

**Behavioral and Neurological Visual Responses under Roll Vection-inducing
Stimulation: Potential Predictors for Motion Sickness Susceptibility**

by

WEI Yue

A Thesis Submitted to
The Hong Kong University of Science and Technology
in Partial Fulfillment of the Requirements for
the Degree of Doctor of Philosophy
in Bioengineering Graduate Program

July 2018, Hong Kong

Authorization

I hereby declare that I am the sole author of the thesis.

I authorize the Hong Kong University of Science and Technology to lend this thesis to other institutions or individuals for the purpose of scholarly research.

I further authorize the Hong Kong University of Science and Technology to reproduce the thesis by photocopying or by other means, in total or in part, at the request of other institutions or individuals for the purpose of scholarly research.

12
12/11/18

WEI Yue

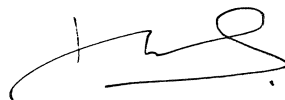
06 July 2018

**Behavioral and Neurological Visual Responses under Roll Vection-inducing
Stimulation: Potential Predictors for Motion Sickness Susceptibility**

by

WEI Yue

This is to certify that I have examined the above PhD thesis
and have found that it is complete and satisfactory in all respects,
and that any and all revisions required by
the thesis examination committee have been made.



Professor Richard Hau Yue SO, Thesis Supervisor
Department of Industrial Engineering and Decision Analytics
Department of Chemical and Biological Engineering



Professor I-Ming HSING
Director, Bioengineering Graduate Program
Head, Department of Chemical and Biological Engineering

School of Engineering, HKUST

06 July 2018

Acknowledgments

I would like to send sincere thanks to my supervisor, Prof. Richard SO, for his generous guidance and support through the whole process. He has not only led me with his foresight, profound knowledge and rich research experiences, but also provided a nice platform and plenty of opportunities for me to evolve my research skills. His patience, spirit and rigorous attitude have always inspired me a lot.

I want to especially thank all the participants who joined our research experiments. Without them, we can never collect those valuable data. I also want to thank my PG fellows in the group for their generous support and warm encouragement along the way, especially to ZHENG Jiayue, FU Xiaojin and Yehur CHEONG for helping me with experiments; to BAO Beisheng, Du Bo and ZHAO Yue for teaching me various experiment procedures.

Moreover, I would like to thank Prof. Michael WONG for encouraging me to join their group meeting. I learned many things and received a lot of help from him. I want to thank PG fellows from his group for their kindly help and inspiring discussions on my research projects, especially to WANG he and YAN min.

In addition, I wish to thank Prof. Keiichi Kitajo from RIKEN for hosting me during the summer program. I learned many advanced data analysis methods from him and his research group. I also want to thank for the generous support and kind help during my stay in Japan, especially to Yuka San and Hiroki San.

I also want to send my gratitude to Ms. Winnie LEUNG for her warm help on tedious student affairs and all the technicians from IELM department for their support and help on equipment. Last but not least, I would like to thank my family for their sustained love, understanding and consideration over the years.

TABLE OF CONTENTS

Title Page.....	i
Authorization Page.....	ii
Signature Page.....	iii
Acknowledgments.....	iv
Table of Contents	v
List of Figures	xi
List of Tables.....	xviii
Abstract	xx
CHAPTER 1 Motivations	1
1.1 Background	1
1.2 General introduction to self-motion perception	2
1.3 Vection and illusory self-motion.....	4
1.4 Visually induced motion sickness susceptibility (VIMSS).....	7
1.5 Central and peripheral vision	8
1.6 Electroencephalography (EEG).....	9
1.7 Terminology, definitions and abbreviations.....	10
1.8 Overview of current research	13
1.9 Thesis outline	13
CHAPTER 2 Literature Review.....	18
2.1 Review on vection.....	18
2.1.1 Behavioral study.....	18
2.1.2 Neurological study	20
2.1.3 Objective indicators for vection	27
2.1.4 Current challenges.....	32
2.2 Review on VIMSS	32
2.2.1 VIMS theories	32
2.2.2 Neurological study	33

2.2.3 Factors affecting VIMSS.....	38
2.2.4 Objective predictors for VIMSS	39
2.2.5 Current challenges.....	41
2.3 Previous works on both vection and VIMSS	41
2.3.1 Current challenges.....	42
CHAPTER 3 Research Gaps and Solutions.....	43
3.1 GAP1: Vection covariates with well-controlled confounding factors	43
3.1.1 Explore vection covariates by method with a higher time resolution	43
3.1.2 Explore vection covariates while controlling VIMSS.....	43
3.1.3 Separate & compare vection covariates originated from CVF and PVF	44
3.1.4 Explore vection covariates with synchronization method and network analysis.....	47
3.2 GAP2: Objective predictors for VIMSS	49
3.2.1 Explore objective VIMSS predictors (without making participants sick)	49
3.2.2 Explore VIMSS predictors while controlling the perception of vection.....	49
3.2.3 Separate & compare VIMSS predictors originated from CVF and PVF	50
3.2.4 Explore VIMSS predictors with synchronization method and network analysis.....	50
CHAPTER 4 Study One – Performance of Behavioral Visual Tasks under Vection-inducing Stimulation	51
4.1 Introduction	51
4.2 Experiment 1a	51
4.2.1 Hypothesis.....	51
4.2.2 Methods.....	52
4.2.3 Results	56
4.2.4 Discussion	60
4.3 Experiment 1b	61
4.3.1 Hypotheses	61
4.3.2 Method	61
4.3.3 Results	63
4.3.4 Discussion	68
4.4 Experiment 2	69

4.4.1 Hypotheses	69
4.4.2 Method	69
4.4.3 Results	70
4.4.4 Discussion	72
4.5 Summary	72
4.5.1 New findings and contributions	72
4.5.2 Raised further questions and focus of follow-up works.....	73
CHAPTER 5 Study Two – Pattern-reversal and Motion-onset Transient VEP Responses under Vection-inducing Stimulation	75
5.1 Introduction	75
5.2 Objective and hypotheses.....	75
5.3 Methods.....	76
5.3.1 Participants	76
5.3.2 Stimuli, apparatus, task and procedures	76
5.3.3 Response measures.....	79
5.4 Data analysis and result.....	80
5.4.1 PRVEP	80
5.4.2 MOVEP	82
5.4.3 Models with MSSQ scores	82
5.4.4 Vection and VIMS reports	87
5.5 Discussion	87
5.6 Summary	89
5.6.1 New findings and contributions	89
5.6.2 Raised further questions and focus of follow-up works.....	90
CHAPTER 6 Study Three – Steady-state VEP Responses under Vection-inducing Stimulation	92
6.1 Introduction	92
6.2 Objective and hypotheses.....	92
6.3 Methods.....	93
6.3.1 Participants	93
6.3.2 Stimuli, apparatus, task and procedures	94

6.3.3 Response measures.....	97
6.4 Data analysis and result.....	99
6.4.1 Vection and VIMS reports	99
6.4.2 SSVEP results	100
6.4.3 Vection covariates.....	103
6.4.4 VIMSS covariates	107
6.4.5 Interaction of attention allocation and vection.....	109
6.4.6 Effect during vection onset	114
6.5 Discussion	115
6.5.1 Differentiated response for CVF and PVF	115
6.5.2 Vection effect: power shift from occipital to parietal	116
6.5.3 Top-down regulation: direct processing from CVF to PVF at frequency domain.....	118
6.5.4 Potential Limitations and Validations	120
6.6 Summary	121
6.6.1 New findings and contributions	121
6.6.2 Raised further questions and focus of follow-up works.....	122
CHAPTER 7 Study Four – Dynamic Links and Connectivity Maps under Vection-inducing Stimulation	124
7.1 Introduction	124
7.2 Objective and hypotheses.....	124
7.3 Methods.....	125
7.3.1 Participants	125
7.3.2 Stimuli, apparatus, task and procedures	126
7.3.3 Response measures.....	127
7.4 Result.....	130
7.4.1 Behavioral results and subjective reports.....	130
7.4.2 VEP results	130
7.4.3 Dynamic node density in phase synchrony networks	135
7.4.4 The distribution and range of phase synchrony	136
7.5 Discussion	146

7.5.1 VEP components	146
7.5.2 Theta-band phase synchrony network.....	148
7.5.3 EEG signatures correlated with VIMS susceptibility	151
7.5.4 Potential limitations and validations	154
7.6 Summary	155
CHAPTER 8 Summary and Comparison on Identified VIMSS Covariates.....	156
8.1 Introduction	156
8.2 Objective	156
8.3 Explanation power.....	156
8.3.1 Data and method.....	156
8.3.2 Results	158
8.3.3 Discussion	161
8.4 Stability and Discrimination ability	163
8.4.1 Data and method.....	163
8.4.2 Results	164
8.4.3 Discussion	166
8.5 Difficulty and cost.....	167
8.6 Summary	168
CHAPTER 9 Conclusions.....	171
9.1 Conclusions	171
9.1.1 Response associate with vection	171
9.1.2 Effects associated with VIMSS.....	172
9.1.3 Guideline for VIMS sensible applications	173
9.2 Summary on contributions	174
Bibliography.....	175
APPENDIX A List of Publications and Conferences	199
Journal articles.....	199
Conference presentations	199
APPENDIX B Visual Stimulation Setups.....	201
APPENDIX C EEG System Setups	202

APPENDIX D Consent Form 203

APPENDIX E MSSQ-short & Pre/post-SSQ..... 204

APPENDIX F MSSQ Score Distribution of Participants in Each Study 205

APPENDIX G Vection Intensity Scale 212

APPENDIX H International 10-10 System for EEG 213

APPENDIX I Example for Training Instructions and Experiment Instructions 214

APPENDIX J List of Hypothesis for Each Study 216

LIST OF FIGURES

<i>Number</i>	<i>Page</i>
Figure 1.1 Major modalities that contributed to self-motion perception. The size of illustrations roughly represents the importance and contribution of each modality. The visual receptors are located in the eye with an eye-centered reference. The auditory and vestibular receptors are located in the head which is naturally head-centered. The somatosensory and proprioceptive receptors are widely distributed in our entire body.	3
Figure 1.2 Illustration on the definition of vection and the type of stimulation we focused.	6
Figure 1.3 An illustration on central and peripheral vision (The pictures are downloaded from https://en.wikipedia.org/wiki/Peripheral_vision#/media/File:Field_of_view.svg and https://en.wikipedia.org/wiki/Peripheral_vision#/media/File:Peripheral_vision.svg on 1:40pm, UTC+8, Mar 12 th 2018).	9
Figure 1.4 Illustration on thesis outline.	17
Figure 2.1 Illustration on the general time course of roll vection under constant velocity stimulation.	20
Figure 3.1 Procedure a typical SART used in this research. (In this illustration, the trial duration of targets is 500ms, while the inter trail interval is randomized from 1s to 1.5s. A red disc shows up in the first frame as an illustration of target presentation in PVF. A green disc shows up in the third frame as an illustration of target presentation in CVF. Note that the ratio of screen and target size is not according to real parameters, since the sizes of targets have been exaggerated for illustration)	45
Figure 3.2 Comparing SSVEP and transient VEP (This is an illustrations obtained from Vialatte, F. B., Maurice, M., Dauwels, J., & Cichocki, A. (2010). Steady-state visually evoked potentials: Focus on essential paradigms and future perspectives. Progress in Neurobiology. http://doi.org/10.1016/j.pneurobio.2009.11.005)	46

Figure 4.1 Illustration of the stimuli and target positions for study one. (W indicates the half length of screen vertical width; r indicates the radius of central black area in Exp.1b; Green shadow is only for illustration of CVF/PVF areas and was not presented in actual stimuli; target diameter is 0.53 cm in Exp.1a and 1.06 cm in Exp.1b; target luminance: 5.86 cd/m^2 for red disc and 10.80 cd/m^2 for green disc)	55
Figure 4.2 Effects of visual response regulation reflected in Exp. 1a and Exp. 1b and their correlation with MSSQ scores illustrated in scatter plots. a. Interaction effect of vection and visual location on SART performance in Exp.1a; note that the effect direction of RT in CVF is subjected to individual MSSQ scores (see Figure 4.2b); ACC=Accuracy; *_vection=averaged from vection trials in CRS condition; *_control=averaged from control trials in IRS condition; b. Correlation of RT effects and MSSQ scores illustrated by scatter plots; MSSQ_T=MSSQ total scale; MSSQ_C=MSSQ child scale; TRT=total effect; DRT_C=delay of RT in CVF	57
Figure 4.3 The modulation of strong vection on RT for target in PVF moving at different speed in Exp.1b (notice that there is no significant difference across all speed under IRS condition)	65
Figure 4.4 Effects of SART-guided attention reallocation on vection intensity and duration. (Task type: CF=central focused, PF=peripheral focused; Targets type: SC=self-motion cues, NC=non-cues; Vection intensity measured by self-report scale: 1=no vection; 5=saturated vection; Vection duration measures by self-rating scale: 0=no experience of vection; 10=experiencing vection all the time).....	71
Figure 5.1 Illustration on the visual stimuli. (the averaged luminance for black cells in checkerboard are 0.70 cd/m^2 , and for white cells are 17.75 cd/m^2 , so the contrast is 92.42%; Note that checkerboard is encircled by grey bar with luminance of 0.35 cd/m^2 and width of 2.1cm; for PRVEP, checkboard has 48×36 cells with size of 0.53cm; for MOVEP, checkboard has 24×18 cells with size of 1.06cm which is twice larger than PRVEP cells).....	77
Figure 5.2 Comparisons of VEP for vection-perception contrasts for all three occipital electrodes. (The red markers indicated the significant/or marginal simple effects for each electrode and their p-values; note that with vection the P1 and N1 are significantly	

smaller, while the P3 is not significantly different between RN and RV; note that all PRVEP is referenced to Fz channel based on previous studies).....	81
Figure 5.3 Comparisons of VEP for stimuli-motion contrasts for all three occipital electrodes. (The red markers indicated the significant simple effects for each electrode and their p-values; note that the P1 and N1 are no significant difference, while the P3 is significantly larger in STA and ROT).....	81
Figure 5.4 Comparisons of VEP under all conditions for three occipital electrodes. (Note that the peak amplitude is larger in right hemisphere, with O2>O1; No peak amplitude difference was revealed for all contrast, but STA is marginally larger than ROT condition; note that all MOVEP are referenced to linked mastoid indicated as A1A2 based on previous studies).....	83
Figure 5.5 Scatter plot for the visual response indicator (increment of N2 peak amplitude at O1 electrode) and child scale of MSSQ (In general, for resistant participants the increment N2 during vection period is positive, while for susceptible people the increment is negative).	86
Figure 5.6 Scatter plot for the visual response indicator (advance of N2 peak latency at Oz electrode) and percentile score of MSSQ adult scale (Note that for resistant people N2 peak latency tend to be shorter during vection, while for susceptible people the Plat tend to be longer during vection)	86
Figure 6.1 Illustration on the visual stimuli. (The averaged luminance for black cells in checkerboard are 0.62 <i>cd/m2</i> , and for white cells are 10 <i>cd/m2</i> , so the contrast is 88.32%; Note that checkerboard is encircled by grey bar with a luminance of 1.54 <i>cd/m2</i> and a width of 0.53cm; the highlighted grey area is just for illustration, so it is larger than actual stimuli; checkboard has 24×18 cells with a size of 0.53cm).....	95
Figure 6.2 The procedure of each trial. (Note that participants are required to indicate their vection perception state by pressing the response button under the ROT stimulation)	96
Figure 6.3 The comparison of vection duration among different attention tasks. (Note that pairwise comparisons only reported a significant difference between SAT and SMO; the error bars are standard errors calculated based on repeated measures model)....	100

Figure 6.4 Topography of SSVEP power at stimuli frequencies and the power spectrum of EOIs.	
a. Topography of SSVEP power at stimuli frequencies. (Left graph shows the topography for CVF stimulation frequency at 8.6 Hz; right graph shows the topography for PVF stimulation frequency at 12Hz)	
b. The comparison on power spectrum at EOIs between the control (COT) condition and dots pattern rotating (ROT) condition (left graph shows the power spectrum of Oz electrode which is the EOI for CVF stimuli; right graph shows the power spectrum of Pz electrode which is the EOI for PVF stimuli; Note that the ROT showed significant larger power than COT at all stimuli frequencies and their 2 nd harmonics in both Oz and Pz)	101
Figure 6.5 Interaction of power between stimuli condition and frequency	102
Figure 6.6 Interaction of power between stimuli EOI position and frequency	103
Figure 6.7 Difference topography obtained by subtracting the power of RN condition from the power of RV condition (DiffRV – RN).	104
Figure 6.8 Interaction on power between vection and position of electrode.	105
Figure 6.9 Interaction on power between the vection and frequency. (Note that this group averaged effect is hid by the significant interaction with individual MSSQ scores)	105
Figure 6.10 Simple interaction on power illustrated for the trinomial interaction between the vection, position and frequency. a. the simple interaction at 8.6Hz between the vection and position. b. the the simple interaction at 12Hz between the vection and position. (Note that the triple interaction ididcated that trend of power shift from Pz to Oz is consistant at the two frequencies, although the dominance frequency for Pz and Oz is different)	106
Figure 6.11 Scatter plot for the MSSQ_T score and the decrease of power during vection at 8.6Hz from Oz electrode	108
Figure 6.12 Scatter plot for the MSSQ_C score and the decrease of power during vection at 8.6Hz from Oz electrode	108
Figure 6.13 Difference topography obtained by subtracting the power of STA condition from the power of SMO condition (DiffSMO – STA). (Upper two topographies are ROT condition without vection perception; lower two are ROT condition with vection)	110
Figure 6.14 Interaction of power between focus condition and frequency	111

Figure 6.15 Interaction of power between focus condition and vection at 8.6 Hz (Note that the simple interaction effect is marginally significant with $p=0.064$)	112
Figure 6.16 Interaction of power between focus condition and vection at 12 Hz. (Note that the trinomial interaction term is significant, while the simple effect at 12 Hz is not significant).....	112
Figure 6.17 Difference topography obtained by subtracting the power of RV condition from the power of RN condition (DiffRV – RN). (Upper two topographies are STA condition; lower two are SMO condition).....	113
Figure 6.18 Topography of power difference between VEON and RV condition	114
Figure 7.1 The procedure of each trial. (Note that participants are required to indicate the onset of vection by pressing once the response button under the ROT stimulation).....	126
Figure 7.2 Averaged VEP for two stimuli conditions at electrodes of interest (shadowed area illustrate the time window for each components).	132
Figure 7.3 The topography map of VEP amplitude under ROT and COT condition.	133
Figure 7.4 VEP results for N=26 participants. a. demonstrate the interaction of VIMS group \times visual stimuli on N223 amplitude (** $p=0.001$; * $p<0.05$). b. the scatter plot for vection intensity and the increment of N223 (amplitude in ROT condition subtracting amplitude in COT condition).	134
Figure 7.5 Topography illustrating the changes of node density in phase synchrony networks under ROT condition (Note that the nodes density reach peak at 200-400ms; and those nodes demonstrating the highest density are the dynamic hubs in the network).	136
Figure 7.6 Illustration for the significant positive clusters which showed higher nodes density in ROT than COT condition. [The line graphs demonstrate the averaged node density across all nodes for each VIMS group. The upper topographies show the two positive clusters in VRE group along with the distribution of connections to NOIs passing the positive threshold (indicating higher $PLVz$ in ROT than COT within each assessed window period). The lower topography shows the positive cluster in VSU group (Note the cluster is much narrower than VRE group)].	137
Figure 7.7 The changed of node density in phase synchrony network before and after the vection onset. (Note that the line graph shows the averaged node density across all nodes for	

VRE and VSU group with baseline corrected by BVEC period from -1500 to -1000ms).....	138
Figure 7.8 The significant negative cluster in VRE group (indicating AVEC<BVEC) and the distribution of connections to right central NOIs passing the negative threshold (indicating smaller <i>PLVz</i> in AVEC than BVEC within assessed window period)..	139
Figure 7.9 scatter plot for MSSQ scores and the indicator calculated from degree of the right central NOIs (Fz/F4) in negative subnetwork (number links indicating smaller <i>PLVz</i> in AVEC than BVEC).....	140
Figure 7.10 Positive and negative subnetwork connected to NOIs (Cpz/Pz and C4) calculated from group averaged PLV node density difference between ROT and COT condition at 208-419ms (two left graphs showed the distribution of connection to NOIs which passed the positive threshold; two right graphs showed the connections to NOIs which passed the negative threshold; RE: the VIMS resistant group; SU: the VIMS susceptible group)	142
Figure 7.11 Positive and negative subnetwork connected to NOIs (P8) calculated from group averaged PLV node density difference between ROT and COT condition at 646-816ms (two left graphs showed the distribution of connection to NOIs which passed the positive threshold; two right graphs showed the connections to NOIs which passed the negative threshold; RE: the VIMS resistant group; SU: the VIMS susceptible group)	143
Figure 7.12 Positive and negative subnetwork connected to NOIs (Pz/Cpz and P8) calculated from group averaged PLV node density difference between ROT and COT condition at 1000-2500ms (two left graphs showed the distribution of connection to NOIs which passed the positive threshold; two right graphs showed the connections to NOIs which passed the negative threshold; RE: the VIMS resistant group; SU: the VIMS susceptible group)	144
Figure 7.13 Positive and negative subnetwork connected to NOIs (F4/Fz) calculated from group averaged PLV node density difference between BVEC and AVEC windows (two left graphs showed the distribution of connection to NOIs which passed the positive threshold; two right graphs showed the connections to NOIs which passed the	

negative threshold; RE: the VIMS resistant group; SU: the VIMS susceptible group)	
.....	145

LIST OF TABLES

<i>Number</i>	<i>Page</i>
Table 2.1 Summary of visual stimuli FOV and neural covariates revealed in recent human vection studies. (Studies used multiple FOV sizes or applied different stimuli in CVF and PVF is showed in bold. fMRI: functional magnetic resonance imaging; BOLD: blood oxygen level dependent; PET: positron emission tomography; rCBF: regional cerebral blood flow; BA: Brodmann area; V1-V6, V3A: human visual areas; MT/ MT+: middle temporal motion area/human MT complex; MST/MST+: medial superior temporal area/MST complex; Csv: cingulate sulcus visual area; PcM: Precuneus motion area ; PIVC: parieto-insular vestibular cortex; IPS: intraparietal sulcus; VIP: ventral intraparietal area; PO: parieto-occipital ; ST: superior temporal area; P1/P3: positive VEP component appeared at around 100ms/300ms; N1/N2: negative VEP component appeared at around 100ms/200ms; TOP: Topography).....	25
Table 2.2 Pros and Cons of current and potential vection measures.....	30
Table 2.3 Summary on neural covariates with VIMS and general motion sickness (MS). (For participants, the group number is demonstrated by: total=resistant + susceptible; if no number for group member, then this study only conducted correlation analysis; for visual stimuli, the FOV is illustrated by: horizontal FOV × vertical FOV; MT+: human middle temporal complex; FIC: right frontoinsula cortex; secondary (SII) and primary (SI) somatosensory cortices; ACC/PCC: anterior/posterior cingulate cortex; PFC: prefrontal cortex; OM: occipital midline; ICA: independent component analysis; mar sig.: marginal significant)	37
Table 2.4 Pros and Cons of current and potential VIMSS predictors.	40
Table 4.1 Vection report in Experiments 1a and 1b.....	59
Table 4.2 Correlations and regression models for visual response indicators predicting MSSQ scores.....	67
Table 5.1 Trial and block summary for each VEP types	80

Table 5.2 Correlations and regression models for VEP indicators predicting MSSQ scores	85
Table 6.1 Summary for block, trial and epoch numbers in experimental conditions	98
Table 6.2 Mean and SD of subjective vection measures.....	99
Table 6.3 Correlations and regression models for SSVEP indicators predicting MSSQ scores.	109
Table 7.1 Group characteristics in demography, VIMS reports and vection perception	131
Table 7.2 Regression models for MSSQ scores with EEG signatures as predictors	141
Table 8.1 Best explanation power for each type of objective indicators in single variable model	159
Table 8.2 Best explanation power for each type of objective indicators in multiple variables model.....	160
Table 8.3 The discrimination ability evaluated by <i>Scored1</i> for different types of indicator	165
Table 8.4 The discrimination ability evaluated by <i>Scored2</i> for different types of indicator	165

Behavioral and Neurological Responses under Roll Vection-inducing Stimulation: Potential Predictors for Motion Sickness Susceptibility

by

WEI Yue

Bioengineering Graduate Program
The Hong Kong University of Science and Technology

ABSTRACT

Visually induced motion sickness (VIMS) is a response commonly reported by viewers exposing to visual stimulation that can provoke self-motion perception (vection). The VIMS susceptibility (VIMSS) varies largely in the population and the neural mechanism for the variation is still unclear. Based on the sensory conflict theory, VIMSS depends on the ability to regulate visual response and coordinate self-motion information between visual and extra-visual modalities under vection-inducing stimulation. However, those hypotheses have not yet been systematically tested. To bridge current research gaps, we need to identify new behavioral and neurological covariates for both vection and VIMSS. In particular, we need indicators that: 1) are of higher time resolution; 2) can reflect the difference of central and peripheral vision; and 3) can reflect information coordination between visual and extra-visual modalities. This research comprises

four studies to explore both behavioral task performances and electroencephalography (EEG) signatures that correlate with vection qualitatively (assess the existence of vection) and quantitatively (assess the magnitude of vection intensity). Study one discovered that under vection, the visual performance of sustained attention to response task (SART) is impaired in central vision and strengthened in peripheral vision to facilitate the processing of self-motion cues. Study two examined the temporal characteristics of transient visually evoked potentials (VEP) from central visual field under the same peripheral vection-inducing stimulation. Results suggest that earlier VEP components are more closely associated with vection perception than VEP components observed later ($>350\text{ms}$). Study three examined the more stable steady-state VEP with frequency tags at central and peripheral visual field to explore more reliable indicators along with the spatial properties of effects. Results revealed a shift of visual information processing emphasis from occipital to parietal under vection. Study four investigated the phase synchrony between visual and extra-visual regions. Results suggest the information coordination between parietal regions and other widely distributed regions are strengthened under vection-inducing stimulation. Furthermore, the magnitudes of those vection associated effects are negatively associated with the VIMSS of participants, hence, can serve as indicators to differentiate VIMS susceptible and resistant groups: the more people are resistant to VIMS, the stronger are the vection effects. In general, our findings support the sensory conflict theory from the perspective of individual differences. Identified behavioral and EEG signatures can contribute to not only the better understanding of VIMS, but also the development of new objective vection measures and VIMS predictors.

CHAPTER 1 MOTIVATIONS

1.1 Background

Self-motion perception can be very crucial for human beings to move effectively from one location to another. It affects not only spatial navigation (Britten 2008; Deangelis and Angelaki 2012), but also many other cognitive and motor functions (Popp et al. 2017), including the bodily self-consciousness (Lopez 2015; Smith and Zheng 2013), the postural control (Freitas Júnior and Barela 2004) and even the reward-based attention (Blini et al. 2018). Although we can make use of information obtained from multiple senses (e.g. visual, auditory, vestibular, somatosensory and proprioceptive modalities: Carriot, Brooks, & Cullen, 2013; Dichgans & Brandt, 1978), human perceives self-motion mainly through vision (Britten 2008; Warren and Kurtz 1992), more specifically, from coherent patterns of visual motion that dominate our peripheral vision (Brandt et al. 1998; Warren, Morris, and Kalish 1988) [See **section 1.2** for more details].

When stationary viewers are exposed to coherent patterns of visual motion, they sometimes can experience illusory self-motion sensation. This phenomenon, commonly experienced in our daily lives (e.g. when observing adjacent train departing or clouds moving), is traditionally referred to as ‘vection’ (Dichgans and Brandt 1978). Although effects of vection have been popular research topics for many years (Hettinger et al. 1990; Palmisano et al. 2015), unresolved challenges and unknowns still exist. In particular, further explorations on objective covariates of vection are needed (Palmisano et al. 2015) (See **section 1.3** for more details).

Currently, vection is also widely utilized in virtual reality (VR) applications to simulate movements in all kinds of vivid environments (Riecke 2011). Given the advanced computing power in recent years, VR technology acquired the unlimited capability to create a various interactive synthetic world with almost perfect photorealism and vivid sensation of motion (Burdea and Coiffet 2003; Rory 2016). This evolves VR into an effective and powerful tool

for many fields, including education (Eschenbrenner, Nah, and Siau 2008; Psotka 1995; Wickens 1992), medicine (Coleman, Nduka, and Darzi 1994; Parsons and Cobb 2011; Wilson, Foreman, and Stanton 1997), entertainment (Beveridge, Wilson, and Coyle 2016; Caroux, Le Bigot, and Vibert 2013) and manufacturing industry (Lu, Shpitalni, and Gadh 1999; Ye et al. 2006).

One major concern accompanied with widespread VR applications is that users may develop symptoms similar to motion sickness (Gallagher and Ferrè 2018). As visual stimulation dominates the VR environment, this experience is often more specifically referred to as visually induced motion sickness (VIMS) (Keshavarz, Riecke, et al. 2015). Although VIMS is usually reported together with vection, the etiology of VIMS and how it related to vection is still vague (Hettinger et al. 1990; Keshavarz, Riecke, et al. 2015). One interesting fact often being underestimated is that the VIMS susceptibility (VIMSS) actually varies a lot in the population (Golding 2006). About one third of people are relatively resistant to VIMS, when exposed to vection-inducing stimulation (Chen et al. 2015; Griffin 2012; Stanney, Kingdon, and Kennedy 2002). Thus, exploring how the response to vection-inducing stimulation of resistant people differs from susceptible people might provide a possible breach. [See **section 1.4**].

In summary, both the fundamental research and industry VR applications call for further investigation on objective covariates of vection along with the VIMSS.

1.2 General introduction to self-motion perception

It is well known that self-motion perception is a multisensory process. Almost all human sensory systems (e.g. visual, vestibular and proprioceptive modalities, see Figure 1.1), to some extent, can provide various information (e.g. speed, direction) regarding the body movement of ourselves, which mostly in a redundancy manner (Campos and Bühlhoff 2012; Cullen 2011; Deangelis and Angelaki 2012). Human perceptive self-motion through the integration of information from multiple modalities.

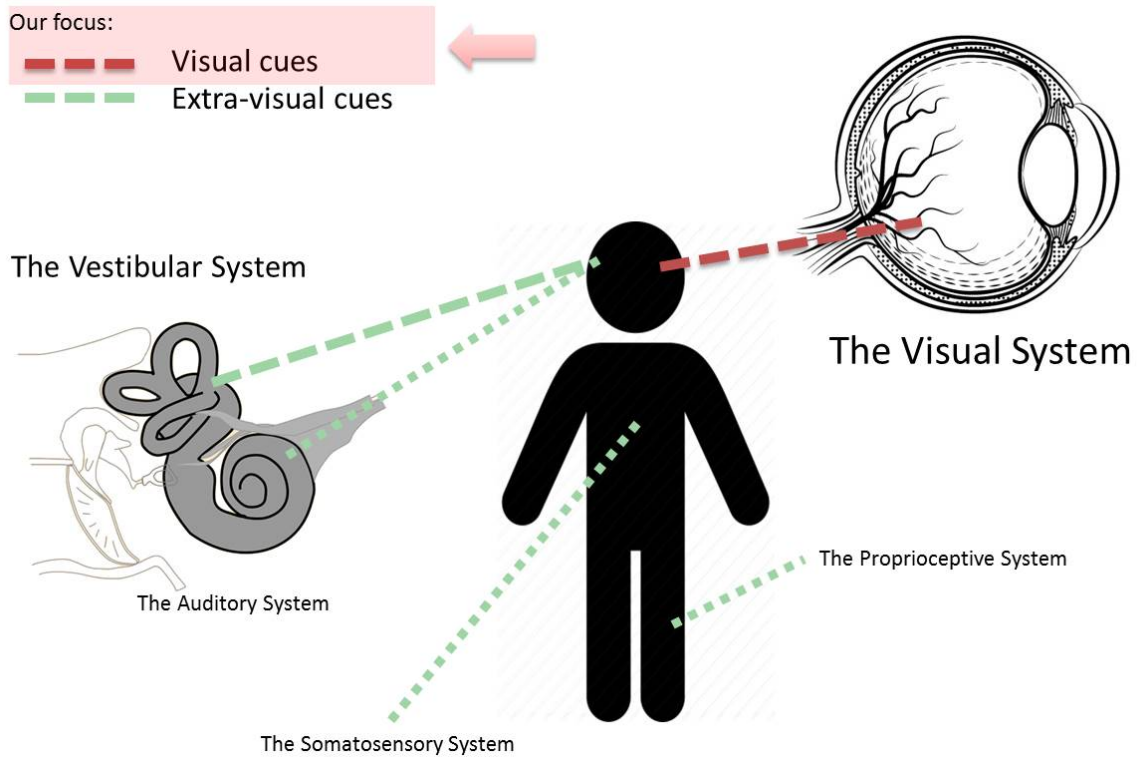


Figure 1.1 Major modalities that contributed to self-motion perception. The size of illustrations roughly represents the importance and contribution of each modality. The visual receptors are located in the eye with an eye-centered reference. The auditory and vestibular receptors are located in the head which is naturally head-centered. The somatosensory and proprioceptive receptors are widely distributed in our entire body.

Among those sensory modalities, visual system dominates our self-motion perception and contributes most of information in plenty of situations (Bremmer et al. 2016; Deangelis and Angelaki 2012), especially in VR environments (Riecke 2011; Wilson 1997). For conciseness, in this work, we refer cues from other sensory modalities as extra-visual cues in general.

For extra-visual cues, the most crucial cue is the inertial motion sensed by labyrinth (the vestibular receptor), often referred to as vestibular input in sensory integration models (Bremmer et al. 2016; Gu, Angelaki, and Deangelis 2008; De Winkel et al. 2013). As visual

and vestibular input generally dominate the sensory information for the self-motion sensation, many researches often focus on visual-vestibular interaction when addressing the sensory coupling or dynamic coordination during self-motion sensation (Dichgans and Brandt 1978; Frank et al. 2014; Gu et al. 2008; Roberts et al. 2016). Nevertheless, other cues from auditory (Keshavarz, Lawrence J Hettinger, et al. 2014; Riecke, Feuereissen, and Rieser 2008), somatosensory (Blanchard et al. 2011; Probst, Straube, and Bles 1985) and proprioceptive (Blanchard et al. 2011; Lackner 1988) system, though limited, also contribute to the self-motion perception.

For visual cues, the most import and intensely explored cue is the optic flow received by retina (Bremmer et al. 2016; Field, Inman, and Li 2015). Optic flow is described as a pattern of motion projected to our retina when we move (Gibson 1950), providing information regarding the speed and direction of our movements relative to the environment (Bremmer et al. 2016; Warren et al. 1988). As the original optic flow based on eye-centered reference frame, when our eye, head and body moves freely, this primary visual cue needs to be decomposed or transformed into other reference frames (e.g. head-centered, body-centered) in a complicated manner (Lappe 2000; Orban 2001), which is often referred to as the ‘rotation problem’ (Bremmer et al. 2016). In current research, we focus on optic flow and restrict to situations, where the three types of egocentric reference frames should yield same movement information, to avoid the interference of ‘rotation problem’.

1.3 Vection and illusory self-motion

The dominance of visual system in self-motion perception is closely associated with one type of illusory sensation of self-motion. When exposed to certain type of visual motion pattern (e.g. optic flow), stationary viewers can experience the illusory sensation of self-motion with a latency of several seconds, which often addressed as ‘vection’.

1.3.1 Definition of vection

Originally, vection was described as the illusion of self-motion triggered by visual stimulation alone, and firstly investigated in laboratory by Mach in 1875 (Dichgans and Brandt 1978; Mach 1875). However, it is worth mentioning that over the years the term 'vection' was subsequently extended to illusions of self-motion triggered by other senses, such as auditory (Keshavarz, Lawrence J Hettinger, et al. 2014; Riecke et al. 2008), tactile and proprioceptive sense (Blanchard et al. 2011), or even applied to real physical motion perception that is mediated by visual stimuli (Ash and Palmisano 2012). In this research, we only focus on the original and most widely examined type of vection: visual cues triggered, illusory self-motion perception (see Figure 1.2).

Moreover, earlier researchers also categorized vection into different types based on the motion type: illusions of self-rotation and self-translation were named 'circular vection' (CV) and 'linear vection' (LV) respectively (Palmisano et al. 2015). For the CV, it can be further divided into three types: yaw, roll and pitch vection, based on the rotating plane (Dichgans and Brandt 1978).

In this research, we mainly test roll vection with a constant rotating speed (see Figure 1.2). We choose this type of vection as the investigation niche for two reasons. Firstly, this type of motion stimuli has been well explored in previous behavioral and neurological studies (Du 2016; Thilo, Kleinschmidt, and Gresty 2003; Zhao 2017; Zheng 2016), so we are able to select most suitable and appropriate parameters for our current research purpose. Secondly, roll rotation has been reported to more closely associated with motion sickness than other types of movements (Diaz Artiles et al. 2016; Van Ombergen et al. 2016).

1.3.2 Measures of vection

Currently, the most commonly used measures for vection is the subjective estimation (Keshavarz, Campos, and Berti 2015), where participants are trained to indicate their experienced intensity of self-motion by operating a joystick or report numerical ratings, either by comparing the experience with a reference, such as the saturated full vection (i.e.,

experience strong illusory self-motion while the moving stimuli appear to be stationary) (Ji, So, and Cheung 2009), or a previously defined stable modulus (Carpenter-Smith and Parker 1992; Webb and Griffin 2003).

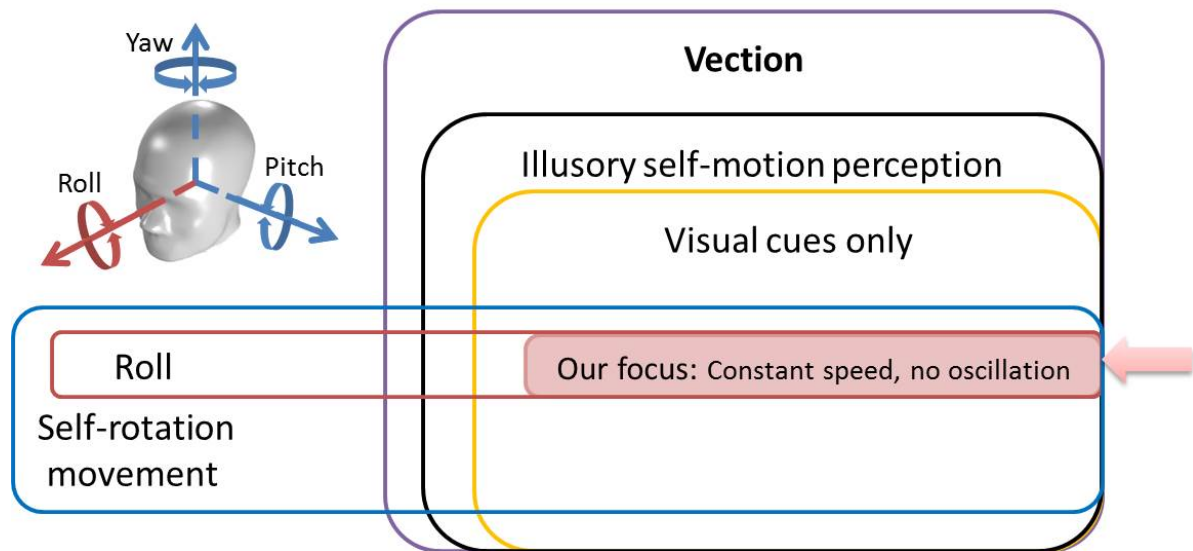


Figure 1.2 Illustration on the definition of vection and the type of stimulation we focused.

However, subjective estimation has been criticized for increasing reasons over the years (e.g. unrealistic presumptions, inconsistency, the subjective and experimental bias) (Carpenter-Smith, Futamura, and Parker 1995; Palmisano et al. 2015; Teghtsoonian 1971). As the modern vection research focus has been directed to less compelling vection conditions, where subjective estimation is even less effective (Palmisano et al. 2015). Therefore, searching for a reliable and practical objective measure for vection has become more and more important for modern vection studies [see **section 2.1** for a detailed review on vection].

To deal with this challenge in modern vection research, we need to further explore behavioral and neurological objective covariates of vection, while indicators obtained from electroencephalography (EEG) signal has been suggested to be a very promising candidate

(Keshavarz, Campos, et al. 2015; Palmisano et al. 2015). Thus, our first research target is to identify objective covariates of vection, mainly on EEG indicators.

1.4 Visually induced motion sickness susceptibility (VIMSS)

Exposure to prolonged vection-inducing stimulation can provoke symptoms similar to motion sickness in stationary viewers, typically including disorientation, oculomotor disturbances and gastrointestinal discomfort (Hettinger et al. 1990; Keshavarz, Riecke, et al. 2015; Zhang et al. 2015). This experience is usually referred to as visually induced motion sickness (VIMS) given the dominance of visual input. VIMS is one of the biggest human factor concerns and popular research topics in a VR environment (Diels and Howarth 2011, 2013; Keshavarz, Riecke, et al. 2015).

Although researches found out that modify the properties of visual stimuli can reduce or prevent VIMS, those methods also generally impaired or destroyed the vection experience (Bonato, Bubka, and Thornton 2015; Golding et al. 2012; Stern et al. 1990). Since vection is very crucial to the user experience and effectiveness of VR applications (Riecke 2011; Riecke et al. 2012), those solutions are not very desirable.

One fact that often ignored or underestimated by previous works is that, the VIMS susceptibility (VIMSS) actually varies a lot in the population, with about one-third of the viewers relatively resistant to VIMS when experiencing vection (Chen et al. 2015; Griffin 2012; Stanney et al. 2002) [see **section 2.2** for a review of VIMSS]. Hence, if we can better capture how those VIMS resistant people differently respond to vection-inducing stimulation (behaviourally and neurologically) as compared to susceptible people, it might shed lights on VIMS preventions that do not hurt vection.

Moreover, the basic processes behind the VIMSS are still vague. Although it is reported that female and children are more susceptible to motion sickness, large variations still exist after controlling age and gender (Golding 1998, 2006; Golding, Kadzere, and Gresty 2005; Paillard et al. 2013; So, Finney, and Goonetilleke 1999; Turner and Griffin 1999).

Furthermore, we are still in short of reliable objective predictors for VIMSS without making people sick currently (Guo et al. 2017). At the ISO Workshop Agreement held in Tokyo in 2005, experts concluded that more studies were needed to explore basic processes underlie the VIMSS (ISO 2005).

Therefore, our second research target is to identify objective indicators (mainly on EEG indicators) that vary according to VIMSS or differentiate VIMS resistant subjects from resistant subjects.

1.5 Central and peripheral vision

One important visual factor affecting both the vection and VIMSS is the functional differences between central and peripheral vision (Brandt, Dichgans, and Koenig 1973; Webb and Griffin 2003; Wei, Zheng, and So 2018).

It is well-known that human visual system process multiple tasks in parallel, where central and peripheral vision are primarily responsible for different tasks respectively (Strasburger, Rentschler, and Jüttner 2011; Zeki 1990). In general, peripheral vision is more responsible for the ‘where’ function (e.g. location, spatial navigation and motion perception) (Agyei et al. 2015; Dichgans and Brandt 1978; Uesaki and Ashida 2015), while the central vision contributes more to the ‘what’ function (e.g. colour, contrast and object recognition) (Ungerleider 1994; Wandell, Brewer, and Dougherty 2005; Zeki et al. 1991). To describe the ‘spatial array of visual sensations available to observation in introspectionist psychological experiments (Smythies 1996), researchers used the term ‘visual field’. In this work, central visual field (CVF) and peripheral visual field (PVF) refer to the visual field perceived by central and peripheral vision pathways respectively.

As mentioned above, self-motion perception primarily involves the optic flow presented in PVF. Previous experiments also suggested that the PVF and CVF play different roles in provoking vection and VIMS (Warren and Kurtz 1992; Webb and Griffin 2003). Therefore, the visual responses originated from central and peripheral vision pathways are very likely to

be affected differently in self-motion related sensory coordination and integration. However, this factor is generally not well-controlled in previous studies, when exploringvection and VIMSS behavioural and neurological covariates [see **section 2** for detailed review]. Therefore, in this research we will also explore specific objective indicators that are able to reflect the visual responses that originated from PVF and CVF respectively.

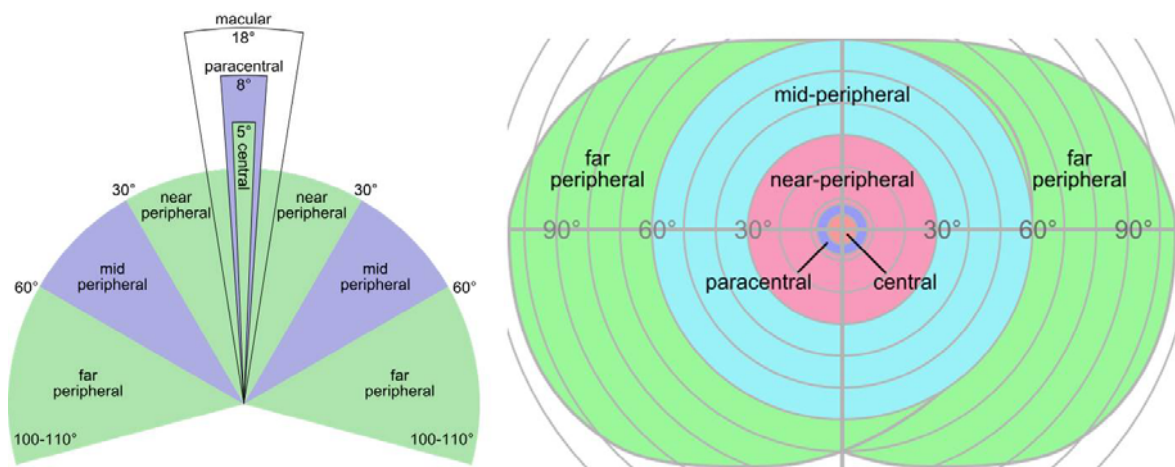


Figure 1.3 An illustration on central and peripheral vision (The pictures are downloaded from https://en.wikipedia.org/wiki/Peripheral_vision#/media/File:Field_of_view.svg and https://en.wikipedia.org/wiki/Peripheral_vision#/media/File:Peripheral_vision.svg on 1:40pm, UTC+8, Mar 12th 2018).

1.6 Electroencephalography (EEG)

Electroencephalography (EEG) is an electrophysiological method that can record the electrical-neurological activity of the brain (Niedermeyer and Lopes da Silva 2005). For the typical noninvasive EEG adopted in most of academic researches, it measures the voltage fluctuations on the scalp that are believed to be originated from ionic current within neurons in our brain (Tyner, Knott, and Mayer 1983).

As EEG is capable to capture the tiny cortical activities with excellent time resolution, it stands out among other neurological measures with several advantages for identifying neural covariates for self-motion perception [see **section 2.1.3** for a detailed review on EEG indicators]: Firstly, EEG signal can be collected without any explicit task or response. This will not only effectively reduce the training procedures and cognitive demands on the capabilities of subjects, but also enable us to collect data under conditions where active behavioral response is not feasible. Secondly, as EEG reflected electrophysiological activities, original EEG data preserves very high temporal resolution. This feature, along with the modern multi-channel EEG systems, empowers researchers to better probe into the dynamic and transient changes during the vection perception. Finally, compared to other non-invasive neural methods such as fMRI and functional Near Infrared Spectroscopy (fNIRS), EEG is portable, easy to manipulate, time-saving and inexpensive, which makes it a very practical measuring apparatus for widespread uses (see Appendix C for illustration on the EEG system adopted in this research).

1.7 Terminology, definitions and abbreviations

A few terminologies, its definition and abbreviation (if applicable) are list as following, subject to the focus and scope of current research as mentioned above.

Self-motion: in this research, it is restricted to the body movement with eye and head position fixed relative to the whole body.

Vection: illusory self-motion perception introduced by visual stimulation alone (Palmisano et al. 2015).

Roll Vection: the illusory sensation of self-rotation about the roll axis (Dichgans and Brandt 1978).

Motion sickness (MS): a group of symptoms provoked by exposure to various kinds of (virtual or real) motion stimulation from various sensory modalities. Typical symptoms

include the disorientation, oculomotor disturbances and gastrointestinal discomfort (Keshavarz, Riecke, et al. 2015; Zhang et al. 2015).

Visually induced motion sickness (VIMS): a group of symptoms similar to motion sickness, but provoked by visual stimulation alone.

Visually induced motion sickness susceptibility (VIMSS): individual susceptibility to VIMS, in this research, the benchmark is obtained by subjective report questionnaire: Motion Sickness Susceptibility Questionnaire (MSSQ) Short-form, which is validated to be an appropriate indicator for VIMSS (Golding 1998; Zhao 2017).

Central visual field (CVF) / Peripheral visual field (PVF): the spatial visual field perceived by central vision / peripheral vision (Smythies 1996). In this research, as the head and eye movement were restricted, the scope of CVF and PVF are treated as generally fixed with the corresponding position on stimuli presenting screen.

Field of view (FOV): describe the degrees of visual angle observable by participants with stable fixation of the eyes (Smythies 1996). In this research, we use FOV to quantify the size of visual field.

Self-motion cues: sensory information which can contribute to the self-motion perception. In current study we only focus on cues received by visual system (optic flow projected to our retina).

Visual response: the response (both transient and steady-state) in visual system when people exposed to vection-inducing stimulation.

Sustained attention to response test (SART): A valid and commonly used measure for sustained visual response (Dillard et al. 2014; Head et al. 2013; Van Schie et al. 2012). SART performance can reflect the sustained response from a particular location in visual field (Manly et al. 1999; Robertson et al. 1997), which is useful for separating and comparing the general visual response in different visual fields (PVF vs. CVF).

Visually evoked potential (VEP): the electrical activity originated from summated postsynaptic potentials in visual cortex, provoked by stimulation on the retina (Niedermeyer and Lopes da Silva 2005; Tyner et al. 1983). VEP is one type of visual responses that measured by EEG. Pattern-reversal VEP (PRVEP) and motion-onset VEP (PRVEP) are two types of well-explored VEPs.

Transient VEP and Steady-state VEP (SSVEP): Transient VEP is the response of the visual system under sudden changes in the visual input, while SSVEP is the sustained response of the system under periodic visual stimulation (usually with a fixed frequency of 3-50Hz) (Vialatte et al. 2010).

Frequency tags: the energy of SSVEP at the frequency of visual stimulation can reflect the processing emphasis of visual system (Camfield et al. 2012; Morgan, Hansen, and Hillyard 1996). In this research, we use specific flickering frequency of the visual stimulation to tag the visual responses originated from CVF and PVF respectively.

Phase synchronization: the process where two or more oscillating signals tend to oscillate with a relative locked delay of phase angle (Lachaux et al. 1999). In this research, we measured the EEG oscillation from electrodes distributed on the scalp and calculate the phase synchronization between electrodes as a reflection of the coordination and integration (Varela et al. 2001). Phase locking value (PLV) is one index that reflecting the strength of phase synchronization (Lachaux et al. 1999).

EEG topography: represent the mapping of EEG features across the scalp (Scarpino, Guidi, and Bolcioni 1990). In this research, we utilize the topography of PLV and VEP (both transient and steady-state VEP) to better capture the spatial distribution of various visual responses.

Electrodes of interest (EOIs): in this research, we select EOI to facilitate analysis based on its location over scalp as well as previous findings which associated those electrodes with optic flow or vection perception.

1.8 Overview of current research

In summary, this research has three major motivations (M1-M3) and four specified research objectives (O1-O4) motivated by them:

(M1) We want to make contributions to the modern vection research by facilitating the development of objective vection measures: for specified research objective, we explore various behavioral and neurological objective covariates of vection (mainly focus on EEG signal and experiment designs) **(O1)**.

(M2) We want to make contributions to the research on VIMSS by exploring basic processes underlie the VIMSS: operationally, we utilize the objective indicators identified in O1 to find out those specific behavioural or neurological responses, which vary according to the VIMSS of participants, or organize differently in the VIMS resistant people and susceptible people **(O2)**.

(M3) We want to support the precautions and solutions for VIMS in VR application by exploring the association between vection covariates and VIMSS: Firstly, we summarize, evaluate and compare those marked responses identified in O2, and then identify promising objective predictors for VIMSS among them **(O3)**. Furthermore, we discuss how VIMS resistant people were able to reduce the potential of VIMS through those marked responses. Guidelines are provided for industry based on our discussion **(O4)**.

To achieve above objectives, we explore various objective indicators (behavioral and EEG) in four sequential studies and approach the O1-3 with each type of indicator. Finally, we approach the O4 based on our summary and discussion of results from all studies.

1.9 Thesis outline

Chapter 1 summarizes the background and the motivations of current research. It also briefly introduces the terminology and methods used in this research.

Chapter 2 presents systematic literature reviews on previous studies investigating our research focus: vection, VIMSS and combined works on both of them. Moreover, it thoroughly reviews current objective measures for vection and objective predictor for VIMSS.

Chapter 3 summarizes the research gaps we want to bridge, our research targets and the new methods we apply to meet those targets. Specifically, the aims of this research are:

- 1) measure objective visual response under vection-inducing stimulation and obtain vection covariates
 - a. explore vection covariates by a method with higher time resolution
 - b. explore vection covariates while controlling VIMSS
 - c. separate & compare vection covariates originated from CVF and PVF
 - d. explore with synchronization method and network analysis
- 2) identify more objective covariates of VIMSS and explore VIMSS predictors
 - a. explore VIMSS predictors without making participants sick
 - b. explore VIMSS predictors while controlling the perception of vection
 - c. separate & compare VIMSS predictors originated from CVF and PVF
 - d. explore with synchronization method and network analysis

Chapter 4 reports the first study measuring the Sustained Attention to Response Test (SART). We conduct three successive behavioral experiments to explore the performance of sustained attention to response test (SART) in PVF and CVF under roll vection inducing stimulation. The **behavioral performances (response time and accuracy) of SART** are revealed to be covariates of vection perception: with vection, the SART performances generally impair in the CVF, while well-directed improve with targets similar to optic flow in the PVF. This study also serves as the validation of our stimuli presenting system and roll vection-inducing stimuli for following EEG studies.

Chapter 5 reports the second study measuring transient VEP. In this study, we go further using visually evoked potential (VEP) to explore the effect revealed by SART. As the SART requires explicit responses that involved many basic cognitive and motor functions, it is vulnerable to plenty of factors unrelated to the vection perception, and inappropriate to use in

a complicated situation when explicit responses are not feasible. To further clarify the basic visual response influenced by the vection perception, we apply two types of procedure to obtain the pattern-reversal VEP (PRVEP) and motion-onset VEP (PRVEP) respectively. The **VEP components (peak amplitude and latency of VEP components)** are revealed to be covariates of vection perception: with vection, N1/P1 components were suppressed, while N2 components were strengthened. As the first EEG experiment, this study also serves as the validation of our EEG setups, signal acquisition and data pre-processing procedures for following studies.

Chapter 6 reports the third study measuring steady-state VEP. In this study, we move further to utilize the 32-channel EEG system to measure widely distributed EEG signal and obtain more spatial information. Since we only explore the signal from occipital electrodes in second study, the spatial information gained by multiple electrodes can shed lights on more sensitive measures for vection. We also make use of frequency tags to differentiate the response from CVF and PVF. **The topography and frequency tags (energy peak at stimuli frequency)** are revealed to be covariates of vection perception: vection is associated with a processing emphasis shift from occipital to parietal area. This study also validated the electrodes of interest (EOI) that primarily responsible for the CVF/PVF stimulation adopted in this research. The identified EOI will be further explored in later study.

Chapter 7 reports the fourth study measuring both the transient VEP and phase synchronization. In this study, we go beyond localization-based methods and explore the functional connectivity between different brain areas. As vection perception is an activity involves multisensory coordination and integration, additional information should lie in the dynamic coordination between visual regions and other widely distributed brain areas. In addition to **VEP components, phase synchronization index (the phase locking value: PLV)** are revealed to be covariates of vection perception: the VEP component (N2) amplitudes are correlated with the vection intensity of participants, while the dynamic links between electrodes over several regions of interest and other widely distributed electrodes (evaluated by network indexes) are enhanced during vection-inducing stimulation.

Chapter 8 summarize and compares all the previously identified objective indicators as predictors for VIMSS. We evaluate the potential of each predictor based on its prediction power over MSSQ scores (child, adult and total scale), along with the difficulty, stability and cost of measurement.

Chapter 9 summarize the basic response associated with vection, and how those responses related to VIMSS. Moreover, we also discuss how VIMS resistant people are able to prevent VIMS through the marked responses differentiate them from the VIMS susceptible group. Guidelines for industry are then provided based on the summary of result.

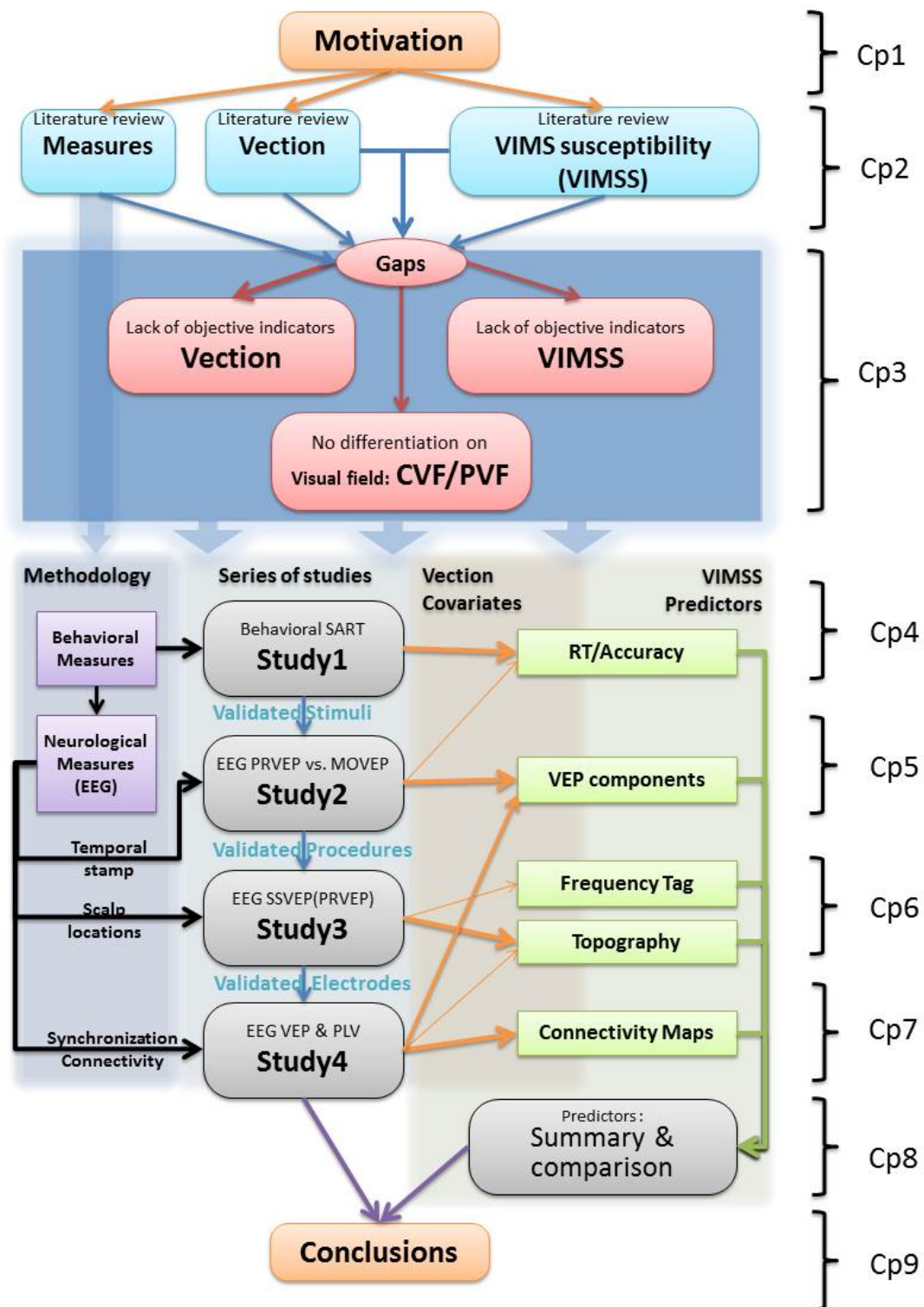


Figure 1.4 Illustration on thesis outline.

CHAPTER 2 LITERATURE REVIEW

2.1 Review on vection

2.1.1 Behavioral study

Although vection has long been a well-known phenomenon among the psychology experimentalists since it is firstly described, its detailed psychophysical characteristics and neurophysiologic basis had not been investigated until recently (Dichgans and Brandt 1978). Early behavioral studies regarding vection mainly focus on describing the motion perception features (e.g. time course of onset and saturated, motion perception velocity, adaptation and displacement) and how they are modulated by stimuli properties (e.g. spatial frequency, velocity, motion plane/axis, eye fixation and visual field of view occupied).

Time Course and vection stages

In general, it has been revealed that the time course of vection is started with a period of onset latency which ranges from 1-10s among different subjects, which is usually shorter for LV than CV (Berthoz, Pavard, and Young 1975). Then it is followed by a period of apparently motion stage for 5-15s where the vection sensation will continually become stronger until it reaches the plateau stage. In some individuals, the perceived vection may reach a 'saturated stage' (also refers to 'full vection'), where subjects experience compelling self-motion sensation while the moving stimuli appear to be stationary (Brandt et al. 1973).

The 'saturated' velocity of CV increase as the stimuli velocity rise, but would start to lag behind when stimuli velocity reach 120°/s and do not exceed 180°/s. When the speed of stimuli is too fast or the visual field occupied by visual stimuli is small (<30°), there will be a mix sensation of self-motion and objective-motion, where both the visual surround and body are perceived to be moving (Dichgans and Brandt 1978).

Vection Intensity

Vection intensity is commonly measured by subjective estimation as an important indicator for the magnitude of vection perceived by participants. The vection intensity is usually described by the relative extent of ‘saturated’ velocity compared with stimuli velocity, rather than an absolute velocity (Riecke, Schulte-Pelkum, and Caniard 2006; Webb and Griffin 2003), in which ‘full vection’ is often selected to be a reference as 100% in the scale (Ji et al. 2009).

Stimuli velocity is obviously one main factor that affecting the vection intensity. With other factors fixed, the perceived vection intensity usually continue to increase as stimuli velocity increase until it reaches a plateau, or start to decrease when it reaches the maximum intensity (Du 2016; Fu et al. 2017). Besides the velocity, some external factors of the stimuli also have some effect. For instance, increasing the field of view (FOV) occupied by visual stimuli or the spatial frequency of visual stimuli will lead to stronger vection intensity, while peripheral stimuli play more important role than central ones, either in terms of retinal or depth (Dichgans and Brandt 1978).

Motion plane and axis is another crucial factor that can affect the vection intensity. For CV, roll vection and pitch vection, referring to the rotation in sagittal and coronal axis respectively, usually weaker and less stable when compared with the yaw CV in horizontal plane (Dichgans and Brandt 1978; Du 2016; Thilo et al. 2003; Zhao 2017), with reduced intensity and even the occurrence of no vection stages during prolonged exposure to constant velocity stimulation (see figure 2.1 for illustration).

The fluctuation and weak intensity of roll vection could possibly due to the persistent relatively high conflicts between visual and extra-visual cues, which make it a nice circumstance for investigating the sensory conflicts and the VIMSS. As mentioned before, roll vection indeed induced more symptoms of motion sickness as compared with other type of movement (Diaz Artiles et al. 2016; Van Ombergen et al. 2016).

Therefore, we want to explore the visual response under the roll vection inducing stimulation. As roll vection is generally weaker, so it is especially beneficial to choose visual stimuli that can introduce a stronger and more stable roll vection. Based on previous works in our lab (Du 2016; Zhao 2017; Zheng 2016), dots pattern rotating at a velocity of $32^\circ/\text{s}$ would introduce strongest intensity for roll vection, with our stimuli presentation setups (see Appendix B). Thus, we select this velocity ($32^\circ/\text{s}$) and controlled other external factors of vection-inducing stimuli in all experiments, to obtain stronger vection and facilitate the inter-study and inter-subject comparisons.

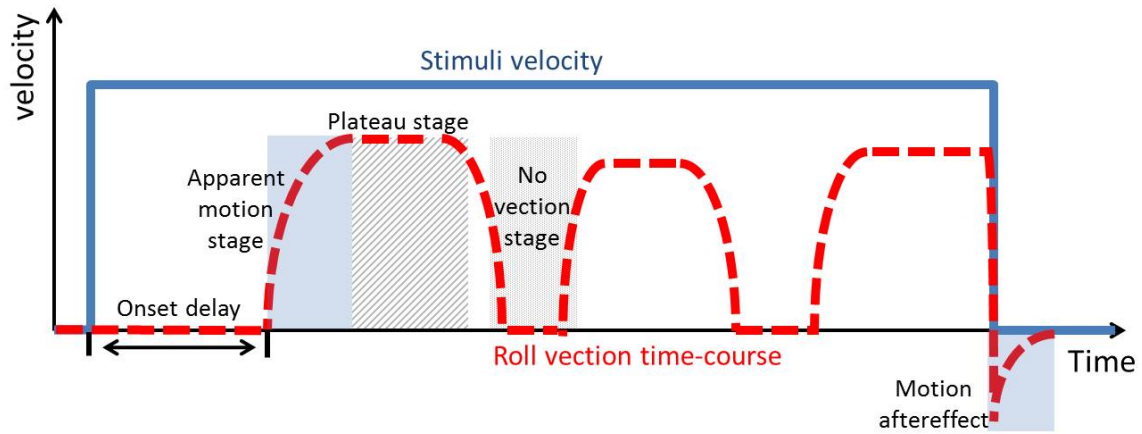


Figure 2.1 Illustration on the general time course of roll vection under constant velocity stimulation.

In this research, we will use subjectively reported time period of vection (e.g. vection onset, duration), along with the vection intensity as a reference benchmark for the objective vection indicators we identified.

2.1.2 Neurological study

Only a small number of studies have tried to penetrate the neural basis of vection as compared with psychophysical studies, while most of animal experiments started around 1970s and human studies adopting non-invasive measurements such as MRI and EEG did not emerge until the last two decades.

Vestibular Nucleus

Over the years, our understanding of vection had been restricted to the fact, that the perception properties of visual stimuli are quite similar to vestibular excitations, until researchers revealed that in goldfish the discharge of neurons in vestibular nucleus (VN) were actually modulated by optic flow (Klinke 1970). This study was followed up by several further experiments in other species, including rabbit (Dichgans and Brandt 1973) and monkey (Henn, Young, and Finley 1974), where different discharging types of neurons were identified.

However, most of these studies were conducted in animals, such as rabbit, cat and fish, where actually no vection perception report can be collected. For human being, there is no doubt the sensory interactions are far more complicated, where higher level cognitive activities, past experiences and training shall play an important role. As a matter of fact, VN was widely admitted to be the least vital sensory interaction site for primates to perceive vection (Keller 1976). In human subjects, CV experiences could still persist even after removing bilateral vestibular nerves (Zee, Yee, and Robinson 1976).

Cortical network underlying the vection or optic flow

Therefore, it is recognized that further investigations in human subjects focusing on brain areas above brainstem are desirable. In fact, understanding the neural basis of vection, has been emphasized as one of the biggest challenges in vection study (Palmisano et al. 2015). Though very limited, increasing neural imaging studies have been carried out recently, attempting to capture the cortical activity during vection. However, few consistent results have been revealed.

Cortical areas identified to be involved in vection perception varied from study to study, which included visual motion processing areas such as V3A (Fischer et al. 2012a), middle temporal area(MT/V5) (Jong et al. 1994; Previc et al. 2014; Watson et al. 1993), MST (Duffy and Wurtz 1991; Pan et al. 2016), kinetic occipital region(KO) (Dupont et al. 1991) and V6

(Cardin and Smith 2011; Fischer et al. 2012b; Pitzalis et al. 2010; Pitzalis, Fattori, and Galletti 2015, 2012) as well as vestibular areas such as parieto-insular vestibular cortex (PIVC) (Bense et al. 2001; Brandt et al. 1998, 2002), some of which (e.g. hMST and PIVC) are also have been proved to be multi-sensory areas that either received the afferent or modulated by from both modalities (see Table 2.1 for a summary).

The attributes of activities also varied across different studies. For example, Brandt and his colleagues found out that PIVC were deactivated duringvection, while visual motion perception related area (middle temporal area, MT+) are intensely activated (Brandt et al. 1998; Dieterich et al. 1998). In conflict with this, MT/V5 are sometimes reported to be deactivated duringvection (illusion of self-motion) perception (Kleinschmidt et al. 2002; Pitzalis et al. 2010), while in other studies, no significant result was found in PIVC area (Bense et al. 2001) or increasing activation were identified (Nishiike et al. 2002; Uesaki and Ashida 2015) which is actually in the contrary with previous studies. To make things more complicated, even for studies that find similar deactivation in PIVC, locations that identified as PIVC area are quite different in different experiments (Brandt et al. 1998; Cardin and Smith 2010; Kleinschmidt et al. 2002).

There are three possible reasons for those inconsistencies:

Lack of synchronization with cognitive state

One biggest concern in interpreting those findings is that most of those experiments primarily focus on brain covariates of visual stimulation, rather than cognitive perception state of participants. As illustrated above (see Figure 2.1), the time course ofvection perception usually does not synchronize with visual stimuli.

Except very few experiments (Kleinschmidt et al. 2002; Kovács, Raabe, and Greenlee 2008; Thilo et al. 2003), most of the studies actually did not bother to examine the capability of their stimuli presenting system in inducingvection or did not required their subjects to report the time course of theirvection perception (Braddick et al. 2001; Brandt et al. 1998;

Deutschländer et al. 2004; Dieterich et al. 1998, 2003; Indovina et al. 2005; Previc et al. 2014; Shipp et al. 1994; Uesaki and Ashida 2015). Since the procedures, stimuli types and different contrast or baseline adopted in previous studies varies between studies, all of those factors could lead to different onset delay, fluctuation, and intensity of vection perception that introduce complicated inter-study conflicts. As the vection perception state fluctuates rapidly and varies for each participant, to better identify neural covariates that can synchronize with vection state, we need to explore neural indicators with higher time resolution.

Lack of control on VIMSS of participants

As mentioned in **section 1.4** above, VIMSS is an important factor that can influence how individual response to vection-inducing stimulation. According to Brandt's theory on the motion sickness (Brandt et al. 1998), people resistant to VIMS shall activate visual system and suppress vestibular system, while susceptible people should fail to implement this mechanism [see detail review in **section 2.2.1**].

Therefore, if experimenter did not control the VIMSS of participants, large inter-subject variations might cancel or hide the activity in brain areas through the averaging of group data. Unfortunately, since VIMSS usually is not the focus of those functional brain studies, few studies have reported the VIMSS of their participants, or screen participants based on VIMSS (Keshavarz, Riecke, et al. 2015; Palmisano et al. 2015). This situation also can lead to inconsistent results in identifying vection covariates. Thus, it is necessary to control VIMSS when explore the vection covariates and validate how vection covariates vary according to VIMSS.

Lack of separation for CVF and PVF

Another factor need to be taken into account, is the functional difference between central and peripheral vision. As introduced in **section 1.5 & 2.1.1**, the PVF and CVF contribute to the self-motion perception differently.

Therefore, it is very likely that the response in PVF and CVF shall be modulated differently during vection-inducing stimulation. However, most of previous often presented similar visual stimuli to CVF and PVF together and measured whole brain responses to their stimulation (Barry et al. 2014; Becker-Bense et al. 2012; Beer et al. 2002; Braddick et al. 2001; Brandt et al. 1998; Deutschländer et al. 2004; Jong et al. 1994; Kovács et al. 2008; S. Pitzalis et al. 2013; Previc et al. 2014; Uesaki and Ashida 2015; Vilhelmsen, van der Weel, and van der Meer 2015; Wall and Smith 2008). The visual field covered by their stimuli various from a small field of $12.8^{\circ} \times 12.8^{\circ}$ to a very large field of $102^{\circ} \times 114^{\circ}$ (see Table 2.1). As illustrated in Figure 1.3, the precise definition of CVF is the visual angle range within 5° of FOV, while the paracentral and macular visual field extended to 8° and 18° of FOV respectively. Therefore, almost all of previous studies examined a mixed response or modulation effect originated from CVF and PVF together.

Table 2.1 Summary of visual stimuli FOV and neural covariates revealed in recent human vection studies. (Studies used multiple FOV sizes or applied different stimuli in CVF and PVF is showed in bold. fMRI: functional magnetic resonance imaging; BOLD: blood oxygen level dependent; PET: positron emission tomography; rCBF: regional cerebral blood flow; BA: Brodmann area; V1-V6, V3A: human visual areas; MT/ MT+: middle temporal motion area/human MT complex; MST/MST+: medial superior temporal area/MST complex; Csv: cingulate sulcus visual area; PcM: Precuneus motion area ; PIVC: parieto-insular vestibular cortex; IPS: intraparietal sulcus; VIP: ventral intraparietal area; PO: parieto-occipital ; ST: superior temporal area; P1/P3: positive VEP component appeared at around 100ms/300ms; N1/N2: negative VEP component appeared at around 100ms/200ms; TOP: Topography)

Literature	FOV (horizontal ×vertical)	Method	Vection covariates	
			Activated	Suppressed
Jong et al., 1994	40°×30°	PET: rCBF	V3, PcM, occipital-temporal ventral surface, fusiform	-
Brandt et al., 1998	40°×40°	PET: rCBF	PO	MT, BA19/18/21/37, posterior insula
Tokumaru et al., 1999	120°×45°	EEG: TOP	No consistent result between subjects	
Braddick et al., 2001	12.8°×12.8°	fMRI: BOLD	V5, V3A, IPS, ST, occipital ventral surface	V1
Kleinschmidt et al., 2002	45°×45°	fMRI: BOLD	MST, dorsomedial cortex, ST	MT, V4, V3/V3A, V1, PIVC
Beer et al., 2002	102°×114°	PET: rCBF	BA37, Csv, occipital area	MT, frontal gyrus, cuneus
Thilo et al., 2003	CVF: 45°× 33° PVF:110°× 110°	EEG: VEP	-	N1(occipital)
Deutschländer et al., 2004	100°×60°	PET: rCBF	MT, PO	retroinsular regions
Wall et al., 2008	20°×20°	fMRI: BOLD	VIP, Csv, MT, MST	V2, V3, V3A, V4
Kovács et al., 2008	59°×59°	fMRI: BOLD	right MT+, PcM, IPS	-
Becker-Bense et al., 2012	90°×60°	FDG-PET: rCGM	inferior parietal, Csv, PO, frontal eye fields	-
Pitzalis et al., 2013	69°×55°	fMRI: BOLD	V6, IPS, MST+	-
Previc et al.,	114°×102°	PET:	left temporal	right temporal

2014		rCBF	(BA37, BA22),	(BA21), occipital(V1)
Keshavarz et al., 2014	CVF: 45°× 38° PVF: 73°× 61°	EEG: VEP	N2 (right PO)	P1
Barry et al., 2014	whole screen: size not reported	EEG		Desynchronization: low alpha, gamma band
Uesaki et al., 2015	30°×30°	fMRI: BOLD	V6, MT+, VIP, PIVC, CSv	-
Vilhelmsen et al., 2015	71.5°×50.4°	EEG: VEP	N2 (MT)	-
Wada et al., 2016	17~100°× 12~67.7°	fMRI: BOLD	V6, CSv, PcM, MT+, PIVC	-
Stróžak et al., 2016	CVF1:no report CVF2:45°× 30° PVF:96°× 60°	EEG: VEP	N2 (left occipital)	P1(right PO), P3(central)

Only a few studies (see highlighted in Table 2.1) have attempted to present different type of stimulation to CVF and PVF separately (Keshavarz and Berti 2014; Stróžak et al. 2016; Thilo et al. 2003), or examined the visual response under vection-inducing stimulation with various range of FOV (Wada, Sakano, and Ando 2016). However, the CVF defined by those studies generally occupied quite large FOV at about 45°× 30°, which have already covered near- and mid-peripheral visual field. Moreover, some studies present the CVF and PVF stimuli simultaneously and did not apply any specific tag to differentiate the response originated from CVF or PVF (Keshavarz, Lawrence J. Hettinger, et al. 2014; Stróžak et al. 2016), which make it unrealistic to compare the effects between CVF and PVF. Finally, some works focus on the response to optic flow which induced vection (Keshavarz and Berti 2014; Wada et al. 2016), while others focus on visual response to additional visual task (Stróžak et al. 2016; Thilo et al. 2003) during vection, making their findings and interpretations more complicated.

Hence, we are lack of studies on: 1) exploring methods that can **tag the responses originated from CVF and PVF separately**; 2) separating the response triggered by optic flow and the **modulation of visual responses under vection perception**; 3) exploring the modulation of visual responses during vection **in narrower CVF**.

Drawbacks of isolated localization methodology

Furthermore, another limitation of previous studies is that all of them have employed traditional localization methodologies. While most of the previous studies try to identifying associate brain areas by correlating subjective reporting or behavioral conditions with the signal recording from each measuring unit (voxels, channels etc.) one by one (Thilo et al. 2003; Brandt et al. 1998; Kleinschmidt et al. 2002; Kovács, Raabe, and Greenlee 2008; Dieterich et al. 1998, 2003; Indovina et al. 2005; Jong et al. 1994), this methodology may cause inconsistencies or failures in capturing the actual neural activities underlying vection.

First of all, some recent functional brain studies (Haxby et al. 2001; Norman et al. 2006) have proved that the traditional localization analysis could underestimate or distort the cortical activity involved in the complicated cognitive tasks due to the network cancelation or sparse coding in the neural activities.

Furthermore, as shown above, the generation of vection is obviously not achieved by one particular isolated functional area, but rather a complicated network. The fact that vection is shaped by a complicated network where widely distributed brain areas are involved and interact with each other, makes the shortcoming of previous methods which mainly focus on identifying isolated local brain activities becomes salient. The crucial neural mechanism behind vection should have a higher possibility to lie in the information integration and coordination between those multiple brain areas, rather than in the activeness of one or two isolated brain areas. To better capture the issue, new solutions that can better grab the dynamic connectivity changes between brain areas need to be explored.

2.1.3 Objective indicators for vection

As introduced in **section 1.3**, in addition to uncovering the neural basis of vection, another important topic in vection study is to identify practical vection measures. Here we summarize current behavioral and neurological vection covariates and explorations on those covariates as the vection indicator (both the qualitative indicators that only reveal the existence of

vection and the quantitative indicators that can indicate the intensity of vection; see Table 2.2 for a summary).

Behavioral vection indicators

To reveal the presence of vection, there are various behavioral indicators can be utilized, including the heading judgements and the postural adjustment (e.g. body tilt and postural sway) (Carpenter-Smith et al. 1995; Kuno et al. 1999). Although those behavioral indicator usually are easy to measure (e.g. body tilt), they shared a common drawback: insensitive to the strength of vection. Only reporting the existence of vection does not achieve the main targets of objective measures, as it contributes very little to weak vection detection, inter-study and inter-subjects comparisons, or quantitative vection model establishment. Thus, it is important to further explore quantitative indicators.

However, very limited studies have tried to address this challenge, where most of the attempts are somewhat unsatisfactory. For example, the postural sway, defined as the human body movement to keep balance of the body during the changes in the body center of gravity, is one of the first quantitative objective measures for vection (Dichgans and Brandt 1978; Stoffregen 1985). However, the limitations of posture sway have also been revealed soon. It was reported that postural sway is only sensitive to the visual acceleration but attenuated during the persistence of constant-velocity visual motion (Carpenter-Smith et al. 1995; Lestienne, Soechting, and Berthoz 1977). Moreover, the occurrence of vection and postural sway is not always consistent: previous studies showed that postural sway can exist without the experience of vection, and vice versa (Palmisano et al. 2015; Previc and Mullen 1990; Warren 1995).

Other potential measures emerged later also came in the similar situation. They are either requiring too complicated task and procedures [e.g. Inertial nulling paradigm, which is measuring vection via the level of body acceleration required in opposite direction to null the perception of self-motion (Carpenter-Smith et al. 1995; Zacharias and Young 1981)], or non-

effective and inconsistent in various conditions [e.g. eye-movements (Kim and Palmisano 2010; Webb and Griffin 2003)]. We summarize their drawbacks and merits in the Table 2.2.

Neurological indicators

In addition to behavioral indicators, the investigations on neural basis of vection also yield several potential neurological indicators. Previous studies have showed that the activation or suppression activity in several brain areas is correlated with vection perception and vection strength (e.g. PIVC, VIP, MST, CSv and PcM; see Table 2.1 for a summary). Applying multi-voxel pattern analysis in those areas can classify the viewing of vection-inducing stimuli with accuracies at 60-80% (Wada et al. 2016). However, although those brain imaging methods (e.g. PET and fMRI) can provide abundant multi-dimensional information and help us to better locate the source of neural activity, the limitation of those methods as the vection indicator is obvious: the limited time resolution (depending on hemodynamic responses), the expensive brain scans, the huge and importable scanning machine and complicated scanning protocols/procedures make it currently quite impractical to be simply served as a measurement for vection.

Compared with other neurological measurements, EEG has been put forward as a more promising candidate recently (Barry et al. 2014; Keshavarz, Campos, et al. 2015).

Table 2.2 Pros and Cons of current and potential vection measures.

Measures	Qualitative/ Quantitative	Type	Pros	Cons
Body tilt	Qualitative	Behavioral	Easy to obtain	Individual variation; difficult to obtain in sitting/supine position; subject to motion plane
Heading judgement	Qualitative	Behavioral	-	Need explicit response, additional cognitive load, difficult to obtain in weak vection condition
Inertial nulling paradigm	Qualitative/ Quantitative	Behavioral	Can measure vection intensity	Difficult to measure; complicated procedures
Postural sway	Qualitative/ Quantitative	Behavioral	Correlated with vection intensity	Weak/attenuate during constant-velocity visual motion stimulation; can occur without vection
Eye-movements	Qualitative/ Quantitative	Behavioral	Correlated with vection intensity	Non-effective if eye movement is restricted, Non-effective in forward translation/roll/pitch/ vection; onset lag
EEG	Qualitative/ <u>Quantitative?</u>	Neurological	High time resolution; multi- dimensional; portable	<u>Limited exploration;</u> <u>Lack of validations on</u> <u>individual variations</u>
MRI/PET	Qualitative/ Quantitative	Neurological	Multi- dimensional; Correlated with vection intensity	Expensive; importable; complicated procedures; low time resolution; inconsistent results;

EEG indicators

Being a non-invasive measurement that is capable to capture the tiny cortical activities, EEG stands out with several advantages in identifying bio-markers for self-motion perception. Firstly, EEG data can be collected without any explicit task or response, which will not only effectively eliminate most of the current training procedures and experiment demands on the capabilities of observers, but also enable the data collection under conditions where active behavioral response is not feasible. Secondly, as a measurement based on electrophysiological activities, EEG signal bears a rather high temporal resolution. This feature of EEG, along with the multi-dimensional information that can be collected simultaneously, would actually empower researchers to better probe into the dynamic and transient changes accompany with the initiation and persistence of vection, which can facilitate the identification of desirable sensitive indicators for vection intensity. Finally, compared to other non-invasive neural methods such as fMRI and functional Near Infrared Spectroscopy (fNIRS), EEG is portable, easy to manipulate, time-saving and inexpensive, which makes it a very practical measuring apparatus.

However, despite all of those superiorities discussed above, very few attempts have been made on approaching the neural covariates through EEG methodology. Among most of those limited works, vection-inducing stimuli (optic flow) are either presented for too short time period (less than 4s) that usually unable to generate vection (Keshavarz and Berti 2014; Vilhelmsen et al. 2015), or simply compared with motionless baseline using frequency analysis (Barry et al. 2014; Tokumaru et al. 1999) with not well-controlled confounding factors, such as the optokinetic nystagmus, the local visual motion processing and VIMSS.

Moreover, as discussed in above **section 2.1.2**, EEG vection studies also suffer from similar dilemma that most of identified covariates are not synchronized with vection perception but the presence of visual stimuli. The only one exception work was conducted by Thilo (2003). Thilo and his colleagues presented roll rotating radial pattern in the PVF and reversing checkerboard in the CVF (see Table 2.1 for details) to provoke VEP. They found that the

peak amplitude of N1(N70) was significantly reduced during vection (Thilo et al. 2003) as compared with periods without vection but under same visual stimulation.

However, N1 is a very small ERP component that usually requires high contrast stimulation and large numbers of repetitions to obtain effective data (Luck 2005). Furthermore, the N1 component is sensitive to various factors and sometimes are even entirely absent in many individuals (>50%, see Souza et al., 2013). Furthermore, the effect size was not reported to correlate with the vection strength. These all hamper the stability and utility of N1 as a quantitative objective indicator for vection. Further sufficient investigations on more reliable EEG indicators are needed to better develop quantitative indicators for vection (Table 2.2 showed bold and underlined summary).

2.1.4 Current challenges

In summary, there are two big topics in vection studies (a. developing objective measures; b. exploring neural basis of vection). Both of them require more explorations on the vection covariates (especially with EEG) with carefully controlled confounding variables. We will summarize all the gaps, challenges and our solutions for exploring objective vection covariates in chapter 3.

2.2 Review on VIMSS

2.2.1 VIMS theories

As introduced in **section 1.4**, with prolonged exposure to a moving visual scene, most of stationary observers would report VIMS with varying severity (Griffin 2012; Stanney et al. 2002). VIMS is usually addressed as a member of the general family of motion sickness, except that physical motion is absent in VIMS (Hettinger et al. 1990; Keshavarz, Riecke, et al. 2015; Zhang et al. 2015). VIMS has been frequently reported in various virtual motion environments. However, the etiology and neurobiological mechanism of VIMS are still vague (So and Ujike 2010; Zhang et al. 2015).

Several theories have been proposed to explain the origin of VIMS (or general motion sickness): the sensory conflict theory (Reason 1978), which addresses motion sickness as the consequence of conflict sensory information and neural mismatch; the postural stability theory (Riccio and Stoffregen 1991), which emphasizes that the crucial role of postural instability in causing motion sickness; and the eye movement theory (Ebenholtz 1992), which argues that the optokinetic nystagmus (OKN) provoked by optic flow can innervate the vagal nerve and thus lead to VIMS.

2.2.2 Neurological study

Currently, none of the motion sickness theories have been supported by conclusive neurobiological evidence. Among them, the ‘sensory conflict theory’ is believed to be the most promising and has supported by a large number of empirical evidence (Keshavarz, Riecke, et al. 2015; Miyazaki et al. 2015). Although ‘sensory conflict’ has been criticized as unmeasurable (Griffin, 2012), recent advances in brain imaging have shed lights on it (Deutschländer et al. 2002; Keshavarz, Riecke, et al. 2015; Zhang et al. 2015). Moreover, in support to theory assumptions on the processing of sensory input, several recent animal studies have added new evidence by pinpointing the cerebellum and vestibular nuclei neurons that selectively response to passive motion but not motion anticipated by internal models (Angelaki and Cullen 2008; Cullen 2012; Oman and Cullen 2014). Nevertheless, human brain activity is far more complicated even only under visual stimulation. We still do not have a clear idea about how inconsistent sensory inputs lead to neural mismatches, not to mention to locate the neural mismatches that responsible for MS.

What complicate the situation might be the nature and ability of human brain to coordinate and integrate sensory information, even when the sensory input is in conflict with each other. For example, according to Brandt’s theory, visual and extra-visual modalities tend to interact with each other in a reciprocal inhibition manner to reduce the sensory conflicts (Brandt et al. 1998, 2002). As the susceptibility to MS under the same physical stimulation varies a lot in the population (Golding 1998, 2006), it is highly possible that what is crucial in triggering

MS is not the external motion stimulation, but how those motion information is perceived and processed by each individual.

Lack of screening on VIMSS

In the case of VIMS, vection provoking stimuli is usually presented to stationary viewers for a prolonged period, thus visual input is continuously in conflict with other senses (Brandt et al. 1998; Dichgans and Brandt 1978; Reason 1978). These conflicts, if accumulated, should cause VIMS among susceptible individuals, while individuals who are resistance to VIMS should be capable to coordinate and resolve sensory conflicts between visual and extra-visual modalities.

Therefore, previous works which focus on exploring neural covariates for the vection-inducing stimuli (Braddick et al. 2001; Brandt et al. 1998; Deutschländer et al. 2004; Dieterich et al. 1998, 2003; Indovina et al. 2005; Previc et al. 2014; Shipp et al. 1994; Uesaki and Ashida 2015), would contribute very little to theories on VIMS if the experimenter did not examine participants who are highly susceptible to VIMS and compared their response with VIMS resistant people.

Unfortunately, as the VIMSS is usually not the research interest for this track of researchers, actually no studies have reported the VIMSS of their participants, neither did they screen their participants based on VIMSS.

Confounding with VIMS symptoms

For another research track, which mainly focuses on exploring neural covariates for VIMS (MS), researchers usually present their motion sickness provoking stimulation for a very long period until they induced VIMS in participants (see Table 2.3 for summary). However, in those studies, prolonged stimulation only provoked severe nausea symptoms in susceptible participants (Farmer et al. 2015; Miyazaki et al. 2015; Napadow et al. 2013). Since visual induced nausea is linked to massive increases in cortical hemodynamic response (Le et al. 2017; Wilkins 2016), it is unable to ensure that the severe nausea symptoms in susceptible

group would not pollute the BOLD signal and introduce differences between susceptible and resistant groups. Thus, it is possible that the increased BOLD responses of brain regions (Farmer et al. 2015; Napadow et al. 2013) as well as the inter-hemispheric desynchronizations (Miyazaki et al. 2015) revealed in VIMS susceptible group are caused by VIMS symptoms, rather than the process underlie the generation of VIMS.

Therefore, in order to eliminate the interference of nausea symptoms, it is important for future work to control the severity of VIMS symptoms and avoid nausea during the procedure of collecting neurological signals.

Confounding with cognitive states

In order to isolate the cortical coordination associated with VIMSS, there is another important confounding factor that needs to be measured and controlled, that is, the sensation of vection. As introduced in **section 2.1.1**, the onset latencies of individuals vary (Chen, Chow, and So 2011; Keshavarz, Riecke, et al. 2015), and could be different between VIMS resistant and susceptible group.

The onset of vection might indicate a different stage of sensory integration that our inner model has updated toward visual input, and indeed demonstrate different patterns of neural activities in former findings (Kleinschmidt et al. 2002; Stróžak et al. 2016; Thilo et al. 2003). Unfortunately, in this track of previous studies working on VIMS/MS (Table 2.3), no study reported the vection perception of their participants, neither did they verify whether the vection experienced by their VIMS susceptible and resistant group are different or not.

Hence, it is necessary for future works to compare the stage before and after onsets of vection and control it between VIMS resistant and susceptible groups, to ensure that differences between the two groups are not simply caused by their different vection perception stage. As the vection perception changes dynamically in a short time scale, looking for indicators with higher time resolution is the crucial challenge.

Limitation of localizing methodology in approaching VIMS

Most former studies have focused on the localization of VIMS associated brain areas. They identified local BOLD signals or EEG oscillating components correlated with VIMS ratings (Chen et al. 2009; Chuang et al. 2016; Napadow et al. 2013), or searched for cortical areas showing differential responses between VIMS susceptible and resistant groups (Farmer et al. 2015). However, little has been reported on the coordination map between cortical regions for groups of different VIMS susceptibility, and how this map changes in space and time under the visual stimulation that potentially causes VIMS. Miyazaki et al. (2015), as the only exception work, restricted their exploration to the inter-hemispheric synchronizations within visual sensitive cortices.

VIMS is believed to be associated with very complicated cortical interaction where plenty of previously identified functional areas are involved (Brandt et al. 1998, 2002; Miyazaki et al. 2015). For instance, as intact vestibular apparatus is one of the prerequisites for MS generation (Lackner 2014; Zhang et al. 2015), vestibular signal processing and vestibular cortex are revealed to be closely related to VIMS/MS. While no particular primary vestibular cortex is found, the cortical areas that receive vestibular afferent are actually broadly distributed in somatosensory, premotor, posterior parietal cortex, precuneus, temporal-parietal junction cortex and insular lobe (Lopez and Blanke 2011). What's more, since visual-vestibular interaction is widely accepted to be the major conflicts existing in VIMS provoking environments (So and Ujike 2010), visual motion perception and optic-flow related areas (V6/V6A, MT/V5, MST) should also play an unneglectable role in the neural mismatch generation. In addition, many studies have revealed that activities or lesion in emotion and memory associated areas such as the hippocampus (Uno et al. 2000) or anterior cingulate cortex (Napadow et al. 2013) can also correlate with the severity of MS.

Table 2.3 Summary on neural covariates with VIMS and general motion sickness (MS). (For participants, the group number is demonstrated by: total=resistant + susceptible; if no number for group member, then this study only conducted correlation analysis; for visual stimuli, the FOV is illustrated by: horizontal FOV × vertical FOV; MT+: human middle temporal complex; FIC: right frontoinsula cortex; secondary (SII) and primary (SI) somatosensory cortices; ACC/PCC: anterior/posterior cingulate cortex; PFC: prefrontal cortex; OM: occipital midline; ICA: independent component analysis; mar sig.: marginal significant)

Literature (Participant numbers)	Stimuli (FOV, Duration)	Vection report	VIMS/MS covariates	
			Positive	Negative
Chelen et al, 1993 (10,correlation)	Yaw rotating chair+ head tilts (5-15min)	-	delta/theta band EEG power	-
Miller et al., 1996 (no report)	vestibular stimulation (side-to-side head movements during yaw-axis rotation) or ingest ipecac syrup	-	inferior frontal gyrus	-
Chen et al., 2009 (24,correlation)	driving simulator: visual & vestibular stimuli (full FOV, 40min)	-	EEG ICA component:	
			Parietal area	left/right motor, occipital, OM areas
Napadow et al., 2013 (24,correlation)	Vertical stripes, yaw circular rotation at 62.5°/s (150°×150°, 20min)	No	dorsal lateral PFC, FIC, SI, SII, middle ACC, premotor cortex	No found
Farmer et al., 2015 (28=11 + 17)	Landscape video, rotate at 72°/s (28.5°×16.4°, 10min)	No	left inferior PFC, middle occipital area	ACC, PCC, cuneus, lingual gyrus
Miyazaki et al., 2015 (14=6+8)	Room scene video, rotate at 60°/s + translation movement (50°×36°, 6min)	No	MT+ desynchronization	Local activity mar sig. MT+/V1
Chuang et al., 2016 (19,correlation)	virtual-reality driving environment	-	EEG components covering motor, parietal, occipital areas	-

As the process underlying VIMS might locate in a complicated network where widely distributed brain areas are involved and interact with each other, the localization methods which mainly focus on identifying isolated local brain activities becomes inappropriate. The crucial neural mechanism behind VIMS should have a higher possibility to lie in the information integration and interaction between visual and other sensory modalities, than in the activeness of one or two isolated brain areas. To better capture the issue, new solutions that can better grab the whole brain activity at a system level need to be explored.

In summary, the detail neural mechanisms underlying VIMS have not yet been clearly examined. Further explorations taking those challenges and confounding factors into account are desirable.

2.2.3 Factors affecting VIMSS

There are generally two types of factors that can affect the VIMS: a) factors related to the stimuli properties (e.g. FOV, contrast, frequency, duration); b) factors related to individual person (e.g. adaptation, individual difference (VIMSS), drugs uses) (Golding 2006; So et al. 1999). As introduced in **section 1.4**, we will focus on the VIMSS in this research.

Many demographic factors have been found out to correlate with VIMSS. Gender and age are reported to be two demographic factors, where female and children are generally more susceptible (Golding 2006; Paillard et al. 2013). Other procedure factors, including adaptation, previous similar experiences, experiment instructions (provide eye fixation or not) (Guo 2010; Ji et al. 2009), also can influence the VIMSS of individual.

As confounding factors may introduce spurious group and correlation effects, it is very important to control and balance those factors (especially age and gender) in experiment design.

2.2.4 Objective predictors for VIMSS

The most common method for assessing VIMSS is through the subjectively reported questionnaires (Guo et al. 2017). Among them, the simulator sickness questionnaire (SSQ) (Kennedy et al. 1993), the nausea rating (Golding and Kerguelen 1992) and the motion sickness susceptibility questionnaire (MSSQ) short form (Golding 1998) are the three top choices. Since both SSQ and nausea rating can only obtain after participants develop VIMS symptoms which means they cannot serve as a real predictor, in this research, we choose MSSQ-short to be a bench mark to validate our new objective predictors.

Although subjective questionnaires are popular due to inexpensive and convenience, it still relies heavily on the ability of participant to correctly assess and report they feelings. This hinders the inter-study comparison and restricts the use of VIMSS predictors among people who have difficulties in self-description and evaluating themselves. Therefore, developing objective VIMSS predictors is desirable both for academic research and industry (Guo et al. 2017; IWA 3 2005).

Among the track of developing predictors for individual MS susceptibility predictors, there are generally three directions (Zhang et al. 2015): a) measuring vestibular related functions [e.g. the vestibular-ocular reflex (VOR) (Gordon et al. 1996; Nachum et al. 2002), optokinetic after-nystagmus (OKAN) (Guo et al. 2017), caloric stimulation and vestibular-evoked myogenic potential (VEMP) (Fowler, Sweet, and Steffel 2014; Tal et al. 2013), eye blinks (Dennison, Wisti, and D’Zmura 2016)] ; b) measuring postural instability (e.g. body sway or body tilt) (Koslucher, Haaland, and Stoffregen 2016; Varlet et al. 2015); c) measuring other sense related functions [e.g. odor (Paillard et al. 2014) and taster sensitivity (Sharma et al. 2008)]. Most of those attempts are unsatisfactory due to tedious measuring procedures, low prediction power and unable to assess in many participants (e.g. high dropout rate) (see table 2.4 for a thorough summary).

Table 2.4 Pros and Cons of current and potential VIMSS predictors.

Predictors	Qualitative/ Quantitative	Type	Pros	Cons
Vestibular related functions	Qualitative	Electro-physiology	Correlated with VIMS severity	Individual variation; difficult to measure; high dropout rate ($\geq 30\%$)
Postural instability	Qualitative	Behavioral	-	Usually cannot predict VIMS/MS severity; Low prediction power
Other sense related functions	Qualitative/ Quantitative	Mainly behavioral	-	Low prediction power
EEG	Qualitative/ Quantitative	Mainly cortical	Multi-dimensional; portable; inexpensive; Correlated with VIMS severity	<u>Limited exploration; pollution of nausea symptoms; no control on vection perception</u>
MRI/PET	Qualitative/ Quantitative	Mainly cortical	Multi-dimensional; Correlated with VIMS severity	Expensive; importable; difficult to measure; pollution of nausea symptoms; inconsistent results

The whole brain activities, which reflecting both local activities and interaction between multiple sensory modalities might be a promising potential candidate for predicting the VIMSS. Among another track of explorations focusing on identifying VIMS cortical covariates using EEG or neural imaging methods, the local activities of many brain regions have been revealed to be correlated with VIMS (see table 2.3). However, as mentioned in **section 2.2.2**, most of those studies present prolonged stimuli until participants develop

various symptoms. Therefore, currently we are still lack of real cortical predictors for VIMS. As EEG is more portable and inexpensive than other methods to be utilized in various scenarios, this research mainly focuses on searching EEG predictors for VIMSS.

2.2.5 Current challenges

In summary, further exploring the neural covariates for VIMSS with higher temporal resolution (e.g. EEG) at a system level (e.g. network analysis), while controlling confounding factors (e.g. vection perception state, nausea symptoms) is important both for investigating the neural basis of VIMSS predictors. Detail research gaps and our solutions in this work will be described in chapter 3 (the main drawbacks with EEG are showed in bold and underlined words in Table 2.4).

2.3 Previous works on both vection and VIMSS

In fact, the track of vection studies usually tries to prevent their participants from any uncomfortable feelings or even exclude VIMS susceptible participants, while the track of VIMS studies usually does not care about the vection perception. Thus, only a few studies have reported both vection intensity and VIMS (Keshavarz, Riecke, et al. 2015). Although none of those works has clarified the relationship between the vection and VIMS, it does provide some valuable hints for future explorations.

Firstly, it has been revealed that sensation of vection is not a sufficient condition for VIMS. As introduced above in **section 2.2.3**, many other factors, including intra-individual differences, the motion profile (e.g. constant or oscillation, translation or rotation, and axes etc.) and the previous experience all have some influence on the occurrence and severity of VIMS. And it is quite possible to for people to experience vection without suffering from any VIMS (Chen et al. 2015; Diels and Howarth 2011; Hettinger et al. 1990; Keshavarz, Riecke, et al. 2015; Nooij et al. 2017; Zhao 2017).

Secondly, previous results revealed that the magnitude of vection and VIMS is not positively correlated. Conditions introducing more vection does not also lead to more severity VIMS (Prothero et al. 1999; Webb and Griffin 2003), and vice versa (Chen et al. 2011; Keshavarz and Hecht 2011). Moreover, individuals who report stronger vection do not also report stronger VIMS symptoms (Chen et al. 2015; Keshavarz and Berti 2014) or more susceptible to VIMS (Wei et al. 2018).

Finally, it is possible to develop VIMS symptoms without the perception of vection (Ji et al. 2009). Although currently only one study has explored this topic, it implies that the perception of vection might not be a prerequisite for VIMS.

2.3.1 Current challenges

All of the facts above suggested that there might be some intermediary factors between the psychical stimulation and the development of the vection and VIMS. This not only re-emphasizes the importance of exploring vection together with VIMSS, but also imposes higher requirements on exploring the dynamic development of vection perception rather than treat vection as a state attributes under certain visual stimulation. In this research, we explore more indicators with high time resolution to cope with this challenge (see **section 3** for detail solutions).

CHAPTER 3 RESEARCH GAPS AND SOLUTIONS

3.1 GAP1: Vection covariates with well-controlled confounding factors

3.1.1 Explore vection covariates by method with a higher time resolution

As introduced in **section 2.1**, the rapid variation in vection perception state requires higher time resolution on the objective measurement as vection indicator. As EEG possesses higher time resolution as compared with other neural imaging methods, we cope with this challenge by searching for EEG indicators in study two-4.

3.1.2 Explore vection covariates while controlling VIMSS

As described in **section 2.1**, one current gap in identifying vection covariates is that the confounding VIMSS of participants is not controlled. There are several ways to both control and observe the effect associated with VIMSS. In this research, we apply two approaches: 1) explore how the vection indicators vary according to VIMSS, and add them as covariates when we analyze the vection indicators; 2) separate participants into susceptible group and resistant group based on their VIMSS, and explore whether vection indicators behave differently between the two groups.

The biggest challenge of screening VIMSS is to carefully balance or control other external factors which highly correlated with VIMSS (e.g. gender, age, training and experience) of participants to avoid the interference of confounding factors. In this research, gender is balanced in all study; while age and experiences are controlled by recruiting healthy university students who are free from any vestibular diseases or experiences with large FOV video games.

3.1.3 Separate & compare vection covariates originated from CVF and PVF

As it is mentioned previously, another visual factor that needs to be controlled is the difference between CVF and PVF.

The biggest challenge of separating CVF and PVF is that we need the measures that are more dominant in one part of the visual field than other parts. Moreover, this response can be marked or differentiated from each location when we recorded the data (e.g. behavioral performances or EEG signal).

SART task

In study one, we try to cope with this challenge by testing the performance of Sustained Attention to Response Test (SART) in CVF and PVF separately (see chapter 4). As a valid and frequently used measure for sustained visual response (Dillard et al. 2014; Head et al. 2013; Van Schie et al. 2012), by varying the size and location of SART targets, its performance can reflect the sustained visual processing resource (or attention resource) assigned to a particular visual location (Manly et al. 1999; Robertson et al. 1997). This property is very useful for experimenter to separate and compare the visual response originated from different visual locations (PVF vs. CVF). Moreover, SART can be conducted superimposed on other visual stimuli (Dillard et al. 2014), and hence it is applicable to be assessed while participants are also exposed to vection-inducing stimulation. Finally, performance in SART is measured by response time and accuracy (Manly et al. 1999), which can be obtained from quick and simple paradigms (Manly et al., 1999; Robertson et al., 1997).

During a typical SART, a series of targets would appear sequentially within an uninterrupted time period called a 'block' (usually shorter than 5 min). Within each block, the presence of each target is called a trial. For each trial, the time period that a target preserves on the screen after its appearance is called the trial duration. The inter trial interval (ITI) in this research is defined as the time period between the presence of two consecutive targets. To conduct SART, subjects should respond to a common target (e.g. red disc) and withhold their

response to a rare target (e.g. green disc). Figure 3.1 shows the typical procedure of two consecutive trials in SART.

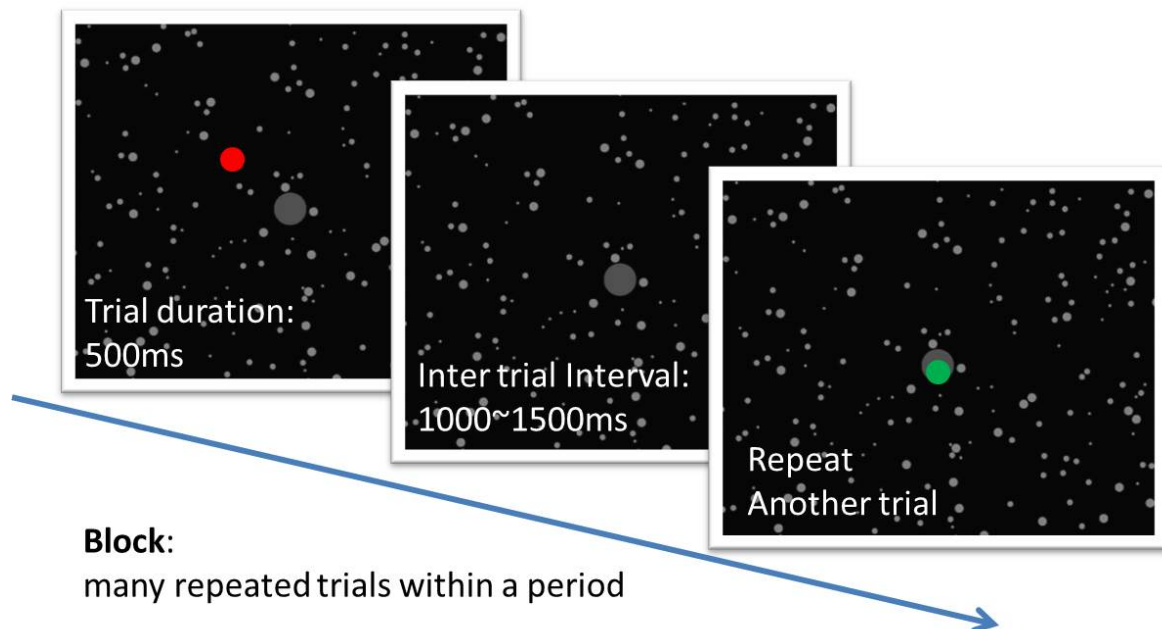
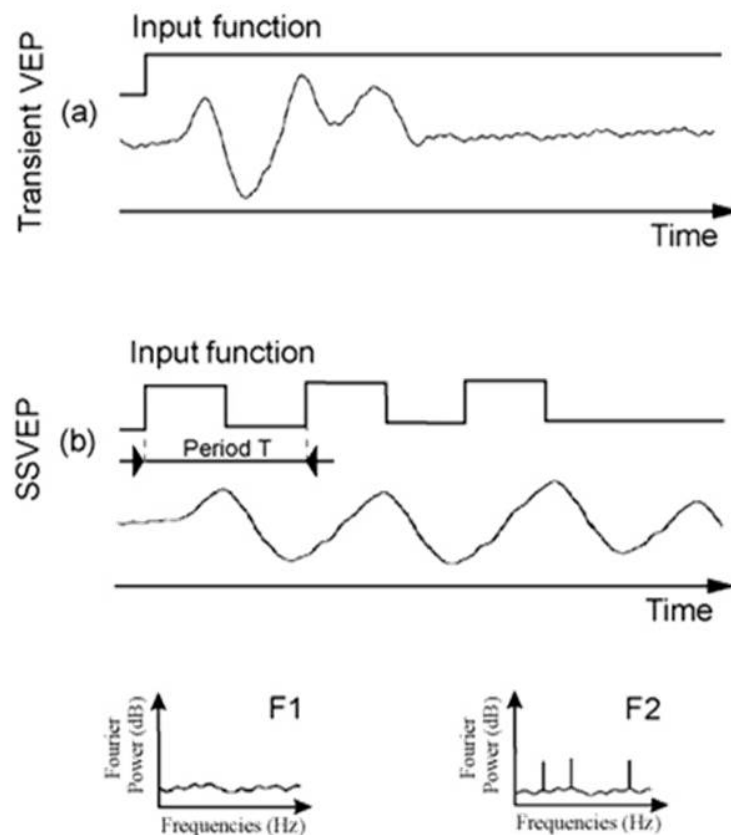


Figure 3.1 Procedure a typical SART used in this research. (In this illustration, the trial duration of targets is 500ms, while the inter trail interval is randomized from 1s to 1.5s. A red disc shows up in the first frame as an illustration of target presentation in PVF. A green disc shows up in the third frame as an illustration of target presentation in CVF. Note that the ratio of screen and target size is not according to real parameters, since the sizes of targets have been exaggerated for illustration)

SSVEP and frequency tag

In study three, we explore another solution by utilizing the properties of VEP. We explore the possibility of using different frequencies of flickering stimuli to mark specific visual location and extract the visual response information from SSVEP energy at different frequencies respectively (see chapter 6).



Francois-Benoit Vialatte et al., 2010

Figure 3.2 Comparing SSVEP and transient VEP (This is an illustrations obtained from Vialatte, F. B., Maurice, M., Dauwels, J., & Cichocki, A. (2010). Steady-state visually evoked potentials: Focus on essential paradigms and future perspectives. *Progress in Neurobiology*. <http://doi.org/10.1016/j.pneurobio.2009.11.005>)

As introduced above in **section 1.7**, the SSVEP reflect the sustained response of visual system under repeated periodic visual stimulation. Compared to the commonly adopted transient VEP that reflected a single sudden perturbation to the visual system, the SSVEP possess many advantages: a) more resistant to EEG artifacts (e.g. eye movement, which is the biggest concern under vection-inducing stimulation); b) when adopted as a measurement, it preserves higher signal to noise ratio; c) the SSVEP can be clearly observed in frequency

or time-frequency domain, with local peaks at the specific frequency of visual stimulation and its 2nd harmonic; d) the processing emphasis of visual system can be reflected by the peaks in frequency domain that correspond to stimuli frequencies (Camfield et al. 2012; Keil et al. 2005; Müller et al. 1998).

With all of the merits above, we can record SSVEP and tag different visual locations (PVF and CVF) with stimuli flip at a different frequency. Then, by analyzing the SSVEP response in frequency domain we can better separate and compare the visual responses that originated from different visual locations (see detail in chapter 6).

Separate task triggers and optic flow in PVF

Another challenge of this issue is that under the vection-inducing stimulation, the optic flow which triggered vection is also presented to PVF. So if we apply additional response measures or evoker in PVF to examine vection covariates, it is often blended or interfered with the processing of optic flow in PVF. In study one, we use series of experiments with restricted stimuli FOV to separate the optic flow and task targets (see detail in chapter 4). Moreover, in study three, we try to implement SSVEP trigger and optic flow in different domain to reduce the interference between them: optic flow is perceived by participants in time domain with rather slow changes (rotating velocity: 32°/s, frequency<0.1Hz), while SSVEP trigger is the flip of the contrast in PVF at higher alpha band frequency (12Hz).

3.1.4 Explore vection covariates with synchronization method and network analysis

The last research gap we aim to bridge in vection studies is the utilization of synchronization method and network analysis. As introduced in **section 2.1**, traditional localization methods may not capable to capture the dynamic interactions between multi-modalities and central integration on the perception of self-motion. In study four, we try to cope with this challenge by exploring the phase synchronization of EEG signals and the dynamics of network properties based on graphic metrics.

EEG Phase synchronization

EEG demonstrates excellent temporal properties and has been proved to be particularly useful in addressing temporal relationships among brain areas (Kawasaki, Kitajo, and Yamaguchi 2010). It is supported that the dynamic links of cell assemblies serves for a particular function can be reflected by EEG oscillations, while multi-functional interaction and integration can be reflected by large-scale synchronization of EEG rhythms (Murray et al. 2018; Varela et al. 2001). Hence, by probing into the phase synchrony of EEG oscillations under vection-inducing stimulation, we can capture new connectivity-based neural covariates for vection.

Graph theoretical analysis

With the growing of connectivity researches and the explosion of data in brain network modelling, the newly introduced graph theory is a very promising approach owing to its simplified and powerful capability in quantifying the topological organization with the language of math (Bullmore and Sporns 2009; Fornito, Zalesky, and Breakspear 2013; He and Evans 2010). Since graph theoretical analysis can serve as a perfect method in better qualifying and indicating the network differences at the system level, it can be used to reveal the differences in dynamic connectivity network organization between different VIMS groups. In particular, we will adopt the node degree and node density to evaluate the dynamic network properties in this research.

3.2 GAP2: Objective predictors for VIMSS

3.2.1 Explore objective VIMSS predictors (without making participants sick)

As described in **section 2.2**, one gap in VIMS research is the lack of control on confounding nausea symptoms. Moreover, for the research track of predicting VIMSS, we are still lack of good objective VIMSS predictors that are able to indicate the susceptibility of participants without the prerequisite of observing VIMS symptoms.

Thus, exploring new objective (EEG/behavioral) indicators that correlated with current benchmark of VIMSS predictors (e.g. MSSQ-short) with meticulously controlled VIMS symptoms would contribute to the bridge of both two gaps. The biggest challenge for this target is the control of symptoms in VIMS susceptible group, as they tend to experience more serious nausea symptoms when exposed to same physical stimuli as compared with VIMS resistant group. In all of our following studies, we cope with this challenge by presenting very short periods of vection-inducing stimulation (less than 5 min) with sufficient rest between repetitions to avoid nausea and any other unpleasant feelings. The symptoms are monitored by pre-/post questionnaires (SSQ) and self-report of participants throughout the experiments.

Moreover, we also collect, assess, compare and rank all of the potential VIMSS predictors obtained in our studies to provide an overview picture for the quality of our new VIMSS predictors (see Chapter 8).

3.2.2 Explore VIMSS predictors while controlling the perception of vection

Another gap in VIMS research is the lack of control on confounding cognitive states (vection perception). To bridge this gap, there are two biggest challenges: 1) the record of vection state; 2) indicators with higher time resolution as the vection state changes dynamically.

Since in this research, we explore objective covariates for vection and VIMSS together, our study design would be capable to handle these two challenges naturally.

3.2.3 Separate & compare VIMSS predictors originated from CVF and PVF

3.2.4 Explore VIMSS predictors with synchronization method and network analysis

Similar to the track of vection studies, the separation of CVF and PVF was almost missing in the exploration of VIMS studies. Moreover, most of previous VIMS studies focus on the use of traditional localization methods. The biggest challenge of coping with those two gaps is also similar to the explorations on vection. Therefore, the methodologies and measurements introduced in **section 3.1.3** and **3.1.4** also apply to the exploration on VIMSS predictors.

Procedures of all experiments are approved by the university ethics committee and performed in accordance with the Declaration of Helsinki. All of subjects were recruited in HKUST campus by advertisements post on the Clear Water Bay BBS with full consent regarding the procedures and purpose of our experiments. Note that as we focus on the health university students in this research, therefore all of our conclusions shall be constrained to this targeted group. Researchers need to be cautious when addressing other demographic groups in the population (e.g. children, elderly, etc...), as more validations are needed. As our targeted group is restricted to healthy university student, the sample size of all experiments (N: 14~27) are chosen based on the validation and suggestions from previous works on the methodology of EEG (Luck 2005), as well as the sample size adopted in previous EEG studies focus on vection (Barry et al. 2014; Keshavarz and Berti 2014; Thilo et al. 2003; Tokumaru et al. 1999; Vilhelmsen et al. 2015) and motion sickness (Chelen, Kabrisky, and Rogers 1993; Chen et al. 2009; Chuang et al. 2016).

CHAPTER 4 STUDY ONE – PERFORMANCE OF BEHAVIORAL VISUAL TASKS UNDER VECTION- INDUCING STIMULATION

4.1 Introduction

To explore the performance of behavioral visual attention tasks under vection, this study test SART under the roll vection-inducing stimulation among participants with various degrees of VIMS susceptibility. We presented a coherent rotating dot pattern to introduce roll vection and examined the changes of SART performance in the PVF and CVF during vection. In Experiment 1a (Exp.1a), static targets were used for SART, while in Experiment 1b (Exp.1b) we adopted targets rotating at five different speeds to further examine the properties of the effects of the regulation under vection-inducing stimulation. Furthermore, to further explore the effect of task guided attention allocation on vection perception and to better guide VR applications, the Experiment 2 (Exp. 2) was conducted to explore whether subjects can be trained by visual tasks to regulate their visual response in CVF and PVF separately, and how the vection perception was affected. The result of study one was published in *Ergonomics* 2018 (see Appendix A).

4.2 Experiment 1a

4.2.1 Hypothesis

As introduced in chapter 2, Brandt extended and complemented the sensory-conflict theory by introducing a conflict-reducing mechanism, the reciprocal inhibitory interaction between the visual and vestibular systems (Brandt et al. 1998, 2002). This mechanism facilitates negative regulation on the vestibular system and positive regulation on the visual system during vection resulting in an effective reduction of conflicting self-motion neural signals. Accordingly, individual VIMS susceptibility should depend on the strength of visual-

vestibular reciprocal regulation of the person. Therefore, we expect the visual response regulation during vection to vary according to individual VIMS susceptibility.

Moreover, as explained in chapter 1&2, the peripheral vision contributes more to self-motion perception than central vision. Hence, the regulation on visual response is expected to be mainly directed toward self-motion cues in the PVF. We hypothesized that the influence of visual response regulation measured by SART performance in the presence of vection depends on whether the visual targets are in the PVF or CVF (H1). In particular, we expect the SART performance in the PVF shall be improved with vection (H1a) and weakened in the CVF (H1b). Moreover, as the regulation of visual response is supposed to be a part of the ‘sensory conflict’ reduction mechanism, the magnitudes of individual effect measured by SART performance during vection would vary depending on VIMS susceptibility (H2).

4.2.2 Methods

Participants

Fourteen right-handed university students (8 male and 6 female; Age range: 19-27, mean 23.31, SD 2.02), with 20/20 (or corrected) eyesight and normal color vision, were recruited with complete informed consent (see Appendix D for the template example). This group of participants exhibited a large variation in VIMS susceptibility [measured using the Motion Sickness Susceptibility Questionnaire (MSSQ) Short-form; see Golding 1998], which in general follows the percentile distribution in the population (See Appendix F). All participants are free of any vestibular injury or medical treatment. None of them were heavy video game players or had rich experience with large-screen visual motion stimuli.

Apparatus and stimuli

Grey dots (luminance: 0.27cd/m^2 ; contrast: 58.8%; FOV diameter: 0.5~1.3) were randomly generated on a black background (luminance: 0.07cd/m^2) to provoke roll vection. The stimuli were presented using a 46-in LCD monitor (Screen size: $102.1\times 57.5\text{cm}$; FOV: $93.5^\circ\times 61.8^\circ$; View distance: 48cm). To investigate the visual response regulation associated with

vection rather than local motion or visual complexity, two types of stimuli were designed: coherently rotating stimuli (CRS) and incoherently rotating stimuli (IRS). For CRS, all dots rotated anticlockwise coherently around the center of the LCD screen at $32^\circ/\text{s}$. For IRS, each dot had a different center of rotation and the dots were randomly distributed inside a central window (size: 33.3° of FOV). They had the same angular velocity ($32^\circ/\text{s}$) as dots in CRS and the radius was similarly distributed. During the whole experiment, the dot pattern was randomly distributed on a canvas larger than the screen window, with 600~650 dots visible during each moment. Parameters of stimuli were chosen based on our pilot study and previous findings (Chen et al. 2015; Zhao 2017). The visual stimuli were programmed with Matlab incorporated with Psychtoolbox-3.

A grey disc (FOV size: 5°) was presented at the center of the screen as the fixation marker. All participants were trained to fix their eyes on the disc to suppress optokinetic nystagmus (OKN) (Ji et al. 2009; Wyatt et al. 1995) and control other types of eye movement. Eye movement was monitored using an eye tracker (Eyetechnology, TM3) in a separate session to ensure that participants were capable to keep their eyes on the fixation marker during the experiment block for most of the time.

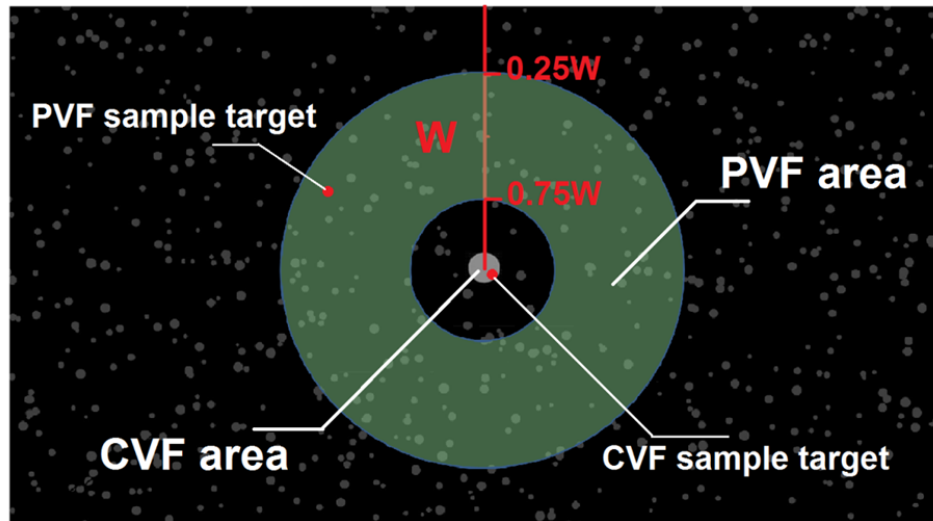
Procedures

As introduced in section 3.1.3, the commonly applied SART paradigm (Manly et al. 1999) was used to explore the regulation on behavioral visual performance during vection in the PVF and CVF respectively. In this study, for each trial, one target (red/green disc, randomized at a ratio of 4/1) was presented on the screen and kept static for 500ms. The interval between two successive trials was randomized in the range 1000~1500 ms so that subjects would not be able to predict the appearance of a target. Subjects were instructed to press a response button as soon as they saw the red disc and do nothing when the green disc appeared. The SART performance of subjects under CRS and IRS conditions was examined. To compare the effects in the PVF and CVF, targets would randomly appear either inside the foveal central area (FOV: $0\sim 2.1^\circ$) or in the peripheral area (FOV: $7.9\sim 24.9^\circ$; see Figure 4.1a)

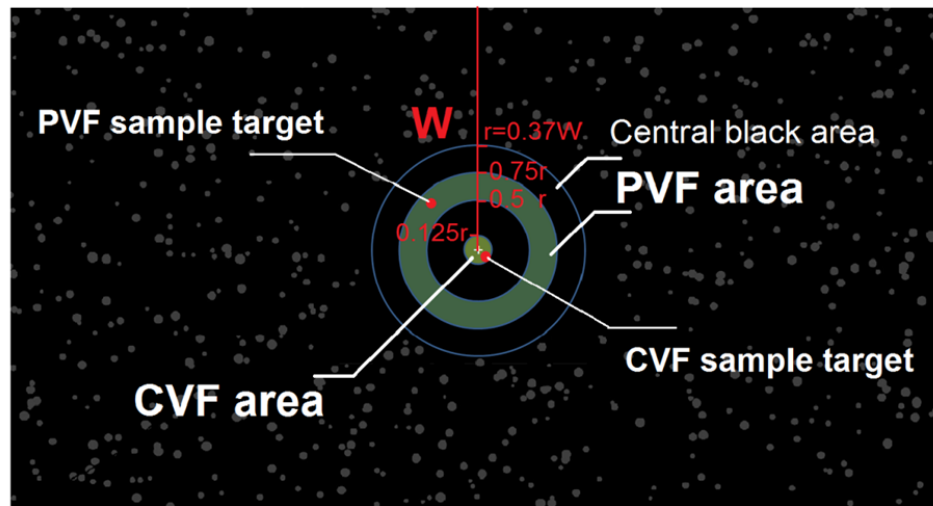
(O'Connell et al. 2017; Webb and Griffin 2003). Total 200 trials were divided into two blocks. In each block, fifty repetitions of the SART trial were conducted for each type of target location (CVF and PVF) under one type of stimulus condition (CRS or IRS). Types of target location were randomized in each block (half CVF and half PVF), while the order of blocks was randomized for subjects.

All subjects received sufficient training on SART and vection onset judgement before taking part in the actual experiment. Throughout the whole experiment, subjects were required to conduct the SART with their left hand, while pressing another vection report button with their right hand to indicate a change in their perception state (i.e. whether experiencing vection or not). SART Trials completed under CRS during the period of vection perception were kept as valid vection trials, while trials completed under IRS during the period of no vection perception were kept as valid control trials. Similar to previous studies, trials conducted within 2 s of a change in perception state were excluded to eliminate the influence of an intermediate state (Kleinschmidt et al. 2002). Total percentage of valid trials was over 88% with no significant differences across blocks. To validate the manipulation of vection strength in the two stimulus conditions (CRS vs. IRS), subjects were trained to report vection intensity after each block based on a 5-point vection magnitude scale revised from previous studies (1=no vection; 5=saturated vection; Webb & Griffin, 2003). To ensure SART performance was not impeded by VIMS symptoms, the block exposure time was kept short (<3 min) with sufficient rest between blocks. We used a chinrest to restrict head and body movement. To reduce environmental influences, ceiling lights were switched off, earplugs were used, and a black curtain was used to cover the monitor and the head of subjects.

a. Exp.1a & Exp.2



b. Exp.1b



Scale: \square 2.1cm = 2.5° of FOV

Figure 4.1 Illustration of the stimuli and target positions for study one. (W indicates the half length of screen vertical width; r indicates the radius of central black area in Exp.1b; Green shadow is only for illustration of CVF/PVF areas and was not presented in actual stimuli; target diameter is 0.53 cm in Exp.1a and 1.06 cm in Exp.1b; target luminance: 5.86 cd/m^2 for red disc and 10.80 cd/m^2 for green disc)

Dependent measures

Response time (RT) of each type of condition was calculated by averaging corrected valid responses made within 200ms~1500ms after the onset of target. The accuracy of each condition was calculated by dividing the number of corrected responses by the total number of valid trials (correct response: press button for red target; no response for green target). VIMS susceptibility data of all participants were assessed using Motion Sickness Susceptibility Questionnaire (MSSQ) Short-form (Golding, 1998), which has been widely adopted and shown to be a proper indicator of VIMS susceptibility (Zhao 2017). The score of the child scale and that of the adult scale were calculated, while adding up the two scores yielded the total score.

4.2.3 Results

A repeated-measures MANOVA (RMANOVA) was conducted for each of RT and accuracy, with vection (vection or control trials) and visual location (CVF or PVF) as within-subject factors and individual MSSQ-Short scores (MSSQ_C for the child scale and MSSQ_A for the adult scale) added as two covariates in the model. Interaction effect of vection \times location was found to be significant both for RT [$F(1,11) = 16.715, p = 0.002$] and accuracy [$F(1,11) = 22.204, p = 0.001$], showing different patterns of performance for the PVF and CVF during vection from those of the controls (supporting H1; see Figure 4.2a). Moreover, the interaction terms of vection \times MSSQ_C [$F(1,11) = 7.614, p = 0.019$] and vection \times location \times MSSQ_A [$F(1,11) = 4.919, p = 0.049$] were also significant for RT (supporting H2). For all comparisons, significant changes in RT were found to be in accordance with accuracy, which ensures the effects were not due to a speed-accuracy trade off. Also, the main effects of location were significant both for RT and accuracy ($p < 0.001$), where subjects generally reacted more quickly and accurately in the CVF than the PVF.

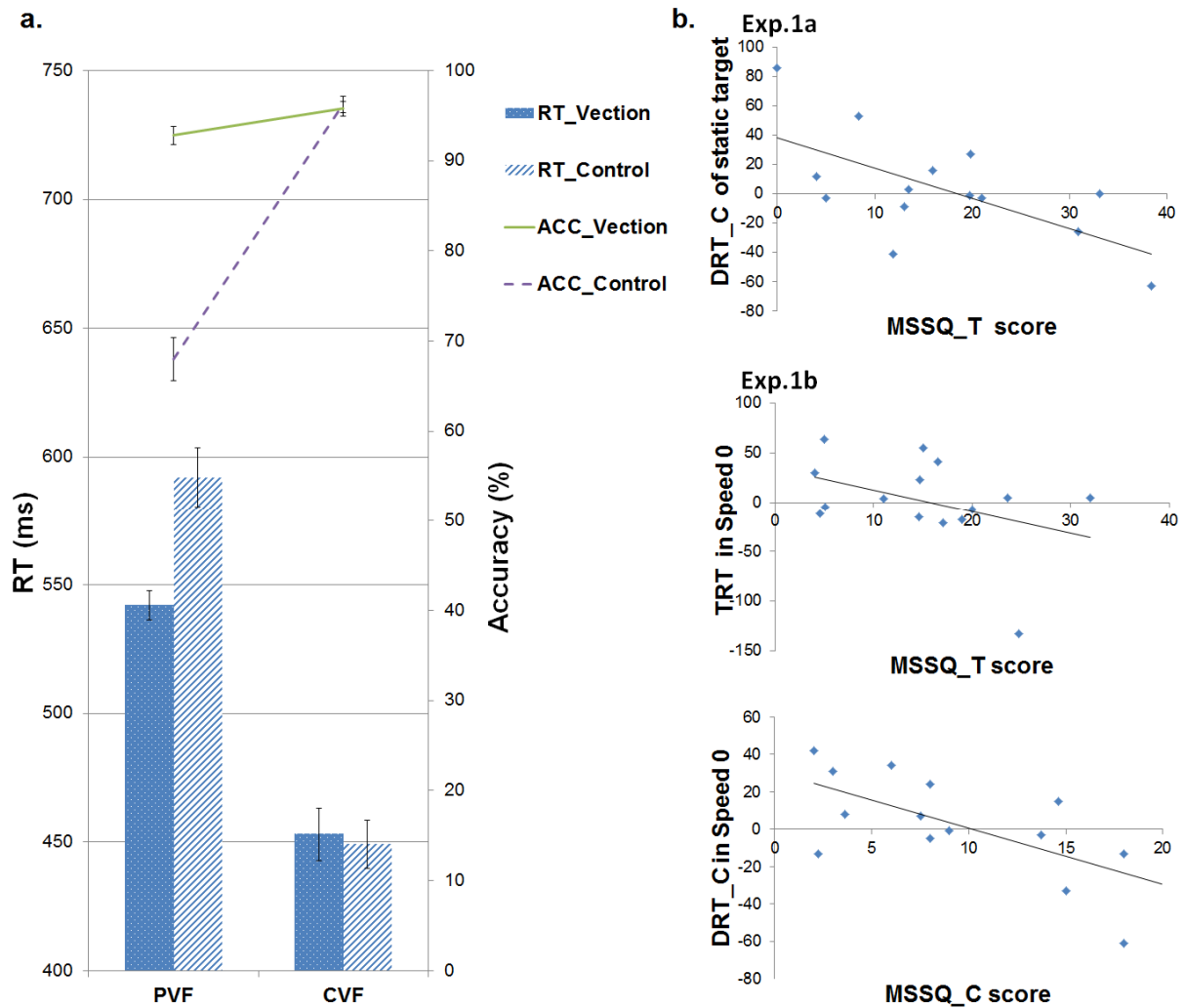


Figure 4.2 Effects of visual response regulation reflected in Exp. 1a and Exp. 1b and their correlation with MSSQ scores illustrated in scatter plots. a. Interaction effect of vection and visual location on SART performance in Exp.1a; note that the effect direction of RT in CVF is subjected to individual MSSQ scores (see Figure 4.2b); ACC=Accuracy; *_vection=averaged from vection trials in CRS condition; *_control=averaged from control trials in IRS condition; b. Correlation of RT effects and MSSQ scores illustrated by scatter plots; MSSQ_T=MSSQ total scale; MSSQ_C=MSSQ child scale; TRT=total effect; DRT_C=delay of RT in CVF

Effects in the PVF

In the PVF, further simple effect analysis showed that SART performance was improved withvection, both for RT [$F(1,11) = 3.628, p = 0.083$] and accuracy [$F(1,11) = 11.0, p = 0.001$] (supporting H1a). Note that the simple mainvection effect of RT is only marginally significant, possibly due to the significant interaction betweenvection \times MSSQ_A [$F(1,11) = 4.884, p = 0.049$], which showed a larger RT improvement for subjects with smaller MSSQ_A scores (supporting H2). No significant interaction term was found for accuracy.

Effects in the CVF

In the CVF, the RT performance in the SART was impaired duringvection [$F(1,11) = 8.895, p = 0.012$]. Moreover, not only the magnitude but also the direction of the CVF effect was different from those of the PVF effect (see Figure 4.2a, supporting H1b). The interaction term ofvection \times MSSQ_C [$F(1,11) = 7.691, p = 0.018$] is also significant, which suggests a larger delay in response for subjects with smaller MSSQ_C scores (support H2). No significant effect was found for accuracy.

Correlation of effect magnitudes and MSSQ scores

Since the interaction between SART performance and MSSQ was only found for RT, we focused on RT and further analysed whether individual RT changes are correlated with MSSQ scores. To quantify the magnitude of individual effect in the PVF, a decrease in RT in the PVF (DRT_P) was calculated as RT (ms) of controls minus the RT duringvection. Note that effects in the CVF are opposite to effects in the PVF, so we used the delay in response in the CVF (DRT_C), calculated as the RT duringvection minus the RT of controls, while the total RT effect (TRT) was calculated by subtracting the DRT_P from the DRT_C (Note that the direction of peripheral and central effect is in opposite). Pearson correlations between MSSQ-Short scores (total, child and adult scales: MSSQ_T, MSSQ_C, MSSQ_A; a higher score indicates a higher VIMS susceptibility; see Golding, 1998) and the indicators of effect

magnitude (DRT_P, DRT_C and TRT) were negative (see Table 4.2 for coefficients and p-values; see Figure 4.2b for scatter plots).

Vection and nausea report

Reported vection intensity and duration were significantly stronger and longer under CRS than IRS (See Table 4.1). No participants experienced nausea, vomiting or other severe discomfort.

Table 4.1 Vection report in Experiments 1a and 1b

Vection Indicators	Exp. 1a			Exp. 1b		
	CRS	IRS	T/Z-value*	CRS	IRS	T/Z-value*
Intensity	2.54	1.50	4.315	2.62	1.76	6.194
	(0.96)	(0.52)	(p=0.001)	(0.40)	(0.62)	(p<0.001)
Duration#	8.83	0.72	15.116	7.12	2.54	6.314
	(1.30)	(1.15)	(p<0.001)	(1.99)	(2.68)	(p<0.001)
Occurrence Ratio[^]			2.449			2.236
	14/14	7/14	(p=0.014)	15/15	10/15	(p=0.025)

* Paired T-test was conducted for intensity/duration; Wilcoxon signed-rank test was conducted for vection occurrence, with Z-value reported. [^] The occurrence ratio represents the number of subjects reporting vection to the total number of subjects. [#] For Exp. 1a, vection duration was calculated as the length of vection time period divided by the total length of time and transformed into an 11-point scale (see Exp. 1b) to facilitate comparison.

4.2.4 Discussion

Results support hypothesis H1 that vection and visual location of targets have significant interaction effects on SART performance. More specifically, data indicate that vection perception is associated with improved SART performance in the PVF and impaired performance in the CVF. Since SART usually reflects sustained visual attention or vigilance (Manly et al. 1999), our results suggest that more attention is directed toward the PVF than the CVF during vection. This finding is consistent with a former study that reported a delayed response of the oddball task in the CVF during horizontal vection (Stróžak et al., 2016). As the total attention resource for visual information processing is limited (Kahneman, 1973; Marois & Ivanoff, 2005), assigning more resource to the PVF for processing self-motion cues could result in less resource directed toward the CVF and thus impaired performance in this field. This difference in changes during vection is consistent with Brandt's (2002) hypothesis on visual response regulation under vection-induced stimulation.

Furthermore, correlations between MSSQ scores and SART performance levels suggest that these effects vary according to VIMS susceptibility (H2). Data indicate that effect in the PVF is associated with the MSSQ adult scale, while effect in the CVF is closely associated with the child scale (Table 4.2). As the child scale can be used as a pre-morbid indicator of motion sickness susceptibility in patients with vestibular disease (Golding 1998), a closer examination of SART in the CVF might lead to useful new assessment tools for clinical consideration. Further correlation analysis showed that the magnitude of visual response regulation is greater for participants who are less susceptible to VIMS, which is consistent with Brandt's theory (1998; 2002). It is worth noting that the effects measured in the CVF showed better predictive power for MSSQ scores (DRT_P is only marginally significant), possibly because improvements in PVF performance had reached the ceiling for most of the subjects (see Figure 4.2a). In addition, as SART targets in the PVF were superimposed on the background with a random dot pattern that possessed a higher visual complexity than the central grey disc (see Figure 4.1a), the visual performance might also be affected by

background visual complexity (Caroux et al. 2013). More investigations controlling for this confounding factor are desirable.

4.3 Experiment 1b

4.3.1 Hypotheses

Experiment 1b (Exp.1b) is a follow-up experiment designed to explore in depth the characteristics of visual response regulation when different SART targets are used during vection while controlling for the confounding factors. As discussed above, it is possible that regulation on visual response is achieved by reallocating one's attention from the CVF to the task of processing self-motion cues in the PVF. Therefore, the benefits of visual response regulation in the PVF are expected to be more evident with targets moving at similar speeds to the self-motion cues (H1c), while the impairment of visual response in the CVF should affect tasks equally regardless of the moving speeds of targets (H1d). Also, as this mechanism is supposed to facilitate sensory conflict reduction, individuals with stronger effect magnitude are expected to be less susceptible to VIMS (same as H2 in Exp. 1a).

4.3.2 Method

Participants

A different group of 15 participants (9 male; Age: 20-27 years old, mean 24.6, SD 2.06) who have attained all of the requirements for Exp. 1a were recruited (see Appendix F for VIMS susceptibility distribution).

Apparatus and stimuli

Targets moving at different speeds were used in SART. Targets would appear for 500 ms and rotate around the screen center at one of five rotating speeds (0, 16, 32, 64, -32°/s; 0=static, positive value=anticlockwise). Moreover, to better control the background of targets and

reduce the interference of rotating dot pattern, a black area (occupying 0~12.5° of FOV) was adopted to separate targets from peripheral vection-provoking stimuli. All targets only appeared within the black area and a white cross was used for fixation (Figure 4.1b). The same apparatus and procedures as those in Exp. 1a were applied to present stimuli and to restrict eye, head, and body movement and other environmental influences.

Procedures

The same SART paradigm from Exp. 1a was adopted. Sixty repetitions were conducted for each stimulus condition (CRS or IRS), each target location (CVF: 0~1.4° or PVF: 6.3~9.4° of FOV; see Figure 4.1b) and each of the five target speeds. This gave 1200 trials (60×2×2×5). The trials were conducted in eight blocks (each containing 150 trials, length: 3~4 min). Repeated trials for each stimulus condition spanned more than four blocks and the combinations of target location and speed were randomized within each block. The order of blocks was randomized for each subject. The SART trial started 3 s after the vection-provoking stimulation to allow time for vection onset. To ensure performance was not affected by VIMS symptoms, participants took enough rest (3~5 min) between blocks. To reduce task difficulty for the sake of developing simple visual response regulation measures, subjects only needed to complete SART with their right hand and verbally report the duration of vection they experienced, based on an 11-point scale (0=experienced no vection; 10=experienced vection the whole time) after each block, as well as reporting the vection intensity. Reported vection intensity and duration were significantly stronger and longer under CRS than IRS (See Table 4.1).

Dependent measures

The RT and accuracy data obtained from all trials were averaged for the two types of stimulus conditions (CRS and IRS). Individual VIMS susceptibility is also measured using MSSQ-Short (Golding 1998) with two sub-scales (adult and child).

4.3.3 Results

An RMANOVA was conducted for each of RT and accuracy, with vection stimulus (CRS or IRS), location (CVF or PVF) and speed (0, 16, 32, 64, or -32°/s) as within-subject factors and individual MSSQ-Short scores (MSSQ_C and MSSQ_A) added as two covariates in the model. For RT, the interaction of vection \times location \times speed \times MSSQ_A was significant for the cubic term [$F(1,12)=5.489$, $p=0.037$] and the interaction of vection \times location \times speed \times MSSQ_C was marginally significant for the linear term [$F(1,12)=3.538$, $p=0.084$]. Due to the complicated interaction introduced by target speed, vection \times location ($p=0.090$) and vection \times location \times MSSQ_C ($p=0.098$) were only marginally significant. As in Exp. 1a, subjects generally reacted more quickly in the CVF than PVF ($p=0.001$). No significant accuracy differences were found, which ensures that no effect was due to a speed-accuracy trade off.

Effects in the PVF

Effects in the PVF diverged for different target speeds. The quadratic term of speed \times MSSQ_C [$F(1,12)=5.435$, $p=0.038$] was significant and speed \times MSSQ_A [$F(1,12)=4.139$, $p=0.065$] was marginally significant, while the cubic term of vection \times speed \times MSSQ_A was significant [$F(1,12)=5.891$, $p=0.032$]. Specifically, strong vection demonstrated significant modulation on RT for targets moving at different speeds. The simple main effect of speed was significant under CRS [$F(4,56)=3.303$, $p=0.017$, see Figure 4.3] with the shortest RT for speed 32°/s and the longest RT for speed -32°/s, while no difference was found under IRS. Figure 4.3 better illustrates the effect of vection: participants reacted more quickly when targets were moving at similar speeds to the self-motion cues (especially for speed 32°/s, which was the same speed and direction with vection-inducing stimuli that providing self-motion cues), while more slowly when targets were moving at other speeds (especially for -32°/s, which was in the opposite direction to self-motion cues). In summary, specific improvement in SART performance was found in the PVF under strong vection condition (CRS), which mainly focus on targets that were similar to self-motion cues (supported H1a).

Effects in the CVF

Similar to Exp. 1a, the vection \times MSSQ_C term is significant [$F(1,12) = 5.634, p = 0.035$]. Likewise, vection simple main effect is marginal [$F(1,12) = 4.006, p = 0.068$], showing a longer RT in vection trials than control trials. Admittedly, the pure effect of vection was anticipated to be attenuated compared with that in Exp. 1a (simplified tasks might have made it impossible to exclude mixed vection trials under CRS/IRS). To further show that the delayed RT (DRT) in the CVF was associated with vection perception, we calculated the Pearson correlation between the vection duration (VD) difference ($VD_{CRS} - VD_{IRS}$) and DRT ($RT_{CRS} - RT_{IRS}$) of subjects. Results showed that subjects experienced vection for a longer period of time demonstrating larger performance impairments. The correlations were significant for all speeds (speed 0: $r=0.689, p=0.002$; speed 16: $r=0.684, p=0.002$; speed 32: $r=0.700, p=0.002$; speed 64: $r=0.548, p=0.017$; speed -32: $r=0.502, p=0.028$). Moreover, the simple interaction effect of vection \times speed and the simple main effect of speed were not significant. In summary, general SART performance in the CVF was impaired under strong vection-inducing stimulation, regardless of target speed (supported H1b).

Interaction effects with speeds similar to those in Exp. 1a

To validate the findings in Exp. 1a, we further analyzed that the data with speeds similar to Exp.1a (also similar to self-motion cues as explain above: 0, 16, and 32°/s) included in the model. Both vection \times location [$F(1,12)=5.173, p=0.042$] and vection \times location \times MSSQ_C [$F(1,12)=7.256, p=0.020$] were significant with no speed interaction, showing the exactly same pattern as in Exp.1a.

Correlation of effect magnitudes and MSSQ scores

As in Exp. 1a, to quantify the visual response regulation effects during vection, the delayed RT in the CVF (DRT_C), decrease in RT in the PVF (DRT_P) and total RT effects (TRT) were calculated for three speeds (0, 16, and 32°/s) that showed the same pattern as in Exp. 1a. To examine the relationship between effect magnitudes and MSSQ scores, negative Pearson

correlations between MSSQ-Short scores (MSSQ_T, MSSQ_C, and MSSQ_A) and the magnitude of effects (DRT_C, DRT_P, and TRT) were tested (see Table 4.2 for coefficients and p-values; see Figure 4.2b for scatter plots).

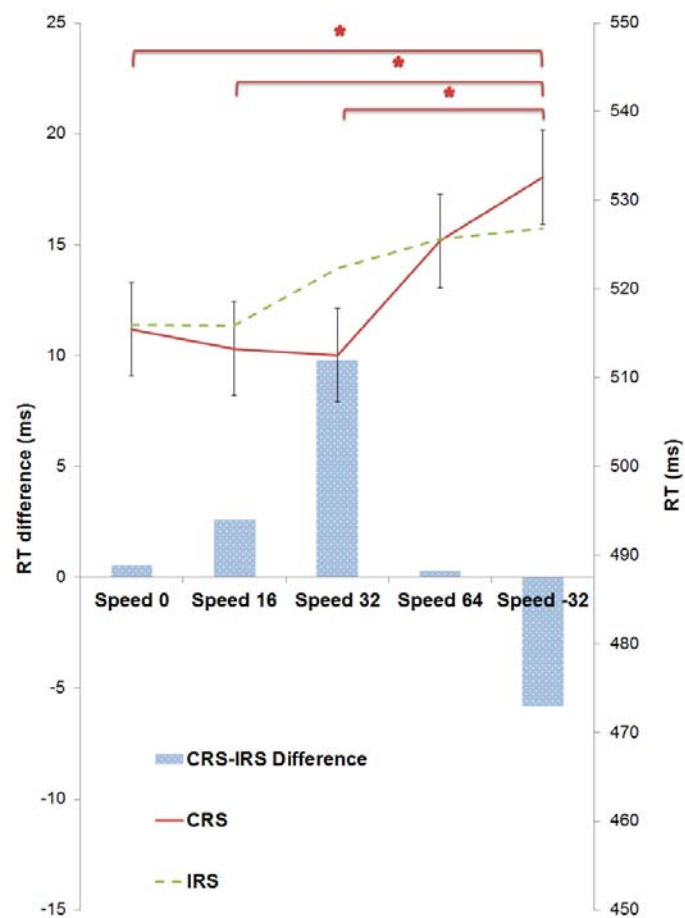


Figure 4.3 The modulation of strongvection on RT for target in PVF moving at different speed in Exp.1b (notice that there is no significant difference across all speed under IRS condition)

Furthermore, to evaluate the predictive power of effect magnitudes for MSSQ scores, we standardized and pooled the effects of static targets from all 29 subjects (including those in Exp. 1a and Exp. 1b). Three linear regression models (Model 1: central effects; Model 2: total effects; Model 3: central and total effects) for MSSQ_T and one model for MSSQ_C were tested using the stepwise method, where independent factors that contributed insignificantly were excluded (Table 4.2). Model 3 demonstrated the highest predictive power [$R^2 = 0.396$; $F = 8.535$, $p = 0.001$].

In summary, visual response regulation effects were negatively correlated with MSSQ scores, where VIMS-resistant subjects showed stronger effects than their susceptible counterparts (supporting H2).

Vection and nausea report

Reported vection intensity and duration were significantly stronger and longer in CRS than IRS (See Table 4.1). No participants reported nausea, vomiting or other severe discomfort.

Table 4.2 Correlations and regression models for visual response indicators predicting MSSQ scores.

Visual Response Indicators			MSSQ Scale Score		
Experiment	Location	Target	MSSQ_C	MSSQ_A	MSSQ_T
Exp.1a	DRT_C		-0.628* (p=0.011)	-	-0.505* (p=0.039)
	DRT_P	Static	-	-0.573* (p=0.020)	-
	TRT		-	-0.595* (p=0.012)	-0.479* (p=0.042)
Exp.1b	DRT_C	S0	-0.688** (p=0.002)	-	-0.543* (p=0.018)
		S16	-0.468* (p=0.039)	-	-0.431^ (p=0.055)
		S32	-0.527* (p=0.022)	-	-0.353^ (p=0.098)
	DRT_P	S0	-0.534* (p=0.025)	-	-0.423^ (p=0.066)
		S16	-	-	-
		S32	-0.413^ (p=0.068)	-	-
	TRT	S0	-0.468* (p=0.039)	-	-0.393^ (p=0.074)
		S16	-	-	-
		S32	-0.476* (p=0.037)	-	-0.303 (p=0.136)
Regression Model Summary					
Models	Predictors	Beta	R	R ²	F
1	SDRT_C	-0.307 (p=0.105)	0.307	0.094	2.813 (p=0.105)
2	STRT	-0.434* (p=0.019)	0.434	0.188	6.249* (p=0.019)
3	STRT	-0.575** (p=0.001)	0.630	0.396	8.535** (p=0.001)
	SDRT_C	-0.478** (p=0.006)			
	SDRT_P	Excluded			
4	SDRT_P	-0.455* (p=0.013)	0.455	0.207	7.034* (p=0.013)
	SDRT_C	Excluded			

Two-tailed p-value: ** p<0.01; * p<0.05; ^ p<0.1; S0, S16, and S32 represent the speeds of 0, 16, and 32°/s respectively. DRT correlation coefficients had controlled for individual overall RT; only marginal/significant results are included. SDRT_C, SDRT_P, and STRT represent standardized DRT_C, DRT_P and TRT respectively pooled from Exp. 1a and Exp. 1b. Model 1, 2 and 3 predict the MSSQ_T score; Model 4 (including SDRT_C & SDRT_P) specifically predicts MSSQ_C to address clinical concerns.

4.3.4 Discussion

Firstly, results of Exp. 1b confirmed the vection \times location interaction findings from Exp. 1a with 15 different subjects and with tighter control of the background visual complexity. Furthermore, results support H1c and H1d, showing a general performance impairment in the CVF and specific improvement in the processing of self-motion cues in the PVF during vection. Note that this specific improvement also ensured that PVF effects were not due to the PVF targets blending in with the rotating dot pattern, or opposite results would have been obtained. As discussed in the section on Exp. 1a above, diverging SART performance suggests the reallocation of attention from the CVF to the PVF during vection. Increasing attention assignment can increase neuron reliability of the current visual input (Martínez-Trujillo and Treue 2002; Mitchell, Sundberg, and Reynolds 2007). According to previous studies, increased visual reliability would facilitate the weight shifting from vestibular to visual modality (Fetsch et al. 2012; Gu et al. 2008), which may yield less sensory conflict between the inner model and the visual input (Brandt et al. 2002; Reason 1978) under ambiguous vection-inducing conditions. This is also consistent with former studies reporting that VIMS is worse when vection is changing (less reliable) rather than stable (more reliable) (Bonato et al. 2008; Bonato, Bubka, and Story 2005). In summary, individuals who are able to reallocate their attention may be more resistant to VIMS, while those who fail to do so may be more vulnerable to optokinetic stimulation. This may explain the correlations we identified between visual response effects and MSSQ scores.

In addition, Exp. 1b also validated the negative correlation between individual VIMS susceptibility and magnitude of visual response regulation effects (H2). Although the simplified procedure mixed vection and no-vection trials which reduced the absolute effect size that could be measured, it still revealed that effect magnitudes and MSSQ_C scores were significant correlated. Note that the use of static targets generally produced higher correlation coefficients, suggesting that this SART paradigm can be a promising candidate for VIMS susceptibility measurement. We explored the potential of static targets by pooling the results from Exp. 1a and Exp. 1b and obtained acceptable predictive power for MSSQ scores.

4.4 Experiment 2

4.4.1 Hypotheses

As the previous two experiments suggested that visual regulations on CVF and PVF is associate with VIMSS, we went on to explore whether the top-down visual regulation could be guided using a revised SART and how it interact with individual vection perception. We hypothesize that: when participants are only allowed to react to PVF targets while ignoring CVF targets, their vection experience is stronger and more stable, as compared with the vection experience when they are only allowed to do opposite reactions (response to CVF targets while ignoring PVF targets) (H3); the enhancement of vection is stronger when the PVF targets are moving at the same speed as the visual self-motion cues, as compared with the enhancement when targets are moving in conflict with the visual self-motion cues (H4).

4.4.2 Method

Participants

Thirteen of the 29 subjects who participated in Exp. 1a or Exp. 1b were invited to join Exp. 2 (7 male; Age: 19-27 years old).

Apparatus, stimuli and procedures

The same set of apparatus as that used in Exp. 1a and Exp. b was adopted. The same coherent rotating stimuli (CRS) used in Exp. 1a were presented. To test H3, two modified SARTs were used to facilitate and control visual attention allocation in accordance to conditions. Such manipulation is a common paradigm for visual attention studies (Eggemeir and Wilson 1991; Morgan et al. 1996; Müller et al. 1998). For the central-focused (CF) condition, subjects were instructed to press the response button as soon as targets appeared in the CVF, while ignoring targets appearing in the PVF. For the peripheral-focused (PF) condition, subjects were instructed to attend to the peripheral targets and ignore the central targets. The targets were all red discs (CVF/PVF ratio: 1/1). To test H4, two types of targets were

designed: Self-motion cue targets which rotated at the same speed and in the same direction as coherent rotating stimuli; and non-cue targets (targets that do not provide self-motion cues) which rotated at the other speeds tested in Exp. 1b with equal probability. Target duration, trial interval and fixation were kept the same as in Exp. 1a. A total of 12 blocks (each containing 30 trials) were conducted, with three repetition blocks for each of the four experimental conditions in a randomized sequence (factorial combinations: 2 attention conditions \times 2 target types \times 3 repetitions = 12 blocks). All subjects received sufficient training before the actual experiment to ensure their response accuracy reached manipulation requirement ($>95\%$). An eye tracker was used during the training session and throughout the actual experiment to ensure all subjects kept their eyes on the fixation circle for most of the time ($>80\%$).

Dependent measures

Subjects were required to report their vection intensity and duration after each block based on the scales used in Exp. 1b. The ratings were averaged for each condition.

4.4.3 Results

All subjects accomplished responses for the two types of targets (attended targets/non-attended) with overall accuracy exceeding 95%. The main effect of attention allocation condition is significant for vection duration [$F(1,12)=11.164$, $p=0.006$] and marginally significant for vection intensity [$F(1,12)=4.125$, $p=0.065$], with subjects demonstrating stronger and a longer period of vection in the PF condition than the CF condition (supporting H3). Further simple effect analysis showed that the vection duration was only significantly different between PF and CF when self-motion cue targets were used [$F(1,12)=7.341$, $p=0.019$], but not when non-cue targets were used (supporting H4). Admittedly, the interaction between task type (PF or CF) and target type (self-motion cue or non-cue) is not significant [vection duration: $p=0.218$; vection intensity: $p=0.425$] (Figure 4.4), possibly due to the large individual variations.

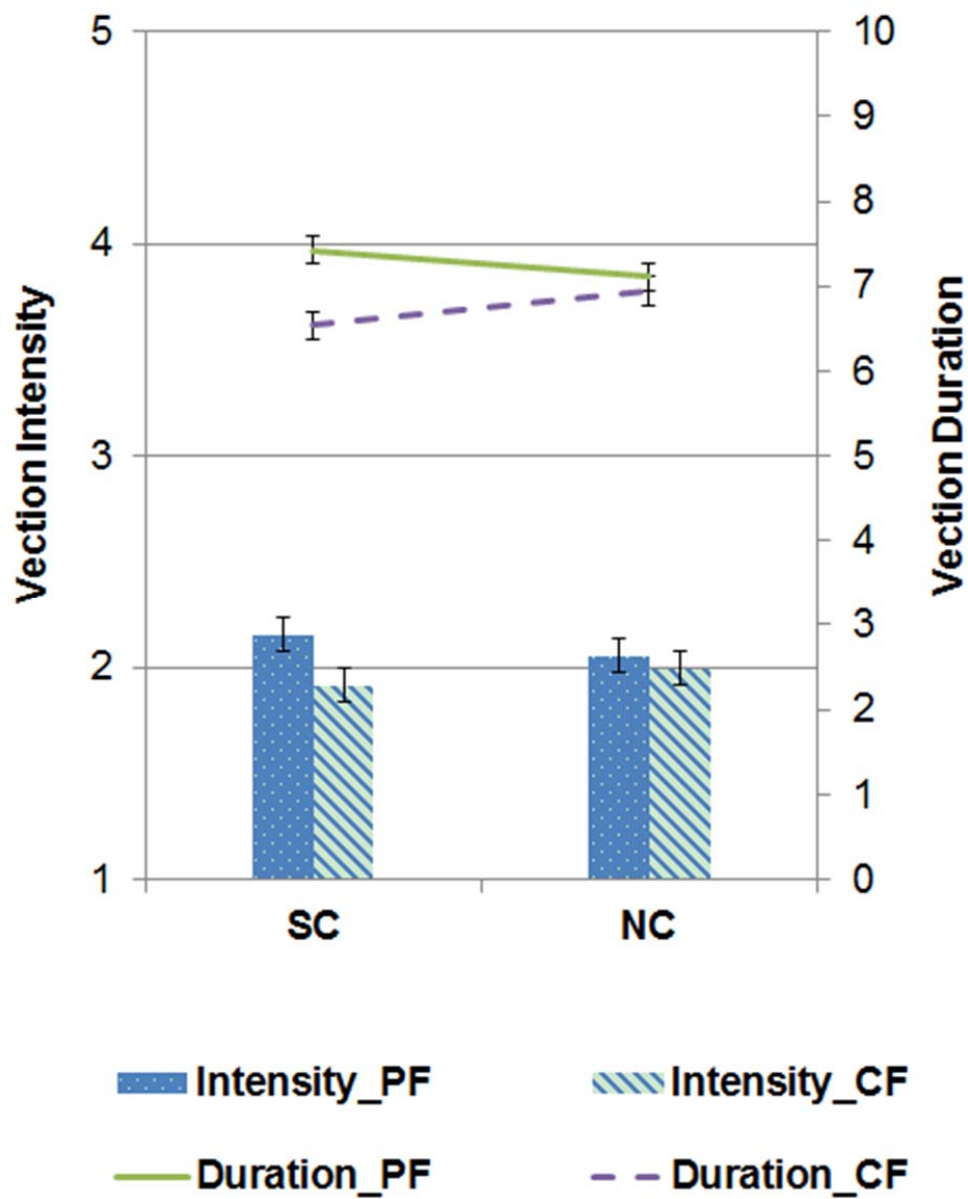


Figure 4.4 Effects of SART-guided attention reallocation on vection intensity and duration. (Task type: CF=central focused, PF=peripheral focused; Targets type: SC=self-motion cues, NC=non-cues; Vection intensity measured by self-report scale: 1=no vection; 5=saturated vection; Vection duration measures by self-rating scale: 0=no experience of vection; 10=experiencing vection all the time)

4.4.4 Discussion

This exploratory work demonstrated the promising effectiveness of SART training for attention reallocation under vection-inducing stimulation. Moreover, a more reliable and stable perception of vection was achieved during peripheral focused task, which is appealing for VR applications (e.g. video games). This suggests the possibility of redesigning visual tasks that are superimposed on a moving background to strengthen the vection perception. Moreover, this approach may also prevent VIMS, since more reliable and stable vection actually cause less VIMS (Bonato et al. 2008, 2005; Reason 1978). Future studies exploring more direct evidence with a larger group sample are desirable.

4.5 Summary

4.5.1 New findings and contributions

This study concludes that performance of visual tasks changes in the presence of vection. In particular, we find that the performance of visual tasks is impaired in the central visual field (CVF) and improved in the peripheral visual field (PVF). As discussed above, the current results and Brandt et al.'s (2002) findings on the activation of visual cortices during vection suggest that people direct more attention to the PVF and less attention to the CVF when perceiving vection. Most importantly, the effect size of this attention reallocation is negatively correlated with VIMS susceptibility. In other words, individuals who are able to shift more of their attention to the PVF are also more resistant to VIMS. The shift in visual attention may imply an enhanced reliability of visual inputs and a relative reduction of vestibular weightings in the sensory integration, which, in a sensory conflicting situation, can reduce the conflicts (Brandt et al. 2002; Bremmer et al. 2016; Martínez-Trujillo and Treue 2002) and reduce VIMS (Reason 1978).

It is worth mention that, the mechanism uncovered in this study focus on stabilizing the visual motion input, which is different from traditional perspective that aiming to attenuate the motion input. As the self-motion perception and objective-motion (viewer stationary) perception are bi-stable states during vection-provoking stimulation (Kleinschmidt et al. 2002; Thilo et al. 2003), to reduce sensory conflict based on Reason's theory (1978), it should exist two optimization directions: one traditional way is to reduce the peripheral visual motion and stabilize the stationary perception, which inevitably hurt the vection experience (Bonato et al. 2015; Golding et al. 2012; Stern et al. 1990); the other solution is to preserve the self-motion input and stabilizing the self-motion perception (at the constant speed). The phenomenon revealed in this study might be following the second direction, which can be quite promising, since it does not hurt the vection experience.

Moreover, results showed that attention re-allocation can be trained, which agreed with previous findings (Szalma et al. 2017). Moreover, our results showed that this attention re-allocation can lead to a more reliable and stable perception of vection under exactly the same visual stimuli. Since a more stable perception of vection may cause less VIMS (Bonato et al. 2008, 2005), it is possible to redesign practical visual tasks in a VR environment to reduce motion sickness while maintaining the vection experience in VR. Follow-up studies to validate and further explore the relationship between VIMS and cognitive attention reallocation are appealing.

4.5.2 Raised further questions and focus of follow-up works

One prominent attribute of explicit behavioral performance indicators is that they are general indicators reflecting the accumulated effects from a sequence of multiple basic cognitive procedures and even the motor functions (if a response button is required for collecting the performance) with one single dimension index. Therefore, the delayed response (or decreased accuracy) uncovered in CVF during vection could be result of the impairment of various basic visual procedures. With behavioral performance indicators, it is very difficult to answer the question regarding more detail procedures of visual information processing (e.g. does the

earlier visual processing functions such as contrast detection being regulated during vection? Or all the visual functions are general impaired for CVF?).

Moreover, owing to this accumulating and imprecise attribute, the behavioral indicators are susceptible to many external and internal interference factors (e.g. the motor function) which might introduce more noises and variations than more pinpointed and well-directed indicators. As we reported in study one, the changes in reaction time and accuracy can only reflect the existence of vection, but not the individual magnitude of vection intensity perceived by each participant. What's more, behavioral performances usually required the explicit response, which cost additional cognitive resources of participants and thus hinder the measurement in various scenarios. Therefore, although the SART task might serve as a rough indicator for the existence of vection, it is not very favorable to develop quantitative measures for vection with indicators simply relying on behavioral performance.

Since high dimension EEG data with good time resolution can better handle these issues, we move on and focus on explore EEG indicators in followed studies by adopting the roll-vection stimulation validated by study one.

CHAPTER 5 STUDY TWO – PATTERN-REVERSAL AND MOTION-ONSET TRANSIENT VEP RESPONSES UNDER VECTION-INDUCING STIMULATION

5.1 Introduction

To further investigate how vection shaped the basic visual responses using EEG, study two measured transient VEP under vection-inducing stimulation among participants with various VIMS susceptibility. We present the same random dots rotating pattern adopted in study one to PVF to provoke roll vection. In the meantime, checkerboard is presented to CVF with two procedure paradigms to evoke two types of transient VEP: pattern-reversal VEP (PRVEP) and motion-onset VEP (MOVEP). Peak amplitudes and peak latencies of VEP components (N1, P1, P3 from PRVEP; N2 from MOVEP) collected from occipital electrodes are explored as vection covariates respectively.

5.2 Objective and hypotheses

The objectives of this study are: 1) replicate the EEG results from previous vection study (Thilo et al. 2003) to validate our EEG set-ups and procedures; 2) explore PRVEP and MOVEP with carefully controlled confounding factors to identify proper EEG indicators for vection; 3) explore how the modulation of vection on visual responses varies corresponding to individual VIMS susceptibility and identify EEG predictors for VIMS susceptibility. Thus in study two, we focus on exploring EEG indicators mainly evoked from CVF for two reasons: 1) to follow previous paradigm and design for validation purpose; 2) it is revealed in study one that CVF effect has better prediction power for MSSQ scores.

Based on Brandt's theory (1998) and our findings in study one, we expect the visual information processing system should withdraw resource from other visual functions (e.g. contrast, object detection) to motion processing in order to facilitate the self-motion

perception. Hence, The influence of visual response regulation under vection reflected VEP components depends on the intrinsic functions and properties of VEP components (H5): the earlier VEP components, which are observed around 100ms and more responsible to contrast processing (N1 and P1 from PRVEP), shall be suppressed during vection (H5a); the N2 component, which is observed around 200ms and more closely associated with motion processing, shall be strengthened during vection (H5b). Furthermore, as it is hypothesized that this visual response regulation is part of the mechanism for sensory conflict reduction, we expected the magnitudes of regulation effect reflected by peak amplitude and peak latency of VEP components should be negatively correlated with VIMS susceptibility (H6).

5.3 Methods

5.3.1 Participants

Fourteen right-handed university students (8 male; Age: 20-27 years old, mean 23.07, SD 2.27), with 20/20 (or corrected) eyesight and normal color vision, were recruited with complete informed consent. This group of participants exhibits a large variation in VIMS susceptibility [measured using the Motion Sickness Susceptibility Questionnaire (MSSQ) Short-form; see Golding 1998] from 0-96% in percentile, which in general follows the percentile distribution in the population (See Appendix F). All participants are free of any vestibular injury or medical treatment. None of them were heavy video game players or had rich experience with large-screen visual motion stimuli.

5.3.2 Stimuli, apparatus, task and procedures

Stimuli and task

Same as study one, grey dots with exactly same parameters (luminance: 0.27cd/m^2 ; contrast: 58.8%; FOV diameter: $0.5\sim 1.3^\circ$) were randomly generated on a black background and all grey dots coherently rotated anticlockwise (angular velocity: $32^\circ/\text{s}$) to provoke roll vection. Achromatic checkerboard (occupied $29.8\times 22.6^\circ$ of FOV; contrast: 92.4%) was presented in

the central screen to evoke VEPs, while the dots pattern in PVF was either static or rotating (see Figure 5.1). Similar to Exp.1a in study one, subjects were trained to indicate their vection perception state continually under the ROT condition by pressing response buttons using right hand. In order to distinguish the effect associated with stimuli motion (STM) and the effect with vection perception (VEC), we designed two types of contrast: the stimuli-motion contrast is compared between the trials recorded when PVF dots pattern is either static (STA) or rotating (ROT), while the vection-perception contrast is compared between the trials recorded under same ROT condition but within time periods indicated by participants as different perception state (ROT during vection: RV; or no-vection: RN).

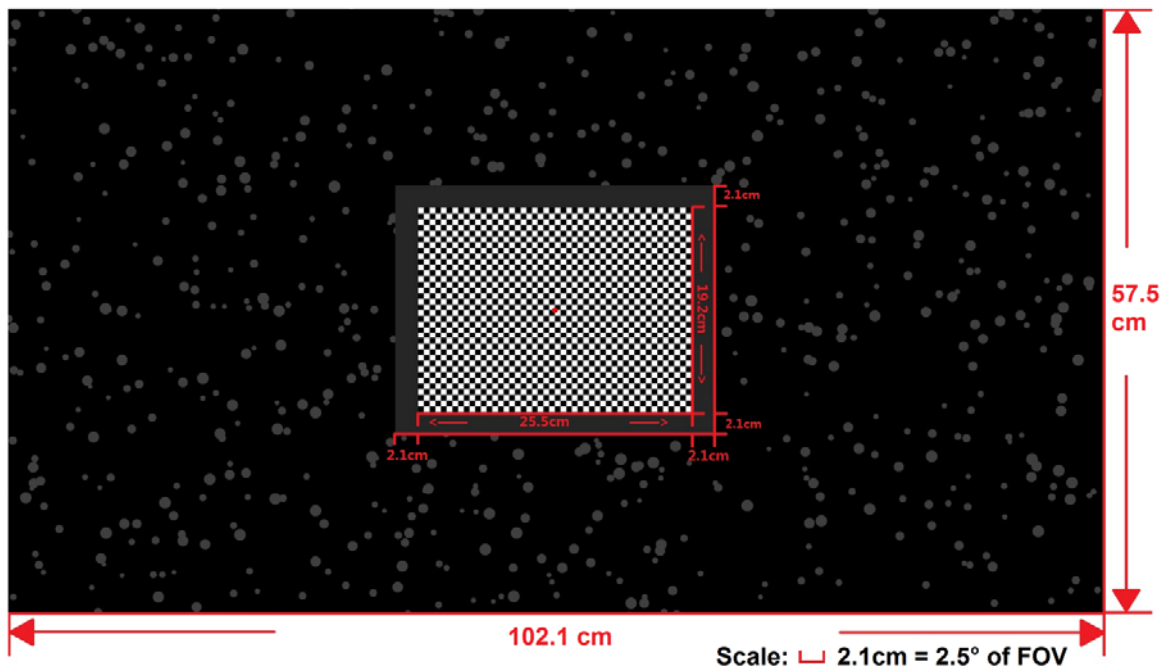


Figure 5.1 Illustration on the visual stimuli. (the averaged luminance for black cells in checkerboard are 0.70 cd/m^2 , and for white cells are 17.75 cd/m^2 , so the contrast is 92.42%; Note that checkerboard is encircled by grey bar with luminance of 0.35 cd/m^2 and width of 2.1cm; for PRVEP, checkerboard has 48×36 cells with size of 0.53cm; for MOVEP, checkerboard has 24×18 cells with size of 1.06cm which is twice larger than PRVEP cells)

Procedures

For each pattern-reversal VEP (PRVEP) trial, the black and white cells in the checkerboard flip their positions. The flipping frequency is 2Hz, so the trial length of PRVEP is 500ms. For each motion-onset VEP (MOVEP) trial, the checkerboard texture would move rightward or leftward randomly for 200ms (speed: 12.6° of FOV/s) inside the checkerboard window (the area within the grey bars) with a duty cycle of 200/1200ms, so the trial length is 1200ms for MOVEP. Both PRVEP and MOVEP had conducted for 400/1000 trials under the STA/ROT condition respectively. Trials with the same stimuli-motion type (STA/ROT) and same VEP type (MOVEP/PRVEP) were grouped into short blocks at similar length (4-5 min, see Table 5.1 for illustration on the trial numbers contained in each block and block numbers for each condition). The sequence of each block is randomized among participants with sufficient rest between successive blocks (see Table 5.1 for detail parameters). Same as study one, trials which recorded within 2s of each perception state changes (from vection to no-vection, or vice versa) were excluded to eliminate the influence of intermediate state and hand movement artifacts. All procedures were approved by the ethics committee of the Hong Kong University of Science Technology and performed in accordance with the Declaration of Helsinki.

Apparatus and EEG recording

The stimuli were presented using the same 46-in LCD monitor (Screen FOV: 93.5°× 61.8°; View distance: 48cm) with the same setups to control the head/body movement and eliminate environment visual cues as study one (Appendix B). Participants were instructed to fix their eyes on a center red dot (diameter: 0.6° of FOV) to suppress OKN and other eye movements. Visual stimuli were synchronized with EEG recording by sending TTL level triggers to the amplifier through a parallel port. EEG from eight channels (Fz/AFz/Cz/A1/A2/O1/Oz/O2, Ag/AgCl sintered, QuikCaps, Compumedics Neuroscan, USA) complying the 10-20 system (Appendix H) were recorded together with four EOG channel (for eye movement control and eye artifacts rejection). Impedances between all channels and ground channel (AFz) were kept below 5kΩ for a DC-coupled, 22 bit, monopolar amplifier (Nuamps, Compumedics

Neuroscan). All stimuli and EEG synchronization triggers are programmed by the Matlab using the Psychtoolbox-3 extensions (Brainard 1997; Pelli 1997).

5.3.3 Response measures

Subjective vection and VIMSS reports

Same as in study one, participants were trained to report their vection intensity based on a 5-point vection magnitude scale revised from previous studies (1=no vection; 5=saturated vection; Webb & Griffin, 2003; see Appendix G). The percentage of vection duration under each condition can be obtained from the response from participants. VIMS susceptibility data were assessed using Motion Sickness Susceptibility Questionnaire (MSSQ) Short-form (Golding, 1998), which included two subscale (child scale: MSSQ_C; adult scale: MSSQ_A).

EEG signal

EEG data were digitized at a sampling rate of 1000 Hz, filtered in bandpass range from 1.6 Hz to 30 Hz and segmented into epochs starting from 100ms prior to the onset of each trial and ending at 400ms after it. Baseline was removed based on pre-onset 100ms. According to previous studies, PRVEP epochs were referenced to channel Fz (Thilo et al. 2003), while MOVEP epochs were referenced to linked mastoids (Kubová et al. 1995). Saccade artifacts were removed by rejecting epochs based on step-like artifacts test in HEOG channel (window width: 400ms; step: 50ms; threshold: $\pm 30 \mu\text{V}$). Epochs polluted by other eye movement, eye-blinks and other artifacts were rejected using moving window peak-to-peak method (window size: 200ms; step: 50ms; threshold: $\pm 100 \mu\text{V}$) for all channel. Remaining valid epochs were averaged for four conditions (STA: static condition; ROT: rotating condition; RN: ROT without vection; RV: ROT with vection; note that $\text{ROT} = \text{RN} + \text{RV}$) respectively (see Table 5.1 for mean epoch numbers included for each type of VEP at each condition). The peak amplitude and peak latency of N1/P1/P3 in PRVEP and N2 in MOVEP were measured from averaged VEP waves of each participant. The selection of VEP components are based on the common dominant components of each VEP type (Bach and Ullrich 1997; Kubová et al.

1995) and previous reported VEP components associated with vection [N1: (Thilo et al. 2003); P1: (Stróžak et al. 2016); N2: (Keshavarz and Berti 2014; Stróžak et al. 2016; Vilhelmsen et al. 2015); P3: (Stróžak et al. 2016)].

Table 5.1 Trial and block summary for each VEP types

VEPs	Reversing Rate	Duty Cycle	Trial length	Trials per block		Block length	Total Blocks	Mean (SD) for Valid epoch	
PRVEP	2Hz	-	500ms	STA	400	200s	1	367.5 (37.6)	
				ROT	500	250s	2	RN	407.9(284.1)
								RV	550.6(334.3)
MOVEP	-	0.2/1.2s	1200ms	STA	200	240s	2	373.1 (18.8)	
				ROT			5	RN	365.3(139.7)
Total			-				10	2553.8 (443.9)	

5.4 Data analysis and result

Peak amplitudes (PAmp) and peak latencies (PLat) of each VEP component (N1, P1 & P3 of RPVEP; N2 of MOVEP) were measured from the average EEG epochs of each subject at each condition. Repeated measures MANOVAs were then conducted separately for each component indicator with the paired contrast factors (stimuli-motion: STA/ROT; vection-perception: RV/RN) and laterality factor (O1-left/Oz-middle/O2-right).

5.4.1 PRVEP

For RPVEP, significant vection-perception main effect was found in both the peak amplitude of N1 [$F(1,13) = 5.599, p = 0.034$] and P1 [$F(1,13) = 11.396, p = 0.005$], where RV (vection) condition in general showed smaller peak amplitude than RN (no-vection) condition (Figure 5.2). Results supported the H5a. Moreover, marginal significant laterality main effect was found for P1 [$F(2,26) = 2.654, p = 0.078$], with Bonferroni-corrected post hoc comparisons revealed that O1 peak amplitude was smaller than Oz ($p < 0.05$). It is noteworthy that no stimuli-motion main effect was found for either N1 or P1 peak amplitude.

However, for P3 peak amplitude, there was significant main effect of stimuli-motion [$F(1,13) = 14.537, p = 0.002$] rather than vection-perception (Figure 5.2), with STA condition larger than ROT condition and no difference between RN & RV.

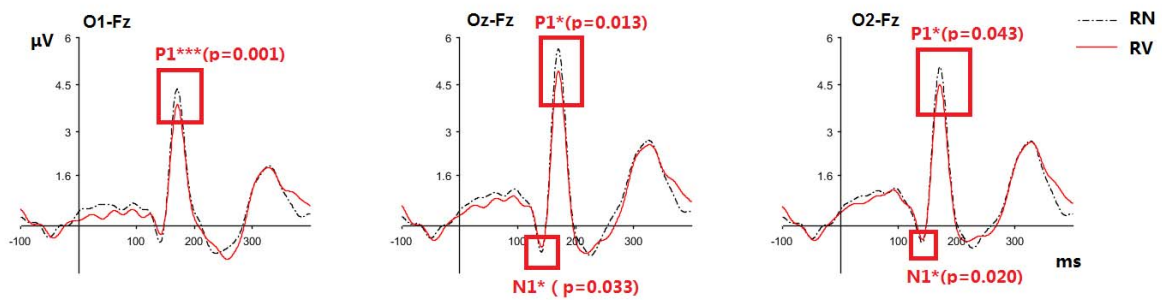


Figure 5.2 Comparisons of VEP for vection-perception contrasts for all three occipital electrodes. (The red markers indicated the significant/or marginal simple effects for each electrode and their p-values; note that with vection the P1 and N1 are significantly smaller, while the P3 is not significantly different between RN and RV; note that all PRVEP is referenced to Fz channel based on previous studies).

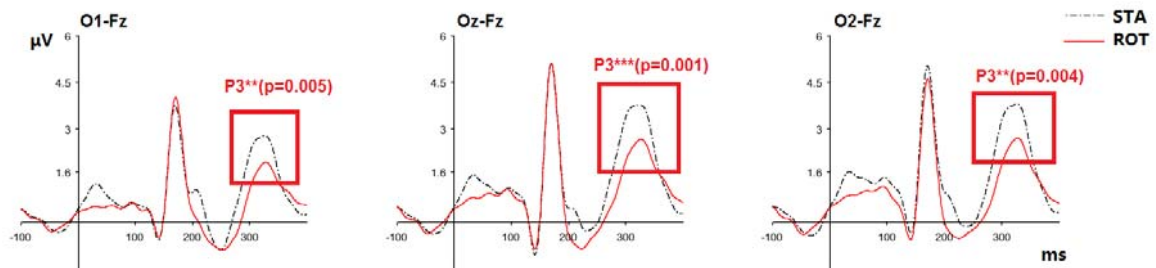


Figure 5.3 Comparisons of VEP for stimuli-motion contrasts for all three occipital electrodes. (The red markers indicated the significant simple effects for each electrode and their p-values; note that the P1 and N1 are no significant difference, while the P3 is significantly larger in STA and ROT).

As for peak latency, no significant difference was found between all conditions for N1 or P1. For P3 latency, significant stimuli-motion main effect [$F(1,13) = 11.792, p = 0.004$] and marginal significant vection-perception main effect [$F(1,13) = 3.424, p = 0.087$] were revealed, with STA shorter than ROT condition and RN shorter than RV condition. No interaction effect and laterality effect were identified for peak latency.

5.4.2 MOVEP

For MOVEP, N2 peak amplitude was neither significant for the stimuli-motion or vection-perception contrast, but the peak amplitude in STA condition is marginally larger than ROT condition [$F(1,13) = 3.534, p = 0.083$]. Moreover, it is worth mentioning that N2 peak latency of Oz tended to be shorter during vection (RV < RN). This peak latency difference was significantly positively correlated with the individual vection duration ($r = 0.467, p = 0.046$), where subjects who experienced longer vection demonstrate larger advances of peak latency. Results are in line with the H5b. Furthermore, we found significant main effect on laterality for stimuli-motion contrast model [$01 < Oz < 02; F(2,26) = 3.407, p = 0.049$], where N2 peak amplitude demonstrated a right hemispheric emphasis.

5.4.3 Models with MSSQ scores

Similar to study one, as we are interested in how the regulations on VEP during vection varied according to the VIMS susceptibility of participants, we also conducted separated MANOVA models with MSSQ scores (MSSQ_A; MSSQ_C) added as covariates. The interaction term with MSSQ scores was revealed significant in peak amplitude of N2 from MOVEP and child scale of MSSQ [$N2_{PAmp} \times MSSQ_C: F(1,12) = 5.635, p = 0.035$], where resistant people generally showed larger N2 peak amplitude during vection than no-vection period and susceptible people demonstrated opposite effects. This significant interaction term explains why no main effects of vection were revealed in peak amplitude of N2 in vection-perception contrast without adding MSSQ scores in the model (see 5.4.3) and also supports the H6.

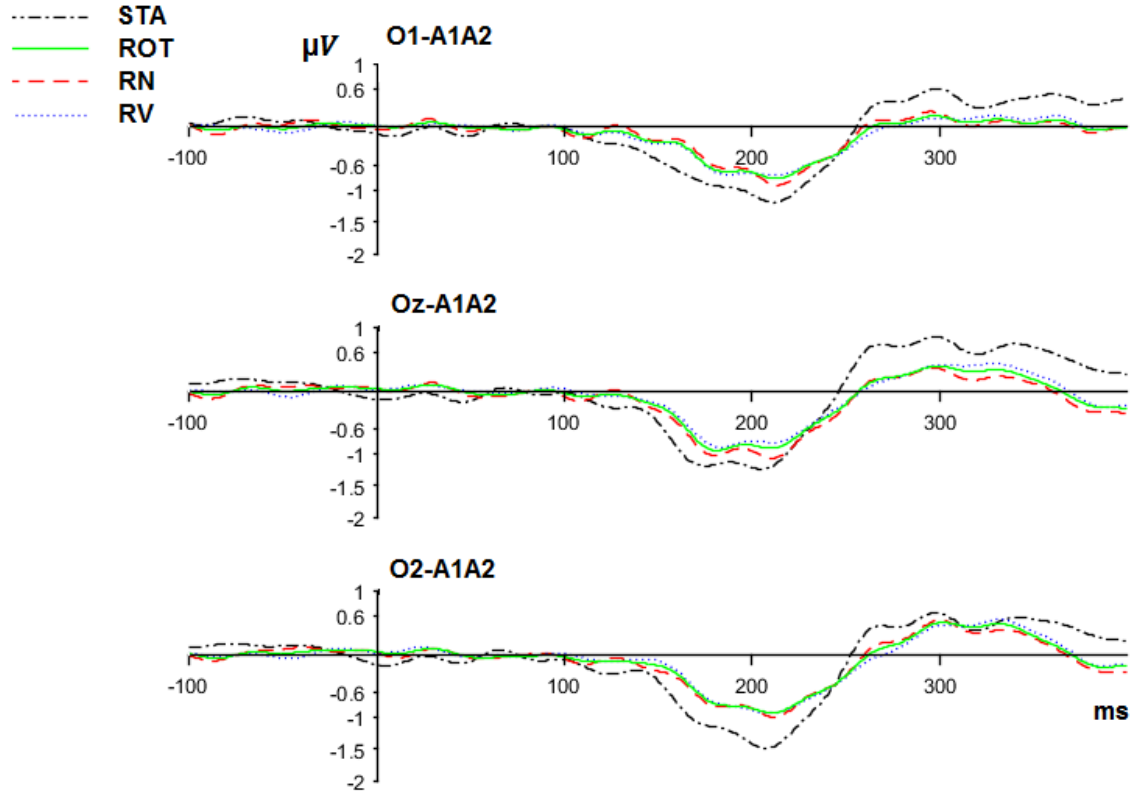


Figure 5.4 Comparisons of VEP under all conditions for three occipital electrodes. (Note that the peak amplitude is larger in right hemisphere, with $O2 > O1$; No peak amplitude difference was revealed for all contrast, but STA is marginally larger than ROT condition; note that all MOVEP are referenced to linked mastoid indicated as A1A2 based on previous studies)

Moreover, in consistent with the positive correlation between vection and advanced N2 peak latency, the vection main effect was found to be significant in the model with MSSQ_A added as covariates [vection-perception : $F(1,12) = 5.503, p = 0.037$], where RV showed advanced Plat than RN. This supported the H5b. The interaction term is also significant for vection-perception contrast and adult scale of MSSQ: [$N2_{PLat} \times MSSQ_A: F(1,12) = 7.587, p = 0.017$], with resistant people showing facilitated N2 while susceptible people showing delayed N2 during vection. This significant interaction term explains why no

significant effects ofvection were revealed in peak latency of N2 invection-perception contrast without adding MSSQ scores in the model (see 5.4.3) and also supports the H6.

To quantify the effect size in N2 peak amplitude for each participant, we calculate the increment of N2 peak amplitude ($N2_{PAmp_inc}$) by using peak amplitude in RV condition subtracting peak amplitude in RN condition ($N2_{PAmp_inc} = N2_{PAmp_RV} - N2_{PAmp_RN}$). For the effect size of N2 peak latency, we calculate the advance of N2 peak latency ($N2_{PLat_adv}$) by using peak amplitude in RN condition subtracting peak amplitude in RV condition ($N2_{PLat_adv} = N2_{PLat_RN} - N2_{PLat_RV}$).

Further correlation and regression analysis revealed that the $N2_{PAmp_inc}$ and $N2_{PLat_adv}$ from different occipital electrodes are significantly negatively correlated with MSSQ scores (see Table 5.2 for the coefficient and Figure 5.5 for scatter plot). To evaluate the prediction power of identified predictors, we conduct a separate regression model for the raw score and percentile score of two MSSQ subscales. Results showed that the $N2_{PAmp_inc}$ from the O1 electrode showed the best prediction power for the raw score of MSSQ_C, and $N2_{PLat_adv}$ from the Oz electrode showed the best prediction power for the percentile score of MSSQ_A (see table 5.2), which supports the H6.

EEG data analyses were validated using both Curry 7.0.8 signal processing package (Compumedics Neuroscan, USA) and Eeglab/Erplab (Delorme and Makeig 2004; Lopez-Calderon and Luck 2014) with various commonly applied pre-processing and artifacts removing/rejecting methods. All results remain robust regardless of different EEG pre-processing procedures.

Table 5.2 Correlations and regression models for VEP indicators predicting MSSQ scores

Visual Response Indicators		MSSQ Scale Score			
VEP indicators	Electrodes	MSSQ_C	MSSQ_C_P	MSSQ_A	MSSQ_A_P
N2 _{PAmp_inc}	O1	-0.598* (p=0.024)	-0.499^ (p=0.069)	-	-
	Oz	-0.579* (p=0.030)	-0.519^ (p=0.057)	-	-
	O2	-	-	-	-
N2 _{PLat_adv}	O1	-	-	-	-0.438^ (p=0.117)
	Oz	-	-	-	-0.540* (p=0.046)
	O2	-	-	-	-0.414^ (p=0.141)
Regression Model Summary					
Models	Predictors	Beta	R	R ²	F
1. MSSQ_C	N2 _{PAmp_inc_O1}	-0.598* (p=0.024)	0.598	0.358	6.693* (p=0.024)
	N2 _{PAmp_inc_Oz}	Excluded			
	N2 _{PAmp_inc_O2}	Excluded			
2. MSSQ_A_P	N2 _{PLat_adv_O1}	Excluded	0.540	0.292	4.938* (p=0.046)
	N2 _{PLat_adv_Oz}	-0.540* (p=0.046)			
	N2 _{PLat_adv_O2}	Excluded			

Two-tailed p-value: ** p<0.01; * p<0.05; ^ p<0.15. MSSQ_C, MSSQ_C_P represent the raw and percentile score of MSSQ child scale; MSSQ_A, MSSQ_A_P represent the raw and percentile score of MSSQ adult scale; N2_{PAmp_inc_O1}, N2_{PAmp_inc_Oz} and N2_{PAmp_inc_O2} represent the increment of peak amplitude of N2 component at O1, Oz and O2 electrodes respectively. N2_{PLat_adv_O1}, N2_{PLat_adv_Oz} and N2_{PLat_adv_O2} represent the increment of peak amplitude of N2 component at O1, Oz and O2 electrodes respectively; only marginal/significant correlation results are included. Model 1 predicts the MSSQ_C score; Model 2 predicts MSSQ_A. Note that no predictor is found to be significant for the total scale of MSSQ.

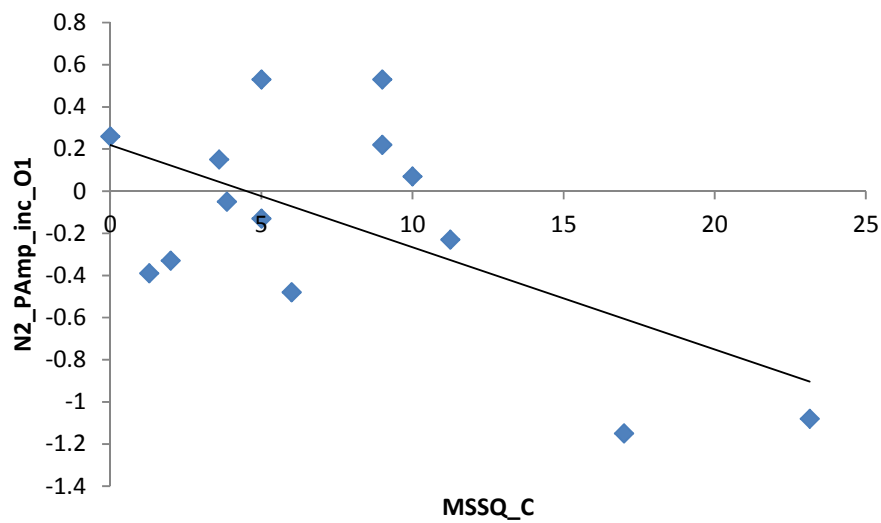


Figure 5.5 Scatter plot for the visual response indicator (increment of N2 peak amplitude at O1 electrode) and child scale of MSSQ (In general, for resistant participants the increment N2 during vection period is positive, while for susceptible people the increment is negative).

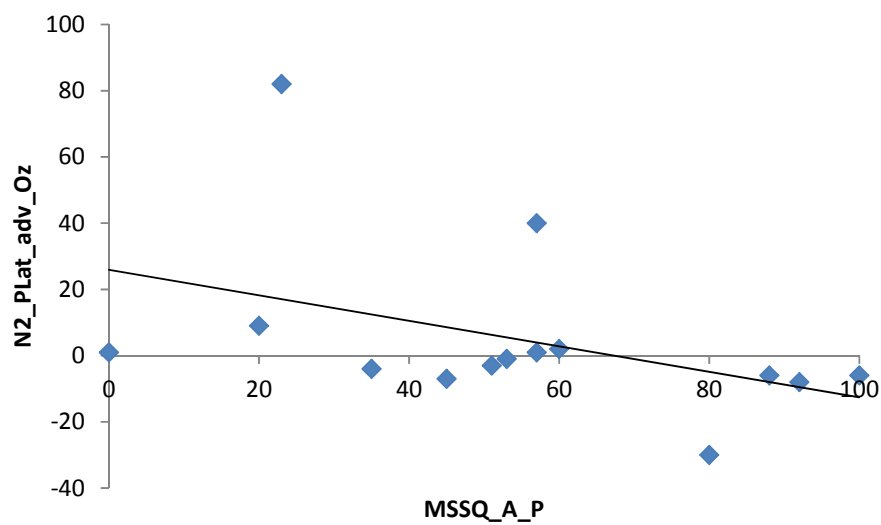


Figure 5.6 Scatter plot for the visual response indicator (advance of N2 peak latency at Oz electrode) and percentile score of MSSQ adult scale (Note that for resistant people N2 peak latency tend to be shorter during vection, while for susceptible people the Plat tend to be longer during vection)

5.4.4 Vection and VIMS reports

Additionally, we also conducted repeated measures MANOVAs for vection intensity and duration separately. There is no significant difference in vection intensity and the percentages of vection duration for PRVEP and MOVEP under the ROT condition, so the vection data are pooled together for each participant. The mean and SD for vection intensity and the vection duration (in percentage) are 2.64 ± 0.84 and 55.42 ± 16.61 (%). The percentile score of VIMSS varies among participants from 0 to 96% (see Appendix F). Since the block exposure time was controlled to be short (≤ 250 s) with sufficient rest between blocks, no subjects experienced nausea, vomiting or other severe unpleasant feelings.

5.5 Discussion

This study examined the regulation on two types of VEP responses (PRVEP and MOVEP) under vection-inducing stimulation. We found earlier VEP components from PRVEP (N1/P1) to be suppressed during vection perception, while the N2 components from MOVEP to be facilitated with the experience of vection. Moreover, the magnitudes of effects on N2 are negatively correlated with the susceptibility to motion sickness.

For PRVEP, both the peak amplitudes of N1 and P1 were found to be significantly decreased during vection as compared with no vection perception period under same roll vection-inducing stimulation. Those findings are agreed with our results in study one that visual performances in CVF are generally impaired (see chapter 4), as well as previous related EEG findings which adopted radial or straight stripe stimuli (Stróžak et al. 2016; Vilhelmsen et al. 2015). Thilo (2003) reported reduced N1 amplitudes of PRVEP for occipital channels during self-motion perception when subjects were exposed to peripheral optokinetic stimulation. In another recent study, the amplitudes of P1 and P3 event-related potential triggered by oddball task were found to be smaller in horizontal moving condition than static controls (Stróžak et al. 2016). In this study, we designedly separated the comparison for stimuli-motion and vection-perception conditions. As the N1/P1 amplitude reduction only occurred with

subjective perception of vection (under same visual stimulation) instead of the rotating of peripheral dot pattern (Figure 5.2), our findings suggested that the N1/P1 suppression effect shall be mainly attributed to vection perception rather than the stimuli motion as well as the nystagmus introduced by optokinetic stimulation. Moreover, as the amplitudes of P3 component showed significant difference for stimuli motion contrast instead of the vection perception contrast (Figure 5.3), researchers should be more conservative regarding the suppression effects reported with later VEP components (P3), since it might be largely due to stimuli motion rather than vection. In sum, results suggested that the regulations during vection perception are mainly direct at earlier VEP components, which are responsible for primary and fundamental visual functions (e.g. contrast processing), than later components which are responsible for more complicated cognitive functions (e.g. pattern recognition; object detection) (Luck 2005).

More interestingly, for MOVEP, instead of suppression effect, shorter latency of N2 was found to be positively correlated with vection perception duration. Moreover, significantly larger N2 amplitudes were revealed in vection period for VIMS susceptible people. Those results are also consistent with previous horizontal vection studies (Keshavarz and Berti 2014; Stróžak et al. 2016; Vilhelmsen et al. 2015), where enhanced N2 components were found for conditions that capable to introduced stronger vection. Since most of previous study did not present vection-inducing stimulation for a period long enough to introduce vection perception when collecting VEPs (Keshavarz and Berti 2014; Vilhelmsen et al. 2015), our study is actually the first work that found peak latency of N2 to be correlated with the individual subjective vection reports. According to former studies, N1/P1 potential generated from PRVEP can serve as an indicator for the contrast processing, while the N2 potential generated from MOVEP could be more associated with the motion-processing (Bach and Ullrich 1997; Kubová et al. 1995; Souza et al. 2013). Furthermore, it was revealed by considerable studies that the modulation on VEP components can reflect the shift of processing emphasis of our visual system (Hillyard, Vogel, and Luck 1998; Mangun 1995). For example, P1 amplitude is decreased when stimuli are unattended, while shorter N2 latency was found when more attention resource is directed to process the stimuli (Correa et

al. 2006; Kempel et al. 2003). Therefore, it is possible that the opposite modulation effect on N2 could be due to a general processing emphasis from other functions to motion processing duringvection.

Note that in this study, the N2 amplitude is significantly different between RV and RN only after controlling the VIMS susceptibility, which suggested that more emphasis shall be put on the association between this regulation effect and susceptibility to VIMS. Further correlation and regression analysis supported our hypothesis H2 that the regulation on VEP components should depend on the susceptibility to VIMS. We found that resistant people tend to facilitate N2 during the perception ofvection, while susceptible people showed an opposite trend. This might suggest that resistant people better achieved the direction of processing emphasis to motion processing than susceptible people. Admittedly, since the percentile of VIMS susceptibility is widely distributed in our participant group, we have very limited participants (<6) who are extremely susceptible or extremely resistant to VIMS. Moreover, since this effect is obtained by the relative difference betweenvection and novection period, we have no idea whether this effect is due to susceptible people produce larger N2 under RN condition or they generate smaller N2 under RV condition, as compared to resistant people. New motion baseline that unable to inducevection (with the local motion and visual complexity controlled) to serve as contrast for both RV and RN condition is necessary for clarify this ambiguity. Therefore, further explorations should explore how N2 signatures are differently organized in VIMS susceptible and resistant people (with a more representative group of subjects), while they are exposed tovection-inducing stimulation and new motion baseline.

5.6 Summary

5.6.1 New findings and contributions

In this study, we further explored the impaired visual response in CVF revealed by SART in study one. More specifically, we have mainly explored the temporal properties of visual

regulations under vection-inducing stimulation which marked by various VEP components evoked at different time stamp. Results suggested that the impairment of visual performance during vection actually has started as earlier as the N1 component (see Figure 5.2, evoked around 140ms) and P1 component (see Figure 5.2, evoked around 170ms). Moreover, as the P3 (see Figure 5.3, evoked around 310ms) component has been revealed to be associated with stimuli motion rather than vection perception (see Figure 5.2), this implies that the negative regulation of visual response during vection is mainly focused on primary visual functions, rather than more complicated cognitive functions.

Moreover, we also found the enhancement of N2 component during vection and the magnitude of this effect is closely associated with VIMS susceptibility. This result is in line with our main hypothesis that during vection there is a processing emphasis shift from other visual function to motion processing to facilitate and stabilize the vection perception, which contributes to the sensory conflict reduction and thus prevent VIMS.

Furthermore, study two has identified new EEG signatures (peak amplitude of P1/N1/N2 and peak latency of N2) as vection indicators, as well as the N2 signatures (peak amplitude and peak latency) as VIMS predictors. As the first EEG study in this research, our replications on previous experiment findings also validate the EEG set-ups and recording procedures for our following EEG studies.

5.6.2 Raised further questions and focus of follow-up works

Admittedly, we did not found any correlation between identified EEG signatures and vection intensity perceived by individuals. Therefore, those vection indicators can only reflect the presence of vection, rather than the magnitude of vection intensity, which are less promising to be developed into quantitative vection measures.

This might due to the drawbacks of transient VEP—vulnerable to motion artifacts and all kinds of other noise (e.g. eye and head movements, EKG). Because of its relatively low SNR, we need to average plenty of trials to obtain the transient VEP indicators, which also make

those vection indicators impractical and less sensitive to the variation of vection experiences. Also, the large individual variation introduced by VIMS susceptibility might also hide the effects related to vection. Future explorations with a larger and more representative group of subjects are desirable.

Moreover, in study two we only focus on occipital electrodes to explore the temporal properties and replicate the results from Thilo (2003). Further explorations with higher dimensional spatial detectors (e.g. EEG signal collected from electrodes widely distributed over occipital, temporal, parietal and frontal areas) could better assist us to capture the spatial properties on the visual response regulation during vection. This can also facilitate the identification of more reliable EEG indicators, because we might be able to search for better electrode or location on the scalp or even make use of multiple electrodes as vection indicators.

Last but not least, study two focused on VEP mainly evoked from CVF and investigated the modulation of those VEPs under vection-inducing stimulation in PVF. As we discussed in chapter 2, further explorations that are capable to simultaneously measure and differentiate the response both CVF and PVF is more desirable for vection indicators.

Therefore, in the follow up works, we go further to explore the spatial properties of VEP response with higher dimensional EEG channel system (32-channel quick cap) and well-directed indicators that capable to explore and compare response originated from CVF and PVF. Particularly, in study three, we examine the steady-state VEP (SSVEP) and its topography under vection-inducing stimulation. As introduced in chapter 3, SSVEPs preserve better SNR and is less vulnerable to motion artifacts than transient VEPs. Moreover, as described in section 3.1.3, we utilize the frequency tags in visual stimulation to differentiate the SSVEP indicators that are responsible for the CVF and PVF respectively. Furthermore, in following study four, we also try to recruit screened and more representative VIMS susceptible and resistant participants to better explore the N2 signatures and how it differently organized for two VIMS groups.

CHAPTER 6 STUDY THREE – STEADY-STATE VEP RESPONSES UNDER VECTION-INDUCING STIMULATION

6.1 Introduction

This study focuses on investigating the spatial properties of regulation on SSVEP during vection. Specifically, we examine the changes of SSVEP topography under vection-inducing stimulation and searches for EEG covariates with vection among participants with various VIMS susceptibility. Similar stimuli adopted in study two were applied to study three. The dots pattern in PVF and checkerboard in CVF were flickered at two specific frequencies of alpha band (12 and 8.6Hz) respectively to generate SSVEP, while the dots pattern in PVF was rotating to induce vection. The frequency power at two frequency tags was calculated as SSVEP indicators. To explore the vection associated effects, electrodes of interest (EOIs) are selected based on topography of frequency power. Moreover, as the top-down attention regulation can modulate both the perception of vection and SSVEP topography, we design three types of attention allocation task and explore how top-down regulation interaction with the vection and SSVEP effects. Then, those identified effect indicators are further explored as VIMS predictors by analyzing the prediction power for MSSQ scores.

6.2 Objective and hypotheses

The objectives of this study are: 1) explore the topography of SSVEP indicators (two frequency marker: 12 and 8.6Hz) to locate electrode of interest (EOIs) which response strongest to PVF and CVF stimulations for future and follow-up works; 2) explore how the identified SSVEP indicators from EOIs changes with the perception of vection to evaluate their potential as effective vection indicators; 3) explore the interaction between the top-

down attention regulation, vection perception and SSVEP indicators to better understand the properties of SSVEP indicators.

Based on the nature of SSVEP (see section 3.1.3 for introduction), we expected to observe peaks at the flickering frequency of stimulation (8.6Hz for CVF; 12Hz for PVF) and their 2nd harmonics (17.2Hz for CVF; 24Hz for PVF) in the power spectrum of SSVEP (H7).

Moreover, as the cortical region which primarily responsible for processing the CVF and PVF stimuli shall be different, we expect the power topography for two marked frequencies (8.6 and 12Hz) should be significantly different (H8a), where the EOIs produce strongest frequency power should be different (H8b).

According to Brandt's theory (1998) and our findings in study 1&2, it is anticipated that people direct more processing resource from CVF to PVF during vection, hence we expected that vection is associated with a power shift from CVF stimuli EOI to PVF stimuli EOI (H9). Furthermore, as we assume this effect can facilitate the sensory conflict reduction and prevent VIMS, we expected that the magnitudes of the effects are negatively correlated with the MSSQ scores of individual participants (H10). Moreover, we expected the top-down attention regulation should have interaction effect on both vection perception (H11a) and the vection associated effects (H11b).

6.3 Methods

6.3.1 Participants

Fifteen university students (9 male; Age: 24-27 years old, mean 25.40, SD 1.40; 14 right-handed), with 20/20 (or corrected) eyesight and normal color vision, were recruited with complete informed consent. This group of participants exhibits a large variation in VIMS susceptibility [measured using the Motion Sickness Susceptibility Questionnaire (MSSQ) Short-form; see Golding 1998] from 0-85% in percentile, which in general follows the percentile distribution in the population (See Appendix F). All participants are free of any

vestibular injury or medical treatment. None of them were heavy video game players or had rich experience with large-screen visual motion stimuli.

6.3.2 Stimuli, apparatus, task and procedures

Stimuli and task

Same as study two, grey dots (FOV diameter: $0.5\sim1.3^\circ$) were randomly generated on a black background and all grey dots coherently rotated anticlockwise (angular velocity: $32^\circ/\text{s}$) as the ROT condition. To focus on more narrowly defined CVF (as we introduced in section 1.5 and 2.1.2), an achromatic checkerboard occupied $11.4 \times 15.1^\circ$ of FOV (smaller than the one in study two) was presented to CVF (see Figure 6.1). To evoke the SSVEP, the random dots in PVF were alternated between strong (contrast: 91.62%; dots luminance: $1.6\text{ cd}/\text{m}^2$) and weak (contrast: 26.32%; dots luminance: $0.12\text{ cd}/\text{m}^2$) contrast condition at a frequency of 12Hz, while the checkerboard in CVF was reversed at a frequency of 8.6Hz (luminance: $10\text{ cd}/\text{m}^2$ for white cell; $0.62\text{ cd}/\text{m}^2$ for black cell; contrast: 88.32%). To provide a general control for the local visual stimuli motion, a control (COT) condition without flickering is formed by letting the grey dots moved toward randomized directions, while keeping linear velocity paralleled with angular velocity as former studies employed (Brandt et al. 1998; Wei, Fu, and So 2017). Similar to study two, subjects were trained to indicate their vection perception state continually under the ROT condition by pressing response buttons using right hand. Similarly, the vection-perception contrast is compared between the SSVEP recorded under same ROT condition but within time periods indicated by participants as different perception state (ROT during vection: RV; or no-vection: RN). Same as study two, SSVEP recorded within 2s of the perception state changes (from vection to no-vection, or vice versa) were not included in RV/RN conditions as they were conducted within the transition state. Moreover, in this study, we collected SSVEP recorded within 2s of the vection onset (from no-vection to vection, indicated by button pressing of participants) and assigned them into a separate vection onset (VEON) condition to explore the transition state before and after vection onset.

Procedures

Each trial started with a 1.5s-baseline black background (BAS), followed by 15s ROT stimuli. Participants were trained to press a key button with right hand index finger to indicate the onset or offset of roll vection (all participants watched one trial of stimuli demo and received sufficient training on how to identify the state of self-rotational vection). After the ROT stimulation with another 3s-BAS, COT stimuli would last for 3s and this trial end with a 1.5s-BAS (see Figure 6.2).

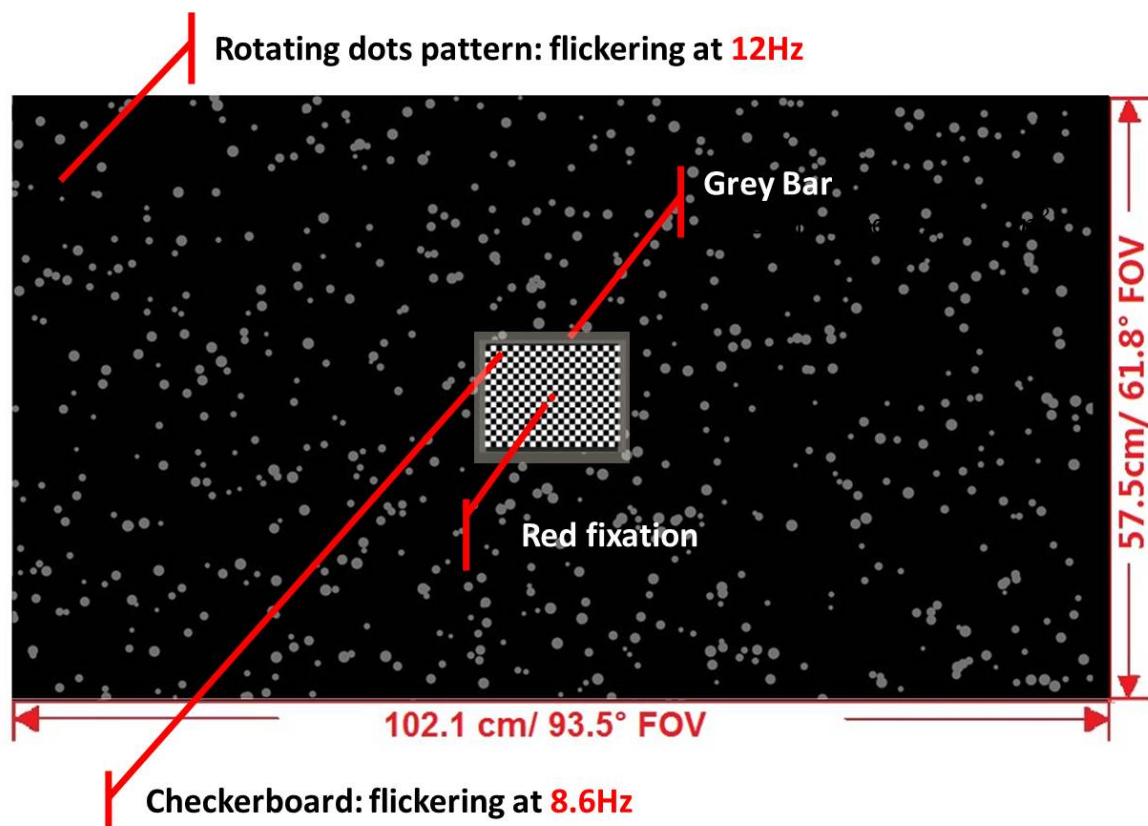


Figure 6.1 Illustration on the visual stimuli. (The averaged luminance for black cells in checkerboard are 0.62 cd/m^2 , and for white cells are 10 cd/m^2 , so the contrast is 88.32%; Note that checkerboard is encircled by grey bar with a luminance of 1.54 cd/m^2 and a width of 0.53cm; the highlighted grey area is just for illustration, so it is larger than actual stimuli; checkerboard has 24×18 cells with a size of 0.53cm)

Hence, each trial cost 24 seconds. And each block consisted of 8 trials ($24 \times 8 = 192$ sec per block). Before next block, participants rested for 3-10min, until no fatigue or discomfort was reported.

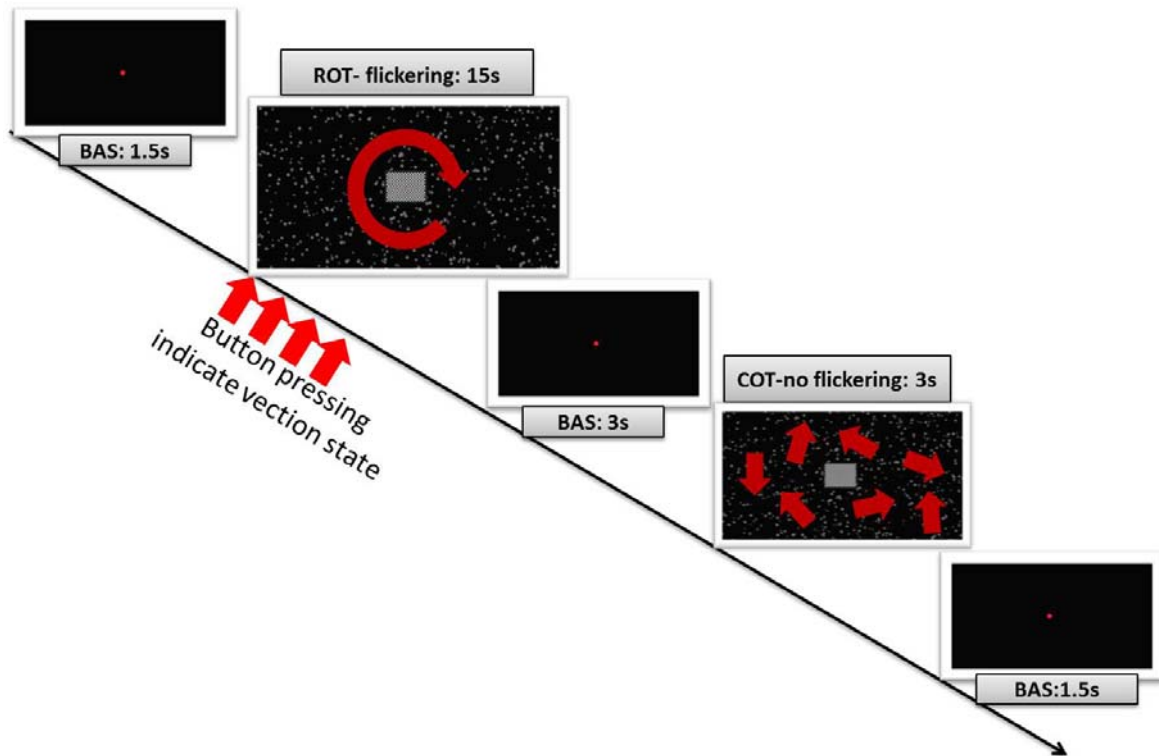


Figure 6.2 The procedure of each trial. (Note that participants are required to indicate their vection perception state by pressing the response button under the ROT stimulation)

To explore the interaction of vection and top-down attention regulation, three types of attention task were conducted with different instructions: 1) stationary focus (STA: participants are instructed to focus on the stationary cues and ignore any self-motion cues to suppress the self-motion perception); 2) self-motion focus (SMO: participants are instructed to focus on the self-motion cues and imagine that they were sitting inside a space ship and looking at the rotating stars in the sky to facilitate the self-motion perception); 3) no focus

requirement (NOF: participants are instructed to assign the attention to whole screen without any particular focus). All participants finished three STA blocks, three SMO blocks and six NOF blocks. The sequence of each block is randomized among participants with sufficient rest between successive blocks (see Table 6.1 for summary).

Apparatus and EEG recording

The stimuli were presented using the same 46-in LCD monitor (Screen FOV: $93.5^{\circ} \times 61.8^{\circ}$; View distance: 48cm; refreshing rate: 60Hz) with the same setups to control the head/body movement and eliminate environment visual cues as study one (Appendix B). Participants were instructed to fix their eyes on a center red dot (diameter: 0.6° of FOV; luminance: 5.05 cd/m^2) to suppress OKN and other types of eye movements. During stimuli presentation, the EEG was recorded together with two horizontal EOG (left and right) and two vertical EOG (upper and lower) channels using a NuAmps Amplifier (DC-coupled, 22 bit, monopolar) from 36-channel Ag/AgCl sintered electrodes (Quik-Cap, Compumedics Neuroscan) based on the international 10-10 system (Appendix H) referenced to linked mastoid electrodes. Impedances between all channels and ground channel (AFz) were kept below $5\text{k}\Omega$. Same procedures and protocols validated in study two for EEG recording and synchronization triggers with visual stimuli were applied in this study.

6.3.3 Response measures

EEG signal preprocessing

Raw EEG data were digitized at a sampling rate of 1000 Hz and a bandwidth of DC-260Hz, and then filtered offline with FIR filter at a band-pass of 1.6-45Hz. Data were segmented into 1167ms-epochs for each type of condition (see Table 6.1 for detail), based on the length of two consecutive cycles of the visual flickers --the refreshing rate of monitor is 60Hz, hence the PVF dots pattern flickers at every fifth screen flip (12Hz) and the CVF checkerboard flickers at every seventh screen flip (8.6Hz); so one complete cycle of visual flicker is $5 \times 7 = 35$ screen flips (each flip $\approx 16.7\text{ms}$, total $\approx 583\text{ms}$).

Independent components analysis (ICA) was then applied to these epochs using EEGLAB (Delorme and Makeig 2004), and components identified as eye movement artifacts were removed using automatic toolbox ADJUST (Mognon et al. 2011). The epochs contaminated by other artifacts were rejected based on moving window peak-to-peak method (window size: 200ms; step: 50ms; threshold: $\pm 100 \mu\text{V}$) and extreme value of remaining components (threshold: $\pm 20 \mu\text{V}$). The average epochs remained for each condition and their standard deviations were listed in the Table 6.1. The averaged epochs were then transformed into power spectrum at frequency domain.

Table 6.1 Summary for block, trial and epoch numbers in experimental conditions

		Attention Allocation Task			Total
		Stationary focus (STA)	Self-motion focus (SMO)	No focus (NFO)	
Block/Trial numbers		3 B/24 T	3 B/24 T	6 B/48 T	12 B/96 T
Mean clean epochs (SD)		227.6 (50.4)	220.5 (46.3)	625 (199.3)	1073.2 (233.9)
<i>Vection conditions</i>					
ROT	RV	77.7 (47.5)	96.2 (47.8)	351.4 (124.3)	173.9 (91.1)
	RN	150.0 (71.0)	124.3 (58.2)	273.7 (137.6)	274.2 (119.5)
	VEON		-		163.7 (47.8)
COT			-		180.3 (27.3)

Subjective vection and VIMSS reports

Participants were trained to report their vection intensity after each block, based on a 5-point vection magnitude scale revised from previous studies (1=no vection; 5=saturated vection; Webb & Griffin, 2003; see Appendix G). The percentage of vection duration under each condition can be obtained from the response from participants. VIMS susceptibility data were

assessed using Motion Sickness Susceptibility Questionnaire (MSSQ) Short-form (Golding, 1998), which included two subscales (child scale: MSSQ_C; adult scale: MSSQ_A).

6.4 Data analysis and result

6.4.1 Vection and VIMS reports

Repeated measures MANOVAs were conducted separately for the vection intensity and percentage of vection duration across different attention allocation tasks. The mean and SD of these subjective vection measures are reported in Table 6.2 and demonstrated in Figure 6.3. Results revealed significant main effect of attention task in the percentage of vection duration [$F(2,28) = 4.269, p = 0.024$], where pairwise comparisons only revealed that SMO condition is larger than STA condition [$p=0.016$]. No significant main effect of attention task was found in vection intensity. The percentile score of VIMSS varies among participants from 0 to 85% (see Appendix F). Since the block exposure time was controlled to be short (192 s) with sufficient rest between blocks, no subjects experienced nausea, vomiting or other severe unpleasant feelings. Results suggested that top-down attention allocation to self-motion perception can actively introduce longer duration of vection, even when participants were exposed to same physical stimulation, which supported H11a.

Table 6.2 Mean and SD of subjective vection measures

Attention task	Stationary focus (STA)	Self-motion focus (SMO)	No focus (NFO)	Averaged
Vection intensity	2.33 (0.63)	2.66 (0.86)	2.40 (0.55)	2.40 (0.47)
Vection duration* (%)	39.32% (20.22)	48.57% (15.48)	47.22% (17.04)	45.04% (15.95)

* Note that the percentage of vection duration is used to facilitate the comparison between conditions with different total stimuli exposure time; calculated by using the length of vection period dividing the length of total stimuli exposure time; the standard deviations are provided in the brackets.

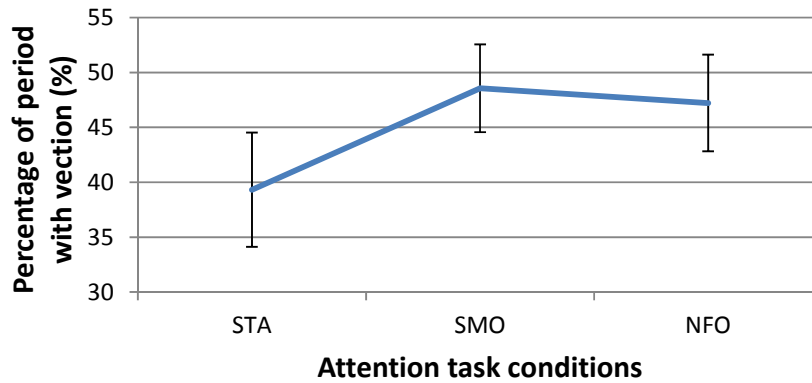


Figure 6.3 The comparison of vection duration among different attention tasks. (Note that pairwise comparisons only reported a significant difference between SAT and SMO; the error bars are standard errors calculated based on repeated measures model)

6.4.2 SSVEP results

Firstly, we conducted initial analysis on the properties of SSVEP by using the data under NFO condition to eliminate the effect due to attention manipulation. As expected, we found four peaks in the frequency power spectrum of averaged SSVEPs, which are corresponding to the PVF stimuli frequency (12Hz), the 2nd harmonic of the PVF stimuli frequency (24Hz), the CVF stimuli frequency (8.6Hz) and the 2nd harmonic of the CVF stimuli frequency (17.2Hz) in all participants (see Figure 6.4 for illustration on group averaged power spectrum at frequency domain), which supported the H7.

To explore the spatial distribution of the SSVEP power at stimuli frequencies we plot the topography of the power at 12Hz (PVF stimuli) and 8.6Hz (CVF stimuli) respectively. As showed in Figure 6.4a, the electrode which response strongest to PVF stimulation (12Hz) is the Pz electrode, while the Oz electrode has showed strongest responses to CVF stimulation (8.6Hz), which supported the H8b. Based on this, Pz and Oz were selected as EOIs for further analysis.

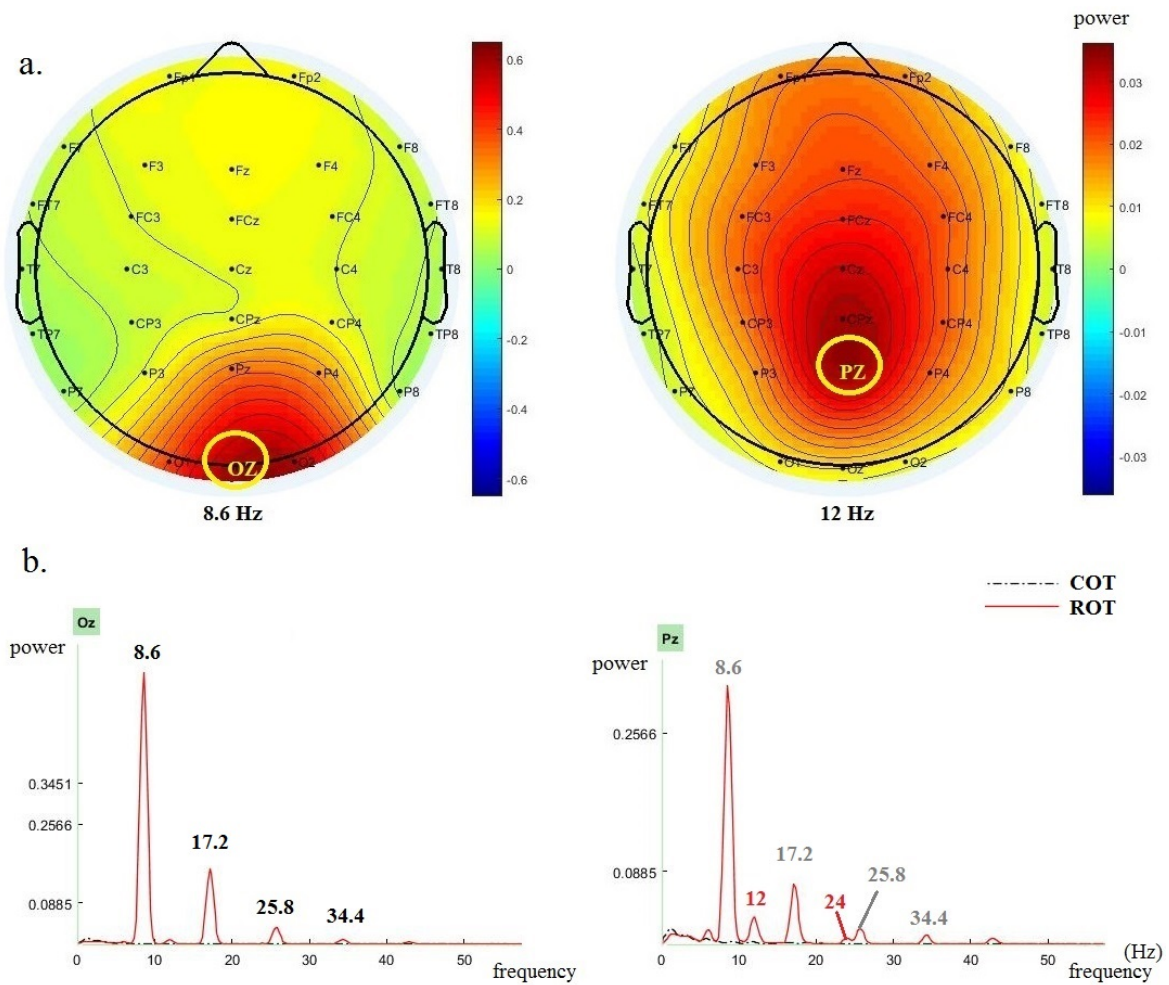


Figure 6.4 Topography of SSVEP power at stimuli frequencies and the power spectrum of EOIs. a. Topography of SSVEP power at stimuli frequencies. (Left graph shows the topography for CVF stimulation frequency at 8.6 Hz; right graph shows the topography for PVF stimulation frequency at 12Hz) b. The comparison on power spectrum at EOIs between the control (COT) condition and dots pattern rotating (ROT) condition (left graph shows the power spectrum of Oz electrode which is the EOI for CVF stimuli; right graph shows the power spectrum of Pz electrode which is the EOI for PVF stimuli; Note that the ROT showed significant larger power than COT at all stimuli frequencies and their 2nd harmonics in both Oz and Pz)

Moreover, further analysis with the SSVEP power at each stimuli frequency and EOI, also confirmed the statistical significance of the observed effects. We conducted one two-level

three factor (Stimuli: ROT/COT; Position: Oz/Pz; Frequency: 8.6/12Hz) repeated measures MANOVA with MSSQ total score added as covariates (similar to previous study). We found power in ROT condition was significantly larger than COT condition [$F(1,13) = 21.912$, $p < 0.001$]. Moreover, the frequency also showed significant main effect [$F(1,13) = 18.667$, $p = 0.001$], where power is stronger at 8.6Hz than 12Hz. The interaction for Stimuli \times Frequency [$F(1,13) = 18.747$, $p = 0.001$], Position \times Frequency [$F(1,13) = 5.174$, $p = 0.041$], and the triple term Stimuli \times Position \times Frequency [$F(1,13) = 5.048$, $p = 0.043$] were also significant (see Figure 6.5& 6.6 for illustration on interactions). Results suggested that the power at CVF and PVF stimuli frequency are differently distribution on EOIs, which supported H8. Note that we also found complicated significant terms with MSSQ scores, which will be further explored and demonstrated in section 6.4.4.

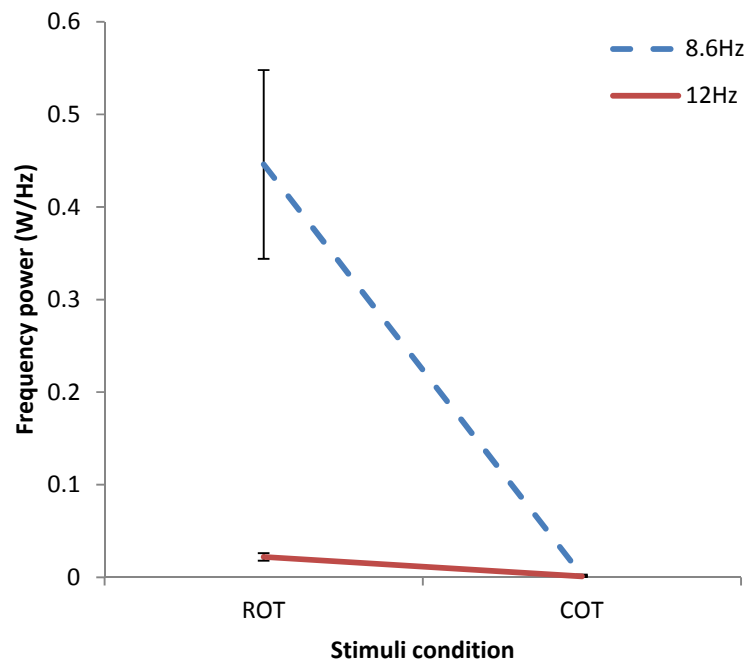


Figure 6.5 Interaction of power between stimuli condition and frequency

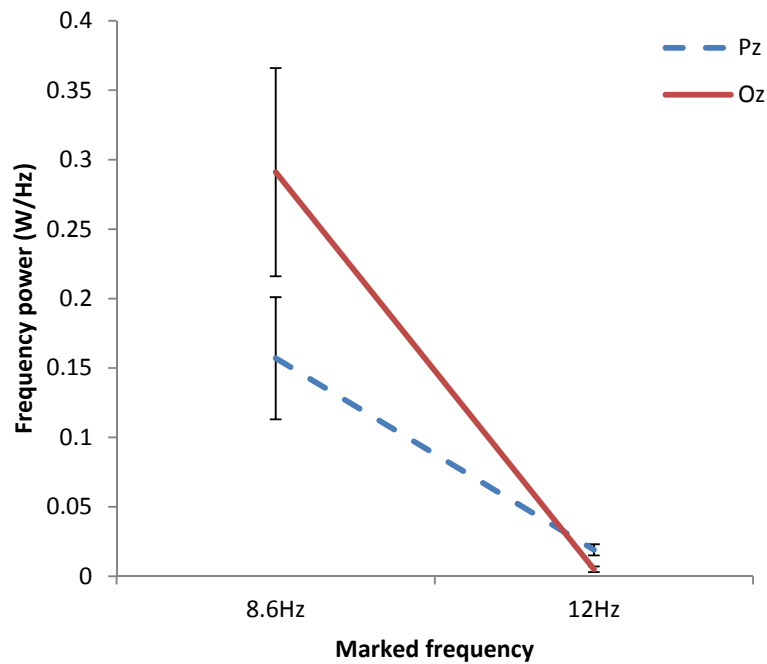


Figure 6.6 Interaction of power between stimuli EOI position and frequency

6.4.3 Vection covariates

To explore the effect associated with vection perception instead of visual stimulation, we generate the vection difference topography by subtracting the power of RN condition from the power of RV condition ($\text{Diff}_{\text{RV-RN}}$). The topography of $\text{Diff}_{\text{RV-RN}}$ for each frequency was showed in Figure 6.7. As demonstrated in the figure, there is a shift of SSVEP power from occipital to parietal region during vection, especially for 8.6 Hz frequency.

To test the statistical significance of the vection effect, we conducted another two-level three factor (Vection: RV/RN; Position: Oz/Pz; Frequency: 8.6/12Hz) repeated measures MANOVA with MSSQ total score added as covariates. We found significant main effect for Frequency [8.6Hz>12Hz; $F(1,13) = 18.720$, $p = 0.001$] and Vection [RN>RV; $F(1,13) = 5.821$, $p = 0.031$], with marginal significant main effect for Position [Oz > Pz; $F(1,13) = 4.167$, $p = 0.062$]. Moreover, the interaction terms were all significant: Vection \times Position

[$F(1,13) = 10.904$, $p = 0.006$], Vection \times Frequency [$F(1,13) = 6.709$, $p = 0.022$], Frequency \times Position [$F(1,13) = 5.172$, $p = 0.041$], and Vection \times Position \times Frequency [$F(1,13) = 10.911$, $p = 0.006$]. The binomial and trinomial interaction effects associated with vection are showed in Figure 6.8-6.10. Results supported that the observed power shift from occipital to parietal is also statistically significant, which supports the H9. Note that simple main effects under the interaction effects are not significant (see Figure 6.8-6.10).

Moreover, further analysis suggested that the increment of SSVEP power under vection at Pz electrode ($P_{inc_pz} = Power_{RV_Pz} - Power_{RN_Pz}$) is positively correlated with the individual vection intensity within the period collected SSVEP [significant for 8.6Hz: $r = 0.554$, $p = 0.032$; marginal significant for 12Hz: $r = 0.494$, $p = 0.061$], while the SSVEP indicators from Oz fail to achieve this (similar as the transient VEP indicators from Oz electrodes which identified in study two).

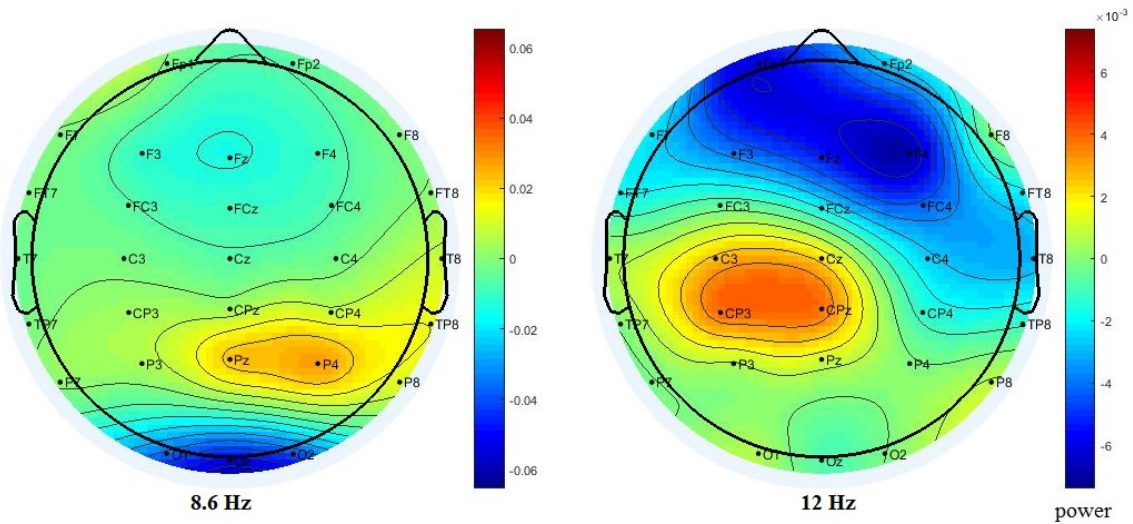


Figure 6.7 Difference topography obtained by subtracting the power of RN condition from the power of RV condition ($Diff_{RV-RN}$).

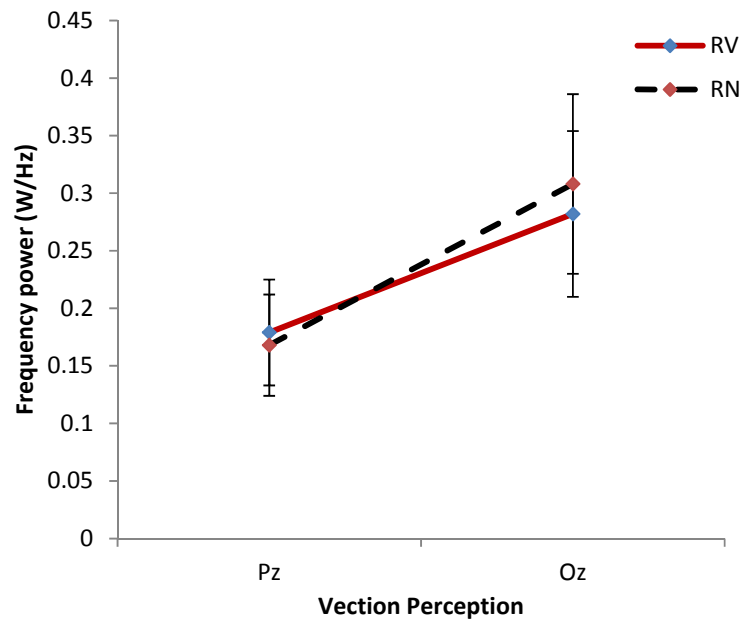


Figure 6.8 Interaction on power between vection and position of electrode.

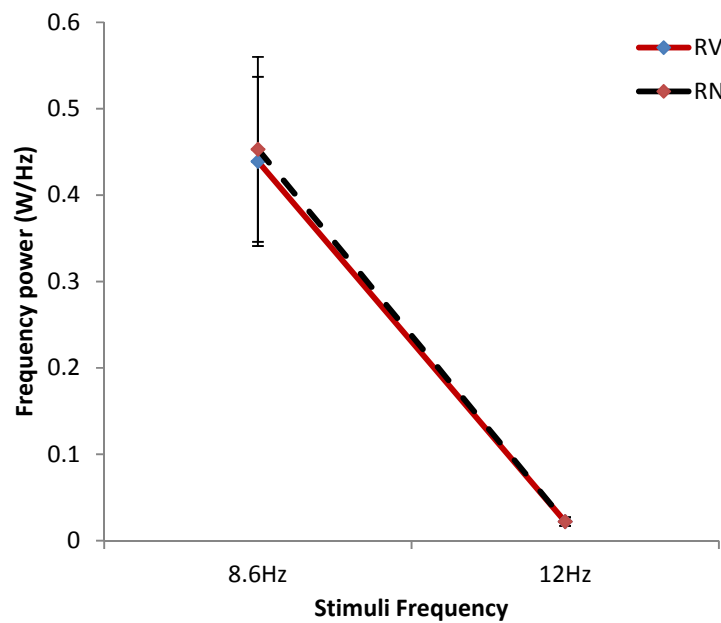


Figure 6.9 Interaction on power between the vection and frequency. (Note that this group averaged effect is hid by the significant interaction with individual MSSQ scores)

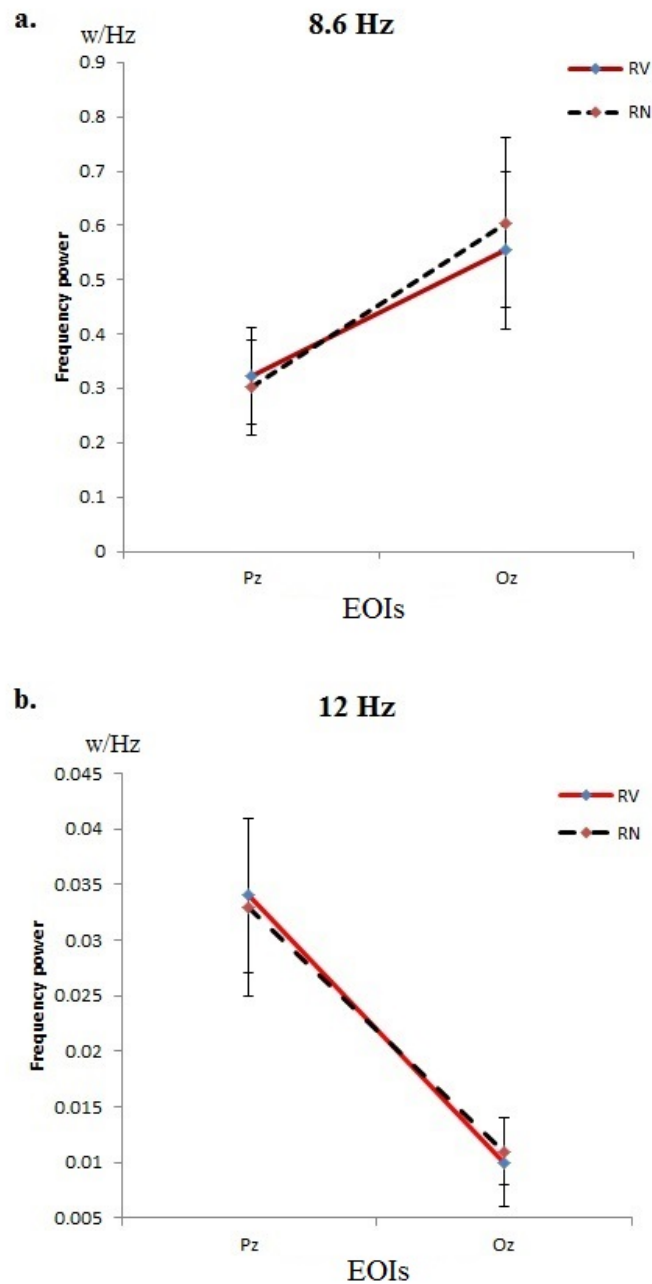


Figure 6.10 Simple interaction on power illustrated for the trinomial interaction between the vection, position and frequency. a. the simple interaction at 8.6Hz between the vection and position. b. the the simple interaction at 12Hz between the vection and position. (Note that the triple interaction idicated that trend of power shift from Pz to Oz is consistant at the two frequencies, although the dominance frequency for Pz and Oz is different)

6.4.4 VIMSS covariates

As expected, we found that several interaction terms between vection associated effects and MSSQ score were also significant or marginal significant: vection \times MSSQ [$F(1,13) = 5.948, p = 0.030$], vection \times Frequency \times MSSQ [$F(1,13) = 6.284, p = 0.026$], vection \times Frequency \times Position \times MSSQ [$F(1,13) = 4.424, p = 0.055$]. This suggested that the vection effect varies according to the MSSQ score of participants, which is consistent with the H10.

To further explore the direction of effects, the power at each vection condition and the decreased power during vection at each stimuli frequency and EOI, along with the combined effects of them, were obtained as the SSVEP indicators. Then we conducted regression models using the SSVEP indicators to predict the total (MSSQ_T) and the two subscales (MSSQ_A & MSSQ_C) scores. As illustrated in Table 6.3, we found that higher MSSQ score is associated with lower SSVEP power at RV (ROT without vection) condition. More importantly, the magnitude of the suppressed power at Oz and the power shift effects (from Oz to Pz) during vection is negatively correlated with MSSQ scores (especially the child subscale), which supported the H10. Furthermore, results also showed that the decrease of SSVEP power during vection at 8.6 Hz from the Oz electrode is correlated with the MSSQ scores with best prediction power (see Figure 6.11-12 for scatter plots) among all the predictors.

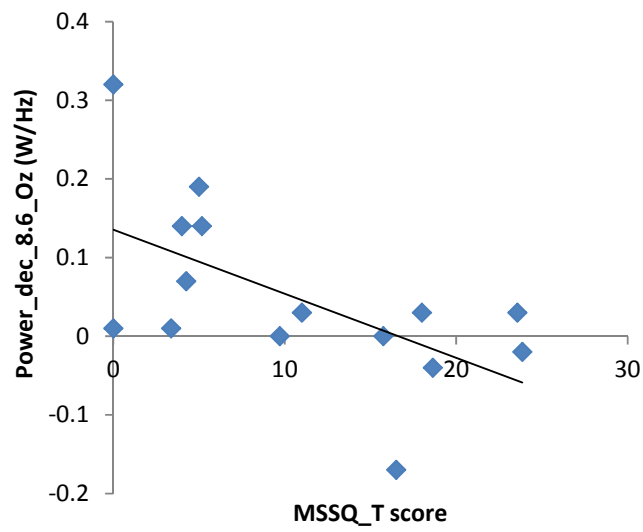


Figure 6.11 Scatter plot for the MSSQ_T score and the decrease of power during vection at 8.6Hz from Oz electrode

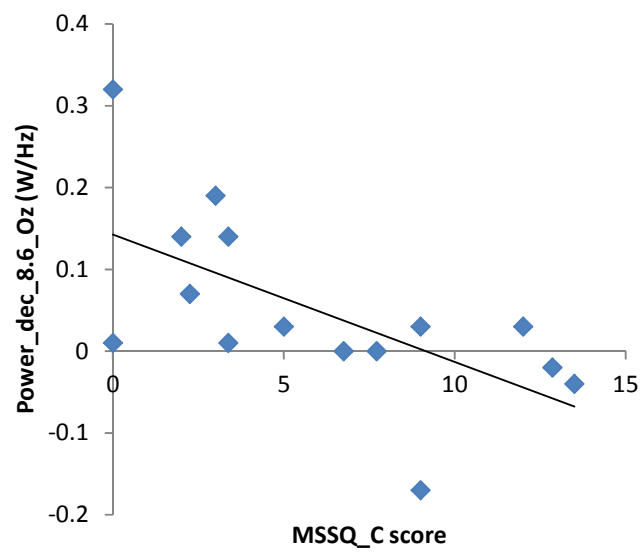


Figure 6.12 Scatter plot for the MSSQ_C score and the decrease of power during vection at 8.6Hz from Oz electrode

Table 6.3 Correlations and regression models for SSVEP indicators predicting MSSQ scores

Visual Response Indicators			MSSQ Scale Score		
SSVEP indicators	EOI	Frequency	MSSQ_T	MSSQ_C	MSSQ_A
Power_{RN}	Pz	8.6Hz	-0.454 [^] (p=0.089)	-	-0.444 [^] (p=0.097)
	Oz	8.6Hz	-0.538* (p=.039)	-0.558* (p=0.031)	-0.461 [^] (p=0.084)
Power_{dec}	Pz	8.6Hz	-	-	-
	Oz	8.6Hz	-0.595* (p=0.019)	-0.622* (p=0.013)	-0.504 [^] (p=0.055)
Power_{dec}	Oz – Pz	8.6Hz	-0.520* (p=0.047)	-0.582* (p=0.023)	-
Power_{dec}	Oz – Pz	8.6 +12 Hz	-0.474 [^] (p=0.074)	-0.546* (p=0.035)	-
Regression Model Summary					
Models	Predictors	Beta	R	R ²	F
1. MSSQ_T	Power_{8.6_dec_Oz}	-0.595* (p=0.019)	0.595	0.354	7.118* (p=0.019)
	Other predictors	Excluded			
2. MSSQ_C	Power_{8.6_dec_Oz}	-0.622* (p=0.013)	0.622	0.387	8.223* (p=0.013)
	Other predictors	Excluded			

Two-tailed p-value: ** p<0.01; * p<0.05; ^ p<0.10. Power_{RN} represents the power of SSVEP at ROT condition without the perception of vection. Power_{dec} represents the decrease of power with vection as compared to period without vection but under same ROT stimulation; The ‘+’ symbol means adding together the effect in two frequency. The ‘-’ symbol means the effect of Pz and Oz is at opposite direction, so it is combined by subtracting the size of Pz effect from the size Oz effect. Only marginal/significant correlation results are included. Model 1 predicts the MSSQ_T score; Model 2 predicts MSSQ_C. Note that all predictors were stepwise added into the regression model, where predictors with less contribution power were excluded. No predictor is found to be significant for the adult scale of MSSQ.

6.4.5 Interaction of attention allocation and vection

To explore the interaction of top-down attention regulation and vection effects on the SSVEP indicators, we go on to analyze the data from STA and SMO condition. We generate the

focus difference topography by subtracting the power of STA condition from the power of SMO condition ($\text{Diff}_{\text{SMO-STA}}$). The topography of $\text{Diff}_{\text{SMO-STA}}$ for each frequency and vection perception state was showed in Figure 6.13.

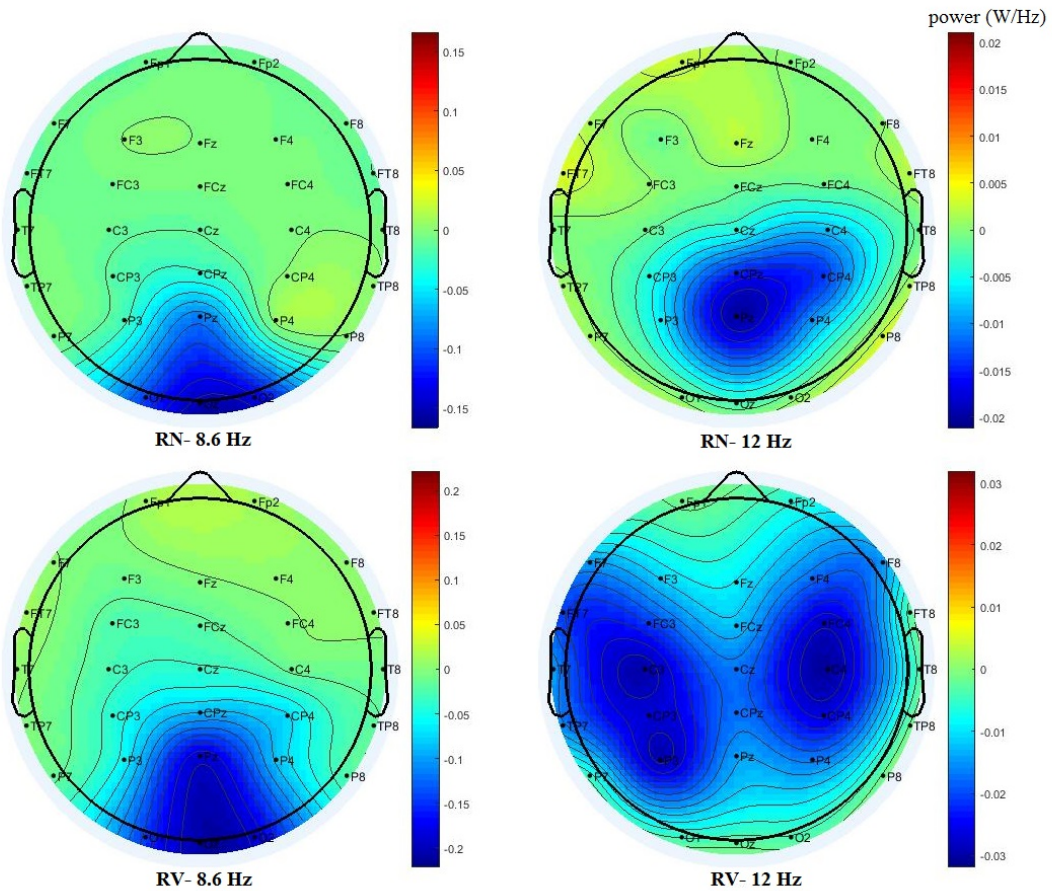


Figure 6.13 Difference topography obtained by subtracting the power of STA condition from the power of SMO condition ($\text{Diff}_{\text{SMO-STA}}$). (Upper two topographies are ROT condition without vection perception; lower two are ROT condition with vection)

As demonstrated in the figure, there is a general suppression of SSVEP power during the SMO condition. It is observed that occipital region is mainly suppressed for 8.6Hz, while the

central-parietal regions are suppressed for 12Hz. Moreover, the suppression at 12Hz showed bilateral patterns during vection, while the suppression was focused in parietal midline and right central parietal area for no vection periods.

For further statistical analysis, we conducted a two-level four factor (Focus: STA/SMO; Vection: RV/RN; Position: Oz/Pz; Frequency: 8.6/12Hz) repeated measures MANOVA. The main effect of focus was found to be significant [$F(1,14) = 12.809$, $p = 0.003$], where SMO showed generally less power than STA condition. The interaction between the Focus \times Frequency [$F(1,14) = 10.098$, $p = 0.007$] (Figure 6.14), the trinomial Focus \times Frequency \times Vection [$F(1,14) = 5.217$, $p = 0.039$] were also significant. As illustrated in Figure 6.15-16, directing attention to self-motion perception from stationary perception has flipped the effect of vection at 8.6Hz, while does not affect the effects at 12Hz.

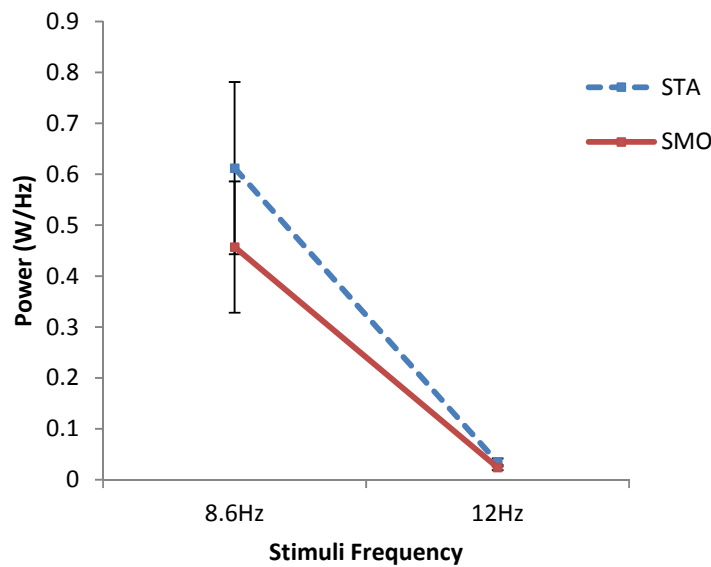


Figure 6.14 Interaction of power between focus condition and frequency

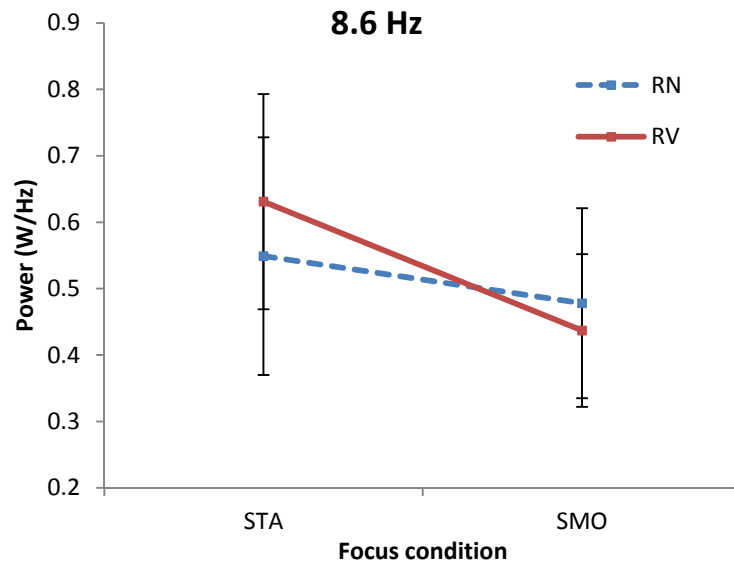


Figure 6.15 Interaction of power between focus condition and vection at 8.6 Hz (Note that the simple interaction effect is marginally significant with $p=0.064$)

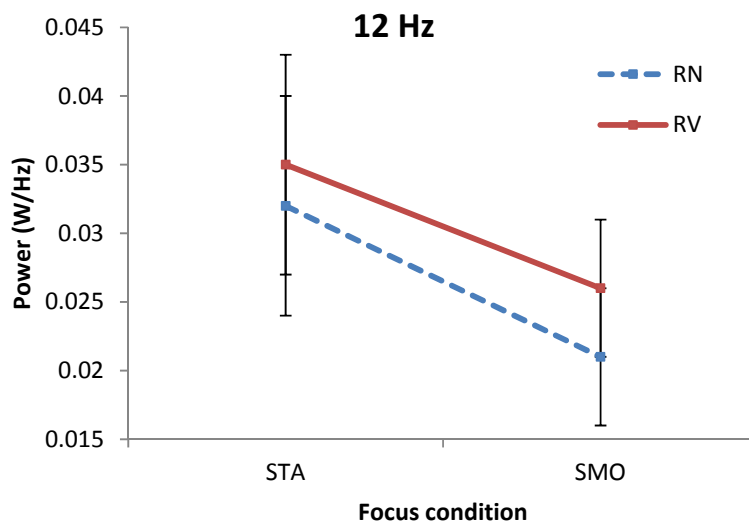


Figure 6.16 Interaction of power between focus condition and vection at 12 Hz. (Note that the trinomial interaction term is significant, while the simple effect at 12 Hz is not significant)

Difference Topography RV-RN

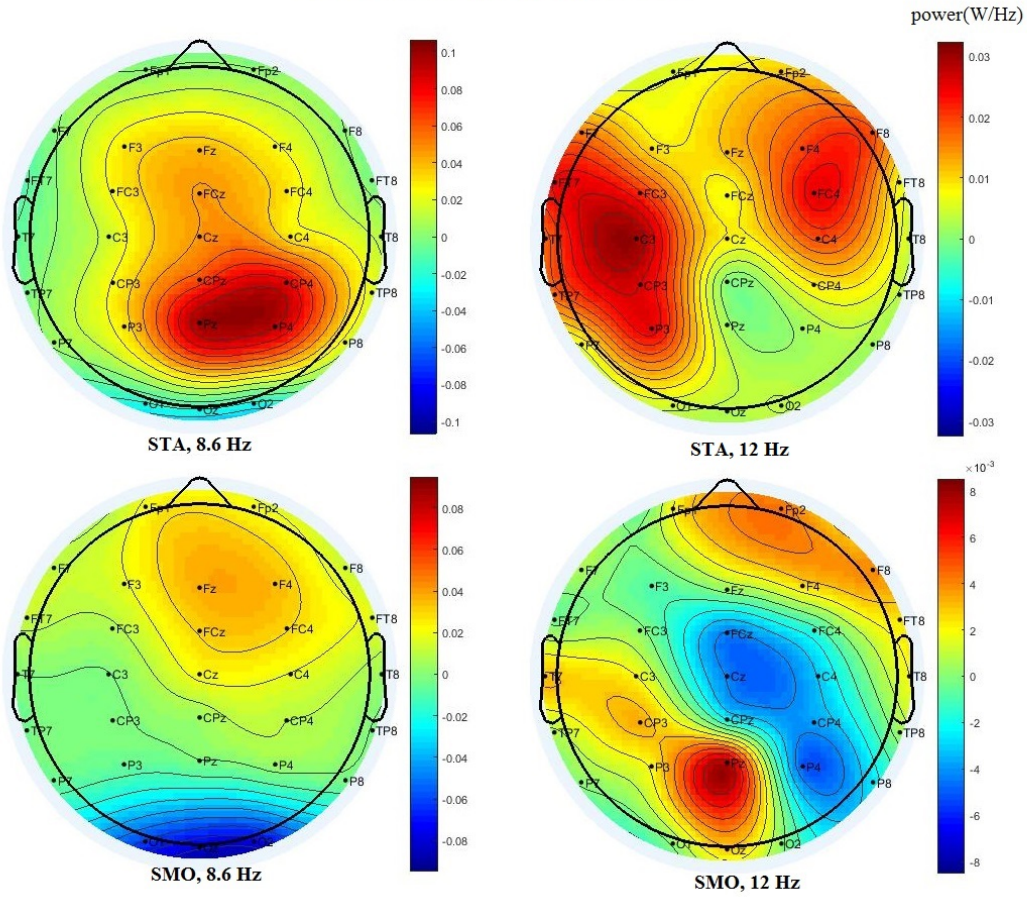


Figure 6.17 Difference topography obtained by subtracting the power of RV condition from the power of RN condition ($\text{Diff}_{\text{RV}-\text{RN}}$). (Upper two topographies are STA condition; lower two are SMO condition)

To better illustrate how the effect distributed in topography, we plot the same vection difference topography as we did for NFO condition in section 6.4.3 (Figure 6.17). Combining the Figure 6.17 and Figure 6.7, we can see that top-down attention allocation to self-motion perception during vection facilitates the suppression in Oz for CVF stimuli frequency (8.6Hz), and facilitates the enhancement in Pz for PVF stimuli frequency (12Hz). Moreover, top-down attention allocation to stationary perception during vection facilitates the enhancement of Pz

for CVF stimuli frequency (8.6Hz), but hindered the enhancement of Pz for PVF stimuli frequency (12Hz) and shifted more energy to bilateral central regions.

Moreover, the main effect of Frequency [8.6Hz>12Hz; $F(1,14) = 11.351$, $p = 0.005$] and the other interaction terms revealed significant in NFO focus were also significant: the Frequency \times Position [$F(1,14) = 4.659$, $p = 0.049$], the trinomial Frequency \times Position \times Vection [$F(1,14) = 5.895$, $p = 0.029$], which also agreed with results in section 6.4.3.

6.4.6 Effect during vection onset

To facilitate the development of vection indicators that can serve as vection onset detector, we also analyzed the SSVEP of epochs that indicated by participants as a transition period from no-vection to vection perception (the vection onset: VEON). We then generate the VEON difference topography by subtracting the power of RN condition (under NFO) from the power of VEON condition ($\text{Diff}_{\text{VEON-RN}}$). The topography of $\text{Diff}_{\text{VEON-RN}}$ for each frequency was showed in Figure 6.18.

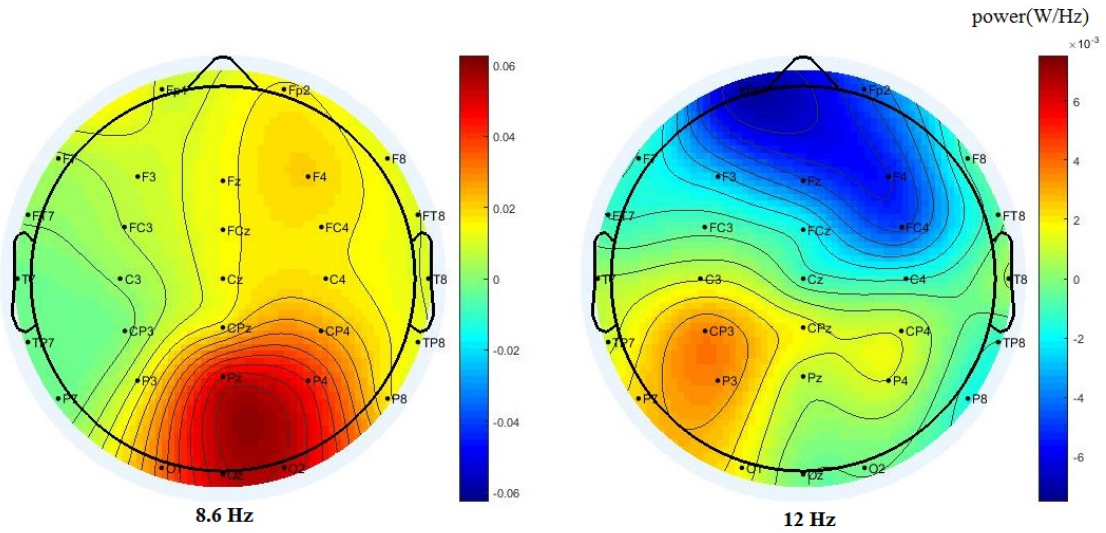


Figure 6.18 Topography of power difference between VEON and RV condition

As illustrated in Figure 6.18, vection onset is associated with enhancement of power in parietal-occipital region at 8.6Hz. For 12 Hz, we found the decrease in frontal region, with enhancement in left parietal regions.

To validate the statistical significance of the effects, we obtained the SSVEP power from P4/Pz/Oz at 8.6Hz. A two-level two factor (Vection onset: VEON/RN; Position: Oz/Pz/P4) repeated measures MANOVA had revealed significant main effect for vection onset [VEON>RN; $F(1,14) = 6.255$, $p = 0.025$], with no other interaction or main effects. As for the 12Hz, we obtained the SSVEP power from Fp1/P3, and conducted a similar two-level two factor repeated measures MANOVA, where only a trend of interaction effect of vection \times position was observed [$p = 0.17$].

6.5 Discussion

6.5.1 Differentiated response for CVF and PVF

Firstly, the findings on the power spectrum of SSVEP supported our hypothesis H7 that predominant peaks shall be observed at the CVF (8.6Hz) and PVF (12Hz) stimulation frequency and their harmonics. This has validated the effectiveness of our SSVEP evoker, the stimuli presentation, the data collection and preprocessing procedures, which also confirms the reliability and effectiveness of our SSVEP indicators: the power at CVF (8.6Hz) and PVF (12 Hz) frequency.

As the power of SSVEP at each marked frequency is able to reflect the visual processing emphasis on the visual location marked by this frequency (Morgan et al. 1996; Silberstein et al. 2001), the differentiated topography between these marked frequency can extract the spatial information in parallel which responsible for the process of visual stimulation at CVF and PVF respectively. Interestingly, we found that Oz electrode response strongest to the CVF stimulation, while Pz response strongest to the PVF stimulation (Figure 6.4), which

consistent with our H8. This differentiated EOI location for each stimuli frequency also agreed with previous knowledge and retinotopic mapping studies (Bridge 2011): the CVF checkerboard stimuli lead to strong activities in occipital regions (around the Occipital Pole & Calcarine Fissure) for the contrast processing (Bach and Ullrich 1997; Griffis et al. 2016; Di Russo et al. 2005), while the rotating PVF stimulation lead to more response in parietal-occipital regions (Sabrina Pitzalis et al. 2013; Uesaki and Ashida 2015; Wada et al. 2016) for the PVF ambient information processing (e.g. large motion patterns). Therefore, our results suggested that the SSVEP indicators from Oz electrode are more responsible to the CVF stimulation, while indicators from Pz electrode are more responsible to the PVF stimulation.

Moreover, we also found significantly stronger power for 8.6Hz than 12Hz. This effect could be explained by several reasons: firstly, the CVF stimulation usually provokes stronger VEP, as larger areas in visual cortex are occupied by CVF receptors (Bridge 2011; Pitzalis et al. 2018). Moreover, the stronger contrast of flicker can lead to larger VEPs (Kubová et al. 1995). As the CVF flicker has stronger contrast than PVF flick, it may also produce stronger SSVEP power. Thirdly, it was reported that the SSVEP at a lower frequency usually generates larger power (Herrmann 2001; Morgan et al. 1996). Since the CVF stimulation (8.6Hz) is smaller than PVF stimulation (12Hz), the power at 8.6Hz could be larger than power at 12Hz. The weaker effects revealed for 12Hz might also due to this prominent main effect.

6.5.2 Vection effect: power shift from occipital to parietal

Then we explored how those SSVEP indicators changed with vection. Interestingly, under vection, a power shift from occipital region to parietal region (Figure 6.7) was observed in the difference topography (especially for 8.6Hz). This effect is also confirmed by statistical test with the responses from Oz electrode (EOI for CVF stimulation) and Pz electrode (EOI for PVF stimulation), where we found a significant interaction effect on vection \times position. Those finding supported our H9 --vection should be associated with the spatial shift of SSVEP power from cortical region more responsible for CVF stimuli to region more

responsible to PVF stimuli. It was also agreed with previous suppression effects reported for occipital electrodes both in our study two (chapter 5) and other EEG studies (Stróžak et al. 2016; Thilo et al. 2003), as well as the activation effects reported for parietal electrodes (Schindler and Bartels 2018; Vilhelmsen et al. 2015).

It is revealed by many previous works that the power strength of SSVEP can reflect the processing emphasis of our visual system: assigning more attention resource, increasing alertness and directed task requirement can strengthen the power of SSVEP, while withdrawing attention or ignoring the stimuli would reduce the power strength of SSVEP (Herrmann 2001; Keil et al. 2005; Morgan et al. 1996; Müller et al. 1998). Hence, the power shift from Oz to Pz may suggest that our visual system withdraw the processing emphasis from occipital region to parietal regions, which can facilitate the processing of self-motion cues in PVF, as many self-motion perception related brain areas located in parietal regions. Moreover, this effect was found to be significantly correlated with the individual MSSQ scores, where that people who are more resistant to VIMS demonstrated stronger effect (Table 6.3). This implied that VIMS resistance is associated with a successful mechanism of directing more processing emphasis from occipital region to parietal region. Therefore, this power shift is also quite consistent with our findings in study one &2 and the general hypothesis that the facilitation of self-motion processing should contribute to the prevention of VIMS.

Interestingly, we found that the SSVEP power increase of the Pz electrode is significantly correlated with the vection intensity of each individual. This implied that the Pz electrode is not only more responsible to the processing of PVF stimulation, but also able to provide better quantitative indicators for vection perception. Although previous works found that the VEPs showed differentiate response to visual stimuli which can introduce different levels of vection (Keshavarz and Berti 2014; Stróžak et al. 2016; Vilhelmsen et al. 2015), this is the first EEG indicator found to be correlated with the individual vection intensity under exposure to same visual stimulation. Therefore, the SSVEP indicators in this study actually showed better the potential as quantitative vection measures.

Furthermore, we also explored the SSVEP indicators for the onset of vection. Interestingly, we identified a significant increase of SSVEP power at 8.6 Hz over right parietal-occipital regions during the onset of vection. Note that this activity is obtained by averaged all completed two cycles of visual stimulation that contained the onset of vection which indicated by the button pressing of participants, hence the window is not locked with the event of button pressing. Owing to this, we also did not observe obvious activity over left motor regions which responsible for the finger movement for pressing the response button. Moreover, the center of uncovered effect originated from the right parietal-occipital regions rather than left hemisphere. Therefore, it is very unlikely that the SSVEP effect revealed in this study was simply due to the right-hand finger movement. Admittedly, to develop a validate indicator for the onset of vection, further explorations on this effect with other experiment procedure designs (e.g. oral report) are necessary. But this study has at least provided valuable and promising information for future works on developing more punctual EEG indicator for vection onset.

6.5.3 Top-down regulation: direct processing from CVF to PVF at frequency domain

Another interesting result revealed in this study is the interaction between the top-down attention regulation and vection. As demonstrated in Table 6.2 and Figure 6.3, when our top-down regulation put more emphasis on the self-motion perception, we experienced longer and more stable roll-vection than when we emphasis the stationary perception. This result is consistent with the finding in study one that re-direct the attention allocation can facilitate the strength of vection perception. According to the two-factor theory on attention mechanism (Egeth and Yantis 1997), the processing priority (or the processing resources) of our visual system can decide by two type of factors: the bottom-up factors (e.g. stimuli frequency, speed and size) and the top-down factors (e.g. experience, instruction and task requirement). In the past, most of EEG vection studies varied the bottom-up factors (e.g. the speed or direction of visual stimuli: Keshavarz, et al 2014; Vilhelmsen, et al 2015; Stróžak, et al 2016), thus very little have been reported how top-down factors modulate the vection effects on EEG

indicators. Hence, capturing the interaction of top-down regulation and EEG vection effects can shed light on the understanding of vection from a new perspective.

By comparing the Figure 6.7 and 6.17, we can found that the top-down attention regulation actually supported and strengthen the shift of power effect with vection by refining the frequency domain. More specifically, focusing on self-motion perception can facilitate the suppression at the occipital region (Oz) for CVF stimuli frequency (8.6Hz), and the activation at parietal region (Pz) for PVF stimuli frequency (12Hz). As discussed in section 6.5.2, the spatial power shift from occipital to parietal region implied the shift of processing emphasis from CVF to PVF in our visual system. As revealed in previous work, the decrease/increase of power at a particular frequency of the stimuli flicker, can indicate the impairment/enhancement of the processing emphasis at the particular visual field where the flick presented to (Morgan et al. 1996; Müller et al. 1998). Therefore, the top-down regulation actually facilitates this power shift of SSVEP by refining it in frequency domain, which shall further support the reallocation of processing emphasis from CVF to PVF and facilitate the perception of vection. Moreover, focus on stationary perception seems to enhance the enhancement of Pz only for the CVF stimuli frequency (8.6Hz), but hindered the enhancement of Pz for PVF stimuli frequency (12Hz) and shifted more energy to bilateral central regions during vection. This implied that top-down regulation reversed the power shift in frequency domain under stationary focus and hindered the processing of visual stimuli in PVF. In summary, the top-regulation effects were quite in line with the behavioral results that participants indeed experienced more vection period when focus on self-motion perception than stationary perception.

As for the simple-main effect of attention focus demonstrated in Figure 6.13, strengthening the self-motion perception suppresses the power of SSVEP whole brain wisely. For the period without vection, we found that this suppression effect was mainly direct at the regions which primarily response to the visual stimulation: the occipital region of 8.6Hz and the parietal-occipital regions for 12Hz. This general power reduction could possibly due to a general drop of processing resource in the visual flicker stimuli during self-motion focus

condition, since more resources have been directed to the processing on the spatial information, ambient motion and even some somatosensory and proprioception functions related to body awareness. Interestingly, we found the suppression effect at 12Hz demonstrated a bilateral pattern (originated from the C3 and C4 electrode) with vection perception, which is different from the centralized pattern (centered at Pz electrode) in the absent of vection (Figure 6.13). Note that the C3 and C4 electrodes are reported to reflect the vestibular activity during similar visual stimulation (Zhao 2017). Therefore, this might imply that during vection, the focus of top-down suppression effects has been shifted to bilateral-central regions which responsible for vestibular functions. Interestingly, this is also in line with Brandt's theory (1998) and many previous studies which reported suppression of vestibular regions during the vection perception (Bense et al. 2001; Brandt et al. 1998, 2002; Deutschländer et al. 2002; Wenzel et al. 1996).

6.5.4 Potential Limitations and Validations

To exclude the potential influence of volume conduction, we also validate the results by applying current source density analysis (parameters: the order of spline, $m=4$; precision of $1.0e-5$) at each electrode position (Kayser and Tenke 2006b, 2006a) before transforming the averaged EEG data into power spectrum at frequency domain. All of the topography maps remained robust with the current source density analysis.

Moreover, another concern is about the frequency selected for CVF and PVF stimulation. Although both 8.6 and 12 Hz are within the range of alpha band, different stimuli frequency may exhibit different baseline power and lead to different effect size introduced by top-down visual regulations under vection-inducing stimulation. However, reducing the PVF frequency ($<12\text{Hz}$) can disrupt the vection perception, as too slow flickering frequency interferes with the motion perception introduced by roll-rotation of random dots pattern. Future works with higher frequency in beta band and more counteract control procedures shall provide valuable validations and more insights on the mechanism of modulations on SSVEP during vection.

6.6 Summary

6.6.1 New findings and contributions

In this study, we further explored the visual responses regulation under vection identified in previous studies for CVF and PVF, using the more noise resistant steady-state VEP (SSVEP). More specifically, we have mainly explored the topography spatial properties of visual regulations at CVF and PVF, marked by different flickering frequency respectively. Results suggested that the processing of CVF stimulation mainly originated from occipital region and better captured by Oz electrode, while the processing of PVF stimulation mainly originated from parietal region and better captured by Pz electrode. Moreover, findings revealed a power shift of SSVEP from occipital region (marked by CVF stimulation) to parietal region (marker by PVF stimulation) during vection perception. This implies that the negative regulation of visual response during vection is mainly focused on the occipital visual cortex which response strongest to CVF stimulation, while the positive regulation mainly focused on the parietal visual areas which response strongest to PVF stimulation.

Moreover, we also found the magnitude of this power shift of SSVEP power during vection (especially for the suppression effect at 8.6Hz obtained from Oz electrode) is closely associated with VIMS susceptibility. This result is in line with our main hypothesis that during vection there is a processing emphasis shift from CVF stimuli to the self-motion cues in PVF to facilitate and stabilize the vection perception, which then contributes to the sensory conflict reduction and thus prevent the VIMS.

Furthermore, study three has identified new EEG signatures (SSVEP power at stimuli frequency from Pz electrodes) as quantitative vection indicators, as well as the SSVEP signatures (magnitudes on power shift from Oz to Pz electrode) as VIMS predictors. As the first EEG study adopted 32-channel covering the whole scalp, our findings are not only in line with previous experiment findings, also identified electrodes of interest (EOIs) for our following EEG study.

Last but not least, we move on with the practice of task-motivated attention re-allocation uncovered in study one. In this study, we not only confirmed that the top-down regulations on attention allocation can strengthen the intensity and stabilize the duration of roll vection perception, we also revealed that those regulations can facilitate the neurological vection effects reflected by the topography of SSVEP power. This further supports that we can use top-down task instruction to modulate the stability of vection perception and perhaps even the resistance to VIMS of viewer, without changing the properties of vection-inducing stimuli. Since this track of strategies does not hurt the experience of vection, these findings can provide good news for industry applications.

6.6.2 Raised further questions and focus of follow-up works

Admittedly, the prediction power of the EEG vection indicators and VIMSS predictors are limited ($R^2 < 0.4$). This might due to the drawbacks of localization method: the analysis of VEP can only reflect the local activity within particular brain function regions. However, as we introduced in chapter 2&3, both the processing and integration of self-motion cues and the reduction of sensory conflict should heavily rely on the cortical coordination between visual and extra-visual regions. Therefore, exploring EEG indicators which can reflect these information integration and coordination under vection-inducing stimulation, is not only important for better understanding of vection, but also may contribute to more reliable and effective EEG indicators for vection and VIMSS.

Moreover, both study two and three were explored with relatively small sample size with large variation in VIMSS ($N < 20$). Firstly, the large individual variation introduced by VIMS susceptibility might hide the effects related to vection. Secondly, we also were lack of sufficient representative participants who are very susceptible or highly resistant to VIMS, which may make some features which are able to differentiate the VIMS group less prominent. Hence, future explorations with a larger and more representative group of subjects are desirable.

Therefore, in the follow up works, we go further to explore the cortical coordination between the visual regions (characterized by the EOIs identified in study three) and other widely distributed brain regions. Particularly, in study four, we examined the phase locking value (PLV) between EEG electrodes under the vection-inducing stimulation. As introduced in chapter 3, PLV can reflect the dynamic links responsible for the cortical coordination between different sensory modalities and the central integration during self-motion perception. Moreover, in study four, we also recruit more representative participants and assign them into different VIMS group (resistant vs. susceptible group) by screening participant with the score of MSSQ-short to ensure participants are either very susceptible to VIMS or highly resistant to it.

CHAPTER 7 STUDY FOUR – DYNAMIC LINKS AND CONNECTIVITY MAPS UNDER VECTION-INDUCING STIMULATION

7.1 Introduction

In this study, we focus on the functional connectivity and its dynamic changes between brain regions under vection-inducing stimulation. More specifically, we explored whether the strength and range of cortical coordination between visual and other regions are differently organized in VIMS susceptible and resistant participants, while controlling the onset of vection and nausea. In particular, we record EEG when VIMS susceptible or resistant participants were exposed to short periods of vection-inducing stimulation (similar to study one) until vection onset, with sufficient rest between repetitions to avoid nausea. Both the VEP and the phase locking value between electrodes during visual stimulation were analyzed. As theta-band synchronization is closely associated with self-motion sensory integration and conflict modulations (Aitake et al. 2011; Araújo, Baffa, and Wakai 2002; Jo, Malinowski, and Schmidt 2017; White et al. 2012) and reported to correlated with motion sickness (Chelen et al. 1993), we would focus on theta band in phase synchronization analysis.

7.2 Objective and hypotheses

The objectives of this study are: 1) explore the dynamic changes of functional connectivity under vection-inducing stimulation; 2) explore the dynamic changes of functional connectivity under vection-inducing stimulation before and after vection onset, and search for vection covariates; 3) explore functional connectivity signatures that differently organized between VIMS susceptible people and resistant people.

Based on the sensory conflict theory and Brandt's theory (Brandt et al. 1998; Reason 1978), processing vection-inducing stimuli requires more between-modality cortical coordination.

Hence, we expected that phase synchronization between electrodes over vection related areas and other extra-visual areas should be stronger under vection inducing-stimulation, as compared to the synchronization under control visual stimuli (H12a). Moreover, as enhanced phase synchrony is reflecting strengthen of cortical coordination (Murray and Wallace 2011; Varela et al. 2001), which can facilitate the reduction of sensory conflicts, we predicted that resistant participants should show stronger effects than susceptible participants (H12b). Furthermore, based on Brandt's theory, the sensory conflict shall be effectively reduced or resolved in resistant participant after vection onset (which means viewer's central integration model successfully updated toward visual system and suppressed other extra-visual systems after vection onset) (Deutschländer et al. 2002), so that the general activity in extra-visual systems shall be suppressed and sustained cortical coordination between central integration and those extra-visual systems shall be decreased. Therefore, reduced phase synchronization after vection onset can reflect the effectiveness of conflict reduction through cortical coordination. As we hypothesized that the sensory conflict reduction is more effective in resistant participants, we expect the reduction of phase synchronizations after vection onset shall be stronger in resistant participant (H13a). The magnitude of effect is negatively correlated with the susceptibility of participants (H13b).

7.3 Methods

7.3.1 Participants

In total 27 right-handed university students, with 20/20 (or corrected) eyesight, were recruited with complete informed consent. Participants were screened by their VIMS susceptibility based on the score of Motion Sickness Susceptible Questionnaire (MSSQ-Short), with child (MSSQ_C), adult (MSSQ_A) and total (MSSQ_T) scale (Golding 1998). Twelve participants scored over 70% percentile in MSSQ_T were included in VIMS susceptible (VSU) group, while fifteen participants scored below 30% percentile in MSSQ_T were included in VIMS resistant (VRE) group. All participants are free of any vestibular injury or medical treatment. None of them were heavy video game players or had rich

experience with large-screen visual motion stimuli. Gender was balanced in each group and there are no group age differences (Table 7.1).

7.3.2 Stimuli, apparatus, task and procedures

Stimuli and task

Same as study three, grey dots (size: $0.5\sim1.3^\circ$ of FOV) were randomly generated on a black background with 700-750 dots visible during all conditions. For vection-inducing stimulation, all grey dots coherently rotated anticlockwise (angular velocity: $32^\circ/\text{s}$) around screen center (ROT). For control (COT) condition, the dots moved toward randomized directions, while keeping linear velocity paralleled with the angular velocity in ROT (same as study three). Participants were instructed to fix their eyes on a center red dot (diameter: 0.6° of FOV; luminance: 5.05 cd/m^2) to suppress OKN and other types of eye movements.

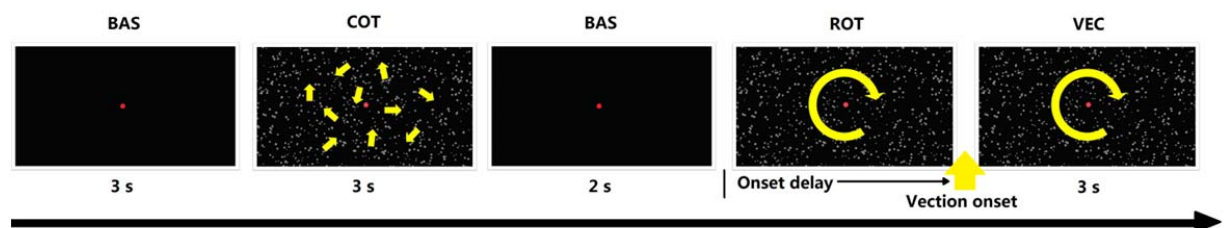


Figure 7.1 The procedure of each trial. (Note that participants are required to indicate the onset of vection by pressing once the response button under the ROT stimulation)

Procedure

Each trial started with 3s baseline black background (BAS), followed by COT stimuli of 3s. Then the ROT stimuli started after a 2s-BAS. Participants were trained to press a key button with right hand index finger to indicate the onset of roll vection (they watched one trial of stimuli demo and received sufficient training on how to identify the onset of self-rotational vection). After the response, ROT stimuli would continue 3s for vection (VEC) condition

(see Figure 7.1). The maximum exposure time was set to 1min. If no response is made, the ROT ends after 1min (see Table 7.1 for response rate). Each block consists of 12 trials with sufficient rest in-between to avoid any nausea. Before next block, participants rested for 3-10min, until no fatigue or discomfort was reported. Most participants completed total 12 blocks (see Table 7.1 for summary). All procedures were approved by the ethics committee of the Hong Kong University of Science Technology and performed in accordance with the Declaration of Helsinki.

Apparatus and EEG recording

The stimuli were presented using the same apparatus (46-in LCD monitor; Screen size: 102.1×57.5cm; FOV: 93.5°× 61.8°; View distance: 48cm), with the same setups used in former study to control the head/body movement and eliminate environment visual cues (Appendix B). Same as in study three, the EEG was recorded together during stimuli presentation with four EOGs (left and right horizontal; upper and lower vertical) channel using a NuAmps Amplifier (DC-coupled, 22 bit, monopolar) from 36-channel Ag/AgCl sintered electrodes (Quik-Cap, Compumedics Neuroscan) based on the international 10-10 system (Appendix H) referenced to linked mastoid electrodes. Impedances between all channels and ground channel (AFz) were kept below 5kΩ. Same procedures and protocols validated in study three for the whole scalp EEG recording and synchronization triggers with visual stimuli were applied in this study.

7.3.3 Response measures

EEG recordings and preprocessing

Raw data were digitized at a sampling rate of 1000 Hz and a bandwidth of DC-260Hz, and then filtered offline with an FIR filter at the band-pass of 1.6-47Hz. Data were segmented into epochs starting from 1.5s prior to the onset of each condition (COT/ROT/VEC) and ending at 3s with baseline corrected for pre-onset 1.5s. Independent components analysis (ICA) was applied to these epochs using EEGLAB (Delorme and Makeig 2004), and

components identified as eye movement artifacts was removed using automatic toolbox ADJUST (Mognon et al. 2011). The epochs contaminated by other artifacts were rejected based on moving window peak-to-peak method (window size: 200ms; step: 50ms; threshold: $\pm 100 \mu\text{V}$) and extreme value of remaining components (threshold: $\pm 20 \mu\text{V}$). One participant (1 female, VSU group) was excluded due to extensive motion artifacts ($> 50\%$ epochs rejected). The average epochs remained for each condition and their standard deviations were as follow: COT (91.6 ± 22.2), ROT (105.5 ± 19.0) and VEC (101.0 ± 21.1). Current source density analysis (parameters: the order of spline, $m=4$; precision of $1.0\text{e-}5$) was then applied at each electrode position to reduce the influence of volume conduction (Kayser and Tenke 2006b, 2006a).

VEP analysis

To analyze the visually evoked potential (VEP), remained clean epochs were trimmed to smaller window (-0.5~1s) and averaged for the two types of visual stimulations (COT, ROT), respectively. Based on the topography of VEP results (see Figure 7.2), the P1, N1/N2 and P3 components at parietal electrodes were analyzed. In detail, the mean amplitudes of the P1 (time window: 135-195ms), the early N2 (time window: 195-250ms) and P3 (time window: 250-395ms) at electrode Pz, the bilateral late N2 (time window: 260-335ms) at electrode P7/P8, and late P3 (time window: 330-410ms) at electrode P3/P4 were calculated for each individual.

Phase synchronization and network analysis

Wavelet analysis was conducted to obtain the instantaneous phase for each time point in clean epochs applying Morlet's mother function. We applied a constant ratio $f/\sigma_f = 6$ with f ranged from 2-46 Hz (1-Hz steps), where $\sigma_f = 1/\sqrt{2\pi}\sigma_t$ and σ_t is the standard deviation of the Gaussian window (Kawasaki, Kitajo, and Yamaguchi 2014; Lachaux, Jean-Philippe Rodriguez et al. 2000). The phase synchronization was evaluated between each electrode pair for each time point in the epoch (-1~3s) of all conditions (ROT, COT, VEC) by phase locking values (PLV) (Lachaux et al. 1999; Totah, Jackson, and Moghaddam 2013) to assess

functional connectivity mediating information integration between distant areas. For time point t , frequency f , and electrode j and k , across the available N epochs, following the equation:

$$PLV_{j,k}(f, t) = N^{-1} | \sum^N e^{i[\phi_j(t) - \phi_k(t)]} |,$$

where $\phi(t)$ is phase at t , i is $\sqrt{-1}$, and $||$ is the complex modulus. As we focused on the theta band, PLV is averaged for theta-band frequency list (4-7Hz) and transformed into PLV_z according to Rayleigh's Z value (Fisher 1993; Totah et al. 2013) to correct for the bias of the number of epochs:

$$PLV_z = N \times PLV^2 \text{ (} N: \text{number of epochs)}.$$

Node density in dynamic phase synchrony network

After obtaining the PLV_z , we formed dynamical phase synchrony networks, where 30 EEG electrodes are nodes and the edge between each node pairs at every time point is weighted by the PLV_z . In connectivity networks analysis, density of each node is calculated by averaging the weight of all connections of this node and high density nodes in the network is referred to as ‘hubs’ (van den Heuvel and Sporns 2013; Stam et al. 2007). These hubs can increase the communication efficiency of the network which facilitate the cortical coordination (van den Heuvel et al. 2013; Hilger et al. 2016; de Reus and van den Heuvel 2013). To demonstrate the dynamic changing of nodes density and hub regions under vection-inducing stimulation, we calculate the density of each node at each time point (see Figure 7.5 for the topography of nodes density distribution in ROT condition).

Vection and VIMS reports

Similar to former studies, participants were trained to report vection intensity after each trial based on a vection magnitude scale (1=no vection; 5=saturated vection; Webb & Griffin, 2003; see Appendix G). The onset latency of vection was obtained by the time period from start of ROT stimuli to the key press for each trial. VIMS symptoms were monitored with

pre-exposure Simulator Sickness Questionnaire (SSQ) before the start of experiment and post-exposure SSQ (Kennedy et al. 1993) after the finish of all blocks.

7.4 Result

7.4.1 Behavioral results and subjective reports

The mean and standard deviation of vection intensity, vection onset delay, strong vection trial percentage (trials with intensity > 2), MSSQ scores and pre-/post-SSQ scores of each VIMS group (VSU/VRE) are reported, along with p-value of between-group two-tailed independent-sample t tests in Table 7.1. Only the MSSQ scores of all scale are significantly higher for VSU group ($P < 0.001$), no other significant difference is inherited with group, including the VIMS symptoms evaluated by SSQ.

7.4.2 VEP results

Two-way mixed measures ANOVAs including the factor of visual stimuli (ROT/COT) and VIMS groups (VSU/VRE) were conducted separately for middle components at Pz electrode (Figure 7.2 & 7.3). For the P1 peak at 178ms (P178), ROT condition showed significantly suppressed amplitude compared to COT [$F(1,24) = 22.41$, $p < 0.001$]. No interaction or VIMS group effects were found for P178. For N2 peak at 223ms (N223), amplitude was significantly increased in ROT compared to COT [$F(1,24) = 31.21$, $p < 0.001$]. Moreover, there is significant interaction for visual stimuli \times VIMS groups, where VSU group showed stronger N223 increase compared to VRE group [$F(1,24) = 5.92$, $p = 0.023$, see Figure 7.4]. The simple main effect for visual stimuli is significant both for VRE ($p=0.011$) and VSU group ($p=0.001$), while no main effect for VIMS group was significant, possible due to large individual variations. For P3 peak at 305ms (P305), amplitude in ROT was significantly larger than COT [$F(1,24) = 31.48$, $p < 0.001$], with no group and interaction effects.

Table 7.1 Group characteristics in demography, VIMS reports and vection perception

	VIMS susceptible	VIMS resistant	<i>P</i>
Age (years)	24.5 ± 1.2	24.3 ± 2.7	0.893
Gender (% male)	54.5%	60%	0.791
MSSQ score*			
Child (0-27)	17.4 ± 3.7	1.7 ± 1.3	<0.001
Adult (0-27)	12.3 ± 5.7	1.3 ± 1.2	<0.001
Total (0-54)	29.6 ± 8.0	3.0 ± 2.1	<0.001
Pre-SSQ score (0-120)	0.5 ± 0.7	2.6 ± 3.8	0.073
Post-SSQ score (0-120)	2.4 ± 2.6	4.6 ± 5.2	0.221
Post-Pre paired T test P value	0.022	0.210	
Vection report			
Intensity (1-5)	2.9 ± 0.6	2.8 ± 0.6	0.666
Strong trial percentage (% intensity>2 trials)	75.0 ± 31.4	73.4 ± 30.7	0.900
Onset delay (Sec)	9.7 ± 9.2	8.6 ± 4.3	0.716
Individual onset delay Std. (Sec)	4.1 ± 4.3	4.3 ± 4.4	0.926
Response rate (%)	99.6 ± 1.3	99.3 ± 1.9	0.560
Total trials completed	135.3 ± 21.9	139.9 ± 9.5	0.525
Total clean epochs	282.9 ± 48.0	309.4 ± 51.5	0.195
EEG quality (% clean epochs)	72.7%	76.8%	0.320

* Except MSSQ score, all group comparisons are not significant with two-tail independent-sample T-test; noted that, SSQ increased only for VSU group after experiments (two-tail paired-sample T-test, $p = 0.022$), but the severity of sickness was kept very low (2.4 in 120), with no severer than VRE group.

Three-way mixed measures ANOVAs including the factor of visual stimuli (ROT/COT), VIMS group (VSU/VRE) and laterality (left/right) were conducted separately for bilateral N2 components at electrodes P7/P8 and P3 components at electrodes P3/P4 (Figure 7.2 & 7.3). For late N2 peak at 290ms (N290), ROT condition showed significantly enhanced amplitude compared to COT [$F(1,24) = 32.46$, $p < 0.001$], with no group and laterality effect. For late P3 peak at 350ms (P350), amplitudes in ROT condition was significantly suppressed compared to COT [$F(1,24) = 8.24$, $p = 0.008$], with no group and laterality effects.

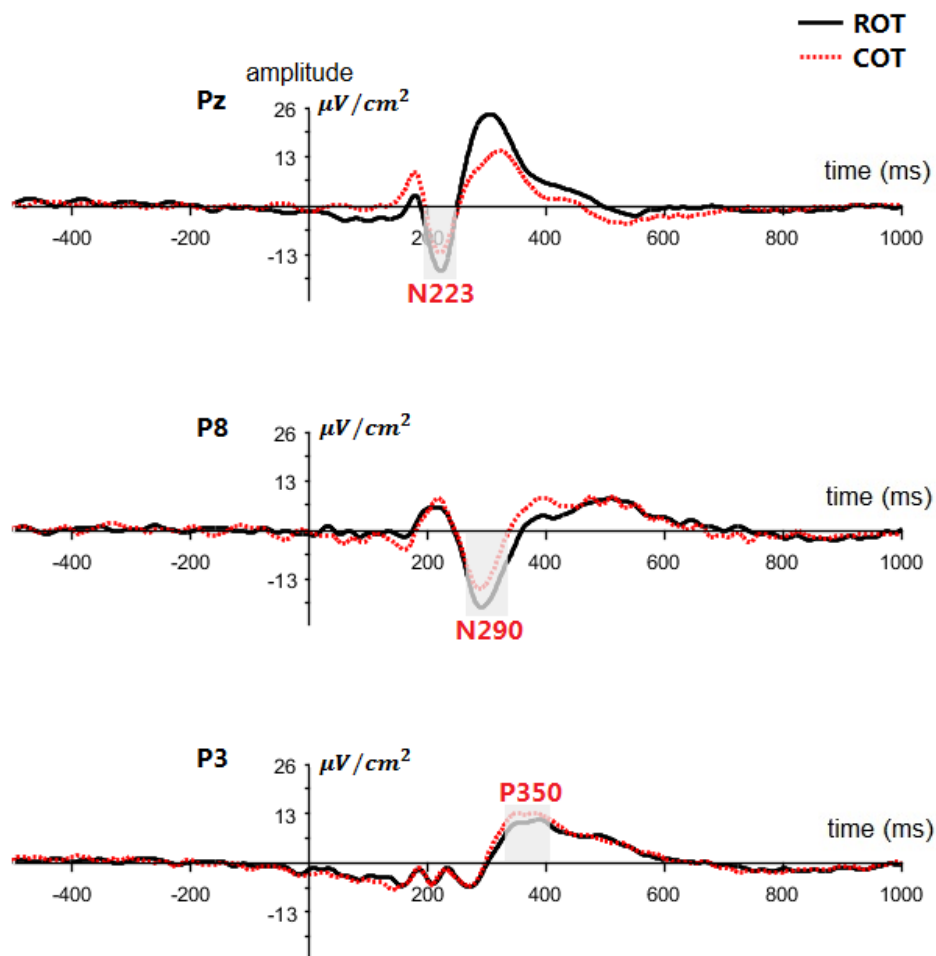


Figure 7.2 Averaged VEP for two stimuli conditions at electrodes of interest (shadowed area illustrate the time window for each components).

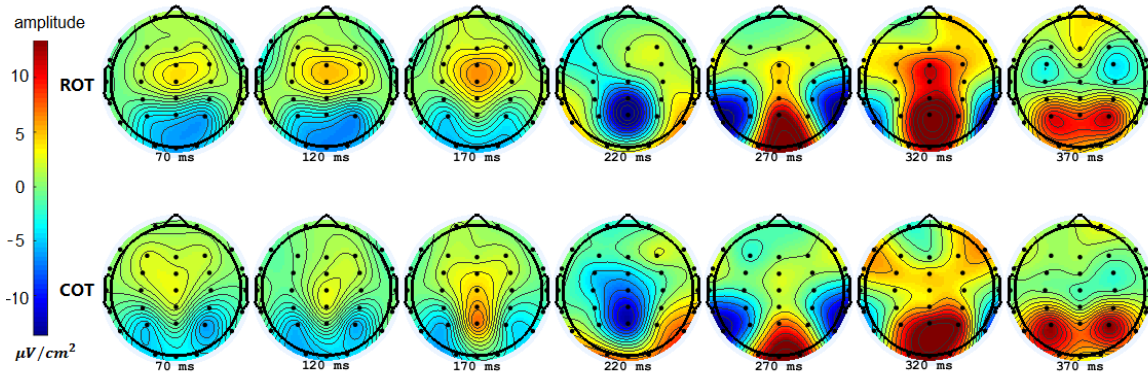


Figure 7.3 The topography map of VEP amplitude under ROT and COT condition.

As N2 is the well-known motion-onset VEP (Anon 2007; Kubová et al. 1995; Pitzalis, Strappini, et al. 2012) and reported as self-motion related VEP in former studies (Keshavarz and Berti 2014; Vilhelmsen et al. 2015), we conducted linear regression models to predict reported vection intensity by adding absolute amplitudes (ROT condition) of N223 at Pz and N290 at P7/P8, along with their amplitude increments (ROT subtract COT condition) as predictors. To control other external factors, the vection intensity, onset delay, epoch numbers were also added in the model in stepwise manner. Results showed that only the increment of N223 amplitude ($N223_{inc}$, $R^2 = 0.27, p = 0.006$) and the absolute N290 amplitude at P8 ($N290_{P8_{ROT}}$, $R^2 = 0.16, p = 0.042$) were positively associated with the averaged vection intensity of each participant (see Figure.2d for scatter plot). No significant effect was found for any model using predictors from P7. Moreover, $N223_{inc}$ was also positively associated with individual MSSQ_T ($R^2 = 0.22$) and MSSQ_C ($R^2 = 0.29$), either with or without controlling other external factors (Table 7.2).

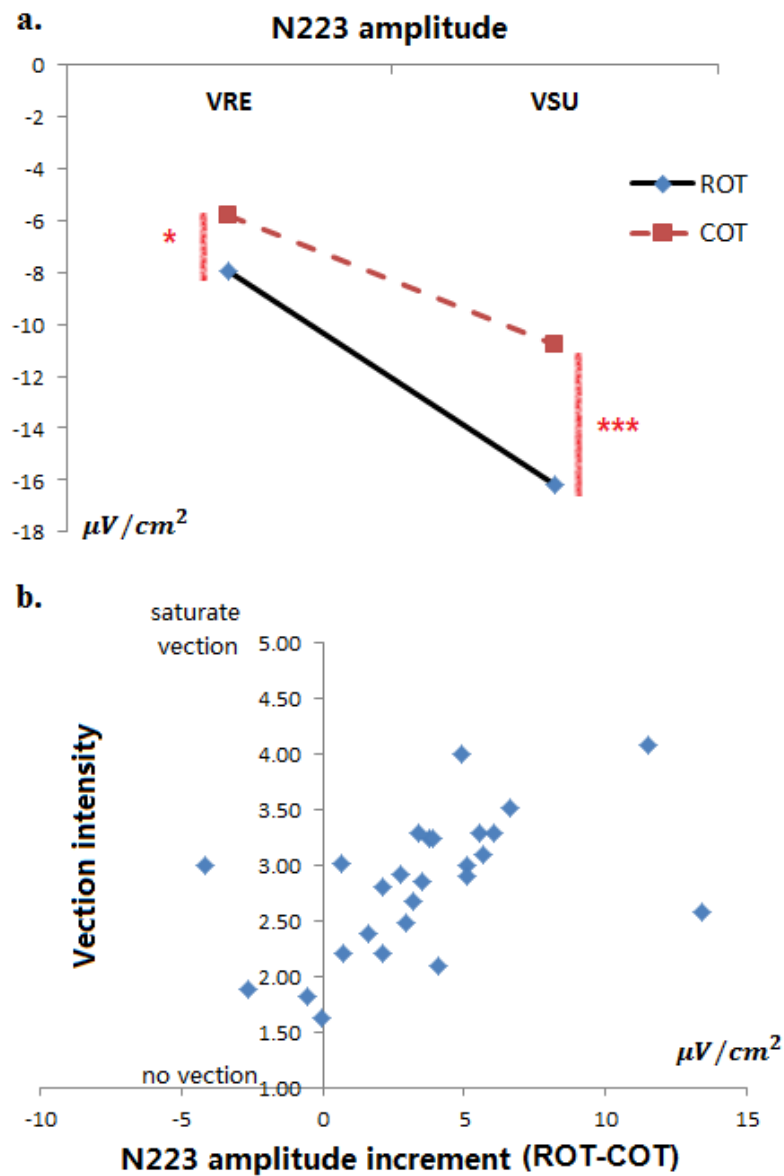


Figure 7.4 VEP results for N=26 participants. a. demonstrate the interaction of VIMS group \times visual stimuli on N223 amplitude (** $p=0.001$; * $p<0.05$). b. the scatter plot for vection intensity and the increment of N223 (amplitude in ROT condition subtracting amplitude in COT condition).

7.4.3 Dynamic node density in phase synchrony networks

For the calculated nodes density of the dynamic phase synchrony network, we conduct cluster-based permutation tests between COT and ROT condition for each VIMS group using Fieldtrip toolbox (Oostenveld et al. 2011). The alpha value of the permutation test for cluster-level statistic is set at 0.025 (two-tailed) to control for the false alarm rate and 2000 times of random draws were conducted to approximate the permutation distribution with a within-subject design (Genovese, Lazar, and Nichols 2002; Maris and Oostenveld 2007). For VRE group, two significant positive clusters were found (see Figure 7.6). First one is located over the parietal and central regions (time window: 208- 419ms, $p=0.005$), and later one is located over the right temporal-parietal regions (time window: 646-816ms, $p=0.008$). For VSU group, only one positive cluster was found (see Figure 7.6). It is located over parietal midline region (time window: 281-405ms, $p=0.006$). Note that no significant negative cluster was found either in VRE or VSU group. In summary, significantly enhanced phase synchrony was showed under vection-inducing stimulation, which supported H12a. Moreover, VIMS resistant participants demonstrated more and larger positive cluster than susceptible participants, which supported H12b.

For the VEC condition, the event window is locked with button pressing response of participant to indicate the onset of vection. Therefore, the period starting from 1s prior to and 0.5s after button pressing was excluded from the analysis to avoid the interference of button pressing and response delay. The density value is then average for a window of 500ms to represent the node density before vection (BVEC) onset and after vection (AVEC) onset under the same visual stimulation for each node (see Figure 7.7). Then cluster-based permutation tests were conducted between BVEC and AVEC for each VIMS group with same parameters (two-tailed, $\alpha=0.025$, permutation numbers=2000, within-subject design). Only one significant negative cluster was found in VRE group, which is located over right central-frontal region (see Figure 7.8, $p=0.006$). No significant cluster was revealed in VSU group. In summary, the strength of phase synchronization is revealed to be reduced

after vection onset for VIMS resistant participants, while no reduction was found for susceptible people, which supported the H13.

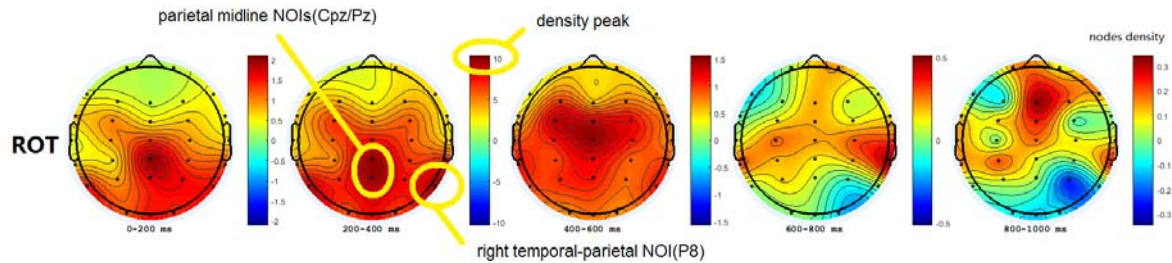


Figure 7.5 Topography illustrating the changes of node density in phase synchrony networks under ROT condition (Note that the nodes density reach peak at 200-400ms; and those nodes demonstrating the highest density are the dynamic hubs in the network).

7.4.4 The distribution and range of phase synchrony

In addition to the total averaged strength of phase synchronization connected to each node (node density), we selected several nodes of interest (NOIs) based on both the hub regions (see Figure 7.5) and significant cluster (see Figure 7.6 & 7.8) to further analyse the distribution and range of the phase synchrony: C4 (right central NOI), Cpz/Pz (parietal midline NOIs), P8 (right temporal-parietal NOI) and Fz/F4 (right central-frontal NOIs).

We assessed the subnetworks connected to cluster NOIs within their cluster window (for ROT/COT, C4 and Cpz/Pz at win1 of 208-419ms; P8 at win2 of 646-816ms; for VEC, Fz/F4 at win3 of 500-1000ms). Moreover, we also assessed the subnetwork of the hub NOIs (see Figure 7.5: Cpz/Pz, P8) within a sustained longer period (win4: 1000ms-2500ms), since this period can reflect the lasting information integration and cortical coordination under vection-inducing stimulation. To obtain a threshold mask for each subnetwork, permutation tests (Sun, Hong, and Tong 2012; Winkler et al. 2016) were conducted for all edges (node pairs). In detail, we shuffled the condition labels (ROT/COT; BVEC/AVEC) of the edge weights (averaged PLV_z of each window) within each subject and obtain group mean difference

between conditions for 2000 times to approximate permutation distribution under the null hypothesis (no condition difference) of our sample. Edges with the increment of weight (ROT subtract COT; BVEC subtract AVEC) that larger than 97.5% percentile or lower than 2.5% percentile in the permutation distributions are marked as passing the positive or negative threshold mask (see Figure 7.10-7.13 for positive and negative averaged group subnetworks at each window for each VIMS group). By applying these threshold masks to each participant, we can obtain positive and negative binary subnetworks and calculated their total node degrees (number of connections) for each participant, where larger node degrees (more connections in the subnetwork) indicate a wider range of phase locking connections.

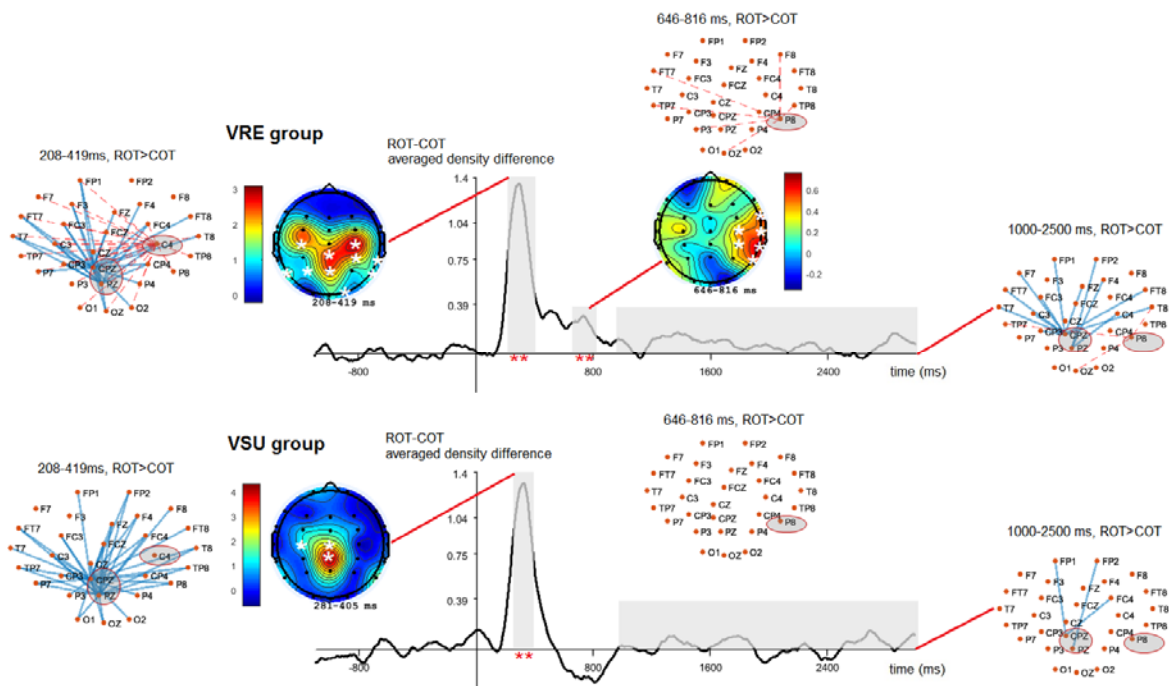


Figure 7.6 Illustration for the significant positive clusters which showed higher nodes density in ROT than COT condition. [The line graphs demonstrate the averaged node density across all nodes for each VIMS group. The upper topographies show the two positive clusters in VRE group along with the distribution of connections to NOIs passing the positive threshold (indicating higher PLV_z in ROT than COT within each assessed window period). The lower topography shows the positive cluster in VSU group (Note the cluster is much narrower than VRE group)].

As the node degrees in the subnetwork for each window period can reflect the wideness and range of phase synchrony in the subnetwork, to examine whether there are group differences in the range of phase synchronization, we conduct between-group independent-sample T-test for node degrees in each subnetwork. Significant higher node degrees were found for VRE group in positive subnetworks of right-central NOI (C4) at win1 [$t = -2.298, p = 0.031$], right temporal-parietal NOI (P8) at win2 [$t = -2.800, p = 0.010$], parietal midline NOIs (CPz/Pz) and right temporal-parietal NOI (P8) at win4 [$t = -2.770, p = 0.011$] (see Figure 7.6 & 7.8 for illustration of significantly different group subnetworks). Moreover, significant higher node degrees were also found for VRE group in negative subnetworks of right central-frontal NOIs (Fz/F4) at win3 [$t = -3.022, p = 0.006$]. In general, VIMS resistant group demonstrated wider range of strengthened phase synchronization than susceptible group under vection-inducing stimulation, which supported **H12b**. Moreover, after vection onset, VIMS resistant group showed wider range of reduction in phase synchronization than susceptible group, which supported **H13**.

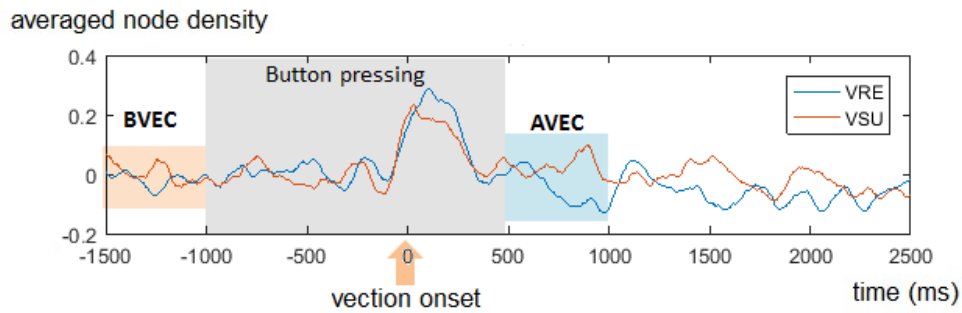


Figure 7.7 The changed of node density in phase synchrony network before and after the vection onset. (Note that the line graph shows the averaged node density across all nodes for VRE and VSU group with baseline corrected by BVEC period from -1500 to -1000ms).

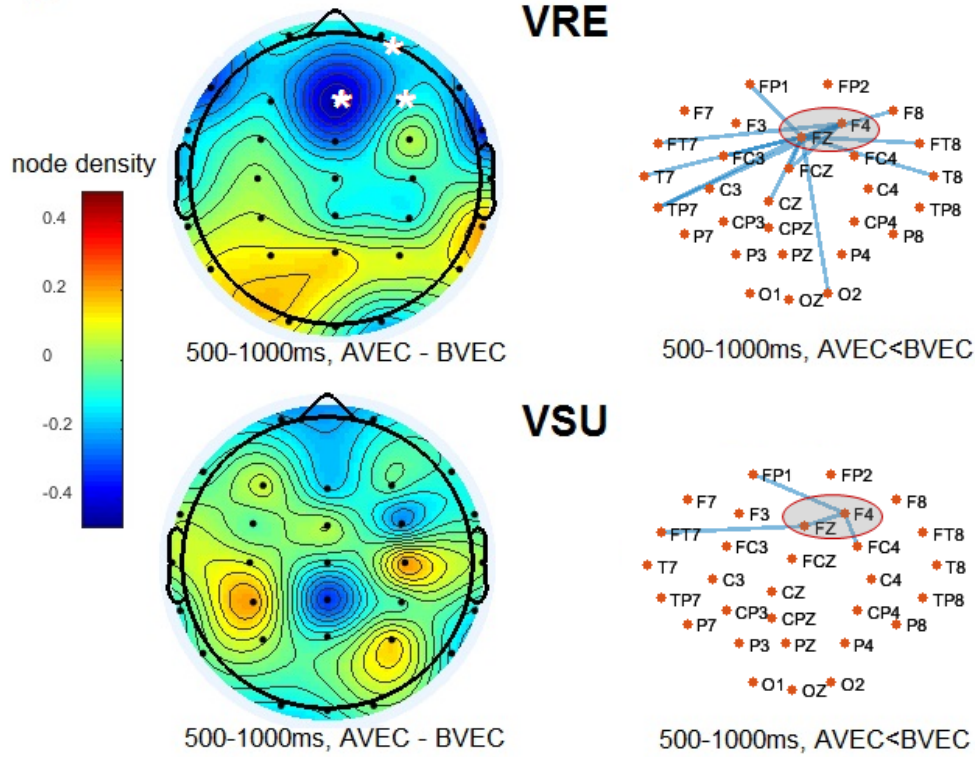


Figure 7.8 The significant negative cluster in VRE group (indicating AVEC<BVEC) and the distribution of connections to right central NOIs passing the negative threshold (indicating smaller PLV_z in AVEC than BVEC within assessed window period).

Furthermore, we find these indexes for phase synchrony network (node degrees in positive subnetwork and negative subnetwork) are negatively correlated with the MSSQ score of participants (see Table 7.2), which supported **H13**. We construct a regression model for each potential indicator with other control variables (the vection intensity, onset delay, and epoch numbers) added in the model. Moreover, a generally model is constructed for each MSSQ scale by stepwise adding all the potential predictors to find the best predictors with highest prediction power and exclude those predictors with low contribution to the model. Table 7.2 contained two coefficient columns for each predictor: the first one shows the coefficient in their simple models, while the second one indicates the contribution to general models. It is revealed that the right central-frontal NOIs and right temporal-parietal NOI (P8) produce the

highest prediction power for total scale [$R^2 = 0.52$]. The results are robust with or without adding the vection intensity, onset delay, and epoch numbers in the regression model.

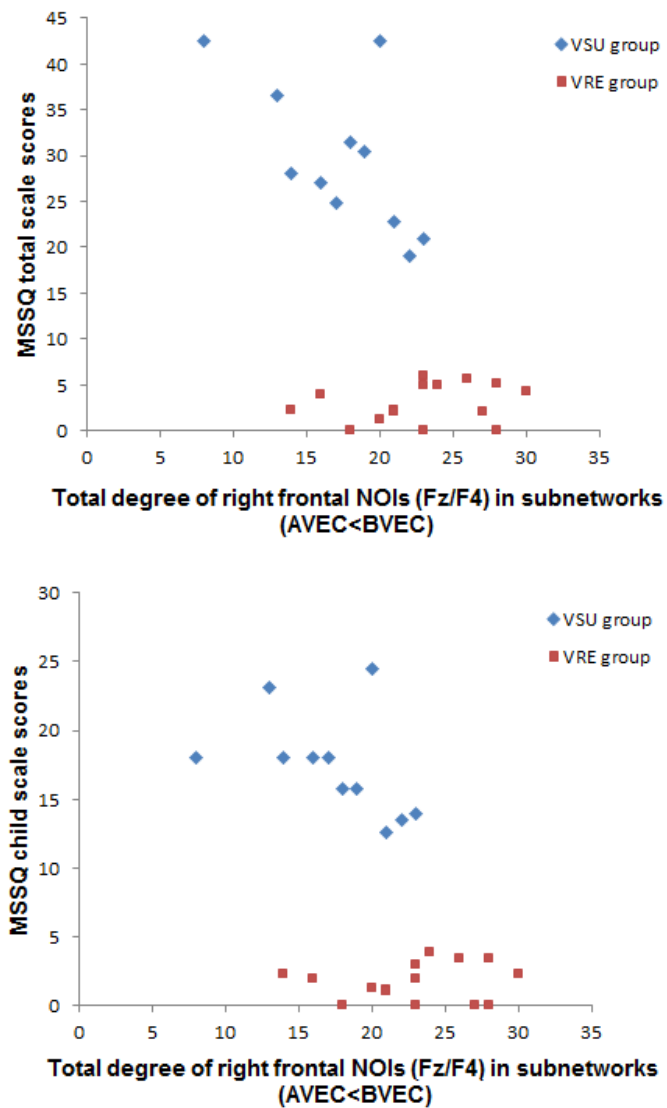


Figure 7.9 scatter plot for MSSQ scores and the indicator calculated from degree of the right central NOIs (Fz/F4) in negative subnetwork (number links indicating smaller PLV_z in AVEC than BVEC).

Table 7.2 Regression models for MSSQ scores with EEG signatures as predictors

predictors	MSSQ scores					
	Child scale		Adult scale		Total scale	
Single model	<i>Beta</i>	<i>R</i> ²	<i>Beta</i>	<i>R</i> ²	<i>Beta</i>	<i>R</i> ²
<i>N223_{Inc}</i>	0.474*	0.22*	-	-	0.474*	0.22*
	(p=0.014)	(p=0.014)			(p=0.014)	(p=0.014)
<i>Degree_{rC_win1}</i>	-0.521**	0.27**	-	-	-0.465*	0.22*
	(p=0.006)	(p=0.006)			(p=0.017)	(p=0.017)
<i>Degree_{rTP_win2}</i>	-0.518**	0.27**	-0.460*	0.21**	-0.543**	0.26**
	(p=0.007)	(p=0.007)	(p=0.018)	(p=0.018)	(p=0.003)	(p=0.003)
<i>Degree_{rF_win3}</i>	-0.559**	0.31**	-0.584**	0.34**	-0.590**	0.32**
	(p=0.003)	(p=0.003)	(p=0.002)	(p=0.002)	(p=0.002)	(p=0.002)
<i>Degree_{hub_win4}</i>	-0.486*	0.24*	-0.391*	0.15*	-0.460**	0.21**
	(p=0.012)	(p=0.012)	(p=0.048)	(p=0.048)	(p=0.018)	(p=0.018)
General model		0.69*** (p<0.001)		0.47** (p=0.001)		0.52*** (p<0.001)
<i>N223_{Inc}</i>	-		-		-	
<i>Degree_{rC_win1}</i>	-0.363* (p=0.011)		-		-	
<i>Degree_{rTP_win2}</i>	-0.427** (p=0.002)		-0.366* (p=0.026)		-0.416** (p=0.010)	0.52*** (p<0.001)
<i>Degree_{rF_win3}</i>	-0.244 (p=0.094)		-0.518** (p=0.003)		-0.515** (p=0.002)	
<i>Degree_{hub_win4}</i>	-0.299* (p=0.032)		-		-	

***p<0.001; ** p<0.01; * p<0.05. *N223_{Inc}* = the increment of N223 amplitude in ROT condition after subtracting amplitude in COT condition. *Degree_{rC_win1}* = the degree of right central NOI (C4) in positive subnetwork showing enhanced *PLV_z* in ROT condition than COT condition at win1(208-419ms). *Degree_{rTP_win2}* = the degree of right temporal-parietal NOI (P8) in positive subnetwork at win2 (646-816ms). *Degree_{hub_win4}* = the degree of hub NOIs (Cpz/Pz; P8) in positive subnetwork at win4 (1000-2500ms). *Degree_{rF_win3}* = the degree of right frontal NOIs (Fz/F4) in negative subnetwork showing less *PLV_z* in AVEC period than BVEC at win3 (500-1000ms). All significant predictors for MSSQ scores remain robust after adding epoch numbers, vection intensity and onset delay in the regression model. Note that after adding synchronization based predictors into stepwise model will exclude localization based predictor *N223_{Inc}*.

Win1:208-419ms NOIs: Cpz/Pz and C4

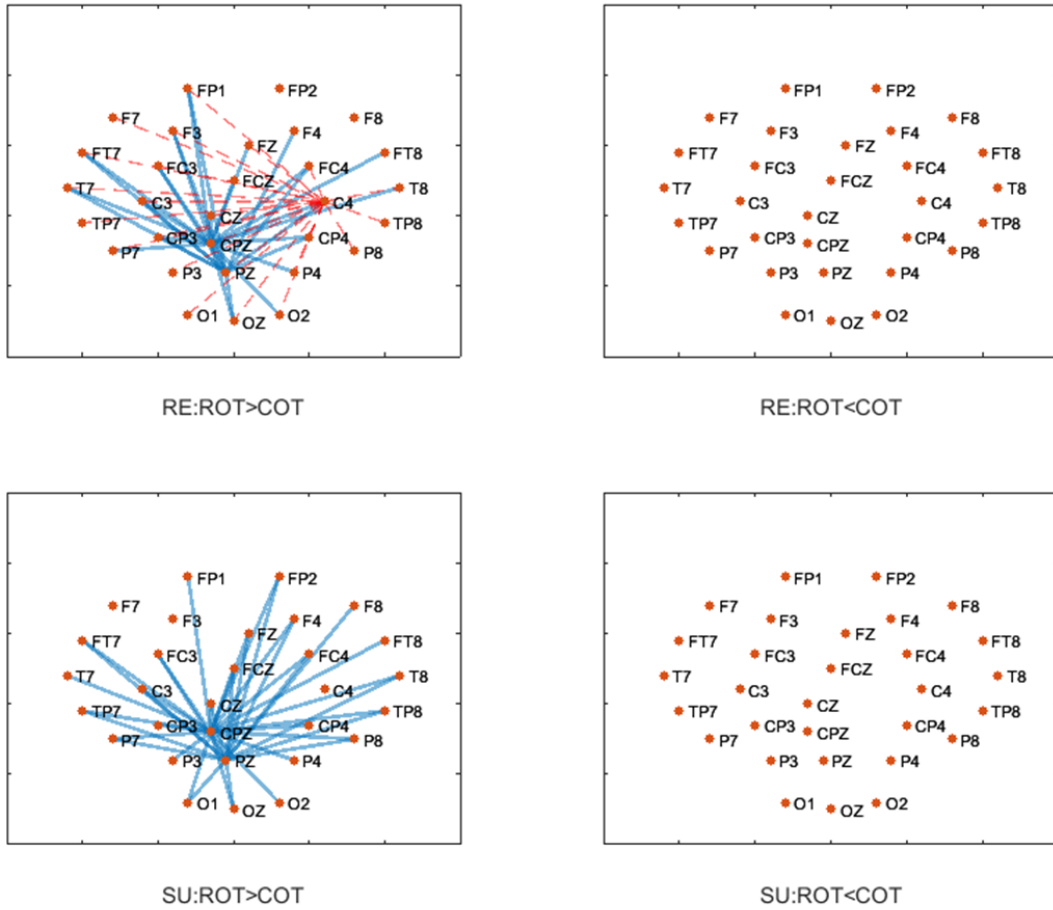


Figure 7.10 Positive and negative subnetwork connected to NOIs (Cpz/Pz and C4) calculated from group averaged PLV node density difference between ROT and COT condition at 208-419ms (two left graphs showed the distribution of connection to NOIs which passed the positive threshold; two right graphs showed the connections to NOIs which passed the negative threshold; RE: the VIMS resistant group; SU: the VIMS susceptible group)

Win2: 646-816ms NOIs: P8

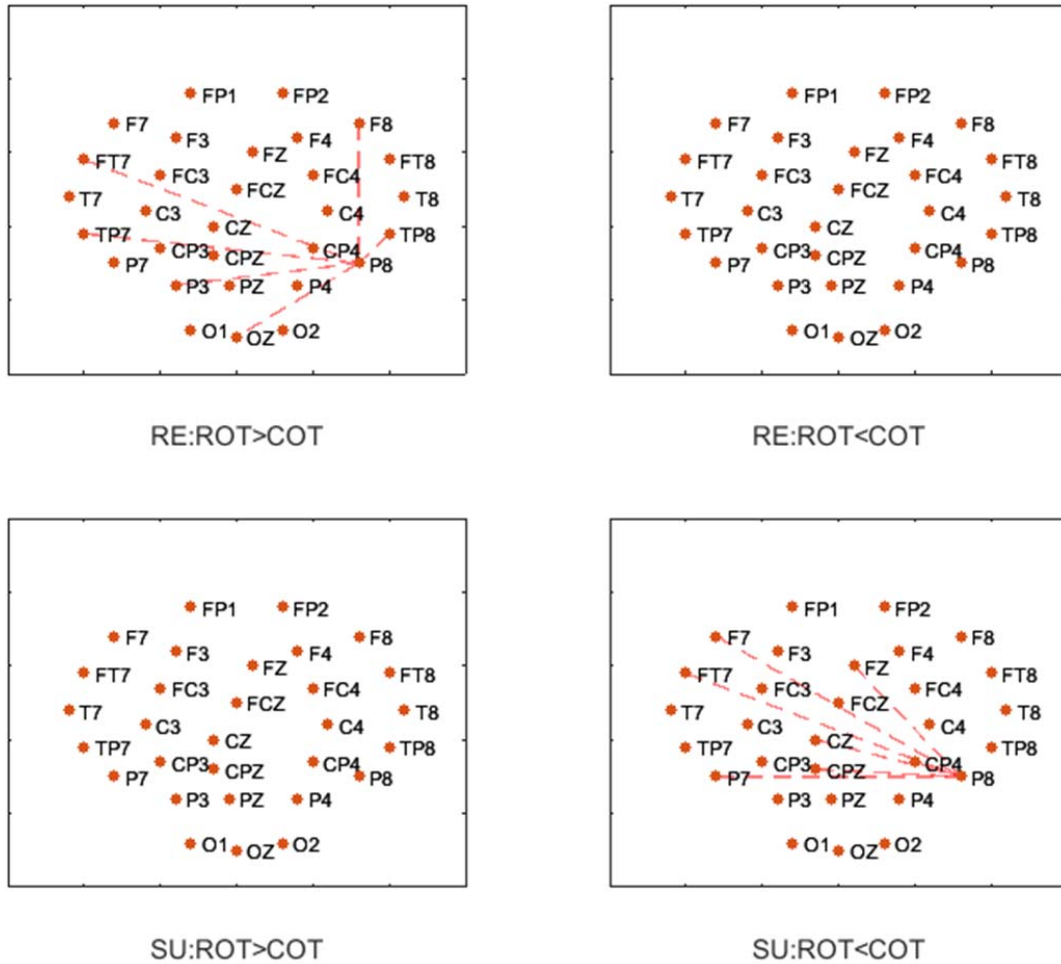


Figure 7.11 Positive and negative subnetwork connected to NOIs (P8) calculated from group averaged PLV node density difference between ROT and COT condition at 646-816ms (two left graphs showed the distribution of connection to NOIs which passed the positive threshold; two right graphs showed the connections to NOIs which passed the negative threshold; RE: the VIMS resistant group; SU: the VIMS susceptible group)

Win4:1000-2500ms NOIs: Cpz/Pz and P8

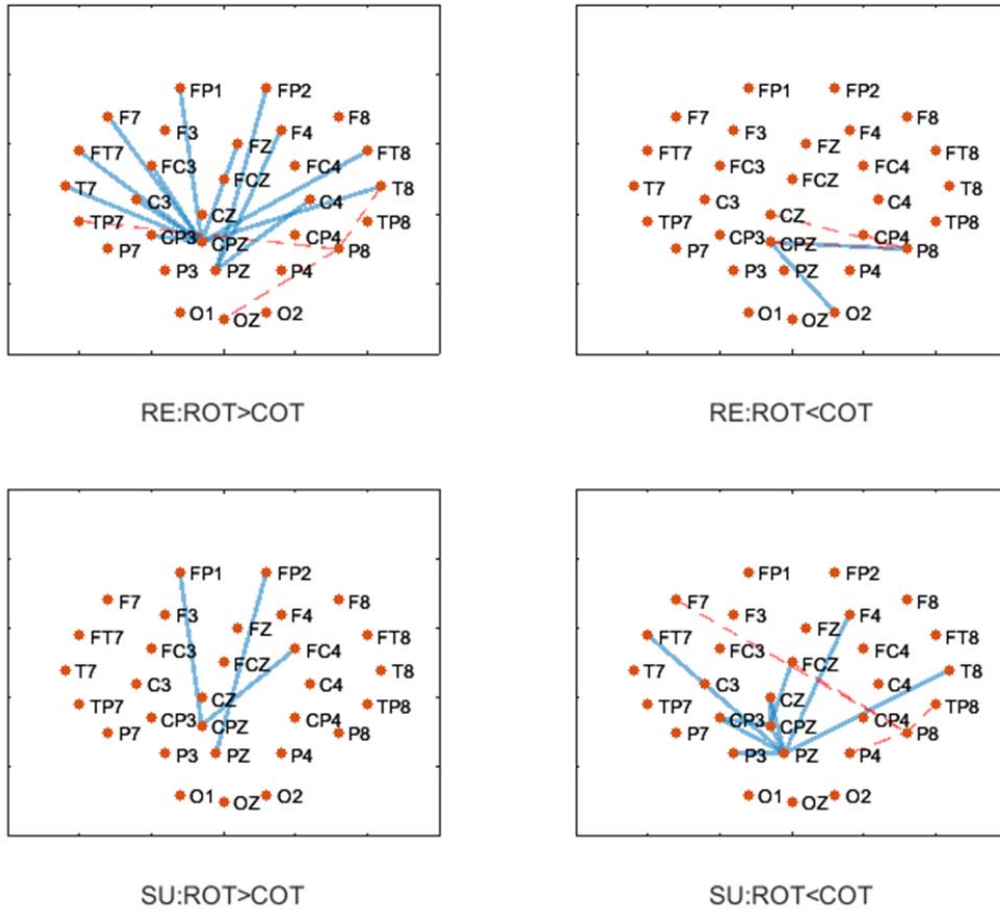
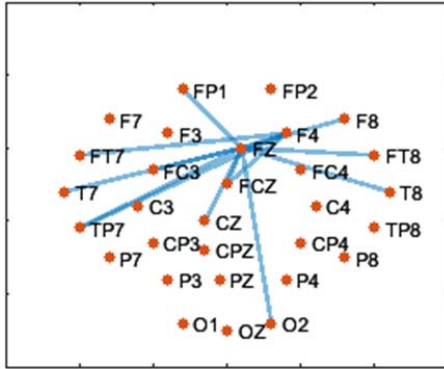
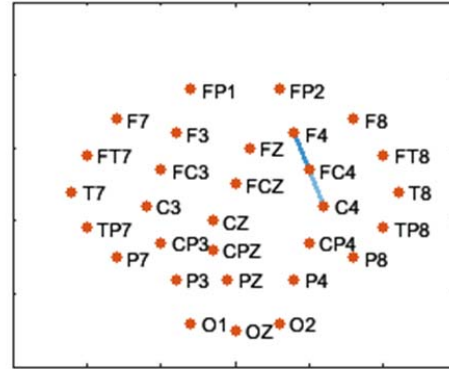


Figure 7.12 Positive and negative subnetwork connected to NOIs (Pz/Cpz and P8) calculated from group averaged PLV node density difference between ROT and COT condition at 1000-2500ms (two left graphs showed the distribution of connection to NOIs which passed the positive threshold; two right graphs showed the connections to NOIs which passed the negative threshold; RE: the VIMS resistant group; SU: the VIMS susceptible group)

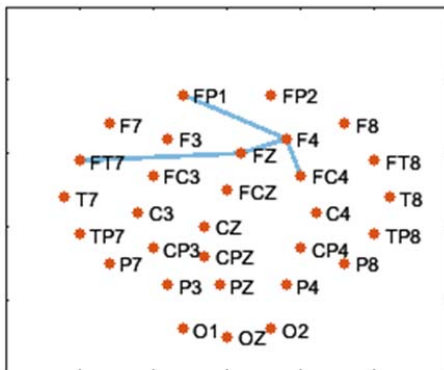
Win4: AVEC 500-1000ms NOIs: F4/Fz



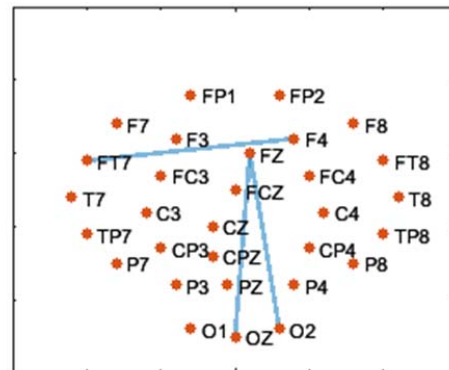
RE: BVEC > AVEC



RE: BVEC < AVEC



SU: BVEC > AVEC



SU: BVEC < AVEC

Figure 7.13 Positive and negative subnetwork connected to NOIs (F4/Fz) calculated from group averaged PLV node density difference between BVEC and AVEC windows (two left graphs showed the distribution of connection to NOIs which passed the positive threshold; two right graphs showed the connections to NOIs which passed the negative threshold; RE: the VIMS resistant group; SU: the VIMS susceptible group)

7.5 Discussion

This study identified several EEG signatures for VIMS susceptibility: we found both excessive N223 amplitude and impaired theta-band phase synchrony in VIMS susceptible people. Particularly, results suggest that the strength and range of dynamic cortical coordination is generally impaired in VIMS susceptible group: when exposed to vection-inducing stimuli, we found that parietal midline (PM), right temporal-parietal (rTP) and right central regions showed strengthened theta-band phase synchrony networks across electrodes over widely distributed brain regions (e.g. frontal, occipital and temporal areas) in VIMS resistant group -- those enhanced synchronization was weaker or disappeared in VIMS susceptible group. Moreover, after vection onset, the strength and range of phase synchronization under visual stimulation is reduced for VIMS resistant people, but not for susceptible people. This suggests that the cortical coordination and sensory conflict reduction is more effective in VIMS resistant people than susceptible people. The VEP results, the theta-band phase synchrony results, and their association with VIMS will be further discussed respectively in detail.

7.5.1 VEP components

Several VEP components with distinct spatial-temporal properties showed differentiate response to roll vection-inducing stimuli, as compared to randomized moving control. Particularly, we found increased amplitude for early N2 (N223) and P3 (P305) components distributed over parietal midline (PM) region (Figure 7.3). Note that the PM region is also suggested to be activated during forward vection-inducing stimulation in another EEG study (Vilhelmsen et al. 2015). There are rich functional areas distributed in PM region which are responsible for ambient visual motion processing: the parietal-occipital visual areas (V3A, V6) (Sabrina Pitzalis et al. 2013; Uesaki and Ashida 2015; Wada et al. 2016), the Precuneus motion area (PcM) (Kovács et al. 2008; Uesaki and Ashida 2015; Wada et al. 2016), and ventral intraparietal (VIP) multisensory area (Uesaki and Ashida 2015; Wall and Smith 2008).

The enhanced amplitudes of N223 and P305 might be associated with increased activities in those functional areas.

Furthermore, we also identified increased amplitude for a bilateral late N2 (N290) component over the temporo-parietal (TP) region (see Figure 7.3). Bilateral N2 components from this region were frequently reported in EEG studies using ambient visual motion stimuli (Keshavarz and Berti 2014; Stróžak et al. 2016; Vilhelmsen et al. 2015). Similar results were found in those works with larger amplitude revealed in conditions that can provoke stronger vection perception (Keshavarz and Berti 2014; Stróžak et al. 2016). This N2 amplitude was addressed as reflecting motion processing (Vilhelmsen et al. 2015) or the integration of peripheral and central motion (Keshavarz and Berti 2014). Moreover, the macaque middle temporal complex (MT+) is a well-known visual motion processing region, and the human areas of MT+ (hMT+) is believed to locate in TP region (Hampson et al. 2004; Strong et al. 2016), which was reported to show increased response for vection-inducing stimuli (Kovács et al. 2008; Uesaki and Ashida 2015).

It is noteworthy that the amplitude increments of N223 and absolute amplitudes of right N290 are positively correlated with the vection intensities perceived by participants. This suggested that these N2 components are not only related to process of ambient visual motion, but also associated with the perception of self-motion. Although recent works found that N2 response varied under different type of visual stimuli (Keshavarz and Berti 2014; Stróžak et al. 2016; Vilhelmsen et al. 2015), this is for the first time to show that, N2 amplitude is correlated with individual vection intensity even under the same visual stimulation. Moreover, these N2 responses are recorded 200-300ms right after visual stimuli onset, while the onset of vection delayed a few seconds. This implies that the individual perception of vection can be influenced by some initial visual processing properties in a quite early stage. Since objective measures for vection is important (Palmisano et al. 2015), N2 components could be a promising EEG measures that facilitate comparison between individuals. Note that only right-side N290 is associated with vection perception – the laterality in self-motion perception was also reported in former findings (Keshavarz and Berti 2014; Kovács et al.

2008), which may relate to the specialization of right hemisphere in visuospatial processing (Ng et al. 2000).

Additionally, we found decreased amplitudes in P1/P3 time window at electrodes over parietal-occipital regions (P178, P350), which is similar to vection studies that reported reduced mean P1/P3 amplitudes at parietal and occipital electrodes for vection-inducing horizontal moving strips (Keshavarz and Berti 2014; Stróžak et al. 2016). This deactivated visual response is addressed as shift of weighting from processing local visual properties to peripheral large field self-motion cues (Stróžak et al. 2016; Thilo et al. 2003). It is also consistent with some neural imaging works, where visual areas V1/V3/V4 (Braddick et al. 2001; Kleinschmidt et al. 2002) or Brodmann area (BA) 17/18 (Brandt et al. 1998) were found to be deactivated during vection-inducing stimulation.

7.5.2 Theta-band phase synchrony network

In supporting to *H12*, we found strengthened theta-band phase synchronization under vection-inducing stimulation as compared to randomized control: the node density of dynamic phase synchrony network weighted by PLV_z was higher in ROT condition than COT condition. Moreover, this effect is stronger and wider in VIMS resistant group than susceptible group, and it can be divided into three stages.

At the first stage of window period at 0.2-0.4s, a large cluster, covering plenty of nodes over central, parietal and temporal regions, demonstrated enhanced node density for VIMS resistant participants. For susceptible people, we only found a quite narrow cluster, covering just a few nodes over the central-parietal regions (see Figure 7.6). This suggests that the strength of dynamic information integration with other extra-visual cortical regions (especially the central region) is generally impaired in VIMS susceptible people. In the further NOI analysis, we assessed NOIs from two dominant regions: the PM (Pz/Cpz) and right central (C4) region. Results further suggested that although the wideness of phase locking with PM region (local activities of this region correlated with visual self-motion perception, as discussed in 4.1) is equivalent for two groups at this early stage, the range of

dynamic coordination with right central region is much narrow or even absent in susceptible people (see Figure 7.6 & 7.10). Interestingly, it is suggested by a work using functional Near-Infrared Spectroscopy (fNIRS) that activities from C4 channel of 10-20 system can reflect the response from somatosensory and vestibular modality under similar visual stimulation (Zhao 2017). Moreover, this region is also covered by the hubs of vestibular network revealed in a recent fMRI study (Kirsch et al. 2018). Therefore, this impaired phase synchrony with right central regions in susceptible individuals might indicate a lack of coordination with somatosensory and vestibular regions in the initial stage of self-motion processing.

At the second stage of window period at 0.6-0.8s, another positive cluster, covering right TP regions was found in resistant people, while no positive cluster was observed in susceptible people. In the further NOI analysis, we found the range of connections with right TP NOI (P8) in positive subnetwork is also significantly wider for resistant group, mainly distributed over occipital and contralateral temporal-parietal regions. Results suggested that the general strength and range of phase synchronization with right TP region is impaired in VIMS susceptible people at this stage. Theta oscillations in right TP region was reported to be correlated with correct navigation performances and addressed as reflecting integration of ego- and allo-centric representations (White et al. 2012). Moreover, our VEP result also revealed that the local activity of right TP region (P8) is correlated with vection intensity. Therefore, those enhanced long-range synchronization with right TP region found in resistant people might indicate the integration of self-motion information under the vection-inducing stimulation. Note that for susceptible group, we not only found less inter-hemispheric in positive subnetworks (indicating enhanced connections), but also marginally more links in negative subnetworks (indicating weakened connections) than resistant group ($t = 1.740, p = 0.095$), where most of those dynamic links are connected to contralateral TP regions (see Figure 7.11). This is quite consistent with a recent fMRI works, where reduced inter-hemispheric synchronization of hMT+ located in TP region was reported to associated with VIMS (Miyazaki et al. 2015). It is possible that those dynamic links connected to right

TP region can reflect the self-motion integration network that facilitates the sensory conflict reduction.

At the third stage of long lasting period at 1-2.5s, no overall node intensity difference was observed between vection-inducing stimulation and control condition for both VIMS groups. In the NOI analysis, we focused on hub NOIs (PM NOIs: Cpz/Pz; right TP NOI: P8) which have demonstrated the highest node density (see Figure 7.5) to explore the range and distribution of enhanced links with those hub regions during this sustained vection-inducing stimulation. Results suggested that enhanced connections during this period are mainly between PM region and frontal regions (see Figure 7.6 & Figure 7.12), where resistant group demonstrated significantly more connections than susceptible group. The theta rhythm in frontal areas are usually associated with detecting mismatched information (Liang, Hu, and Liu 2017) and sensory conflict modulations (Jo et al. 2017), while spatial navigation and self-motion processing is related to theta oscillations from parietal regions (Araújo et al. 2002; White et al. 2012). Moreover, our VEP analysis showed that local activity of PM region (Pz electrode) is correlated with strength of self-motion perception. Therefore, enhanced theta-band phase synchrony between PM and frontal regions might be associated with a sustained detection and coordination of sensory mismatch under lasting vection-inducing stimulation in resistant people, while this function is evidently impaired in VIMS susceptible people.

Note that, after the onset of vection, the strength and range of dynamic links with frontal region (especially right frontal region) has been largely reduced only for resistant people (Figure 7.7-7.9 & 7.13). Moreover, in supporting to **H13**, we found that the number of reduced links is negatively correlated with the MSSQ score of participants (Figure 7.9). This effect shall not be explained by adaptation under a prolonged exposure time, since the vection onset delay is not significantly between the two groups (Table 7.1) and the number of links showing reduced phase locking is not correlated with the length of vection delay. According to Brandt, if our sensory integration is effective, the neural mismatching should be reduced after vection onset. And we should already update our central integration of self-motion state toward our predominant visual input. Hence, the integration weighting for other

modalities has been reduced and the activities in brain regions responsible for extra-visual modalities (especially vestibular) has been suppressed duringvection (Brandt et al. 1998, 2002). Based on Brandt's model, sensory modalities feed forward sensory information to our central integration, while central integration talk to sensory modalities through negative feedbacks. Therefore, both of the feedforward and feedback communication with central integration shall reduce aftervection onset only for resistant participants. As previous studies also supported that lower connectivity with frontal region reflected less mismatched information (Jo et al. 2017; Liang et al. 2017), this may explain the drop of functional connectivity between frontal and other regions in resistant participants, which does not observed in susceptible people. Moreover, the magnitude of this effect was also negatively correlated with the susceptibility of participants, which further support this possibility.

7.5.3 EEG signatures correlated with VIMS susceptibility

Increment of N223 amplitude beforevection

For the local VEP responses, only the N223 demonstrated different effects between VIMS susceptible and resistant group, with larger amplitudes increment for susceptible group (Figure 7.4). Moreover, individual increment of N223 ($N223_{inc}$) is also positively correlated with the MSSQ scores of the participant (Table 7.2). This agrees with Chen's finding (Chen et al. 2009) that activity of parietal midline component was positively correlated with VIMS level. Note that although $N223_{inc}$ is also positively correlated withvection intensity report by participants, there are neither group difference onvection perception nor correlations betweenvection reports and MSSQ scores. Former findings also supported thatvection magnitude is not correlated with VIMS magnitude (Keshavarz, Riecke, et al. 2015; Keshavarz and Berti 2014). When split the two group, we found that $N223_{inc}$ was correlated withvection intensity ($R^2 = 0.38$) and MSSQ_C ($R^2 = 0.44$) in susceptible group with even higher prediction power, while no longer significant in resistant group. It is possible that although local initial response tovection-inducing stimulation can indicate our perceived motion strength, other later mechanisms (e.g. sensory integration), especially in VIMS

resistance people, coordinate sensory inputs and further shaped our updates on self-motion perception. Therefore, it is possible that what resistant people achieve is to reduce the excessive initial N2 response provoked by vection-inducing stimulation before the vection onset, as the central integration have not undated toward visual stimulation yet and there would be large sensory conflict at this stage if the visual motion input is too strong at this initial stage.

Note that this N2 effect is totally different from the effect N2 effect we uncovered in study two: in this study what we compared is the difference between ROT (VEP evoked by vection-inducing rotation stimuli; before vection onset) and COT condition (VEP evoked by random moving control; not vection-inducing), while in study two what we compared is the difference between RV (VEP evoked by checkerboard under rotation stimuli; during vection) and RN condition (VEP evoked by checkerboard under rotation stimuli; without vection; similar to ROT in study 4). Hence the direction of the two effects regarding VIMSS is actually in opposite direction, where the results from the two studies complement each other: 1) resistant people showed less excessive initial N2 response, as the central integration state is stationary before vection onset (ROT-COT in study four); 2) resistant people demonstrated larger enhancement of N2 after vection onset, as central integration state is self-rotation (RV-RN in study two). Both of the two mechanisms are in line with the principle for reducing sensory conflict between central integration state and visual input.

Enhanced phase locking before vection and reduced after vection onset

For the phase synchrony, as discussed in previous section, we found impaired strength and range of theta-band phase synchronization with PM, right TP and right central region during vection stimulation in susceptible group (Figure 7.6). Those indices reflecting the wideness of dynamic links are negatively correlated with the MSSQ scores of individual participants (Table 7.2), where the index indicating synchronization with right TP region shows strongest prediction power (Table 7.2). Moreover, we also found that the reduced strength and range of theta-band phase locking with right frontal region after vection onset is negatively correlated

with MSSQ scores with higher R^2 than other predictors including $N223_{inc}$ in the regression model (Table 7.2). In the general model, the combine of index of right TP region and right frontal region produce the best prediction power for total scale. As discussed before, it is possible that the phase locking with right TP region reflects the strength of sensory integration for self-motion, while the reduced communication with frontal regions (responsible for conflict detection and modulation) aftervection onset indicate the individual effectiveness of conflict reduction. This agreed with former findings that in addition to parietal-occipital regions, frontal activities were also associated with VIMS (Chen et al. 2009; Farmer et al. 2015; Napadow et al. 2013).

It is worth mention that, we focus on searching for EEG signatures differentiate the susceptibility of individual before the symptoms occurred, so that none of the participants experienced any obvious VIMS symptoms (including eye fatigues, disorientation and nausea) in our study, even for the susceptible group. This validated that our findings were not caused by VIMS symptoms. Interestingly, we revealed that synchronization-based EEG signatures showed better prediction power than localization based signatures ($N223_{inc}$) in all of the MSSQ subscale, as the $N223_{inc}$ is excluded from regression model due to lower prediction power. This supported that sensory integration and long range interactions shall be able to better capture the susceptibility to VIMS than localization methodologies. VIMS might be better characterized as an impairment of cortical coordination rather than abnormalities in locally activities.

Moreover, MSSQ is a general questionnaire indicate motion sickness (MS) occurrence in various motion scenarios (Golding 1998). Therefore, the signatures we reported have showed potential properties associated with the general occurrence of sickness rather than specific stimuli we used in laboratory. Admittedly, this also leads to complicated situation that a participant reported mild MS in several scenarios could result in same MSSQ score with a participant reported moderate MS in only one scenario. Further works with more meticulous differentiation on subtypes of MS are desirable.

7.5.4 Potential limitations and validations

To exclude the influence of possible confounding factors involved in procedures, we generate validation datasets to test the robustness of results. Firstly, as PLVs were calculated across all clean epochs remained in each condition (COT/ROT/VEC), the epoch numbers can vary among conditions. To eliminate the alternative explanation that within-subject effects might cause by unequal epoch numbers, for each participant, we randomly sampled epochs in each condition at the size of least remained epochs to generate a smaller validation dataset to calculate PLV. Thus, the remained epoch number is the same across all condition for each participant ($N=85.2 \pm 16.0$ for group). All within-subject effects remained robust in the validation. Similarly, to exclude the influenced of variations in individual epoch numbers on between-subject effects, we sampled epochs in ROT condition at least remained ROT epochs among participants to generate another validation dataset. Therefore, epochs ($N=59$) used for PLV calculation is the same for all participants. The group effects remained robust.

Another concern is that although the mean onset delay of vection is around 10s, there are three participants (1 from VRE, 2 from VSU) had some onset delay less than 3s. The button pressing task for vection onset indication in those subjects might pollute the ROT epochs. We formed smaller validation dataset by excluding them ($N=23$). All effects remained robust in the validation. Another support is that, to control the individual variation in vection onset delay, we included onset delay in the regression models for predicting MSSQ scores and vection intensity. The prediction power of all EEG signatures is robust. Note that in this work, the regression models were conducted to better control other external factors. To reveal the causal relationship between the EEG signatures and VIMS susceptibility is out of the scope of this work. Thus direction implied in the model was not designed to reveal causal relationship between the variables, but only association between the variables.

7.6 Summary

This study compared the VEP components and phase synchrony network under vection-inducing stimulation between VIMS susceptible and resistant people, to identify EEG signatures for VIMS susceptibility. We found higher VIMS susceptibility is weakly associated with excessive initial local responses in parietal regions (N223 amplitude), and strongly linked to impaired theta-band phase synchrony network (especially in the subnetwork with parietal midline, right temporal-parietal and right-central region). Results support that the susceptibility to VIMS can be better captured by phase synchronization of cortical activities than local activities. By applying the procedure in future validations and explorations using methods with higher spatial resolution (e.g. MEG, fMRI), we may be able to reveal more precise functional networks and further understand the neural mechanism underlying VIMS susceptibility. Moreover, collecting EEG signatures identified in our study does not need to cause motion sickness in participant. Given validations with larger group sample in the future, it is possible to develop those EEG signatures into applicable predictors for VIMS that can facilitate sickness precautions and solutions for industry applications.

CHAPTER 8 SUMMARY AND COMPARISON ON IDENTIFIED VIMSS COVARIATES

8.1 Introduction

This chapter focuses on summarizing and comparing the objective indicators we obtained from four studies and discuss their potential as VIMSS predictors in the future based on their properties and the results obtained in our studies. To evaluate the quality of those objective indicators, we assessed their explanation power on MSSQ scores (child, adult and total scale), along with the difficulty, the stability (within-subject variations), the discrimination ability (between-subject variations) and cost of measurement. This work could serve as a useful reference for future explorations on objective indicators for VIMSS.

8.2 Objective

The objectives of this chapter are: 1) explore and evaluate the quality of behavioral and EEG indicators as potential new VIMSS predictor; 2) compare the results obtained from four studies and identify most promising EEG indicators; 3) search for methods to minimize the procedure and the difficulty of measurements for practical utilization.

8.3 Explanation power

8.3.1 Data and method

From study 1-4, several objective indicators that measured under the roll vection-inducing stimulation were observed to be associated with the MSSQ-short score of participants. The reliability of MSSQ-short has been validated with sufficient large sample size in the population (Golding 1998; Golding and Kerguelen 1992). Moreover, former work has also supported that the MSSQ-short score can serve as an appropriate measure for VIMS

susceptibility in the participants sample recruited from university students in HKUST (Zhao 2017). Therefore, we use the MSSQ-short scores collected from participants in each study as a benchmark in evaluating the explanation power of those newly identified objective indicators as potential VIMSS predictors. The R^2 in each regression model predicting the MSSQ score (total scale and two subscales respectively) that can be explained by the objective indicator (which identified from each study) was adopted as the evaluation index for the explanation power of this objective indicator.

Four types of objective indicator were evaluated and compared: 1) *DRT*: the delay of response time measured in behavioral study one (data pooled from Exp.1a&1b); 2) *I_{Amp}_{N2}*: the increment of transient amplitude N2 VEP component measured in EEG study two and study four (note that as we discussed in **section 7.5.1**, the contrast of study four and two are differently organized, so the meaning and direction of two effects actually are different; here we only focus on the measuring method of the indicators, thus we group them together only because they are both transient VEP results of N2 component); 3) *D_{Power}_{8.6Hz}*: the decrease of SSVEP power at CVF frequency (8.6Hz) measured in EEG study three; 4) *N_{Deg}*: the nodes degree in dynamic functional connectivity subnetworks measured in EEG study four.

For each type of indicator (*DRT*, *I_{Amp}*, *D_{Power}* and *N_{Deg}*) we may have identified multiple indicators that are correlated with MSSQ scores (e.g. different target types, different electrode or combined effects) in most studies. For the sake of evaluating the indicator types, we have selected the one that produces strongest explanation power in the regression model for each type of indicator to facilitate the comparison across different indicator types. Moreover, two types of model were evaluated: 1) the single independent variable model adopts only one single indicator with best explanation power; 2) the multiple independent variables model which allowed the adding of multiple indicators in stepwise manner (indicators with limited newly contribution would be excluded) and the combination produce best explanation power is kept. As more variables added in the model usually generate larger R^2 , we adopted adjusted R^2 following the equation to prevent the overestimation of the strength of association (Cohen and Cohen 2003):

$$R_{adj}^2 = \frac{(1-R^2)(N-1)}{N-k-1},$$

where the N is total sample size, the R^2 is the R-square of the sample, R_{adj}^2 is the adjusted R-square, k is the number of predictors.

8.3.2 Results

As for the *DRT* measured from behavioral study one (see chapter 4 for detail), the best single indicator for total scale and adult scale is the total RT effect, while the best single indicator for child scale is the peripheral RT effect. For the multiple indicators model, two indicators model are only found to be beneficial for the MSSQ total scale, with total RT effect and central RT effect generating best explanation power.

As for the *Iamp* of N2 component obtained by EEG, the amplitude increment at the O1 electrode measured in study two is the best single indicator for child scale, while the amplitude increment at the Pz electrode measured in study four is the best single indicator for total scale. For the multiple indicators model, more indicators are found to be not beneficial (no new contributions when adding more indicators into the model) for all of the MSSQ total scale and subscales.

As for the *DPower* measured from the EEG study three, the decrease of SSVEP power at CVF stimuli frequency (8.6Hz) from Oz electrode is found to be best single indicator for both total scale and child scale. No indicator is found to be able to produce significant model for adult scale. For the multiple indicators model, more indicators are found to be not beneficial for all of the MSSQ total scale and subscales.

As for the *NDeg* measured from EEG study four, nodes degree in the positive dynamic connectivity subnetworks of right-frontal NOIs (links showing reduced phase synchrony strength after vection onset, see chapter 7 for details) is the best single indicator for all MSSQ scales. For the multiple indicators model, more indicators are found to be rather beneficial. Adding nodes degree in the positive dynamic connectivity subnetworks of different NOIs

into the model has significantly improved the R^2_{adj} . The best model for child scale accepted four indicators from NOIs at four regions: C4 (right central NOI), Cpz/Pz (parietal midline NOIs), P8 (right temporal-parietal NOI) and Fz/F4 (right central-frontal NOIs); the best model for adult scale accepted three indicators: nodes degree in positive and negative subnetwork of right central-frontal NOIs, as well as the positive subnetwork of right temporal-parietal NOI; the best model for total scale accepted two indicators from NOIs at two regions: right temporal-parietal NOI and right central-frontal NOIs.

Table 8.1 Best explanation power for each type of objective indicators in single variable model

Indicator type		R^2_{adj} (p-value)			Sample size (N)	Data source
		MSSQ_C	MSSQ_A	MSSQ_T		
behavioral	<i>DRT</i>	0.177* (p=0.013)	0.108* (p=0.046)	0.158* (p=0.019)	29	Study 1
	<i>IAmp</i>	0.305* (p=0.024)	-	0.192* (p=0.014)	14 / 26	Study 2 & 4
EEG	<i>DPower</i>	0.340* (p=0.013)	-	0.304* (p=0.019)	15	Study 3
	<i>NDeg</i>	0.283** (p=0.003)	0.314** (p=0.002)	0.321** (p=0.002)	26	Study 4

*** p<0.001, ** p<0.01, * P<0.05; only significant indicators are showed; MSSQ_C, MSSQ_A and MSSQ_T represent the child scale, adult scale and total scale respectively.

The summary of best indicator from four different types (*DRT*, *IAmp*, *DPower* and *NDeg*) is showed in Table 8.1 &8.2. For single variable models, we can see that the three type of EEG indicators all showed higher explanation power than the behavioral indicator in total scale and subscales. Moreover, among the EEG indicators, the network based indexes (*NDeg*) showed highest explanation power for total scale and adult scale, while the SSVEP indicator

(*DPower*) showed highest explanatory power for child scale. In general, SSVEP indicator produces higher explanation power than transient VEP indicator (*Iamp*), while network based indicator shows higher capacity than localization-based indicators (*DPower*, *Iamp*).

As for the multiple variable models (see Table 8.2), combination of behavioral indicators actually shows better explanation power than localization-based indicators (*DPower*, *Iamp*). For EEG indicators, only network-based indicator (*NDeg*) gain adequate benefit by adding more indicators measured from various condition and regions, while no evident contribution is obtained by adding various VEP indicators into the model. The network based indicator in general produce best (and quite promising) explanation power even for adjusted R^2 .

Table 8.2 Best explanation power for each type of objective indicators in multiple variables model

Indicator type		R^2_{adj} (p-value)			Sample size (N)	Data source
		MSSQ_C	MSSQ_A	MSSQ_T		
behavioral	<i>DRT</i>	0.177*	0.108*	0.350**	29	Study 1
		(p=0.013, k=1)	(p=0.046, k=1)	(p=0.001, k=2)		
		0.305*		0.192*		
	<i>Iamp</i>	(p=0.024, k=1)	-	(p=0.014, k=1)	14 / 26	Study 2 & 4
EEG	<i>DPower</i>	0.340*		0.304*	15	Study 3
		(p=0.013, k=1)	-	(p=0.019, k=1)		
		0.633***	0.499***	0.474***		
	<i>NDeg</i>	(p<0.001, k=4)	(p<0.001, k=3)	(p<0.001, k=2)	26	Study 4

*** p<0.001, ** p<0.01, * P<0.05; k represents number of kept in the final model after adding all significant available indicators into the model in a stepwise manner (thus low contribution variables will be excluded); MSSQ_C, MSSQ_A and MSSQ_T represent the child scale, adult scale and total scale respectively.

8.3.3 Discussion

In this section, we evaluate and compare the potential of different types of objective indicators (behavioral indicator: *DRT*; transient VEP indicator: *IAmp*; SSVEP indicator: *DPower*; network-based indicator: *Ndeg*) in terms of their explanation power for VIMSS. We select the best indicator from each type of objective indicator (we explored in study 1-4) to represent its indicator type respectively.

Results suggested that the EEG indicators, in general, demonstrate stronger association than the behavioral indicator (DRT). As we discussed in chapter 4, this may due to the fact the behavioral measures all depended on some explicit response to be made by participants. Thus, in the procedure of generating targeted response, plenty of other unrelated factors (e.g. motor control ability, decision making, and recognition function...) can influence the response time and introduce more noise in the measurement. Compared to behavioral indicators, EEG indicators can reflect the earlier visual response with better time resolution (Keshavarz, Campos, et al. 2015), where the procedure of explicit response is also bypassed. Therefore, well-measured EEG indicators shall reflect the visual response during vection more directly and may be able to better capture the individual difference that characterizes the VIMSS. As first preliminary work to compare the performance of both behavioral and EEG indicator, our comparison on the explanation power has supported above hypothesis. This shall encourage more explorations on EEG indicators.

More interestingly, our results suggest that the network-based indicators precede other localization-based EEG indicators (*IAmp*, *DPower*) especially for the explanation power in total scale and the adult scale, while localization-based EEG indicators outperform the network-based indicators in child scale. This phenomenon mutually supports current findings: child scale scores represent more inherent characteristics, while adult scale score is more adjusted by experience and learning (Golding 2006). As sensory integration and long range interactions developed later and more inclined to experiences than local properties (Calvert et al. 2004), it may explain why phase synchrony signatures might be a better

predictor for adult VIMS susceptibility than locally VEP responses. Since the adult scale shall be more useful in predicting the VIMS of users at current situations, while the child scale is more useful for clinical uses. Further explorations and validations on this phenomenon may facilitate the development of variant VIMSS indicators with inclinations to different aspect of the VIMS.

Moreover, the connectivity network-based indicators are also found to be more promising in terms of the separated contribution to the explanatory power. For other localization-based EEG indicators, adding more indicators from different location/brain regions did not contribute more new information in the model, hence they are not much benefit by multiple variables model. Future work aiming to search for better VIMSS indicators should put more emphasis on network-based indicators. Many potential useful network indexes in addition to nodes degree, including the path length, global efficiency, local efficiency, cluster coefficient (Bullmore and Sporns 2009; He and Evans 2010), are available for further exploration.

Note that, as we already discussed in chapter 7, sensory conflicts is referred to as the general origin of all types of motion sickness (MS), while VIMS is considered as a specific type of MS introduced by virtual motion in this research. VIMS susceptibility was accordingly quantified by MSSQ, which is a general questionnaire for MS (Golding 1998). As mentioned in chapter 2&3, we selected MSSQ-short as our bench mark for comparison, for the sake of its representativeness and reliability tested and verified in previous studies (Golding 1998; Zhao 2017). Thus, the explanatory power evaluated here actually is related to the general susceptibility to all types of motion, rather than restricted to visually induced motion sickness or the particular situation measured in the lab. Since certain differences exist between VIMS and motion sickness caused by physical motion (Zhang et al. 2015), it is also necessary to further explore whether the effects identified in this study may be more closely associated with other VIMS measures in the future. Admittedly, the subjective self-report questionnaire (MSSQ) itself is also suffering from some drawbacks and can be influenced by many factors relied on participants (e.g. the veracity of recall, the individual inclination) (Golding 1998).

Hence, future explorations with other complimentary procedures to validate the VIMSS are desirable.

8.4 Stability and Discrimination ability

8.4.1 Data and method

Another important aspect need to take into account is the stability (or reliability) and the discrimination ability of the measurement among participants. As we aim to develop the uncovered indicators into objective predictors for VIMSS, it is important that the variance of the measured indicator from each participant should be small as compared to the magnitude of between-subject variance among participants, so that magnitude of the indicator can be able to differentiate people with various degrees of VIMSS.

In order to evaluate this aspect, we firstly calculated the within-subject standard error ($STE_{within-sub}$) of those best indicators obtained for each type of indicator (behavioral indicator: DRT ; transient VEP indicator: I_{Amp} ; SSVEP indicator: D_{Power}) to reflect the within-subject variations between repeated measurements obtained from each subject. The within-subject repeated measurement refers to each single trial conducted under each type of task condition in our studies. Secondly, we calculated the between-subject standard deviation ($STD_{between-sub}$) and the range ($RA_{between-sub}$) of those best indicators in sampled participant group (dividing the total percentage of VIMSS percentile covered by this participant group to normalize the covered range in population) to reflect the between-subject variation between participants. Finally, as we need to compare indicators with different type of units, we use an evaluation scores ($Score_{d1}, Score_{d2}$) calculated based on following equations to evaluate the discrimination ability of each indicator:

$$Score_{d1} = \frac{STD_{between-sub}}{STE_{within-sub}},$$

$$Score_{d2} = \frac{RA_{between-sub}}{STE_{within-sub}}.$$

For the *Ndeg* measured in study four, as the calculation of PLV is based on coherence of phase across multiple epochs and the data type does not follow the normal distribution, it is hard to be compared with other types of indicator. Thus the *Ndeg* is not compared together with other three types of indicator. We will discuss it separately.

8.4.2 Results

For the *DRT* measured in study one, we calculated the evaluation scores for the central effect and peripheral effect with static target for experiment 1a&1b respectively, since the tasks and procedures are slightly different for the two experiments and can lead to different stability and discrimination ability. For the *Iamp*, we calculated the evaluation scores for the effect of N2 amplitude at the O1 electrode measured in study two, and the effect at the Pz electrode in study four. In particular, we use the standard error of preprocessed EEG data averaged across the N2 window of each participant for the $STE_{within-sub}$ (note that in study four we transformed the EEG data into current source density before averaging the epochs, hence the unit for *Iamp* from two studies is different). For the *DPower* measured in study three, we calculated the evaluation scores for the effect of SSVEP power at CVF stimuli frequency (8.6Hz) from Oz electrode. The selection of indicator for assessment is based on section 8.3, where those indicators are found to be promising indicators with best prediction power.

The result of $Score_{d1}$ and $Score_{d2}$ calculated for each indicator are showed in the Table 8.3 and Table 8.4 respectively. In general, behavioral and EEG indicator showed equivalently discriminative ability, while both of them have good indicator with high evaluation scores and less competitive indicators with lower scores. For behavioral indicators, both the central and peripheral effect demonstrated higher discriminative ability in Exp.1b. Moreover, the peripheral effect in Exp.1b showed generally worse discriminative ability than other behavioral indicators reflected by both $Score_{d1}$ and $Score_{d2}$. For the EEG indicators, the SSVEP indicator (*DPower*) showed prominently better discriminative ability than transient VEP indicators (*Iamp*) in all evaluation scores, where the *DPower* yield highest $Score_{d2}$ and the *Iamp* showed lowest scores in both evaluation score.

Table 8.3 The discrimination ability evaluated by $Score_{d1}$ for different types of indicator

Indicator type	Evaluation indicators			Sample size (N)	Data source
	$STE_{within-sub}$	$STD_{between-sub}^*$	$Score_{d1}$		
behavioral	<i>DRT_C</i>	21.1±7.7(ms)	36.74 (ms)	1.74	Study 1
	<i>DRT_P</i>	33.7±9.2(ms)	52.58 (ms)	1.56	Exp.1a
	<i>DRT_C</i>	18.7±8.3(ms)	35.93 (ms)	1.92	Study 1
	<i>DRT_P</i>	19.3±9.1(ms)	38.83 (ms)	2.01	Exp.1b
EEG	<i>Iamp</i>	0.45±0.10(μv)	0.52 (μv)	1.16	Study 2
	<i>Iamp</i>	3.32±1.06 (μv/cm ²)	3.74 (μv/cm ²)	1.12	Study 4
	<i>DPower</i>	0.078±0.042 (w/Hz)	0.133 (w/Hz)	1.71	Study 3

DRT_C=central effect of DRT; DRT_P=peripheral effect of DRT; $Score_{d1}$ is calculated using the mean $STE_{within-sub}$ of participants in the sample group. The unit for each indicator is illustrated in the brackets. * Note that the MSSQ percentile cover range for each study are: study 1 Exp.1a is 0-100%, study 1 Exp.1b is 19.5-96.2%, study 2 is 0-99.3%, study 3 is 0-85.2%, study 4 is 0-99.2% and the indicators have been normalized based on their coverage.

Table 8.4 The discrimination ability evaluated by $Score_{d2}$ for different types of indicator

Indicator type	Evaluation indicators			Sample size (N)	Data source
	$STE_{within-sub}$	$RA_{between-sub}^*$	$Score_{d2}$		
behavioral	<i>DRT_C</i>	21.1±7.7(ms)	149 (ms)	7.06	Study 1
	<i>DRT_P</i>	33.7±9.2(ms)	191 (ms)	5.67	Exp.1a
	<i>DRT_C</i>	18.7±8.3(ms)	134 (ms)	7.17	Study 1
	<i>DRT_P</i>	19.3±9.1(ms)	138 (ms)	7.15	Exp.1b
EEG	<i>Iamp</i>	0.45±0.10(μv)	1.69 (μv)	3.76	Study 2
	<i>Iamp</i>	3.32±1.06 (μv/cm ²)	17.69 (μv/cm ²)	5.33	Study 4
	<i>DPower</i>	0.078±0.042 (w/Hz)	0.575 (w/Hz)	7.37	Study 3

DRT_C=central effect of DRT; DRT_P=peripheral effect of DRT; $Score_{d2}$ is calculated using the mean $STE_{within-sub}$ of participants in the sample group. * Note that the indicators have been normalized based on their corresponding MSSQ coverage.

8.4.3 Discussion

In general, the results agreed with our observation and expectation regarding the experiment designs. For behavioral indicator, we found that the procedure in Exp.1b yielded higher stability (lower $STE_{within-sub}$) than Exp.1a. As we described in chapter 4, the task has been simplified in Exp.1b (participants only need to conduct SART with right hand), while in Exp.1a, participant need to carry out dual task (use right hand to indicate vection perception state; use left hand to conduct SART). Moreover, as all of the participants are right-handed, changing the SART task from left hand to right hand also reduce the difficulty of task. Hence, the procedures in Exp.1a are more demanding both in terms of cognitive load and motor functions, which may lead to larger within-subjects variations and smaller discrimination ability than Exp.1b.

Another interesting finding is that the peripheral effect showed significantly lower stability (higher $STE_{within-sub}$) than the central effect only in Exp.1a [$t(13) = 4.512, p < 0.001$]. This actually is consistent with our discussion: the peripheral targets might be mixed with the vection-inducing stimuli presents to PVF in Exp.1a and introduce more noise to the response time of SART or reduce the stability by reducing response accuracy (validated trials reduce due to low accuracy in PVF, which may also increase the $STE_{within-sub}$). While in Exp.1b, both PVF and CVF targets appeared in central black area which eliminated the influence of vection-inducing stimuli in PVF. Moreover, no significant different accuracy difference was found in Exp.1b, which ensure the validate trail numbers were the same for two types of task. Hence, we found equivalent stability and discriminative ability for central and peripheral effect in Exp.1b (the $Score_{d1}$ of peripheral effect was even higher than the score of central effect).

For the EEG indicators, we found that the transient VEP indicators (IAmp) generally yield weaker discriminative ability than the SSVEP indicator (DPower). This is consistent with the high SNR property of SSVEP as compared to transient VEP, since SSVEP is more resistant to eye and body motion artifacts and able to convey more information within a fixed time

period (Vialatte et al. 2010). In fact, the SSVEP based indicator actually showed largest discrimination ability as reflected by $Score_{d2}$, which further confirm the potential of SSVEP indicator as future VIMSS predictor.

Last but not least, our results suggested that the behavioral indicators in general showed equivalent (or even better) discrimination ability with the EEG indicators in our experiment design and procedures. In our work, behavioral indicators were obtained by averaging across around 50 trials, while EEG studies indicators were generally obtained by averaging across 150~250 trials (even over 350 trials in transient VEP at study 2). This may imply that behavioral task actually has higher reliability than EEG indicator and required less repeated measurements. This data can be a useful reference for future studies.

Note that we did not evaluate the network based indicators which calculated from phase locking value between electrodes, since the distribution, data format and calculation method are differently organized, and it is impossible to obtain single trial value for standard error calculation with this fourth type of indicator. Nevertheless, as we described in the chapter 7, we conducted multiple validations by randomly pick trials and re-calculated those indicators. As the effects remain robust in these newly generated smaller measure samples (Mean Trials 59 or 85), those validations can provide indirect evidence supporting the reliability of the network based indicators.

8.5 Difficulty and cost

The quality of a useful VIMSS predictor also depends on the difficulty and cost of the measurement required for obtaining the indicator. As we introduced in chapter 2, tedious procedures and too expensive measurements will hinder the practical utilizations the future VIMSS predictors developed from our indicators.

Undoubtedly, the behavioral indicator identified in study one, has outperformed the EEG indicators in this aspect. Since SART can be conducted with few requirements on participants and results can be obtained quickly and easily (the test time shall be less than

10min if only static central targets are presented), it is a very promising candidate for measuring VIMS susceptibility and deserves to be further developed and validated, especially for situations when quick and less precise predictors are desirable.

Compared to behavioral SART, collecting clean EEG signal in general required more complicated procedure: to obtain EEG data with acceptable SNR, firstly we need to inject conductive gel between the EEG electrodes and the scalp of participants to reduce the impedance—thus the cost of time and money increase as the number of EEG electrodes used; secondly, to increase SNR, we need to repeat large numbers of epochs and average across those epochs. The required average epochs vary for different types of indicator: for reliable transient VEP components, researcher usually need to average around 200 epochs, while for SSVEP, fewer epochs are needed since it has higher SNR than transient VEP (Luck 2005; Vialatte et al. 2010). As we mentioned in section 8.4, to achieve acceptable discrimination ability, the transient VEP required over 350 trials for each condition, while SSVEP required 100~250 trials. Not to mention that the discrimination ability obtained by transient VEP is still weaker than that obtained by SSVEP. As for the network based indicators, our validation has supported that 50~100 trials are generally sufficient for measuring the effects. Thus the measuring difficulty in general can be ranked as follows: SART indicator (*DRT*) < Network based indicator (*Ndeg*) <= SSVEP indicator (*DPower*) < transient VEP indicator (*Iamp*). Note that, this rank is based on measuring all 30 EEG channels as default. For transient VEP and SSVEP, it is possible to further reduce the procedure and cost by selecting and focusing on the channels with best explanation power, while this is not applicable for network based indicators, as obtaining those indicators always require channels cover the whole scalp.

8.6 Summary

In this chapter, we evaluated and compared all types of objective indicators that identify to be correlated with VIMSS to assess their potential as future objective VIMSS predictors. Four types of objective indicators (behavioral based indicator: *DRT*; transient VEP based indicator: *Iamp*; SSVEP based indicator: *DPower*; network based indicator: *Ndeg*) were evaluated in

terms of three aspects: 1) the explanatory power, 2) the stability/discrimination ability and 3) the difficult and cost.

In general, EEG based indicators (*IAmp*, *DPower*, *Ndeg*) showed better explanatory power than behavioral based indicators (*DRT*), while behavioral indicators demand less cost (in time, procedures and other resources) than EEG indicators. Among the EEG indicators, SSVEP based indicator (*DPower*) is best in explanatory power for VIMSS in childhood (inherited traits), while network based indicators (*Ndeg*) is best in explanatory power for current adult VIMSS (acquired coordination ability) and general VIMSS (combine child and adult scores). Moreover, measuring network based indicators required least cost as compared with other EEG indicators, while measuring transient VEP general demand largest cost, and SSVEP yield moderate costs. For the stability and discrimination ability, the behavioral indicators produce equivalent (or even better) discrimination ability with the EEG indicators. Among behavioral indicators, the simplified task in Exp.1b is better than the complicated dual task in Exp.1a. For EEG indicators, SSVEP indicators also outperform the transient VEP.

In summary, the SSVEP based indicator and network based indicator are the most promising EEG candidates with strong explanatory power and moderate measuring cost. Further exploration on simplified the measuring procedure (e.g. select conditions with best stability and explanatory power, pick electrode or reduced combinations with best explanatory power) are desirable and valuable for developing those for practical uses. Furthermore, additional exploration and validations (e.g. evaluate the test-retest reliability) with a larger sample size are desirable to further assess their eligibility as reliable predictors.

Moreover, the behavioral indicators are also promising for situation where simpler and less precise predictors are desirable. Developing simple objective measures to predict individuals' susceptibility to VIMS without making people sick is quite useful for many industry applications (IWA3, 2005). The simplified DRT indicator measured in the Exp.1b of study one can be obtained quickly and easily with very few requirements on participants. Moreover,

we found out that combining the central effect size along with the total effect of DRT in multivariable model can yield quite competitive explanatory power ($R_{adj}^2=0.35$) for VIMSS (measured by MSSQ-short total scale). Therefore, DRT (with procedures in Exp.1b) can be another quite promising candidate for VIMSS predictor and deserves to be further validation and development.

CHAPTER 9 CONCLUSIONS

9.1 Conclusions

9.1.1 Response associate with vection

This research carried out four experiments studying various types of behavioral and EEG based visual responses under the roll vection-inducing stimulation. We identified signatures that correlate with vection in both qualitative (assess the existence of vection) and quantitative manner (assess the magnitude of vection intensity).

For the qualitative covariates, several behavioral and EEG signatures are found to be sensitive to the occurrence of vection: 1) the behavioral performance (reflected by response time and accuracy of Sustained Attention to Response Test) are impaired in central visual field, while they are improved in peripheral visual field with vection (study one); 2) the early transient visually evoked potential (VEP) components (reflected by amplitude) (N1/P1) are found to be suppressed, while the motion related VEP component (N2) are found to be strengthened with vection (study two & four); 3) the power of steady state VEP is found to be suppressed in occipital region, while it is strengthened in parietal region during vection (study three); 4) the phase synchronization links (reflected by theta-band phase locking value between electrodes) connected to right central region and parietal region are found to be strengthened before vection onset, while the links connected to right-frontal regions are reduced after vection onset (study four).

For the qualitative covariates, two EEG signatures are revealed to vary according to the vection intensity of participants: the increment of SSVEP power (during vection) in study three and the increment of N2 amplitude at Pz electrode (evoked before vection onset) in study four are found to be positively correlated with vection intensity of participants.

In summary, those effects implied three consistent principles of visual information processing undervection: 1) shift processing emphasis from central visual field to peripheral visual field duringvection perception period; 2) shift processing emphasis from other visual functions (especially primary function like contrast processing) to the motion perception functions duringvection perception period; and 3) strengthen functional coordination with other sensory or integration regions beforevection onset, while reducing the coordination (especially with the right-frontal region) aftervection onset. As we discussed in previous chapters, those mechanisms can facilitate the processing of visual self-motion cues collaboratively and contribute to the sensory conflict reduction, which is in line with sensory conflict theory (Reason 1978) and Brandt's theory (1998).

9.1.2 Effects associated with VIMSS

Moreover, in supporting to our main hypothesis (vection effects shall vary according to VIMSS), all of thevection associated effects are revealed to negatively associated with VIMSS, where the effect size is weaker, absent or even in opposite direction for VIMS susceptible people as compared to their VIMS resistant contemporaries. This implies that thosevection related effects (described in 9.1.1) could be associated with mechanisms that facilitate the suppression of VIMS (e.g. reduction of sensory conflict).

Several effect indicators that negatively correlated with MSSQ scores of participants are found to be promising candidates for future VIMSS predictors: 1) the peripheral and central effect on response time (DRT) undervection period (study one); 2) the increment of N2 amplitude (IAmp) and advance of N2 latency at occipital electrodes undervection period (study two); 3) the suppression of N2 amplitude at Pz electrode beforevection (negative IAmp, study four); 4) the decrease of SSVEP power at Oz electrode duringvection (study three); 5) the increased dynamic phase locking to right-central, right-temporal-parietal and parietal-midline region beforevection onset (study four); 6) the reduced dynamic phase locking to right-frontal region aftervection onset (study four).

Based on the measuring methods, we grouped those identified indicators into four types (behavioral based indicator: *DRT*; transient VEP based indicator: *I_{Amp}*; SSVEP based indicator: *D_{Power}*; network based indicator: *Ndeg*). In chapter 8, we further evaluated and compared the explanatory power, the stability/discrimination ability, the difficulty and cost of this four types of indicator. Result suggested that the EEG indicators yield higher explanatory power than behavioral indicators. Among EEG indicators, SSVEP based indicator and network based indicator are most promising EEG indicators which deserved further explorations in the future.

9.1.3 Guideline for VIMS sensible applications

For the sake of training and practical applications, we also explored how the task motivated top-down attention allocation modulates the vection perception and visual response associated with it. Results suggested that two of the visual processing principle during vection (1.shift processing emphasis from central visual field to peripheral visual field; 2.shift processing emphasis from other function to the self-motion perception) can be enhanced with task requirements. The attention re-allocation does not only stabilize and strengthen the perception of vection, but also facilitate the vection associated effects reflected by SSVEP. Those vection effects could be associated with mechanisms that facilitate the suppression of VIMS through the stabilization of vection, since unstable vection actually introduce more severe VIMS (Bonato et al. 2008, 2005). Therefore, the task applied in this research actually provides a potential approach to reduce the occurrence of VIMS.

Moreover, based on the general theory and hypothesis, other tasks which motivated attention re-allocation following the two principles mentioned above could also benefit the VIMS sensible application, which enables plenty of possible solutions and designs. This solution is quite appealing as it does not hurt the vection experience, but actually facilitate the perception of vection. Perhaps one day we can actively reduce our susceptibility to VIMS simply by shifting our attention. Future work to realize the principles into design methodology or automatic quality control software for VR game designers is desirable. Data

reported in this research will also be useful in updating ISO/TR 9241, Part 393 – Ergonomics of human-system interaction – structured literature review of visually induced motion sickness during watching electronic images (ISO n.d.).

9.2 Summary on contributions

In summary, our findings support the sensory conflict theory (SCT) from the perspective of individual differences. We explore the visual response at different perception stage under roll vection-inducing stimulation (Figure 2.1), including the period during the plateau vection periods (study 1-3), as well as the period before and after vection onset (study 4). Those visual response effects uncovered were in line with the general sensory conflict theory and Brandt's complimentary theory (1998): under vection-inducing stimulation, our visual system facilitates the self-motion perception to reduce the sensory conflict. Importantly, we further test the hypothesis regarding SCT by exploring the effects among participants with various VIMSS. By uncovering the negative correlation between those effects and individual VIMSS of participants, we further supported that those mechanisms are closely associated with the reduction of sensory conflict and resistance to VIMS.

Furthermore, those identified behavioral and EEG signatures not only contribution to the better understanding of VIMS, but also facilitate the development of new objective vection measures and VIMS predictors. With high explanatory power for VIMSS, the SSVEP and network based indicators uncovered in study three and four can be served as potential objective predictor for VIMSS, while the SART based indicators identified in study one might serve as simple and quick predictors when less precision are demanded. Moreover, since several EEG signatures (SSVEP power and N2 amplitude) from Pz electrode yield quantitative assessing ability for vection intensity, the Pz electrode can be a promising candidate for vection measures and deserved more explorations when developing EEG markers for vection.

BIBLIOGRAPHY

- Agyei, Seth B., Magnus Holth, F. R. Ruud van der Weel, and Audrey L. H. van der Meer. 2015. "Longitudinal Study of Perception of Structured Optic Flow and Random Visual Motion in Infants Using High-Density EEG." *Developmental science* 18(3):436–51.
- Aitake, Michiyo et al. 2011. "Sensory Mismatch Induces Autonomic Responses Associated with Hippocampal Theta Waves in Rats." *Behavioural Brain Research* 220(1):244–53.
- Angelaki, Dora E., and Kathleen E. Cullen. 2008. "Vestibular System: The Many Facets of a Multimodal Sense." *Annual review of neuroscience* 31:125–50.
- Anon. 2007. "Motion-Onset VEPs: Characteristics, Methods, and Diagnostic Use." *Vision Research* 47(2):189–202.
- Araújo, Dráulio B. de, Oswaldo Baffa, and Ronald T. Wakai. 2002. "Theta Oscillations and Human Navigation: A Magnetoencephalography Study." *Journal of Cognitive Neuroscience* 14(1):70–78.
- Ash, April, and Stephen Palmisano. 2012. "Vection during Conflicting Multisensory Information about the Axis, Magnitude, and Direction of Self-Motion." *Perception* 41(3):253–67.
- Bach, Michael, and Dieter Ullrich. 1997. "Contrast Dependency of Motion-Onset and Pattern-Reversal VEPs: Interaction of Stimulus Type, Recording Site and Response Component." *Vision Research* 37(13):1845–49.
- Barry, R. J. et al. 2014. "EEG Markers of Visually Experienced Self-Motion (Vection)." in *Front. Hum. Neurosci. Conference Abstract: Australasian Society for Psychophysiology, Inc.*
- Becker-Bense, Sandra et al. 2012. "Ventral and Dorsal Streams Processing Visual Motion Perception (FDG-PET Study)." *BMC neuroscience* 13:81.
- Beer, Jeremy, Colin Blakemore, Fred H. Previc, and Mario Liotti. 2002. "Areas of the Human Brain Activated by Ambient Visual Motion, Indicating Three Kinds of Self-Movement." *Experimental brain research* 143(1):78–88.

- Bense, S., T. Stephan, T. A. Yousry, T. Brandt, and M. Dieterich. 2001. "Multisensory Cortical Signal Increases and Decreases during Vestibular Galvanic Stimulation (fMRI)." *Journal of neurophysiology* 85(2):886–99.
- Berthoz, A., B. Pavard, and L. R. Young. 1975. "Perception of Linear Horizontal Self-Motion Induced by Peripheral Vision (Linearvection) Basic Characteristics and Visual-Vestibular Interactions." *Experimental brain research* 23(5):471–89.
- Beveridge, R., S. Wilson, and D. Coyle. 2016. "3D Graphics, Virtual Reality, and Motion-Onset Visual Evoked Potentials in Neurogaming." in *Progress in Brain Research*.
- Blanchard, Caroline, Régine Roll, Jean-Pierre Roll, and Anne Kavounoudias. 2011. "Combined Contribution of Tactile and Proprioceptive Feedback to Hand Movement Perception." *Brain research* 1382:219–29.
- Blini, Elvio, Caroline Tilikete, Alessandro Farnè, and Fadila Hadj-Bouziane. 2018. "Probing the Role of the Vestibular System in Motivation and Reward-Based Attention." *Cortex* 103:82–99.
- Bonato, Frederick, Andrea Bubka, Stephen Palmisano, Danielle Phillip, and Giselle Moreno. 2008. "Vection Change Exacerbates Simulator Sickness in Virtual Environments." *Presence: Teleoperators and Virtual Environments* 17(3):283–92.
- Bonato, Frederick, Andrea Bubka, and Meredith Story. 2005. "Rotation Direction Change Hastens Motion Sickness Onset in an Optokinetic Drum." *Aviation, space, and environmental medicine* 76(9):823–27.
- Bonato, Frederick, Andrea Bubka, and William Thornton. 2015. "Visual Blur and Motion Sickness in an Optokinetic Drum." *Aerospace medicine and human performance* 86(5):440–44.
- Braddick, O. J. et al. 2001. "Brain Areas Sensitive to Coherent Visual Motion." *Perception* 30(1):61–72.
- Brainard, David H. 1997. "The Psychophysics Toolbox." *Spatial Vision* 10(4):433–36.
- Brandt, Thomas et al. 2002. "Visual-Vestibular and Visuovisual Cortical Interaction: New Insights from fMRI and PET." *Annals of the New York Academy of Sciences* 956:230–41.

- Brandt, Thomas, P. Bartenstein, A. Janek, and M. Dieterich. 1998. "Reciprocal Inhibitory Visual-Vestibular Interaction. Visual Motion Stimulation Deactivates the Parieto-Insular Vestibular Cortex." *Brain : a journal of neurology* 121 (9):1749–58.
- Brandt, Thomas, J. Dichgans, and E. Koenig. 1973. "Differential Effects of Central versus Peripheral Vision on Egocentric and Exocentric Motion Perception." *Experimental Brain Research* 16(5).
- Bremmer, Frank et al. 2016. "Multisensory Integration in Self Motion Perception." *Multisensory Research*.
- Bridge, H. 2011. "Mapping the Visual Brain: How and Why." *Eye (London, England)* 25(3):291–96.
- Britten, Kenneth H. 2008. "Mechanisms of Self-Motion Perception." *Annual review of neuroscience* 31:389–410.
- Bullmore, Ed, and Olaf Sporns. 2009. "Complex Brain Networks: Graph Theoretical Analysis of Structural and Functional Systems." *Nature reviews. Neuroscience* 10(3):186–98.
- Burdea, Grigore C., and Philippe Coiffet. 2003. "Virtual Reality Technology."
- Calvert, Gemma., Charles. Spence, Barry E. Stein, and MITCogNet. 2004. *The Handbook of Multisensory Processes*. MIT Press.
- Camfield, D. A. et al. 2012. "Steady State Visually Evoked Potential (SSVEP) Topography Changes Associated with Cocoa Flavanol Consumption." *Physiology & Behavior* 105(4):948–57.
- Campos, Jennifer L., and Heinrich H. Bühlhoff. 2012. *Multimodal Integration during Self-Motion in Virtual Reality*. CRC Press/Taylor & Francis.
- Cardin, Velia, and Andrew T. Smith. 2010. "Sensitivity of Human Visual and Vestibular Cortical Regions to Egomotion-Compatible Visual Stimulation." *Cerebral cortex (New York, N.Y. : 1991)* 20(8):1964–73.
- Cardin, Velia, and Andrew T. Smith. 2011. "Sensitivity of Human Visual Cortical Area V6 to Stereoscopic Depth Gradients Associated with Self-Motion." *Journal of neurophysiology* 106(3):1240–49.

- Caroux, Loïc, Ludovic Le Bigot, and Nicolas Vibert. 2013. "Impact of the Motion and Visual Complexity of the Background on Players' Performance in Video Game-like Displays." *Ergonomics* 56(12):1863–76.
- Carpenter-Smith, T. R., Robert G. Futamura, and Donald E. Parker. 1995. "Inertial Acceleration as a Measure of Linear Vection: An Alternative to Magnitude Estimation." *Perception & Psychophysics* 57(1):35–42.
- Carpenter-Smith, T. R., and D. E. Parker. 1992. "The Effects of Unidirectional Visual Surround Translation on Detection of Physical Linear Motion Direction. A Psychophysical Scale for Vection." *Annals of the New York Academy of Sciences* 656:817–19.
- Carriot, Jerome, Jessica X. Brooks, and Kathleen E. Cullen. 2013. "Multimodal Integration of Self-Motion Cues in the Vestibular System: Active versus Passive Translations." *The Journal of neuroscience: the official journal of the Society for Neuroscience* 33(50):19555–66.
- Chelen, W. E., M. Kabrisky, and S. K. Rogers. 1993. "Spectral Analysis of the Electroencephalographic Response to Motion Sickness." *Aviation, space, and environmental medicine* 64(1):24–29.
- Chen, Daniel J. Z., Eric H. C. Chow, and Richard H. Y. So. 2011. "The Relationship between Spatial Velocity, Vection, and Visually Induced Motion Sickness: An Experimental Study." *i-Perception* 2(4):415–415.
- Chen, Daniel Jinzhao, Beisheng Bao, Yue Zhao, and Richard H. Y. So. 2015. "Visually Induced Motion Sickness When Viewing Visual Oscillations of Different Frequencies along the Fore-and-Aft Axis: Keeping Velocity versus Amplitude Constant." *Ergonomics* 0139(July):1–9.
- Chen, Y. C. et al. 2009. "Motion-Sickness Related Brain Areas and EEG Power Activates." Pp. 348–54 in. Springer, Berlin, Heidelberg.
- Chuang, S., C. Chuang, Y. Yu, J. King, and C. Lin. 2016. "EEG Alpha and Gamma Modulators Mediate Motion Sickness-Related Spectral Responses." *International journal of neural systems* 1650007.

- Cohen, Jacob, and Jacob Cohen. 2003. *Applied Multiple Regression/Correlation Analysis for the Behavioral Sciences*. L. Erlbaum Associates.
- Coleman, J., C. C. Nduka, and A. Darzi. 1994. "Virtual Reality and Laparoscopic Surgery." *British Journal of Surgery* 81(12):1709–11.
- Correa, Ángel, Juan Lupiáñez, Eduardo Madrid, and Pío Tudela. 2006. "Temporal Attention Enhances Early Visual Processing: A Review and New Evidence from Event-Related Potentials." *Brain Research* 1076(1):116–28.
- Cullen, Kathleen E. 2011. "The Neural Encoding of Self-Motion." *Current Opinion in Neurobiology* 21(4):587–95.
- Cullen, Kathleen E. 2012. "The Vestibular System: Multimodal Integration and Encoding of Self-Motion for Motor Control." *Trends in neurosciences* 35(3):185–96.
- Deangelis, Gregory C., and Dora E. Angelaki. 2012. "Visual-Vestibular Integration for Self-Motion Perception." Pp. 1100–1113 in *The neural bases of multisensory processes*. CRC Press/Taylor & Francis.
- Delorme, Arnaud, and Scott Makeig. 2004. "EEGLAB: An Open Source Toolbox for Analysis of Single-Trial EEG Dynamics Including Independent Component Analysis." *Journal of Neuroscience Methods* 134(1):9–21.
- Dennison, Mark S., A. Zachary Wisti, and Michael D’Zmura. 2016. "Use of Physiological Signals to Predict Cybersickness." *Displays* 44:42–52.
- Deutschländer, Angela et al. 2002. "Sensory System Interactions during Simultaneous Vestibular and Visual Stimulation in PET." *Human brain mapping* 16(2):92–103.
- Deutschländer, Angela et al. 2004. "Rollvection versus Linearvection: Comparison of Brain Activations in PET." *Human brain mapping* 21(3):143–53.
- Diaz Artiles, Ana et al. 2016. "The Impact of Oral Promethazine on Human Whole-Body Motion Perceptual Thresholds." *Journal of Association for Research in Otolaryngology (Submitted)* 1–10.
- Dichgans, J., and T. Brandt. 1973. "Optokinetic Motion Sickness and Pseudo-Coriolis Effects Induced by Moving Visual Stimuli." *Acta oto-laryngologica* 76(5):339–48.
- Dichgans, J., and T. Brandt. 1978. "Visual-Vestibular Interactions : Effects of Self-Motion

- Perception and Postural Control.” *Handbook of sensory physiology* 8:755–804.
- Diels, Cyriel, and Peter a. Howarth. 2013. “Frequency Characteristics of Visually Induced Motion Sickness.” *Human factors* 55(3):595–604.
- Diels, Cyriel, and Peter A. Howarth. 2011. “Visually Induced Motion Sickness: Single-versus Dual-Axis Motion.” *Displays* 32(4):175–80.
- Dieterich, M., S. F. Bucher, K. C. Seelos, and T. Brandt. 1998. “Horizontal or Vertical Optokinetic Stimulation Activates Visual Motion-Sensitive, Ocular Motor and Vestibular Cortex Areas with Right Hemispheric Dominance. An FMRI Study.” *Brain : a journal of neurology* 121 (Pt 8:1479–95.
- Dieterich, Marianne, Sandra Bense, Thomas Stephan, Tarek A. Yousry, and Thomas Brandt. 2003. “FMRI Signal Increases and Decreases in Cortical Areas during Small-Field Optokinetic Stimulation and Central Fixation.” *Experimental brain research* 148(1):117–27.
- Dillard, Michael B. et al. 2014. “The Sustained Attention to Response Task (SART) Does Not Promote Mindlessness During Vigilance Performance.” *Human Factors: The Journal of the Human Factors and Ergonomics Society* 56(8):1364–79.
- Du, Bo. 2016. “Perception of Circular Vection under Different Viewing Conditions.” The Hong Kong University of Science and Technology, Clear Water Bay, Kowloon, Hong Kong.
- Duffy, C. J., and R. H. Wurtz. 1991. “Sensitivity of MST Neurons to Optic Flow Stimuli. I. A Continuum of Response Selectivity to Large-Field Stimuli.” *Journal of neurophysiology* 65(6):1329–45.
- Dupont, P. et al. 1991. “The Kinetic Occipital Region in Human Visual Cortex.” *Cerebral cortex (New York, N.Y. : 1991)* 7(3):283–92.
- Ebenholtz, Sheldon M. 1992. “Motion Sickness and Oculomotor Systems in Virtual Environments.” *Presence: Teleoperators and Virtual Environments* 1(3):302–5.
- Egeth, Howard E., and Steven Yantis. 1997. “VISUAL ATTENTION: Control, Representation, and Time Course.” *Annual Review of Psychology* 48(1):269–97.
- Eggemeir, F. T., and G. F. Wilson. 1991. “Multiple-Task Performance.” Pp. 217–78 in

- Multiple-Task Performance*. Taylor & Francis.
- Eschenbrenner, Brenda, Fiona Fui-Hoon Nah, and Keng Siau. 2008. "3-D Virtual Worlds in Education." *Journal of Database Management* 19(4):91–110.
- Farmer, Adam D. et al. 2015. "Visually Induced Nausea Causes Characteristic Changes in Cerebral, Autonomic and Endocrine Function in Humans." *The Journal of Physiology* 593(5):1183–96.
- Fetsch, Christopher R., Alexandre Pouget, Gregory C. DeAngelis, and Dora E. Angelaki. 2012. "Neural Correlates of Reliability-Based Cue Weighting during Multisensory Integration." *Nature neuroscience* 15(1):146–54.
- Field, David T., Laura A. Inman, and Li Li. 2015. "Visual Processing of Optic Flow and Motor Control in the Human Posterior Cingulate Sulcus." *Cortex* 71:377–89.
- Fischer, Elvira, Heinrich H. Bühlhoff, Nikos K. Logothetis, and Andreas Bartels. 2012a. "Human Areas V3A and V6 Compensate for Self-Induced Planar Visual Motion." *Neuron* 73(6):1228–40.
- Fischer, Elvira, Heinrich H. Bühlhoff, Nikos K. Logothetis, and Andreas Bartels. 2012b. "Human Areas V3A and V6 Compensate for Self-Induced Planar Visual Motion." *Neuron* 73(6):1228–40.
- Fisher, N. I. 1993. *Statistical Analysis of Circular Data*. Cambridge: Cambridge University Press.
- Fornito, Alex, Andrew Zalesky, and Michael Breakspear. 2013. "Graph Analysis of the Human Connectome: Promise, Progress, and Pitfalls." *NeuroImage* 80:426–44.
- Fowler, Cynthia G., Amanda Sweet, and Emily Steffel. 2014. "Effects of Motion Sickness Severity on the Vestibular-Evoked Myogenic Potentials." *Journal of the American Academy of Audiology* 25(9):814–22.
- Frank, Sebastian M., Oliver Baumann, Jason B. Mattingley, and Mark W. Greenlee. 2014. "Vestibular and Visual Responses in Human Posterior Insular Cortex." *Journal of neurophysiology* 112(10):2481–91.
- Freitas Júnior, Paulo B., and José A. Barela. 2004. "Postural Control as a Function of Self- and Object-Motion Perception." *Neuroscience Letters* 369(1):64–68.

- Fu, Xiao, Yue Wei, Daniel Chen, and Richard So. 2017. "Interaction Effect of Frequency, Velocity and Amplitude on Perceived Vection Magnitude for Yaw Visual Oscillation." *Journal of Vision* 17(10):364.
- Gallagher, Maria, and Elisa Raffaella Ferrè. 2018. "Cybersickness: A Multisensory Integration Perspective." *Multisensory Research*.
- Genovese, Christopher R., Nicole A. Lazar, and Thomas Nichols. 2002. "Thresholding of Statistical Maps in Functional Neuroimaging Using the False Discovery Rate." *NeuroImage* 15(4):870–78.
- Gibson, J. J. 1950. *Perception of the Visual World*. Oxford, England: Houghton Mifflin.
- Golding, J. F. 1998. "Motion Sickness Susceptibility Questionnaire Revised and Its Relationship to Other Forms of Sickness." *Brain research bulletin* 47(5):507–16.
- Golding, J. F. 2006. "Motion Sickness Susceptibility." *Autonomic Neuroscience* 129(1–2):67–76.
- Golding, J. F., and M. Kerguelen. 1992. "A Comparison of the Nauseogenic Potential of Low-Frequency Vertical versus Horizontal Linear Oscillation." *Aviation, space, and environmental medicine* 63(6):491–97.
- Golding, John F., Kim Doolan, Amish Acharya, Maryame Tribak, and Michael A. Gresty. 2012. "Cognitive Cues and Visually Induced Motion Sickness." *Aviation Space and Environmental Medicine* 83(5):477–82.
- Golding, John F., Priscilla Kadzere, and Michael A. Gresty. 2005. "Motion Sickness Susceptibility Fluctuates through the Menstrual Cycle." *Aviation, space, and environmental medicine* 76(10):970–73.
- Gordon, C. R., O. Spitzer, I. Doweck, A. Shupak, and N. Gadoth. 1996. "The Vestibulo-Ocular Reflex and Seasickness Susceptibility." *J. Vestib. Res.-Equilib. Orientat.* 6(October 2015):229–33.
- Griffin, M. J. 2012. *Handbook of Human Vibration*. Academic Press.
- Griffis, JC et al. 2016. "Retinotopic Patterns of Functional Connectivity between V1 and Large-Scale Brain Networks during Resting Fixation." *Unpublished Results* 1.
- Gu, Yong, Dora E. Angelaki, and Gregory C. Deangelis. 2008. "Neural Correlates of

- Multisensory Cue Integration in Macaque MSTd.” *Nature neuroscience* 11(10):1201–10.
- Guo, C. C. T., D. J. Z. Chen, I. Y. Wei, R. H. Y. So, and R. T. F. Cheung. 2017. “Correlations between Individual Susceptibility to Visually Induced Motion Sickness and Decaying Time Constant of After-Nystagmus.” *Applied Ergonomics* 63:1–8.
- Guo, Cuiting. 2010. “Relationships among Optokinetic Nystagmus (OKN), after-OKN and Visually Induced Motion Sickness.” The Hong Kong University of Science and Technology, Clear Water Bay, Kowloon, Hong Kong.
- Hampson, Michelle, Ingrid R. Olson, Hoi-Chung Leung, Pawel Skudlarski, and John C. Gore. 2004. “Changes in Functional Connectivity of Human MT/V5 with Visual Motion Input.” *Neuroreport* 15(8):1315–19.
- Haxby, J. V et al. 2001. “Distributed and Overlapping Representations of Faces and Objects in Ventral Temporal Cortex.” *Science (New York, N.Y.)* 293(5539):2425–30.
- He, Yong, and Alan Evans. 2010. “Graph Theoretical Modeling of Brain Connectivity.” *Current opinion in neurology* 23(4):341–50.
- Head, J., K. Wilson, W. S. Helton, and S. Kemp. 2013. “The Role of Calmness in a High-Go Target Detection Task.” *Proceedings of the Human Factors and Ergonomics Society* 57(1):838–42.
- Henn, V., L. R. Young, and C. Finley. 1974. “Vestibular Nucleus Units in Alert Monkeys Are Also Influenced by Moving Visual Fields.” *Brain Research* 71(1):144–49.
- Herrmann, Christoph S. 2001. “Human EEG Responses to 1-100 Hz Flicker: Resonance Phenomena in Visual Cortex and Their Potential Correlation to Cognitive Phenomena.” *Experimental Brain Research* 137(3–4):346–53.
- Hettinger, L. J., K. S. Berbaum, R. S. Kennedy, W. P. Dunlap, and M. D. Nolan. 1990. “Vection and Simulator Sickness.” *Military psychology: the official journal of the Division of Military Psychology, American Psychological Association* 2(3):171–81.
- van den Heuvel, Martijn P. et al. 2013. “Abnormal Rich Club Organization and Functional Brain Dynamics in Schizophrenia.” *JAMA Psychiatry* 70(8):783.
- van den Heuvel, Martijn P., and Olaf Sporns. 2013. “Network Hubs in the Human Brain.”

- Trends in cognitive sciences* 17(12):683–96.
- Hilger, Kirsten, Matthias Ekman, Christian J. Fiebach, and Ulrike Basten. 2016. “Efficient Hubs in the Intelligent Brain: Nodal Efficiency of Hub Regions in the Salience Network Is Associated with General Intelligence.” *Intelligence*.
- Hillyard, S. A., E. K. Vogel, and S. J. Luck. 1998. “Sensory Gain Control (Amplification) as a Mechanism of Selective Attention: Electrophysiological and Neuroimaging Evidence.” *Philosophical transactions of the Royal Society of London. Series B, Biological sciences* 353(1373):1257–70.
- Indovina, Iole et al. 2005. “Representation of Visual Gravitational Motion in the Human Vestibular Cortex.” *Science (New York, N.Y.)* 308(5720):416–19.
- ISO. 2005. “Ergonomics of Human-System Interaction - Part 393: Structured Literature Review of Visually Induced Motion Sickness during Watching Electronic Images of Human-System Interaction.” *ISO Technical Report 9241-393*. Retrieved November 10, 2017 (<https://www.din.de/en/getting-involved/standards-committees/naerg/projects/wdc-proj:din21:269389016>).
- ISO. n.d. “ISO/TR 9241 Ergonomics of Human-System Interaction — Part 393: Structured Literature Review of Visually Induced Motion Sickness during Watching Electronic Images.” in *ISO/TR 9241 Ergonomics of human-system interaction*. Switzerland.
- IWA 3. 2005. “International Workshop Agreement 3: Image Safety -- Reducing the Incidence of Undesirable Biomedical Effects Caused by Visual Image Sequences.” International Organisation of Standardisation.
- Ji, Jennifer T. T., Richard H. Y. So, and Raymond T. F. Cheung. 2009. “Isolating the Effects of Vection and Optokinetic Nystagmus on Optokinetic Rotation-Induced Motion Sickness.” *Human factors* 51(5):739–51.
- Jo, Han-Gue, Peter Malinowski, and Stefan Schmidt. 2017. “Frontal Theta Dynamics during Response Conflict in Long-Term Mindfulness Meditators.” *Frontiers in Human Neuroscience* 11:299.
- Jong, B. M. d., S. Shipp, B. Skidmore, R. S. J. Frackowiak, and S. Zeki. 1994. “The Cerebral Activity Related to the Visual Perception of Forward Motion in Depth.” *Brain*

117(5):1039–54.

- Kawasaki, Masahiro, Keiichi Kitajo, and Yoko Yamaguchi. 2010. “Dynamic Links between Theta Executive Functions and Alpha Storage Buffers in Auditory and Visual Working Memory.” *European Journal of Neuroscience* 31(9):1683–89.
- Kawasaki, Masahiro, Keiichi Kitajo, and Yoko Yamaguchi. 2014. “Fronto-Parietal and Fronto-Temporal Theta Phase Synchronization for Visual and Auditory-Verbal Working Memory.” *Frontiers in Psychology* 5(MAR):200.
- Kayser, Jürgen, and Craig E. Tenke. 2006a. “Principal Components Analysis of Laplacian Waveforms as a Generic Method for Identifying ERP Generator Patterns: I. Evaluation with Auditory Oddball Tasks.” *Clinical Neurophysiology* 117(2):348–68.
- Kayser, Jürgen, and Craig E. Tenke. 2006b. “Principal Components Analysis of Laplacian Waveforms as a Generic Method for Identifying ERP Generator Patterns: II. Adequacy of Low-Density Estimates.” *Clinical Neurophysiology* 117(2):369–80.
- Keil, Andreas, Stephan Moratti, Dean Sabatinelli, Margaret M. Bradley, and Peter J. Lang. 2005. “Additive Effects of Emotional Content and Spatial Selective Attention on Electrocortical Facilitation.” *Cerebral Cortex* 15(8):1187–97.
- Keller, E. L. 1976. “Behavior of Horizontal Semicircular Canal Afferents in Alert Monkey during Vestibular and Optokinetic Stimulation.” *Experimental Brain Research* 24(5).
- Kempel, P., K. Lampe, R. Parnefjord, J. Hennig, and H. J. Kunert. 2003. “Auditory-Evoked Potentials and Selective Attention: Different Ways of Information Processing in Cannabis Users and Controls.” *Neuropsychobiology* 48(2):95–101.
- Kennedy, Robert S., Norman E. Lane, Kevin S. Berbaum, and Michael G. Lilienthal. 1993. “Simulator Sickness Questionnaire: An Enhanced Method for Quantifying Simulator Sickness.” *The International Journal of Aviation Psychology* 3(3):203–20.
- Keshavarz, Behrang, and Stefan Berti. 2014. “Integration of Sensory Information Precedes the Sensation of Vection: A Combined Behavioral and Event-Related Brain Potential (ERP) Study.” *Behavioural brain research* 259:131–36.
- Keshavarz, Behrang, Jennifer L. Campos, and Stefan Berti. 2015. “Vection Lies in the Brain of the Beholder: EEG Parameters as an Objective Measurement of Vection.” *Frontiers*

in Psychology 6.

- Keshavarz, Behrang, and Heiko Hecht. 2011. "Axis Rotation and Visually Induced Motion Sickness: The Role of Combined Roll, Pitch, and Yaw Motion." *Aviation, space, and environmental medicine* 82(11):1023–29.
- Keshavarz, Behrang, Lawrence J. Hettinger, Robert S. Kennedy, and Jennifer L. Campos. 2014. "Demonstrating the Potential for Dynamic Auditory Stimulation to Contribute to Motion Sickness." *PLoS ONE* 9(7).
- Keshavarz, Behrang, Lawrence J. Hettinger, Daniel Vena, and Jennifer L. Campos. 2014. "Combined Effects of Auditory and Visual Cues on the Perception of Vection." *Experimental brain research* 232(3):827–36.
- Keshavarz, Behrang, Bernhard E. Riecke, Lawrence J. Hettinger, and Jennifer L. Campos. 2015. "Vection and Visually Induced Motion Sickness: How Are They Related?" *Frontiers in psychology* 6:472.
- Kim, Juno, and Stephen Palmisano. 2010. "Eccentric Gaze Dynamics Enhance Vection in Depth." *Journal of vision* 10(12):7.
- Kirsch, Valerie et al. 2018. "Handedness-Dependent Functional Organizational Patterns within the Bilateral Vestibular Cortical Network Revealed by fMRI Connectivity Based Parcellation." *NeuroImage* in press:224–37.
- Kleinschmidt, Andreas et al. 2002. "Neural Correlates of Visual-Motion Perception as Object- or Self-Motion." *NeuroImage* 16(4):873–82.
- Klinke, R. 1970. "Efferent Influence on the Vestibular Organ during Active Movements of the Body." *Pflügers Archiv European Journal of Physiology* 318(4):325–32.
- Koslucher, Frank, Eric Haaland, and Thomas A. Stoffregen. 2016. "Sex Differences in Visual Performance and Postural Sway Precede Sex Differences in Visually Induced Motion Sickness." *Experimental Brain Research* 234(1):313–22.
- Kovács, Gyula, Markus Raabe, and Mark W. Greenlee. 2008. "Neural Correlates of Visually Induced Self-Motion Illusion in Depth." *Cerebral cortex (New York, N.Y. : 1991)* 18(8):1779–87.
- Kubová, Zuzana, Miroslav Kuba, Henk Spekrijse, and Colin Blakemore. 1995. "Contrast

- Dependence of Motion-Onset and Pattern-Reversal Evoked Potentials.” *Vision Research* 35(2):197–205.
- Kuno, S., T. Kawakita, O. Kawakami, Y. Miyake, and S. Watanabe. 1999. “Postural Adjustment Response to Depth Direction Moving Patterns Produced by Virtual Reality Graphics.” *The Japanese journal of physiology* 49(5):417–24.
- Lachaux, Jean-Philippe Rodriguez, Eugenio, Michel Le van Quyen, Antoine Lutz, Jacques Martinerie, and Francisco J. Varela. 2000. “Studying Single-Trials of Phase Synchronous Activity in the Brain.” *International Journal of Bifurcation and Chaos* 10(10):2429–39.
- Lachaux, J. P., E. Rodriguez, J. Martinerie, and F. J. Varela. 1999. “Measuring Phase Synchrony in Brain Signals.” *Human brain mapping* 8(4):194–208.
- Lackner, James R. 1988. “Some Proprioceptive Influences on the Perceptual Representation of Body Shape and Orientation.” *Brain* 111(2):281–97.
- Lackner, James R. 2014. “Motion Sickness: More than Nausea and Vomiting.” *Experimental brain research* 232(8):2493–2510.
- Lappe, Markus. 2000. *Neuronal Processing of Optic Flow*. Academic Press.
- Le, An T. D. et al. 2017. “Discomfort from Urban Scenes: Metabolic Consequences.” *Landscape and Urban Planning* 160:61–68.
- Lestienne, F., J. Soechting, and A. Berthoz. 1977. “Postural Readjustments Induced by Linear Motion of Visual Scenes.” *Experimental Brain Research* 28–28(3–4).
- Liang, Tengfei, Zhonghua Hu, and Qiang Liu. 2017. “Frontal Theta Activity Supports Detecting Mismatched Information in Visual Working Memory.” *Frontiers in Psychology* 8:1821.
- Lopez-Calderon, Javier, and Steven J. Luck. 2014. “ERPLAB: An Open-Source Toolbox for the Analysis of Event-Related Potentials.” *Frontiers in human neuroscience* 8(April):213.
- Lopez, Christophe. 2015. “Making Sense of the Body: The Role of Vestibular Signals.” *Brill*.
- Lopez, Christophe, and Olaf Blanke. 2011. “The Thalamocortical Vestibular System in Animals and Humans.” *Brain research reviews* 67(1–2):119–46.

- Lu, S. .. Y., M. Shpitalni, and Rajit Gadh. 1999. "Virtual and Augmented Reality Technologies for Product Realization." *CIRP Annals - Manufacturing Technology* 48(2):471–95.
- Luck, Stephen J. 2005. *An Introduction to the Event-Related Potential Technique*.
- Mach, Ernst. 1875. *Grundlinien Der Lehre von Den Bewegungsempfindungen*. W. Engelmann.
- Mangun, George R. 1995. "Neural Mechanisms of Visual Selective Attention." *Psychophysiology* 32(1):4–18.
- Manly, Tom, Ian H. Robertson, Maria Galloway, and Kari Hawkins. 1999. "The Absent Mind: Further Investigations of Sustained Attention to Response." *Neuropsychologia* 37(6):661–70.
- Maris, Eric, and Robert Oostenveld. 2007. "Nonparametric Statistical Testing of EEG- and MEG-Data." *Journal of Neuroscience Methods* 164(1):177–90.
- Martínez-Trujillo, Julio C., and Stefan Treue. 2002. "Attentional Modulation Strength in Cortical Area MT Depends on Stimulus Contrast." *Neuron* 35(2):365–70.
- Mitchell, Jude F., Kristy A. Sundberg, and John H. Reynolds. 2007. "Differential Attention-Dependent Response Modulation across Cell Classes in Macaque Visual Area V4." *Neuron* 55(1):131–41.
- Miyazaki, Jungo et al. 2015. "Inter-Hemispheric Desynchronization of the Human MT+ during Visually Induced Motion Sickness." *Experimental brain research*.
- Mognon, Andrea, Jorge Jovicich, Lorenzo Bruzzone, and Marco Buiatti. 2011. "ADJUST: An Automatic EEG Artifact Detector Based on the Joint Use of Spatial and Temporal Features." *Psychophysiology* 48(2):229–40.
- Morgan, S. T., J. C. Hansen, and S. A. Hillyard. 1996. "Selective Attention to Stimulus Location Modulates the Steady-State Visual Evoked Potential." *Proceedings of the National Academy of Sciences of the United States of America* 93(10):4770–74.
- Müller, Matthias M. et al. 1998. "Effects of Spatial Selective Attention on the Steady-State Visual Evoked Potential in the 20-28 Hz Range." *Cognitive Brain Research* 6(4):249–61.

- Murray, Mark, and Micah Wallace. 2011. *The Neural Bases of Multisensory Processes*.
- Murray, Micah M., Antonia Thelen, Silvio Ionta, and Mark T. Wallace. 2018. "Contributions of Intraindividual and Interindividual Differences to Multisensory Processes." *Journal of Cognitive Neuroscience* 1–17.
- Nachum, Zohar, Carlos R. Gordon, Baruch Shahal, Orna Spitzer, and Avi Shupak. 2002. "Active High-Frequency Vestibulo-Ocular Reflex and Seasickness Susceptibility." *Laryngoscope* 112(1):179–82.
- Napadow, Vitaly et al. 2013. "The Brain Circuitry Underlying the Temporal Evolution of Nausea in Humans." *Cerebral cortex (New York, N.Y. : 1991)* 23(4):806–13.
- Ng, V. W. et al. 2000. "Hemispheric Preference in Visuospatial Processing: A Complementary Approach with FMRI and Lesion Studies." *Human brain mapping* 10(2):80–86.
- Niedermeyer, Ernst, and F. H. Lopes da Silva. 2005. *Electroencephalography: Basic Principles, Clinical Applications, and Related Fields*. Lippincott Williams & Wilkins.
- Nishiike, Suetaka et al. 2002. "Magnetic Cortical Responses Evoked by Visual Linear Forward Acceleration." *NeuroReport* 13(14):1805–8.
- Nooij, Suzanne A. E., Paolo Pretto, Daniel Oberfeld, Heiko Hecht, and Heinrich H. Bühlhoff. 2017. "Vection Is the Main Contributor to Motion Sickness Induced by Visual Yaw Rotation: Implications for Conflict and Eye Movement Theories." *PLoS ONE* 12(4).
- Norman, Kenneth A., Sean M. Polyn, Greg J. Detre, and James V Haxby. 2006. "Beyond Mind-Reading: Multi-Voxel Pattern Analysis of FMRI Data." *Trends in cognitive sciences* 10(9):424–30.
- O'Connell, Caitlin et al. 2017. "Effects of Acute Peripheral/Central Visual Field Loss on Standing Balance." *Experimental Brain Research* 1–10.
- Oman, Charles M., and Kathleen E. Cullen. 2014. "Brainstem Processing of Vestibular Sensory Exafference: Implications for Motion Sickness Etiology." *Experimental brain research* 232(8):2483–92.
- Van Ombergen, Angelique et al. 2016. "The Effect of Optokinetic Stimulation on Perceptual and Postural Symptoms in Visual Vestibular Mismatch Patients." *PLoS ONE* 11(4).

- Oostenveld, Robert, Pascal Fries, Eric Maris, and Jan Mathijs Schoffelen. 2011. "FieldTrip: Open Source Software for Advanced Analysis of MEG, EEG, and Invasive Electrophysiological Data." *Computational Intelligence and Neuroscience* 2011:156869.
- Orban, G. A. 2001. "Imaging Image Processing in the Human Brain." *Current Opinion in Neurology* 14(1):47–54.
- Paillard, A. C. et al. 2013. "Motion Sickness Susceptibility in Healthy Subjects and Vestibular Patients: Effects of Gender, Age and Trait-Anxiety." *Journal of Vestibular Research: Equilibrium and Orientation* 23(4–5):203–10.
- Paillard, A. C. et al. 2014. "Is There a Relationship between Odors and Motion Sickness?" *Neuroscience Letters* 566:326–30.
- Palmisano, Stephen, Robert S. Allison, Mark M. Schira, and Robert J. Barry. 2015. "Future Challenges for Vection Research: Definitions, Functional Significance, Measures, and Neural Bases." *Frontiers in psychology* 6:193.
- Pan, Yanxia et al. 2016. "Representation of Illusory and Physical Rotations in Human MST: A Cortical Site for the Pinna Illusion." *Human brain mapping*.
- Parsons, Sarah, and Sue Cobb. 2011. "State-of-the-Art of Virtual Reality Technologies for Children on the Autism Spectrum." *European Journal of Special Needs Education*.
- Pelli, Denis G. 1997. "The VideoToolbox Software for Visual Psychophysics: Transforming Numbers into Movies." *Spatial Vision* 10(4):437–42.
- Pitzalis, S. et al. 2010. "Human v6: The Medial Motion Area." *Cerebral cortex (New York, N.Y. : 1991)* 20(2):411–24.
- Pitzalis, S., F. Strappini, M. de Gasperis, A. Bultrini, and F. Di Russo. 2013. "Spatio-Temporal Brain Mapping of Motion-Onset VEPs Combined with fMRI and Retinotopic Maps." *PLoS ONE* 7(4).
- Pitzalis, Sabrina et al. 2013. "Selectivity to Translational Egomotion in Human Brain Motion Areas." *PLoS ONE* 8(4).
- Pitzalis, Sabrina, Patrizia Fattori, and Claudio Galletti. 2012. "The Functional Role of the Medial Motion Area V6." *Frontiers in behavioral neuroscience* 6:91.

- Pitzalis, SABRINA, PATRIZIA Fattori, and CLAUDIO Galletti. 2015. "The Human Cortical Areas V6 and V6A." *Visual Neuroscience* 32:E007.
- Pitzalis, Sabrina, Francesca Strappini, Alessandro Bultrini, and Francesco Di Russo. 2018. "Detailed Spatiotemporal Brain Mapping of Chromatic Vision Combining High-Resolution VEP with fMRI and Retinotopy." *Human Brain Mapping*.
- Pitzalis, Sabrina, Francesca Strappini, Marco De Gasperis, Alessandro Bultrini, and Francesco Di Russo. 2012. "Spatio-Temporal Brain Mapping of Motion-Onset VEPs Combined with fMRI and Retinotopic Maps" edited by Samuel G. Solomon. *PLoS ONE* 7(4):e35771.
- Popp, Pauline et al. 2017. "Cognitive Deficits in Patients with a Chronic Vestibular Failure." *Journal of Neurology* 264(3):554–63.
- Previc, F. H., and T. J. Mullen. 1990. "A Comparison of the Latencies of Visually Induced Postural Change and Self-Motion Perception." *Journal of vestibular research: equilibrium & orientation* 1(3):317–23.
- Previc, Fred H., Mario Liotti, Colin Blakemore, Jeremy Beer, and Peter Fox. 2014. "Functional Imaging of Brain Areas Involved in the Processing of Coherent and Incoherent Wide Field-of-View Visual Motion." *Experimental Brain Research* 131(4):393–405.
- Probst, Th, A. Straube, and W. Bles. 1985. "Differential Effects of Ambivalent Visual-Vestibular-Somatosensory Stimulation on the Perception of Self-Motion." *Behavioural Brain Research* 16(1):71–79.
- Prothero, J. D., M. H. Draper, T. A. Furness, D. E. Parker, and M. J. Wells. 1999. "The Use of an Independent Visual Background to Reduce Simulator Side-Effects." *Aviation, space, and environmental medicine* 70(3 Pt 1):277–83.
- Psotka, Joseph. 1995. "Immersive Training Systems: Virtual Reality and Education and Training." *Instructional Science* 23(5–6):405–31.
- Reason, J. T. 1978. "Motion Sickness Adaptation: A Neural Mismatch Model." *Journal of the Royal Society of Medicine* 71(11):819–29.
- de Reus, Marcel A., and Martijn P. van den Heuvel. 2013. "The Parcellation-Based

- Connectome: Limitations and Extensions.” *NeuroImage* 80:397–404.
- Riccio, Gary E., and Thomas A. Stoffregen. 1991. “An Ecological Theory of Motion Sickness and Postural Instability.” *Ecological Psychology* 3(3):195–240.
- Riecke, Bernhard E. 2011. *Virtual Reality*. edited by Jae-Jin Kim. InTech.
- Riecke, Bernhard E., Daniel Feuereissen, and John J. Rieser. 2008. “Auditory Self-Motion Illusions (‘circular Vection’) Can Be Facilitated by Vibrations and the Potential for Actual Motion.” P. 147 in *Proceedings of the 5th symposium on Applied perception in graphics and visualization - APGV '08*. New York, New York, USA: ACM Press.
- Riecke, Bernhard E., Daniel Feuereissen, John J. Rieser, and Timothy P. McNamara. 2012. “Self-Motion Illusions (Vection) in VR — Are They Good for Anything?” Pp. 35–38 in *2012 IEEE Virtual Reality (VR)*. IEEE.
- Riecke, Bernhard E., Joerg Schulte-Pelkum, and Franck Caniard. 2006. “Visually Induced Linear Vection Is Enhanced by Small Physical Accelerations.”
- Roberts, R. E. et al. 2016. “Functional Neuroimaging of Visuo-Vestibular Interaction.” *Brain Structure and Function*.
- Robertson, Ian H., Tom Manly, Jackie Andrade, Bart T. Baddeley, and Jenny Yiend. 1997. “‘Oops!’: Performance Correlates of Everyday Attentional Failures in Traumatic Brain Injured and Normal Subjects.” *Neuropsychologia* 35(6):747–58.
- Rory, Cellan-Jones. 2016. “2016: The Year When VR Goes from Virtual to Reality.” *BBC News*.
- Di Russo, Francesco et al. 2005. “Identification of the Neural Sources of the Pattern-Reversal VEP.” *NeuroImage* 24(3):874–86.
- Scarpino, O., M. Guidi, and G. Bolcioni. 1990. “Topographic EEG Analysis. Methods for Graphic Representation and Clinical Applications.” *Acta neurologica* 12(5):410–26.
- Van Schie, Mojca K. M. et al. 2012. “Sustained Attention to Response Task (SART) Shows Impaired Vigilance in a Spectrum of Disorders of Excessive Daytime Sleepiness.” *Journal of Sleep Research* 21(4):390–95.
- Schindler, Andreas, and Andreas Bartels. 2018. “Integration of Visual and Non-Visual Self-Motion Cues during Voluntary Head Movements in the Human Brain.” *NeuroImage*

172:597–607.

- Sharma, K., P. Sharma, A. Sharma, and G. Singh. 2008. "Phenylthiocarbamide Taste Perception and Susceptibility to Motion Sickness: Linking Higher Susceptibility with Higher Phenylthiocarbamide Taste Acuity." *Journal of Laryngology and Otology* 122(10):1064–73.
- Shipp, S., B. M. de Jong, J. Zihl, R. S. Frackowiak, and S. Zeki. 1994. "The Brain Activity Related to Residual Motion Vision in a Patient with Bilateral Lesions of V5." *Brain : a journal of neurology* 117 (Pt 5:1023–38.
- Silberstein, R. B., P. L. Nunez, A. Pipingas, P. Harris, and F. Danieli. 2001. "Steady State Visually Evoked Potential (SSVEP) Topography in a Graded Working Memory Task." *International journal of psychophysiology: official journal of the International Organization of Psychophysiology* 42(2):219–32.
- Smith, Paul F., and Yiwen Zheng. 2013. "From Ear to Uncertainty: Vestibular Contributions to Cognitive Function." *Frontiers in integrative neuroscience* 7(November):84.
- Smythies, John. 1996. "A Note on the Concept of the Visual Field in Neurology, Psychology, and Visual Neuroscience." *Perception* 25(3):369–71.
- So, R. H. Y., C. M. Finney, and R. S. Goonetilleke. 1999. "Motion Sickness Susceptibility and Occurrence in Hong Kong Chinese." in *Contemporary Ergonomics, Taylor & Francis*.
- So, Richard H. Y., and Hiroyasu Ujike. 2010. "Visually Induced Motion Sickness, Visual Stress and Photosensitive Epileptic Seizures: What Do They Have in Common? - Preface to the Special Issue." *Applied Ergonomics*.
- Souza, Givago S. et al. 2013. "Contrast Sensitivity of Pattern Transient VEP Components: Contribution from M and P Pathways." *Psychology & Neuroscience* 6(2):191–98.
- Stam, C. J., B. F. Jones, G. Nolte, M. Breakspear, and Ph Scheltens. 2007. "Small-World Networks and Functional Connectivity in Alzheimer's Disease." *Cerebral cortex (New York, N.Y. : 1991)* 17(1):92–99.
- Stanney, K. M., K. S. Kingdon, and R. S. Kennedy. 2002. "Dropouts and Aftereffects: Examining General Accessibility to Virtual Environment Technology." *Proceedings of*

- the Human Factors and Ergonomics Society Annual Meeting* 46(26):2114–18.
- Stern, R. M., S. Hu, R. B. Anderson, H. W. Leibowitz, and K. L. Koch. 1990. “The Effects of Fixation and Restricted Visual Field on Vection-Induced Motion Sickness.” *Aviation Space and Environmental Medicine* 61(8):712–15.
- Stoffregen, T. A. 1985. “Flow Structure versus Retinal Location in the Optical Control of Stance.” *Journal of experimental psychology. Human perception and performance* 11(5):554–65.
- Strasburger, H., I. Rentschler, and M. Jüttner. 2011. “Peripheral Vision and Pattern Recognition: A Review.” *Journal of Vision* 11(5):13–13.
- Strong, Samantha L., Edward H. Silson, André D. Gouws, Antony B. Morland, and Declan J. McKeefry. 2016. “A Direct Demonstration of Functional Differences between Subdivisions of Human V5/MT+.” *Cerebral Cortex* 1–10.
- Stróżak, Paweł et al. 2016. “ERPs in an Oddball Task under Vection-Inducing Visual Stimulation.” *Experimental Brain Research* 1–10.
- Sun, Junfeng, Xiangfei Hong, and Shanbao Tong. 2012. “Phase Synchronization Analysis of Eeg Signals: An Evaluation Based on Surrogate Tests.” *IEEE Transactions on Biomedical Engineering* 59(8):2254–63.
- Szalma, J. L., T. N. Daly, G. W. L. Teo, G. M. Hancock, and P. A. Hancock. 2017. “Training for Vigilance on the Move: A Video Game-Based Paradigm for Sustained Attention.” *Ergonomics* 1–65.
- Tal, Dror et al. 2013. “Vestibular Evoked Myogenic Potentials and Habituation to Seasickness.” *Clinical Neurophysiology* 124(12):2445–49.
- Teghtsoonian, R. 1971. “On the Exponents in Stevens’ Law and the Constant in Ekman’s Law.” *Psychological review* 78(1):71–80.
- Thilo, Kai V, Andreas Kleinschmidt, and Michael A. Gresty. 2003. “Perception of Self-Motion from Peripheral Optokinetic Stimulation Suppresses Visual Evoked Responses to Central Stimuli.” *Journal of neurophysiology* 90(2):723–30.
- Tokumaru, O., K. Kaida, H. Ashida, I. Yoneda, and J. Tatsuno. 1999. “EEG Topographical Analysis of Spatial Disorientation.” *Aviation, space, and environmental medicine* 70(3

Pt 1):256–63.

- Totah, Nelson K. B., Mark E. Jackson, and Bitu Moghaddam. 2013. “Preparatory Attention Relies on Dynamic Interactions between Prelimbic Cortex and Anterior Cingulate Cortex.” *Cerebral Cortex* 23(3):729–38.
- Turner, Mark, and Michael J. Griffin. 1999. “Motion Sickness in Public Road Transport: Passenger Behaviour and Susceptibility.” *Ergonomics* 42(3):444–61.
- Tyner, Fay S., John R. (John Russell) Knott, and W. Brem. Mayer. 1983. *Fundamentals of EEG Technology*. Raven Press.
- Uesaki, Maiko, and Hiroshi Ashida. 2015. “Optic-Flow Selective Cortical Sensory Regions Associated with Self-Reported States of Vection.” *Frontiers in psychology* 6:775.
- Ungerleider, L. 1994. “‘What’ and ‘Where’ in the Human Brain.” *Current Opinion in Neurobiology* 4(2):157–65.
- Uno, A. et al. 2000. “Effects of Amygdala or Hippocampus Lesion on Hypergravity-Induced Motion Sickness in Rats.” *Acta oto-laryngologica* 120(7):860–65.
- Varela, Francisco, J. P. Lachaux, Eugenio Rodriguez, and Jacques Martinerie. 2001. “The Brainweb: Phase Synchronization and Large-Scale Integration.” *Nature reviews. Neuroscience* 2(4):229–39.
- Varlet, Manuel, Benoît G. Bardy, Fu Chen Chen, Cristina Alcantara, and Thomas A. Stoffregen. 2015. “Coupling of Postural Activity with Motion of a Ship at Sea.” *Experimental Brain Research* 233(5):1607–16.
- Vialatte, Francois Benoit, Monique Maurice, Justin Dauwels, and Andrzej Cichocki. 2010. “Steady-State Visually Evoked Potentials: Focus on Essential Paradigms and Future Perspectives.” *Progress in Neurobiology* 90(4):418–38.
- Vilhelmsen, Kenneth, F. R. (Ruud) van der Weel, and Audrey L. H. van der Meer. 2015. “A High-Density EEG Study of Differences between Three High Speeds of Simulated Forward Motion from Optic Flow in Adult Participants.” *Frontiers in Systems Neuroscience* 9.
- Wada, Atsushi, Yuichi Sakano, and Hiroshi Ando. 2016. “Differential Responses to a Visual Self-Motion Signal in Human Medial Cortical Regions Revealed by Wide-View

- Stimulation.” *Frontiers in psychology* 7:309.
- Wall, Matthew B., and Andrew T. Smith. 2008. “The Representation of Egomotion in the Human Brain.” *Current biology : CB* 18(3):191–94.
- Wandell, Brian A., Alyssa A. Brewer, and Robert F. Dougherty. 2005. “Visual Field Map Clusters in Human Cortex.” *Philosophical transactions of the Royal Society of London. Series B, Biological sciences* 360(1456):693–707.
- Warren, W. H. 1995. “Self-Motion.” Pp. 263–325 in *Perception of Space and Motion*. Elsevier.
- Warren, William H., and Kenneth J. Kurtz. 1992. “The Role of Central and Peripheral Vision in Perceiving the Direction of Self-Motion.” *Perception & Psychophysics* 51(5):443–54.
- Warren, William H., Michael W. Morris, and Michael Kalish. 1988. “Perception of Translational Heading from Optical Flow.” *Journal of Experimental Psychology: Human Perception and Performance* 14(4):646–60.
- Watson, J. D. G. et al. 1993. “Area V5 of the Human Brain: Evidence from a Combined Study Using Positron Emission Tomography and Magnetic Resonance Imaging.” *Cerebral Cortex* 3(2):79–94.
- Webb, Nicholas A., and Michael J. Griffin. 2003. “Eye Movement, Vection, and Motion Sickness with Foveal and Peripheral Vision.” *Aviation, space, and environmental medicine* 74(6 Pt 1):622–25.
- Wei, Y., X. Fu, and Richard H. Y. So. 2017. “Does Your Attention Allocation Affect How Motion Sick You Can Get.” Pp. 167–74 in *Contemporary Ergonomics 2017*.
- Wei, Yue, Jiayue Zheng, and Richard H. Y. So. 2018. “Allocating Less Attention to Central Vision during Vection Is Correlated with Less Motion Sickness.” *Ergonomics* 1–14.
- Wenzel, R. et al. 1996. “Deactivation of Human Visual Cortex during Involuntary Ocular Oscillations. A PET Activation Study.” *Brain : a journal of neurology* 119 (Pt 1:101–10.
- White, David J., Marco Congedo, Joseph Ciorciari, and Richard B. Silberstein. 2012. “Brain Oscillatory Activity during Spatial Navigation: Theta and Gamma Activity Link Medial Temporal and Parietal Regions.” *Journal of Cognitive Neuroscience* 24(3):686–97.

- Wickens, C. D. 1992. "Virtual Reality and Education." Pp. 842–47 in *[Proceedings] 1992 IEEE International Conference on Systems, Man, and Cybernetics*. IEEE.
- Wilkins, A.J. 2016. "A Physiological Basis for Visual Discomfort: Application in Lighting Design." *Lighting Research & Technology* 48(1):44–54.
- Wilson, John R. 1997. "Virtual Environments and Ergonomics: Needs and Opportunities." *Ergonomics* 40(10):1057–77.
- Wilson, Paul N., Nigel Foreman, and Danaë Stanton. 1997. "Virtual Reality, Disability and Rehabilitation." *Disability and rehabilitation* 19(6):213–20.
- De Winkel, K. N. et al. 2013. "Integration of Visual and Inertial Cues in the Perception of Angular Self-Motion." *Experimental Brain Research* 231(2):209–18.
- Winkler, Anderson M. et al. 2016. "Non-Parametric Combination and Related Permutation Tests for Neuroimaging." *Human Brain Mapping* 37(4):1486–1511.
- Wyatt, H. J., J. Pola, M. Lustgarten, and E. Aksionoff. 1995. "Optokinetic Nystagmus (OKN) Suppression by Fixation of a Stabilized Target: The Effect of OKN-Stimulus Predictability." *Vision research* 35(20):2903–10.
- Ye, J., R. I. Campbell, T. Page, and K. S. Badni. 2006. "An Investigation into the Implementation of Virtual Reality Technologies in Support of Conceptual Design." *Design Studies* 27(1):77–97.
- Zacharias, G. L., and L. R. Young. 1981. "Influence of Combined Visual and Vestibular Cues on Human Perception and Control of Horizontal Rotation." *Experimental brain research* 41(2):159–71.
- Zee, D. S., R. D. Yee, and D. A. Robinson. 1976. "Optokinetic Responses in Labyrinthine-Defective Human Beings." *Brain research* 113(2):423–28.
- Zeki, S. 1990. "Parallelism and Functional Specialization in Human Visual Cortex." *Cold Spring Harbor symposia on quantitative biology* 55:651–61.
- Zeki, S. et al. 1991. "A Direct Demonstration of Functional Specialization in Human Visual Cortex." *Journal of Neuroscience* 11(3).
- Zhang, Li-Li et al. 2015. "Motion Sickness: Current Knowledge and Recent Advance." *CNS neuroscience & therapeutics* n/a-n/a.

- Zhao, Yue. 2017. "Identifying Vestibular and Visual Cortical Response during Circular Vection among People with Different Susceptibility to Motion Sickness." The Hong Kong University of Science and Technology, Clear Water Bay, Kowloon, Hong Kong.
- Zheng, Jiayue. 2016. "Brain Wave Signatures Associated with Vection." The Hong Kong University of Science and Technology, Clear Water Bay, Kowloon, Hong Kong.

APPENDIX A LIST OF PUBLICATIONS AND CONFERENCES

Journal articles

- [1] Wei, Y., Zheng, J., & So, R. H. (2018). Allocating less attention to central vision during vection is correlated with less motion sickness. *Ergonomics*, 61(7), 933-946.
- [2] Guo, C. C., Chen, D. J., Wei, I. Y., So, R. H., & Cheung, R. T. (2017). Correlations between individual susceptibility to visually induced motion sickness and decaying time constant of after-nystagmus. *Applied ergonomics*, 63, 1-8.

Conference presentations

- [1] Human Factors and Ergonomics Society Annual Meeting, Oct 2015, LA, USA
- (Oral) Wei, Y., Bao, B., So, R. H., & Wong, K. M. (2015). Heading Discrimination Thresholds and Lateral Heading Detection Thresholds When Exposed to Low-frequency Linear Motion. *Proceedings of the Human Factors and Ergonomics Society Annual Meeting*, Vol. 59, No. 1, pp. 1341-1345.
- [2] Ergonomics & Human Factors, April 2017, Daventry, Northamptonshire, UK
- (Oral) Wei, Y., Fu, X.J., & So, R.H.Y. (2017). Does your attention allocation affect how motion sick you can get? *Contemporary Ergonomics & Human Factors 2017*.
- [3] Vision Sciences Society Seventeenth Annual Meeting, May 2017, St. Pete Beach, Florida, USA

(Oral) Wei, Y., Zheng, J.Y. and So, R.H.Y. (2017). Duration of vection generated by rotating dot patterns in peripheral correlates with VEP suppression in central visual field. *Journal of Vision*. 2017, 17(10):597-597. doi: 10.1167/17.10.597

(Poster) Fu, X., Wei, Y., Chen, J., & So, R. H. (2017). Interaction Effect of Frequency, Velocity and Amplitude on Perceived Vection Magnitude for Yaw Visual Oscillation. *Journal of Vision*. 2017(10):364. doi: 10.1167/17.10.364.

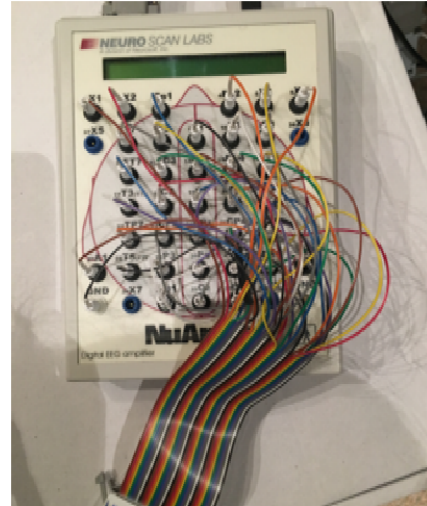
APPENDIX B VISUAL STIMULATION SETUPS



As illustrated in the above photo, the 46-inch Monitor is placed on a table covered by black curtains. The visual field outside the monitor is completely sheltered by black curtains with the ceiling light turned off during the experiment to eliminate all other visual cues.

The chin-rest is placed at the edge of the table. For all experiments, participants need to sit in front of the chin-rest to fix the viewing distance and sitting eye height.

APPENDIX C EEG SYSTEM SETUPS



As illustrated in the above left photo, participants wear the 32 EEG channel plus 4 EOG channel EEG cap (Quick-cap, Compumedics Neuroscan) of small, medium or large size based on their head size (see <http://compumedicsneuroscan.com/wp-content/uploads/Brochure-Quik-Cap-EEG.pdf> for the brochure of the EEG caps)

Above right photo illustrates the 40-channel NuAmps amplifier used in our EEG studies. The NuAmps is a DC-coupled, 22 bit, monopolar amplifier (see <https://compumedicsneuroscan.com/product/nuamps-40-channel-ee-erp-amplifier/> for detail specifications of the amplifier).

APPENDIX D CONSENT FORM

Consent Form For Human Factors Experiment Participation

1. Name _____ Age _____
2. Are you feeling ill in any way? Yes/No
3. Do you suffer from diabetes epilepsy (癲癇症) or other neurological diseases? Yes/No
4. Are you under medical treatment? Yes/No
5. Have you had any intake of alcohol (飲酒) during past 24 hours? Yes /No
6. Have you had injuries or over-exercises during the past 24 hours that will affect your postural stability or perception? Yes /No

If your answer is “Yes” to question (2) to (6), please give details to the Experimenter.

DECLARATION

I consent to take part in the experiment. My replies to the above questions are correct to the best of my belief, and I understand that they will be treated as confidential by the experimenter.

I understand that I may at any time withdraw from the experiment and that I am under no obligation to give reasons for withdraw declared above.

I undertake to obey the regulations of the laboratory and instructions of the experimenter regarding safety only to my right to withdraw declared above.

The purpose and methods of the experiment have been explained to me and I have had the opportunity to ask questions.

I know I will get **50HKD/h** for compensation of participation.

Signature of Subject _____ Date _____

This experiment conforms to the requirement of the University Research Ethic Committee.

Signature of Experimenter _____ Date _____

Starting time _____ Finish time _____

APPENDIX E MSSQ-SHORT & Pre/post-SSQ

MSSQ-short:[illegible]

This questionnaire is designed to find out how susceptible to motion sickness you are, and what sorts of motion are most effective in causing that sickness. Sickness here means feeling queasy or nauseated or actually vomiting.

Your CHILDHOOD Experience Only (before 12 years of age), for each of the following types of transport or entertainment please indicate:

3. As a CHILD (before age 12), how often you Felt Sick or Nauseated (tick boxes):

	Not Applicable - Never Travelled	Never Felt Sick	Rarely Felt Sick	Sometimes Felt Sick	Frequently Felt Sick
Cars					
Buses or Coaches					
Trains					
Aircraft					
Small Boats					
Ships, e.g. Channel Ferries					
Swings in playgrounds					
Roundabouts in playgrounds					
Big Dippers, Funfair Rides					

Your Experience over the LAST 10 YEARS (approximately), for each of the following types of transport or entertainment please indicate:

4. Over the LAST 10 YEARS, how often you Felt Sick or Nauseated (tick boxes):

	Not Applicable - Never Travelled	Never Felt Sick	Rarely Felt Sick	Sometimes Felt Sick	Frequently Felt Sick
Cars					
Buses or Coaches					
Trains					
Aircraft					
Small Boats					
Ships, e.g. Channel Ferries					
Swings in playgrounds					
Roundabouts in playgrounds					
Big Dippers, Funfair Rides					

Pre-SSQ:

SYMPTOM CHECKLIST (Pre-exposure)

Pre-exposure instruction: please fill in this questionnaire. Circle below if any of the symptoms apply to you now.

一般不適	1. General discomfort	None	Slight	Moderate	Severe
疲 倦	2. Fatigue	None	Slight	Moderate	Severe
沉 悶	3. Boredom	None	Slight	Moderate	Severe
想 睡	4. Drowsiness	None	Slight	Moderate	Severe
頭 痛	5. Headache	None	Slight	Moderate	Severe
眼 痛	6. Eyestrain	None	Slight	Moderate	Severe
很難集中視力	7. Difficulty focusing	None	Slight	Moderate	Severe
口水分秘增加	8. Salivation increase	None	Slight	Moderate	Severe
口水分秘減少	Salivation decrease	None	Slight	Moderate	Severe
出 汗	9. Sweating	None	Slight	Moderate	Severe
作 嘔	10. Nausea	None	Slight	Moderate	Severe
很難集中精神	11. Difficulty concentrating	None	Slight	Moderate	Severe
精神的壓抑	12. Mental depression	No	Yes (Slight	Moderate	Severe)
頭 脹	13. "Fullness of the head"	No	Yes (Slight	Moderate	Severe)
視野模糊	14. Blurred vision	No	Yes (Slight	Moderate	Severe)
眼 花 (開)	15. Dizziness eyes open	No	Yes (Slight	Moderate	Severe)
眼 花 (合)	Dizziness eyes close	No	Yes (Slight	Moderate	Severe)
眩 暈	16. Vertigo	No	Yes (Slight	Moderate	Severe)
幻 覺	17. Visual flashbacks*	No	Yes (Slight	Moderate	Severe)
昏 厥	18. Faintness	No	Yes (Slight	Moderate	Severe)
呼吸異樣	19. Aware of breathing	No	Yes (Slight	Moderate	Severe)
胃感覺異樣	20. Stomach awareness	No	Yes (Slight	Moderate	Severe)
沒有胃口	21. Loss of appetite	No	Yes (Slight	Moderate	Severe)
胃口增加	22. Increased appetite	No	Yes (Slight	Moderate	Severe)
想去洗手間	23. Desire to move bowels	No	Yes (Slight	Moderate	Severe)
迷 惘	24. Confusion	No	Yes (Slight	Moderate	Severe)
打 嗝	25. Burping	No	Yes (Slight	Moderate	Severe)
嘔 吐	26. Vomiting	No	Yes (Slight	Moderate	Severe)
其 他	27. Other	No	Yes (Slight	Moderate	Severe)

Post-SSQ:

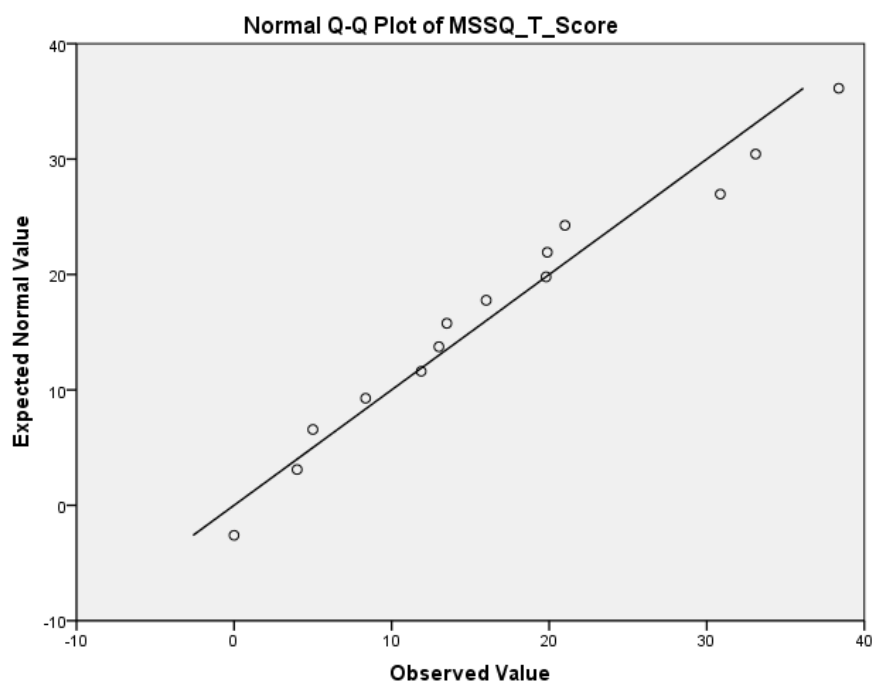
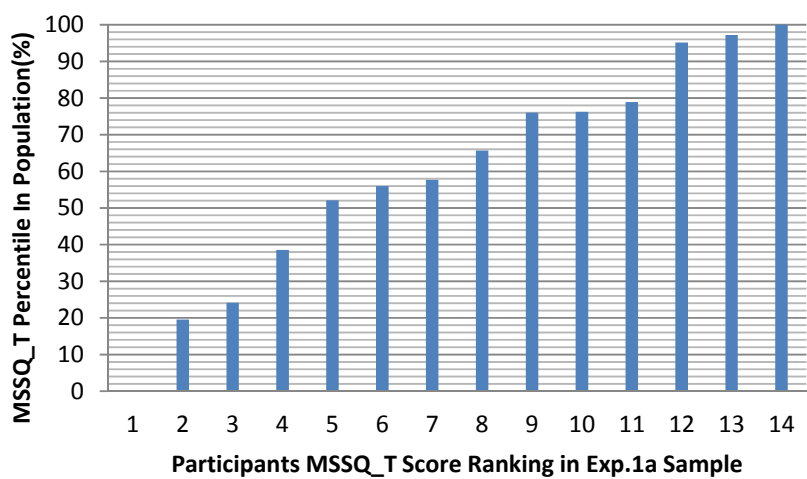
SYMPTOM CHECKLIST (Post-exposure)

Post-exposure instruction: please fill in this questionnaire once more. Circle below if any of the symptoms apply to you now.

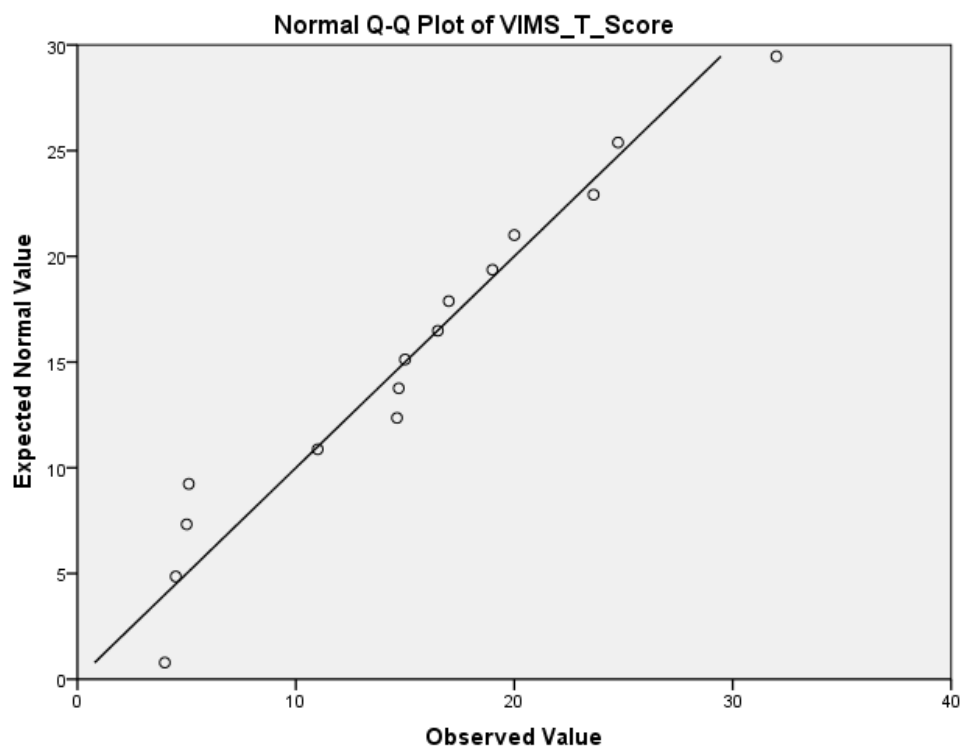
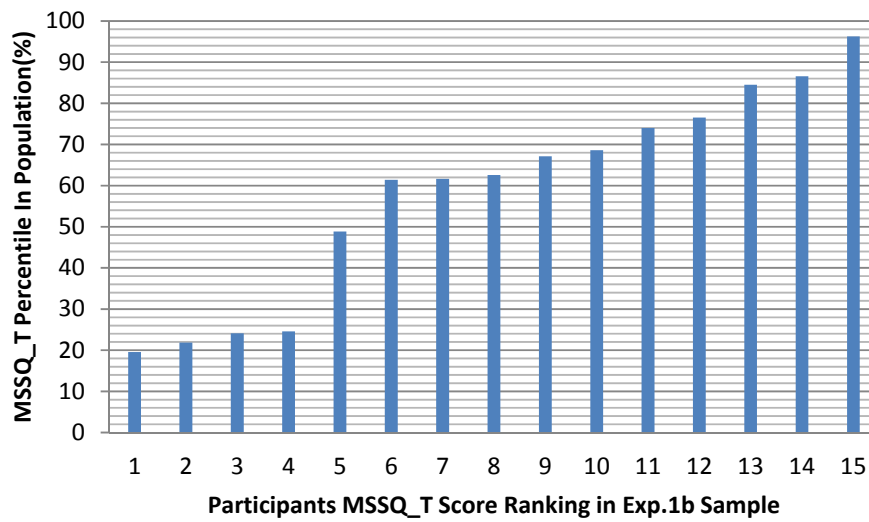
一般不適	1. General discomfort	None	Slight	Moderate	Severe
疲 倦	2. Fatigue	None	Slight	Moderate	Severe
沉 悶	3. Boredom	None	Slight	Moderate	Severe
想 睡	4. Drowsiness	None	Slight	Moderate	Severe
頭 痛	5. Headache	None	Slight	Moderate	Severe
眼 痛	6. Eyestrain	None	Slight	Moderate	Severe
很難集中視力	7. Difficulty focusing	None	Slight	Moderate	Severe
口水分秘增加	8. Salivation increase	None	Slight	Moderate	Severe
口水分秘減少	Salivation decrease	None	Slight	Moderate	Severe
出 汗	9. Sweating	None	Slight	Moderate	Severe
作 嘔	10. Nausea	None	Slight	Moderate	Severe
很難集中精神	11. Difficulty concentrating	None	Slight	Moderate	Severe
精神的壓抑	12. Mental depression	No	Yes (Slight	Moderate	Severe)
頭 脹	13. "Fullness of the head"	No	Yes (Slight	Moderate	Severe)
視野模糊	14. Blurred vision	No	Yes (Slight	Moderate	Severe)
眼 花 (開)	15. Dizziness eyes open	No	Yes (Slight	Moderate	Severe)
眼 花 (合)	Dizziness eyes close	No	Yes (Slight	Moderate	Severe)
眩 暈	16. Vertigo	No	Yes (Slight	Moderate	Severe)
幻 覺	17. Visual flashbacks*	No	Yes (Slight	Moderate	Severe)
昏 厥	18. Faintness	No	Yes (Slight	Moderate	Severe)
呼吸異樣	19. Aware of breathing	No	Yes (Slight	Moderate	Severe)
胃感覺異樣	20. Stomach awareness	No	Yes (Slight	Moderate	Severe)
沒有胃口	21. Loss of appetite	No	Yes (Slight	Moderate	Severe)
胃口增加	22. Increased appetite	No	Yes (Slight	Moderate	Severe)
想去洗手間	23. Desire to move bowels	No	Yes (Slight	Moderate	Severe)
迷 惘	24. Confusion	No	Yes (Slight	Moderate	Severe)
打 嗝	25. Burping	No	Yes (Slight	Moderate	Severe)
嘔 吐	26. Vomiting	No	Yes (Slight	Moderate	Severe)
其 他	27. Other	No	Yes (Slight	Moderate	Severe)

APPENDIX F MSSQ SCORE DISTRIBUTION OF PARTICIPANTS IN EACH STUDY

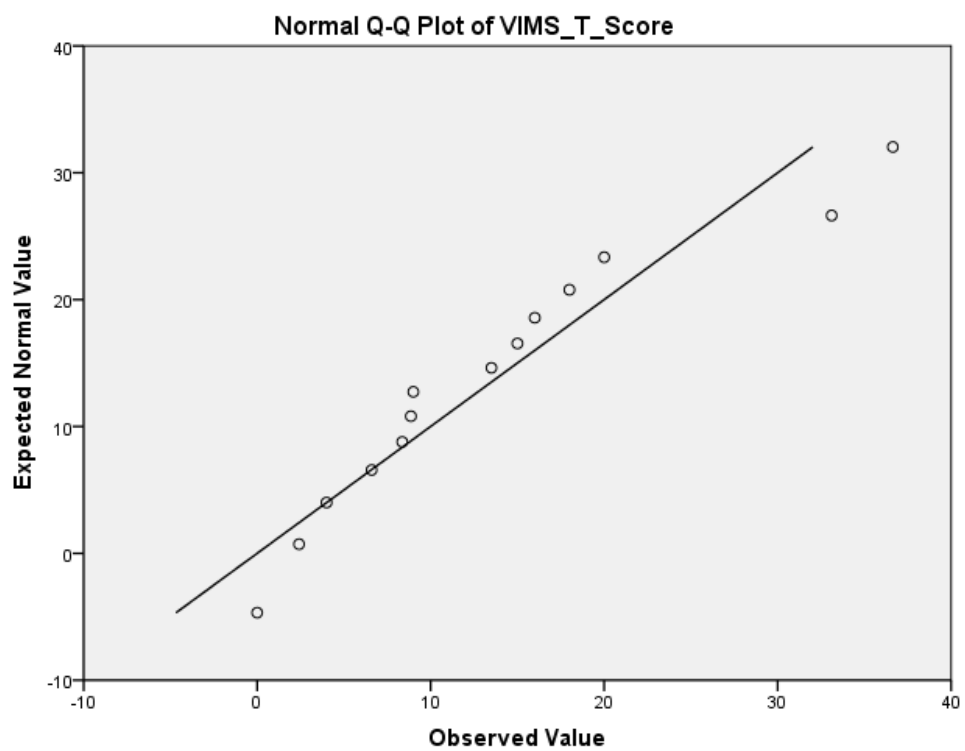
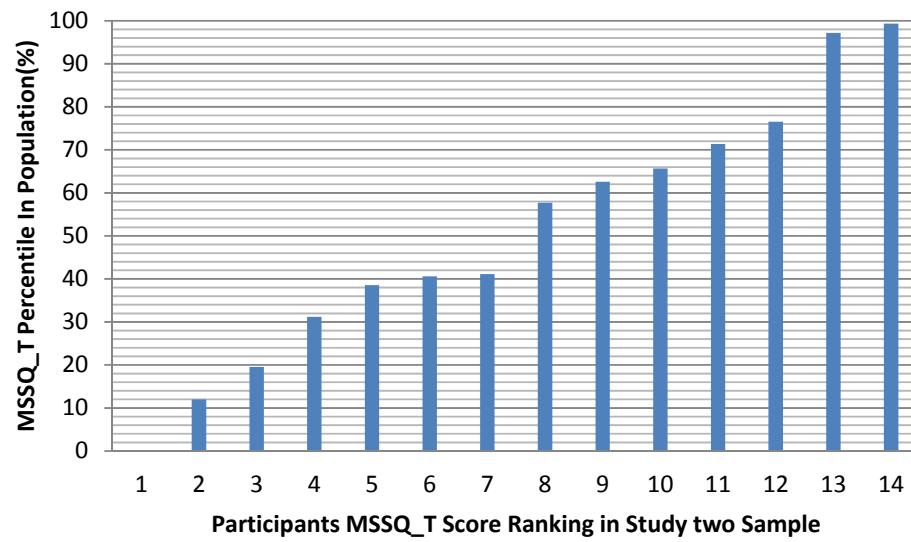
Participants MSSQ score distribution in Study one (Exp.1a)



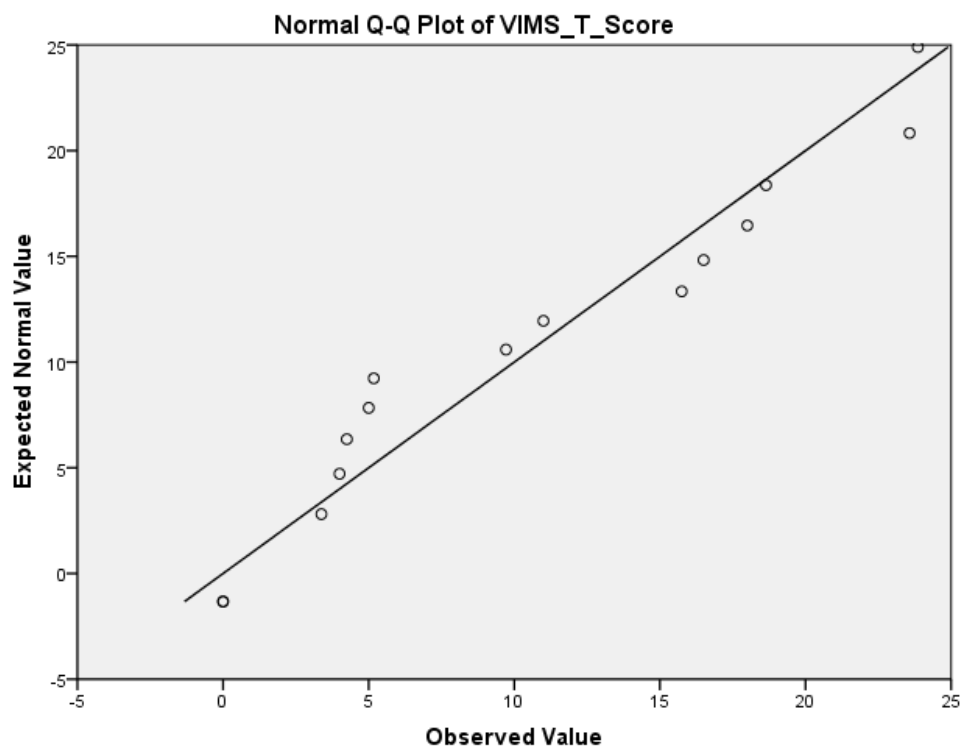
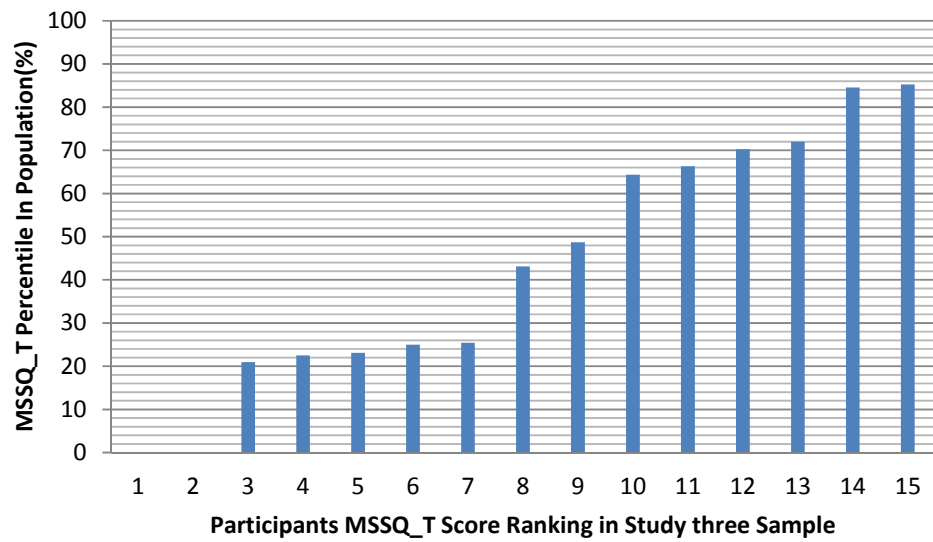
Participants MSSQ score distribution in Study one (Exp.1b)



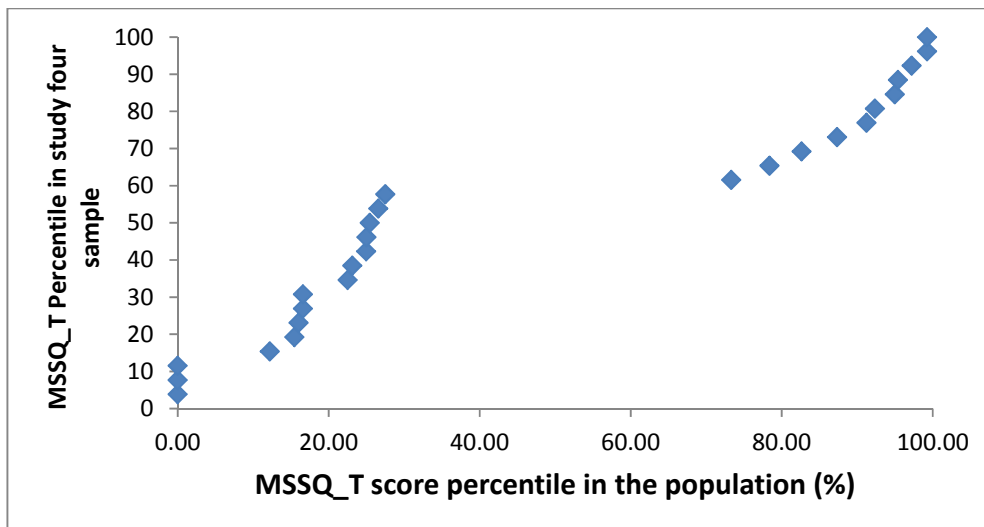
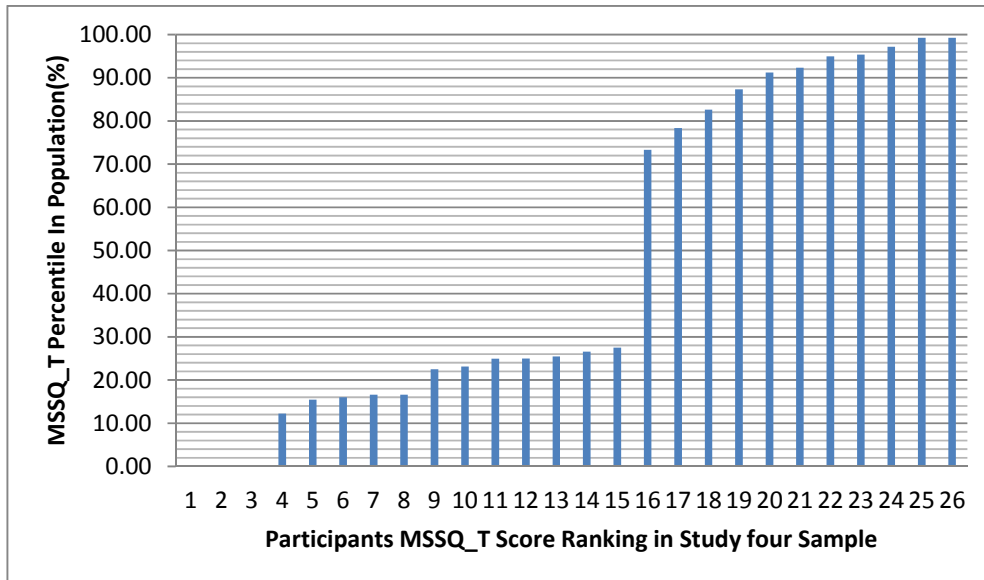
Participants MSSQ score distribution in Study two



Participants MSSQ score distribution in Study three



Participants MSSQ score distribution in Study four



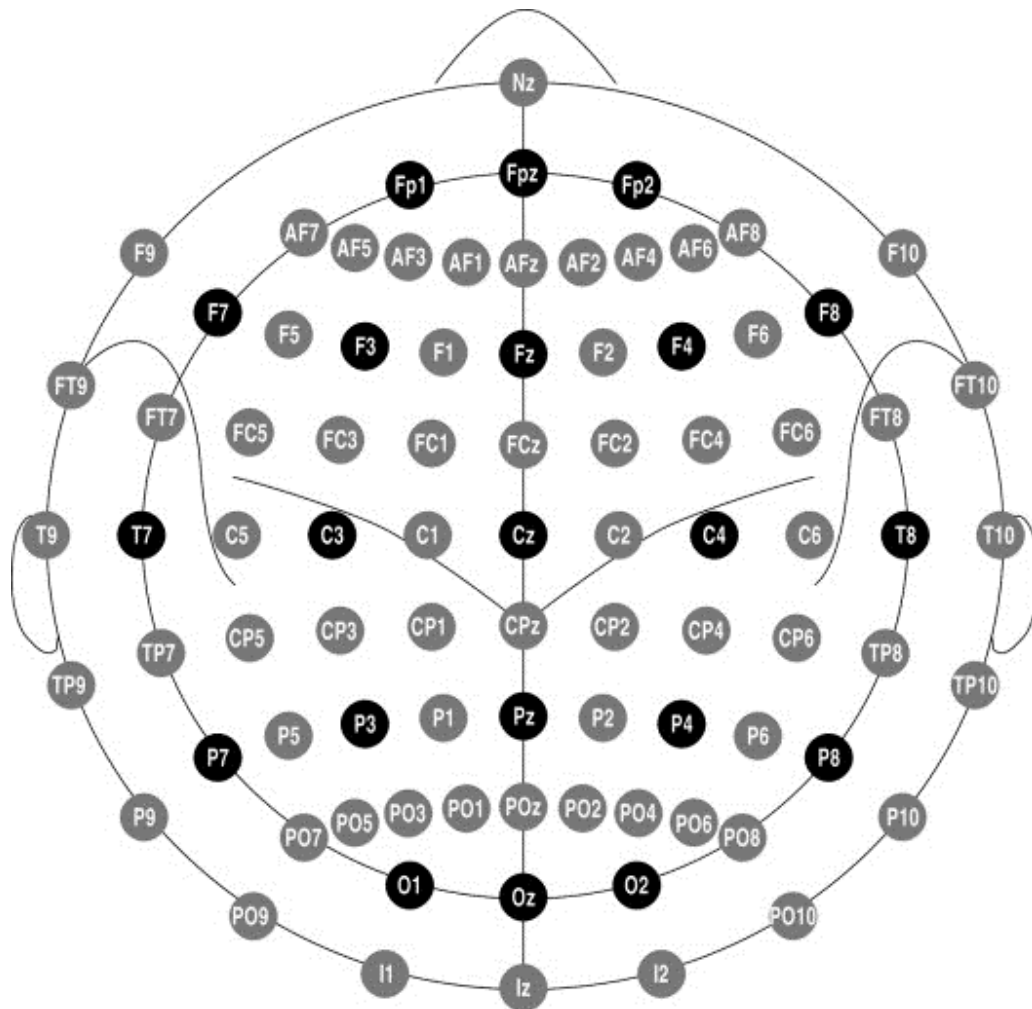
APPENDIX G VECTION INTENSITY SCALE

Subjective reported vection intensity

Perception of motion	Your report
You feel like you are stationary and it is the dot(s) which appear to moving only	1
You feel like you are moving a bit, but the dot(s) are moving more	2
You feel like you are moving at the same speed as the dot(s)	3
You feel like you are moving a lot and the dot(s) are moving a bit	4
You feel like you are moving and the dot(s) appear stationary	5

Participants are trained to report their perception state based on this scale, with intermediate non-integers allowed if they feel applicable (e.g. 2.7, 3.5...).

APPENDIX H INTERNATIONAL 10-10 SYSTEM FOR EEG



Above is the illustration on the international 10-10 system for EEG. Note that channels in dark black colour are the channels used in this study (The pictures are downloaded from <http://searchinsleep.blogspot.com/2012/11/eeg-polarity-2.html> 4:10pm, UTC+8, May 17th 2018).

APPENDIX I EXAMPLE FOR TRAINING INSTRUCTIONS AND EXPERIMENT INSTRUCTIONS

Training Instructions

Project Name: Functional Brain Connectivity Associated with Visually Induced Motion Sickness

Experimenter: WEI Yue (Isabella), email: yweiaj@connect.ust.hk

Supervisor: Prof. Richard So, HKUST

Dear participant:

Thank you for participation in this experiment preparation session. 感谢您参加我们的预实验。

Now we will spend 5-10min to help you get familiar with the task and formal experiment procedures.

现在我们会花费5-10分钟来帮助您熟悉我们的正式实验任务与实验流程。

Sometimes, what we see can cheat on us. For example, when we sit on train, look out of the window and find another train next to us moving, we may feel that our train is moving forward even though we do not move at all. And this is an illusion of self-motion.

有时候我们看到的東西會讓我們產生錯覺，比如當我們坐在靜止的火車上，有時旁邊的另外一輛火車開出車站時，雖然所搭乘的列車並沒有動，但我們有時會產生我們在緩慢地往相反方向運動的錯覺。而這就是一種自我運動的錯覺。

In the experiment, when you stare dot patterns rotating for a while, you may feel the rotation of dots gradually slow down and this is a sign that you are starting to generate an illusion of self-motion.

實驗中，當您觀看點圖旋轉運動時，您有時會覺得點旋轉的速度在漸漸變慢，這就是您開始產生自我運動的錯覺的標志之一。

Then, you may gradually start to feel the TV frame and yourself is tilting or even slowly rotating toward the opposite direction which the dots are moving.

隨後，您可能會漸漸感覺到電視邊框和自己開始往點運動相反的方向傾斜，甚至最終開始整個旋轉起來。

However, different individuals may have slight different feelings, and take different time to initiate the illusion of self-motion feelings. So take your time and there is no need to worry if you do not see the illusive self-motion in the beginning.

不過，每個人的感覺都會各有不同，而不同人需要產生這種感覺的時間長短也不同；這跟人的視覺特點有關並沒有好壞之分，所以請放輕鬆，如果一開始您沒有任何感覺，也完全不必擔心。

Now, let's have a try and watch the dots pattern first.

現在，我們先來看看實驗圖像試試。

Please verbally describe your feelings to experimenter when you feel some changes about the state of dots or yourself.

當您感覺到圖像中的點或自己的狀態有變化時，請將您的感覺到的口頭描述給實驗者。

Experiment procedure

1. Firstly, you will see a page with instructions, which just to remind you about the experiment task. Please put your right forefinger on left-arrow, put your ring finger on right-arrow.

实验开始后，您会看着这样一个有字的页面。它主要是提醒您一下具体的实验任务。请把右手食指放在键盘的左箭头上，无名指放在右箭头上。

When you feel you are ready to start the experiment, just use left forefinger press key 'z' to start it yourself. 当您觉得准备好了的话，您可以把左手食指放在'z'键自己开始实验。



2. After this, you may see lots of grey dots shows up and moving randomly at the black background, or coherently rotating around the grey circle.

在这之后，您会看到一些大小不一的灰点出现的屏幕上随机四处运动，或者所有点一起围绕中央灰圆逆时针旋转。

You will see a grey circle at the center of a black ground for a while. 接下来，您会看到黑底屏幕中央有一个灰色的圆圈。

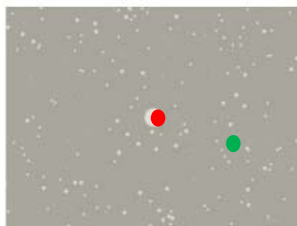
Please fix your eye at the grey circle though the whole experiment. 请在接下来的整个实验过程中，一直保持注视这个灰圆。



If you start feel self-motion, please press the left-arrow (forefinger finger).

当您感觉到自己开始运动时，请并保持按一下左箭头（食指），并松开。

If you feel the self-motion disappear, please press the ring finger. 如果这种感觉消失了，请按一下右箭头（无名指），并松开。



3. During this, you may see some red/green dots shows up at the screen, some may in the center and some may at the peripherals.

与此同时，你有时会看到红色/绿色的点出现在视野里，它们可能出现在视野中央，也可能出现在周围任何位置。

When you see the red dots, press the key 'z' (left forefinger) as quickly as you can.

当你看见红点时，请尽快按下 z 键（左手食指）并松开。

When you see the red dots, do not press any key.

当你看见绿点时，请不要按键。

Before, the experiment start, we will practice 1-2 min to help you familiar with the task.

在实验开始前，我们会练习这个 1-2 两分钟，以帮助你熟悉任务。

APPENDIX J LIST OF HYPHOTHESIS FOR EACH STUDY

Study No.	Hypotheses List (No. : Content)
Study 1	<p>H1: The influence of visual response regulation measured by SART performance in the presence of vection depends on whether the visual targets are in the PVF or CVF</p> <ul style="list-style-type: none"> - H1a: SART performance in the PVF is improved during vection - H1b: SART performance in the CVF is impaired during vection - H1c: The improvement of SART performance in the PVF is more evident with targets moving at similar speeds to the self-motion cues - H1d: The impairment of SART performance in the CVF is equally to all type of targets regardless of the moving speeds of them
	<p>H2: The magnitudes of individual effect measured by SART performance during vection would vary depending on VIMS susceptibility</p>
	<p>H3: When participants are only allowed to react to PVF targets while ignoring CVF targets, their vection experience is stronger and more stable, as compared with the vection experience when they are only allowed to do opposite reactions (response to CVF targets while ignoring PVF targets)</p>
	<p>H4: The enhancement of vection is stronger when the PVF targets are moving at the same speed as the visual self-motion cues, as compared with the enhancement when targets are moving in conflict with the visual self-motion cues</p>
Study 2	<p>H5: The influence of visual response regulation under vection reflected VEP components depends on the intrinsic properties of VEP components</p>
	<ul style="list-style-type: none"> - H5a: The earlier VEP components, which are observed around 100ms and more responsible to contrast processing (N1 and P1 from PRVEP), are suppressed during vection

	<p>- H5b: The N2 component, which is observed around 200ms and more closely associated with motion processing, is strengthened during vection</p> <p>H6: The magnitudes of visual regulation effect reflected by peak amplitude and peak latency of VEP components is negatively correlated with VIMS susceptibility</p>
	<p>H7: There are peaks observed at the flickering frequency of stimulation (8.6Hz for CVF; 12Hz for PVF) and their 2nd harmonics (17.2Hz for CVF; 24Hz for PVF) in the power spectrum of SSVEP</p> <p>H8: The power topography for two marked frequencies (8.6 and 12Hz) should be significantly different (H8a), where the EOIs produce strongest frequency power should be different (H8b)</p>
Study 3	<p>H9: Vection is associated with a power shift from CVF stimuli EOI to PVF stimuli EOI</p> <p>H10: The magnitudes of the effects are negatively correlated with the MSSQ scores of individual participants</p> <p>H11: The top-down attention regulation should have interaction effect on both vection perception (H11a) and the vection associated effects (H11b)</p>
Study 4	<p>H12: Phase synchronization between electrodes over vection related areas and other extra-visual areas should be stronger under vection inducing-stimulation, as compared to the synchronization under control visual stimuli (H12a). Moreover, resistant participants should show stronger effects than susceptible participants (H12b).</p> <p>H13: As we hypothesized that the sensory conflict reduction is more effective in resistant participant, we expect the reduction of phase synchronizations after vection onset shall be stronger in resistant participant (H13a). The magnitude of this effect is negatively correlated with the susceptibility of participants (H13b)</p>